

## Journal of Polymer Science

## Part A-1: Polymer Chemistry

## Contents

KATSUKIYO ITO: Relationship between the Autoacceleration of Polymerization Rate and Conversion in Radical Polymerization . . . . .	1313
CHUJI ASO, SANAE TAGAMI, and TOYOKI KUNITAKE: Polymerization of Aromatic Aldehydes. IV. Cationic Copolymerization of Phthalaldehyde Isomers and Styrene . . . . .	1323
N. R. FETTER and C. M. GRIEVE: Metal Coordination Polymers. III. Molecular Weights of Beryllium Phosphinate Polymers in Chloroform . . . . .	1337
GABRIEL EZRA and ALBERT ZILKHA: Anionic Graft Polymerization and Homopolymerization of Phenyl Glycidyl Ether . . . . .	1343
K. HORIE, H. HIURA, M. SAWADA, I. MITA, and H. KAMBE: Calorimetric Investigation of Polymerization Reactions. III. Curing Reaction of Epoxides with Amines . . . . .	1357
D. R. CRUISE and R. G. LACOMBE: Representation of Terpolymer Kinetics on Triangular Coordinates . . . . .	1373
C. F. HAUSER and NATHAN L. ZUTTY: Quinone Copolymerization. I. Reactions of <i>p</i> -Chloranil, <i>p</i> -Benzoquinone, and 2,5-Dimethyl- <i>p</i> -benzoquinone with Vinyl Monomers under Free-Radical Initiation . . . . .	1385
JOOST MANASSEN and ROBERT REIN: The Reactive Intermediate in Acetylene Polymerization: Results of Quantum Chemical Calculations on Charge Delocalization and Its Consequences . . . . .	1403
R. E. WHITE and Z. G. GARDLUND: Reduction of Pendent Ester Groups in Polycarbonates by Use of Diborane . . . . .	1419
DWAIN M. WHITE and HOWARD J. KLOFFER: Polymerization by Oxidation Coupling. I. A Study of the Oxidation of 2,6-Diphenylphenol to Poly(2,6-diphenyl-1,4-phenylene ether) . . . . .	1427
JOHN N. MAJERUS and ANTHONY R. PITOCELLI: Influence of Microstructure on the Tensile Behavior of Acrylic Copolymers . . . . .	1439
HIDEMASA YAMAGUCHI and YUJI MINOURA: Copolymerization of Optically Active <i>N</i> -Bornylmaleimide with Vinyl Monomers . . . . .	1467
GIANNI LINOLI, ENZO MANNUCCI, and CARLO BERGONZI: Natural and Synthetic Polymers as Reagents. I. Diazonium Salt Derivatives of Polycarboxylic Resins (Insoluble Diazonium Salt Chromogens) . . . . .	1481
SATYENDRA NATH GUPTA and UMA SANKAR NANDI: Role of Dimethyl Sulfoxide as a Solvent for Vinyl Polymerization . . . . .	1493
R. G. CHRISTENSEN and C. A. J. HOEVE: Comparison between Theoretical and Experimental Values of the Volume Changes Accompanying Rubber Extension . . . . .	1503
GEORGE A. MORTIMER: Chain Transfer in Ethylene Polymerization. IV. Additional Study at 1360-Atm and 130°C . . . . .	1513
V. JIŠOVÁ, M. KOLÍNSKÝ, and D. LÍM: Polymerization of Vinyl Chloride by Alkyl-lithium Compounds . . . . .	1525

(continued inside)

Journal of Polymer Science: **Part A-1: Polymer Chemistry**

**Board of Editors:** H. Mark • C. G. Overberger • T. G. Fox

**Advisory Editors:**

R. M. Fuoss • J. J. Hermans • H. W. Melville • G. Smets

**Editor:** C. G. Overberger      **Associate Editor:** E. M. Pearce

**Advisory Board:**

T. Alfrey, Jr.	E. M. Fettes	C. S. Marvel	W. H. Sharkey
W. J. Bailey	N. D. Field	F. R. Mayo	W. R. Sorenson
D. S. Ballantine	F. C. Foster	R. B. Mesrobian	V. T. Stannett
M. B. Birenbaum	H. N. Friedlander	H. Morawetz	J. K. Stille
F. A. Bovey	K. C. Frisch	M. Morton	M. Szwarc
J. W. Breitenbach	N. G. Gaylord	S. Murahashi	A. V. Tobolsky
W. J. Burlant	W. E. Gibbs	G. Natta	E. J. Vandenberg
G. B. Butler	A. R. Gilbert	K. F. O'Driscoll	L. A. Wall
S. Bywater	J. E. Guillet	S. Okamura	F. X. Werber
T. W. Campbell	H. C. Haas	P. Pino	O. Wichterle
W. L. Carrick	J. P. Kennedy	C. C. Price	F. H. Winslow
H. W. Coover, Jr.	W. Kern	B. Rånby	M. Wismer
F. Danusso	J. Lal	J. H. Saunders	E. A. Youngman
F. R. Eirich	R. W. Lenz	C. Schuerch	

*Contents (continued), Vol. 8*

GEORGE A. MORTIMER: Chain Transfer in Ethylene Polymerization. V. The Effect of Temperature.....	1535
GEORGE A. MORTIMER: Chain Transfer in Ethylene Polymerization. VI. The Effect of Pressure.....	1543
PAUL W. TIDWELL and GEORGE A. MORTIMER: Chain Transfer in Ethylene Polymerization. III. An Improved Method of Calculating Polymerization Chain-Transfer Constants.....	1549
J. P. STALLINGS: Preparation, Reaction, and Polymerization of the Nuclear Chlorinated $\alpha$ , $\alpha'$ -Xylylene Diallyl Ethers.....	1557
KOICHI YAMAGUCHI and YUGI MINOURA: Polymerization of Vinyl Monomers with Salts of Bronsted Acids.....	1571

*(continued on inside back cover)*

The Journal of Polymer Science is published in four sections as follows: Part A-1, Polymer Chemistry, monthly; Part A-2, Polymer Physics, monthly; Part B, Polymer Letters, monthly; Part C, Polymer Symposia, irregular.

Published monthly by Interscience Publishers, a Division of John Wiley & Sons, Inc., covering one volume annually. Publication Office at 20th and Northampton Sts., Easton, Pa. 18042. Executive, Editorial, and Circulation Offices at 605 Third Avenue, New York, N. Y. 10016. Second-class postage paid at Easton, Pa. Subscription price, \$325.00 per volume (including Parts A-2, B, and C). Foreign postage \$15.00 per volume (including Parts A-2, B, and C).

Copyright © 1970 by John Wiley & Sons, Inc. All rights reserved. No part of this publication may be reproduced by any means, nor transmitted, or translated into a machine language without the written permission of the publisher.

## Relationship between the Autoacceleration of Polymerization Rate and Conversion in Radical Polymerization

KATSUKIYO ITO, *Government Industrial Research Institute, Nagoya, Kita-ku, Nagoya, Japan*

### Synopsis

By using a simple treatment for the kinetics of radical polymerization with primary radical termination, the ratio  $k_{ty}/k_{tx}$  of chain termination rate constant  $k_{ty}$  at conversion  $y$  to that  $k_{tx}$  at conversion  $x$  and the ratio  $k_{tiy}/k_{tix}$  of the primary radical termination rate constant  $k_{tiy}$  at conversion  $y$  to  $k_{tix}$  at conversion  $x$  were calculated for the polymerizations of methyl methacrylate and ethyl acrylate in the conversion range 0 to 0.4.  $k_{ty}/k_{tx}$  and  $k_{tiy}/k_{tix}$  were treated by using the following equations based on the variation of conversion:

$$\frac{1}{\log(k_{ty}/k_{tx})} = -g(T,y) + \frac{[g(T,y)]^2}{\beta(T)} \left( \frac{1}{x-y} \right)$$

where  $g(T,y)$  is the average fractional free volume of radical chain end at conversion  $y$  and absolute temperature and  $\beta(T)$  is a function depending on  $T$ , and

$$\frac{1}{\log(k_{tiy}/k_{tix})} = -g_i(T,y) + \frac{[g_i(T,y)]^2}{\beta_i(T)} \left( \frac{1}{x-y} \right)$$

where  $g_i(T,y)$  is the average fractional free volume of primary radical at conversion  $y$  and  $T$  and  $\beta_i(T)$  is a function depending on  $T$ . The autoacceleration for the above monomers was successfully interpreted by the above treatment.

### INTRODUCTION

In the past, the autoacceleration of polymerization rate has been interpreted on the assumption that the termination rate constant decreases with decreasing mobility of the polymeric radical. Brunett and Duncan<sup>1</sup> pointed out that due to loss of mobility of the polymeric radical at high conversion, termination for bimolecular reaction between primary radical and polymeric radical (primary radical termination) is a matter of great importance, and termination for bimolecular reaction between polymeric radicals (chain termination) is negligible. The following equation was derived for a relationship between two polymerization rates  $R_x$  and  $R_0$  at conversions  $x$  and 0, respectively:

$$(R_x/R_0 - 1) = K_1(x - x_1)^2 \tag{1}$$

where  $K_1$  is a constant depending on termination rate constant and initiation rate and  $x_1$  is the critical conversion requiring a threshold concentration of polymer for trapping the radicals. If the treatment based on eq. (1) is correct at high conversion, the molecular weight distribution should be observed for a polymerization terminated by primary radical termination at low and high initiation rates rather than by chain termination. However, it was reported that in the bulk polymerization of methyl methacrylate at high conversion, the molecular weight distribution observed at low initiation rate is that with one peak, corresponding to chain termination while at high initiation rate distribution with two peaks is observed, the first and second peaks corresponding to primary radical termination and chain termination, respectively.<sup>2,3</sup> Thus, not every condition can be applicable Brunett and Duncan's treatment. In view of the molecular weight distribution, their treatment is correct under the condition that chain termination is negligible to be compared to primary radical termination.

In the previous papers,<sup>3,4</sup> by using a treatment based on the relationships between conversions and the termination rate constants, it was proved that the termination rate constants for chain termination and primary radical termination are in proportion to the diffusion constants for the radical chain end and primary radical, respectively. By using these treatments, the autoacceleration of the polymerization rate for the polymerization with both chain termination and primary radical termination should be able to be interpreted. In this paper, by using Ito and Matsuda's equation,<sup>5</sup> the ratios of  $k_{ty}/k_{tx}$  and  $k_{tly}/k_{tlx}$  were calculated, where  $k_{tx}$  and  $k_{ty}$  are the chain termination rate constants at conversions  $x$  and  $y$ , respectively, and  $k_{tlx}$  and  $k_{tly}$  are the primary radical termination rate constants at conversions  $x$  and  $y$ , respectively. On extension of the treatments in the previous papers<sup>3,4</sup> to the above ratios, the autoacceleration for the polymerization where chain termination exceeds primary radical termination was interpreted.

## THEORY

### Kinetics for Radical Polymerization with Primary Radical Termination

Using an approximate equation

$$\{1 + 4B(x)[C]^{1/2}\}^{1/2} = 1 + 2B(x)[C]^{1/2} - 2[B(x)]^2[C] \quad (2)$$

Ito and Matsuda<sup>5</sup> derived eq. (3) for the polymerization rate  $R_x$  of chain termination exceeding primary radical termination:

$$R_x = A(x)[C]^{1/2}\{1 - B(x)[C]^{1/2}\} \quad (3)$$

where

$$A(x) = (2fk_d)^{1/2}k_p[M]_0(1-x)/k_{tx}^{1/2} \quad (4)$$

$$B(x) = (2fk_d)^{1/2}k_{tlx}/\{k_tk_i^{1/2}[M]_0(1-x)\} \quad (5)$$

In eqs. (2) and (3),  $[M]_0$  is the initial concentration of monomer,  $[C]$  is the concentration of initiator,  $f$  is initiator efficiency, and  $k_p$ ,  $k_i$ , and  $k_d$  are the rate constants for the propagation, primary radical addition to monomer, and decomposition of initiator, respectively.

On taking eq. (3) and an approximate equation

$$\frac{1}{R(0)} = \frac{1 + B(0)[C]^{1/2}}{A(0)[C]^{1/2}} \quad (6)$$

at conversion  $x = 0$ , in which an approximation

$$1/\{1 - B(0)[C]^{1/2}\} = 1 + B(0)[C]^{1/2} \quad (7)$$

can be used,  $R_x/R_0$  becomes

$$R_x/R_0 = [A(x)/A(0)]\{1 - [B(x) - B(0)][C]^{1/2}\} \quad (8)$$

Taking eq. (3) and the same equation with respect to conversion  $y$  in the conversion range where  $fk_d$ ,  $k_p$ , and  $k_i$  do not depend on conversion, constants,  $k_{ty}/k_{tx}$  and  $k_{tiy}/k_{tiz}$  are given by eqs. (9) and (10), respectively.

$$\frac{k_{ty}}{k_{tx}} = \left[ \frac{A(x)(1-y)}{A(y)(1-x)} \right]^2 \quad (9)$$

$$\frac{k_{tiy}}{k_{tiz}} = \frac{A(x)B(y)}{A(y)B(x)} \left( \frac{1-y}{1-x} \right)^2 \quad (10)$$

### Termination Rate Constants

**Chain Termination Rate Constant.** For a linear relationship to conversions and the chain termination rate constants proportional to the diffusion constant of the radical chain end,<sup>6</sup> eq. (11) was derived on the assumption that an approximation

$$v = 1 - x$$

can be used,<sup>4</sup> where  $v$  is the volume fraction of monomer in the homogeneous solution of monomer molecules and segments:

$$\frac{1}{\log(k_{ty}/k_{tx})} = -g(T,y) + \frac{[g(T,y)]^2}{\beta(T)} \left( \frac{1}{x-y} \right) \quad (11)$$

where

$$g(T,y) = g(T,1) + \beta(T)(1-y) \quad (12)$$

In eq. (11),  $g(T,y)$  is the average fractional free volume of radical chain end at conversion  $y$  and absolute temperature  $T$ , and  $\beta(T)$  is a function depending on  $T$ .

**Primary Radical Termination Rate Constant.** In the previous paper,<sup>6</sup> a primary radical termination rate constant was derived for the first-order reaction on the assumption that the concentration of radical chain ends during a collision between primary radical and polymeric radical is con-

stant. Actually, the reaction between primary radicals and radical chain ends is second-order. Fortunately, when the distance or the time  $t$  for the translation of primary radical during a collision is a sufficiently short, the result obtained for the first-order reaction is equivalent to the result obtained in the second-order reaction. In this paper, taking by assuming a second-order reaction and using the fact that the distance of the translation of primary radical is  $u_i t$  (where  $u_i$  denotes the mean velocity of translation of the primary radical), the rate of this reaction is given by

$$-d[\text{R}]/dt = u_i \gamma_i [\text{R}][\text{S}] \\ = \pi N_L p_{Si} r_{Si}^2 (u_S^2 + u_i^2)^{1/2} [\text{R}][\text{S}] \times 10^{-3} \text{ mole/l.-sec} \quad (13)$$

where  $\gamma_i$  is a reactivity constant,  $[\text{R}]$  and  $[\text{S}]$  are the concentrations of primary radical and radical chain end, respectively in the polymeric radical,  $u_S$  is the mean velocity of translation of radical chain end,  $N_L$  is Avogadro's number,  $p_{Si}$  is the probability of bimolecular combination between primary radical and radical chain end, and  $r_{Si}$  is the average distance of approach of the primary radical and radical chain end during a collision. By using  $\gamma_i$  determined from eq. (13) and the primary radical termination rate constant obtained in the previous paper,<sup>6</sup>  $k_{tir}$  is given by

$$k_{tir} = A_{il} (u_S^2 + u_i^2)^{1/2} \quad (14)$$

where

$$A_{il} = \frac{3}{2} \pi N_L p_{Si} r_{Si}^2 \mu_i (1 - \mu_i)^2 \times 10^{-3}$$

where  $\mu_i$  is the ratio of the length of a primary radical immersed in the polymeric radical to the radius of the polymeric radical.

Under the condition that  $u_S$  is negligible compared to  $u_i$ , and on assuming the validity of eq. (14) and Einstein's equation

$$u_i = 6D_i/h_i \quad (15)$$

where  $D_i$  is the diffusion constant of the primary radical and  $h_i$  is the distance of translation of primary radical per collision between primary radical and solvent molecule, eq. (14) becomes

$$k_{tir} = A_i D_i \quad (16)$$

where

$$A_i = 6A_{il}/h_i \quad (17)$$

On applying this equation similarly to the diffusion constant of radical chain end,<sup>3</sup> the diffusion constant of the primary radical is given by

$$D_i = A_{i2} \exp\{-[1/g_i(T,x)]\} \quad (18)$$

where

$$g_i(T,x) = g_i(T,1) + \beta_i(T)(1-x) \quad (19)$$

In eqs. (18) and (19),  $A_{i2}$  is constant, and  $g_i(T,x)$  and  $\beta_i(T)$  are the average fractional free volume at conversion  $x$  and a function depending on  $T$  for the primary radical, respectively. On the introduction of eq. (18) into eq. (16), eq. (16) becomes

$$k_{tix} = A_1^* \exp \left\{ -1/g_i(T,x) \right\} \tag{20}$$

where

$$A_1^* = A_i A_{i2}. \tag{21}$$

Taking eq. (20) and the same equation with respect to conversion  $y$  to eq. (20), a linear relationship between the primary radical termination rate constants and conversion is given by eq. (22):

$$\frac{1}{\log(k_{tiy}/k_{tiz})} = -g_i(T,y) + \frac{[g_i(T,y)]^2}{\beta_i(T)} \left( \frac{1}{x-y} \right) \tag{22}$$

This equation is applicable under the condition  $u_i \gg u_s$ .

Under the condition  $u_i = u_s$  or  $u_i \ll u_s$ , a linear relationship between primary radical termination rate constants and conversions is given by eq. (23):

$$\frac{1}{\log(k_{tiy}/k_{tiz})} = -g(T,y) + \frac{[g(T,y)]^2}{\beta(T)} \left( \frac{1}{x-y} \right) \tag{23}$$

Under the condition that  $u_i$  is only moderately greater than  $u_s$  or  $u_i$  is only moderately less than  $u_s$ , no convenient linear relationship could be obtained for the primary radical termination rate constant.

## APPLICATIONS AND DISCUSSION

### Determination of $k_{ty}/k_{tz}$ and $k_{tiy}/k_{tiz}$

In the bulk polymerization of methyl methacrylate (MMA) initiated by benzoyl peroxide (BPO) (at concentrations of BPO of 0.0103–0.0826 mole/

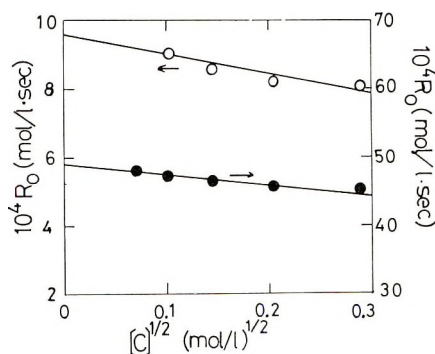


Fig. 1. Relationships between  $R_0$  and  $[C]^{1/2}$  for the polymerization of MMA: (○) at 50°C; (●) at 70°C.

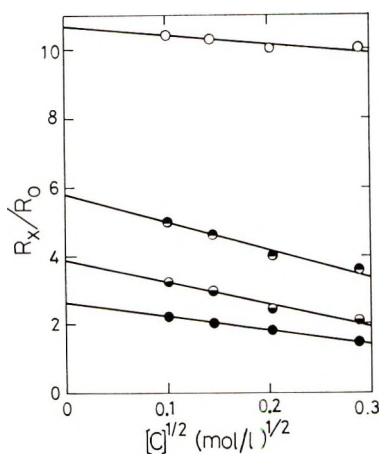


Fig. 2. Relationships between  $R_x/R_0$  and  $[C]^{1/2}$  for the polymerization of MMA at  $50^\circ\text{C}$ : (●)  $x = 0.2$ ; (◐)  $x = 0.25$ ; (◑)  $x = 0.3$ ; (○)  $x = 0.4$ .

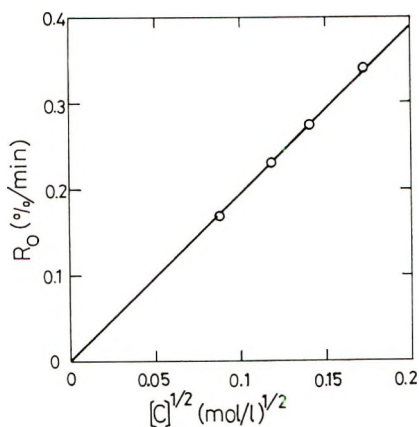


Fig. 3. Relationship between  $R_0$  and  $[C]^{1/2}$  for the polymerization of EA.

1.), and  $R_0/[C]^{1/2}$  was essentially constant,<sup>7</sup> the small decrease of  $R_0/[C]^{1/2}$  with increasing of  $[C]$  observed being attributed to experimental error. Actually, in view of eq. (3) for this polymerization (Fig. 1), this point is

TABLE I  
Values of  $A(x)/A(0)$ ,  $B(x)/B(0)$ ,  $k_{t0}/k_{tx}$ , and  $k_{ti0}/k_{tix}$   
at Conversion  $x$  for the Bulk Polymerization of MMA

$x$	$A(x)/A(0)$	$B(x)/B(0)$	$k_{t0}/k_{tx}$	$k_{ti0}/k_{tix}$
0	1	1	1	1
0.20	2.60	3.91	10.6	1.04
0.25	3.90	4.06	26.9	1.71
0.30	5.80	3.66	68.6	3.25
0.40	10.70	1.53	318.0	19.5



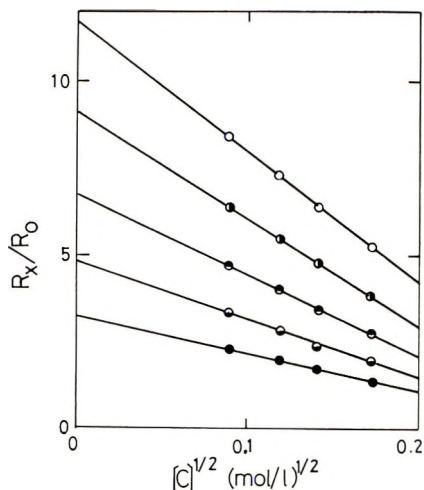


Fig. 4. Relationships between  $R_x/R_0$  and  $[C]^{1/2}$  for the polymerization of EA: (●)  $x = 0.2$ ; (◐)  $x = 0.25$ ; (●)  $x = 0.3$ ; (◐)  $x = 0.35$ ; (○)  $x = 0.4$ .

not correct. The linear relationships in Figure 1 gave  $B(0) = 0.53$  and  $0.30$  at  $50$  and  $70^\circ\text{C}$ , respectively. Because of the small value of  $B(0)[C]^{1/2}$ , on taking  $y = 0$  and using eq. (8), linear relationships between  $R_x/R_0$  and  $[C]^{1/2}$  could be obtained (Fig. 2). By using these linear relationships and  $B(0) = 0.53$ ,  $k_{t0}/k_{tx}$  and  $k_{ti0}/k_{tix}$  were calculated from eqs. (9) and (10), respectively (Table I).

TABLE II  
Values of  $A(x)/A(0)$ ,  $B(x)/B(0.2)$ ,  $k_{t0}/k_{tx}$ , and  $k_{ti0.2}/k_{tix}$  at Conversion  $x$  for the Bulk Polymerization of EA

$x$	$A(x)/A(0)$	$B(x)/B(0.2)$	$k_{t0}/k_{tx}$	$k_{ti0.2}/k_{tix}$
0.20	3.33	1	16.8	1
0.25	4.65	0.972	38.5	1.63
0.27	5.50	0.986	56.8	2.02
0.30	6.72	0.986	92.1	2.75
0.35	9.08	0.968	195.0	4.33
0.40	11.70	0.916	380.0	6.75

A linear relationship between  $R_0$  and  $[C]^{1/2}$  could be obtained for the bulk polymerization of ethyl acrylate<sup>8</sup> (EA) initiated by 2,2'-azobisisobutyronitrile (AIBN) at AIBN concentrations of  $0.0080$ – $0.0030$  mole/l. at  $35^\circ\text{C}$  (Fig. 3). Accordingly,  $B(0) = 0$ . On taking  $y = 0$  and by using eq. (8), linear relationships between  $R_x/R_0$  and  $[C]^{1/2}$  could be obtained (Fig. 4). In these determinations of  $R_x/R_0$ , eq. (1) was used. Using these linear relationships,  $k_{t0}/k_{tx}$  and  $k_{ti0.2}/k_{tix}$  were calculated from Eqs. (9) and (10), respectively (Table II).

### Termination Rate Constants

**Chain Termination Rate Constant.** On application of eq. (11) to the values of  $k_{t0}/k_{tz}$  in Tables I and II, linear relationships between  $k_{t0}/k_{tz}$  and  $1/x$  for the polymerizations of MMA and EA could be obtained (Figs. 5 and 6). Using these linear relationships the eqs. (24) and (25), were obtained for the polymerization of MMA at 50°C and for the polymerization of EA at 35°C, respectively.

$$g(T,x) = 0.084 + 0.031(1 - x) \quad (24)$$

$$g(T,x) = 0.10 + 0.13(1 - x) \quad (25)$$

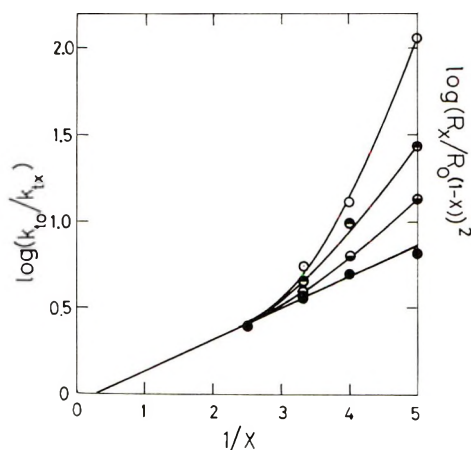


Fig. 5. Relationship between  $1/\log(k_{t0}/k_{tz})$  and  $1/x$ , and relationships between  $[R_x/R_0(1-x)]^2$  and  $1/x$  for the polymerization of MMA: (●) relationship between  $1/\log(k_{t0}/k_{tz})$  and  $1/x$  for  $[C] = 0$ ; (◐)  $[C] = 0.0103$  mole/l.; (◑)  $[C] = 0.0413$  mole/l.; (○)  $[C] = 0.0826$  mole/l.

In the past, in spite of the breakdown of the square-root dependence of the polymerization rate, various rate constants have been calculated on the basis of a second-order termination mechanism between polymeric radicals.<sup>9</sup> However, a linear relationship between  $\log[R_x/R_0(1-x)]^2$  and  $1/x$  at high initiation rate could not be obtained (Figs. 5 and 6). Thus, because of the effect of primary radical termination on the polymerization rate, the rate constants determined on the basis of a second-order termination mechanism between polymeric radicals at high initiation rate are approximate. Generally, the results at high initiation rate are a poorer approximation than the results at low initiation rate.

**Primary Radical Termination Rate Constant.** On the application of eq. (22) or (23) to the values  $k_{t10}/k_{t1z}$  and  $k_{t10.2}/k_{t1z}$  calculated by using  $k_{t10}/k_{t1z}$  in Table I, linear relationships could not be obtained. Thus, it appears that the condition  $u_i \gg u_s$ ,  $u_i = u_s$ , or  $u_i \ll u_s$  was not satisfied for the polymerization of MMA initiated by BPO.

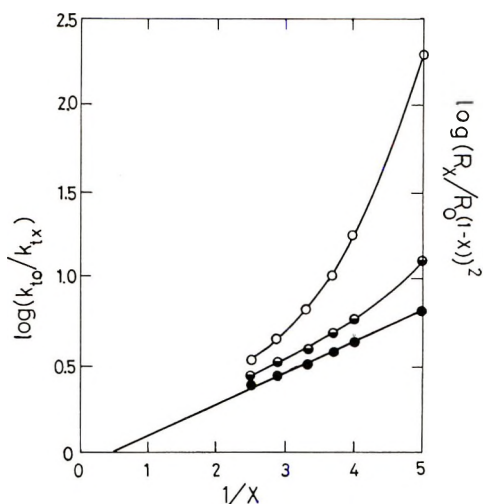


Fig. 6. Relationship between  $1/\log(k_{t0}/k_{tx})$  and  $1/x$  and relationships between  $[R_z/R_o (1-x)]^2$  and  $1/x$  for the polymerization of EA: (●) relationship between  $1/\log(k_{t0}/k_{tx})$  and  $1/x$  for  $[C] = 0$ ; (◐)  $[C] = 0.8 \times 10^{-2}$  mole/l.; (○)  $[C] = 3.0 \times 10^{-2}$  mole/l.

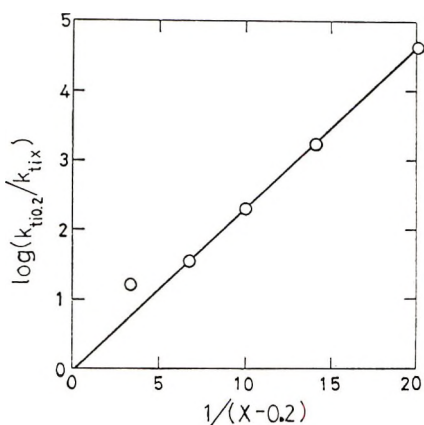


Fig. 7. Relationship between  $1/\log(k_{t0.2}/k_{ttx})$  and  $1/(x-0.2)$  for the polymerization of EA.

On the application of eq. (22) or (23) to the values  $k_{t0.2}/k_{ttx}$  in Table II in the polymerization of EA initiated by using AIBN, a linear relationship between  $1/\log(k_{t0.2}/k_{ttx})$  and  $1/(x-0.2)$  could be obtained (Fig. 7). By using this linear relationship, the eq. (26) was derived.

$$g_i(T,x) = 0.15 + 0.10(1-x) \quad (26)$$

This equation is approximately equivalent to eq. (25). However,  $A_1^*$  and  $A_t^*$ , where  $A_t^*$  is a constant defined by  $k_{ty} = A_t^* \exp\{-1/q(T,x)\}$ , were unknown. Furthermore, because  $g_i(T,0.2)$  has a very small value com-

pared to 1 (Fig. 7), it was difficult graphically to determine the correct value, and eq. (26) was approximate. Thus, to discuss termination rate constants in detail was impossible.

As stated in the theory, eqs. (9) and (10) are correct in the conversion range (0 to 0.4 in this paper) for which  $k_p$ ,  $k_t$ , and  $2fk_d[C]$  are constants and are independent of conversion. The autoacceleration in this conversion range should be interpreted by the same method in this paper. Without this conversion range, the treatment for the kinetics in this paper must be modified for the analysis to experimental results. Furthermore, because eq. (3) is an approximation,<sup>5</sup> eq. (3) should be not applied to polymerizations for which primary radical termination exceeds chain termination. The complete analysis of polymerization with primary radical termination will be reported in a future publication.<sup>10</sup>

The author thanks Dr. T. Matsuda for the treatment of polymerization.

### References

1. G. M. Brunett and G. L. Duncan, *Makromol. Chem.*, **51**, 154, 171, 177 (1961).
2. M. Kawasaki, M. Yano, and T. Imoto, paper presented at 22th Meeting, Chemical Society of Japan, 1969.
3. K. Ito, *J. Polym. Sci., A-1*, **7**, 2995 (1969).
4. K. Ito, *J. Polym. Sci., A-1*, in press.
5. K. Ito and T. Matsuda, *Bull. Chem. Soc. Japan*, **42**, 1758 (1969).
6. K. Ito, *J. Polym. Sci., A-1*, **7**, 2247 (1969).
7. G. V. Schulz and G. Harborth, *Makromol. Chem.*, **1**, 106 (1947).
8. D. Mangraraĳ and S. K. Patra, *Makromol. Chem.*, **104**, 135 (1967).
9. P. Heyden and H. Melville, *J. Polym. Sci.*, **43**, 201 (1960).
10. K. Ito, *J. Applied Polym. Sci.*, in press.

Received August 1, 1969

## Polymerization of Aromatic Aldehydes. IV. Cationic Copolymerization of Phthalaldehyde Isomers and Styrene

CHUJI ASO, SANAE TAGAMI, and TOYOKI KUNITAKE,  
*Department of Organic Synthesis, Faculty of Engineering, Kyushu  
University, Fukuoka, 812, Japan*

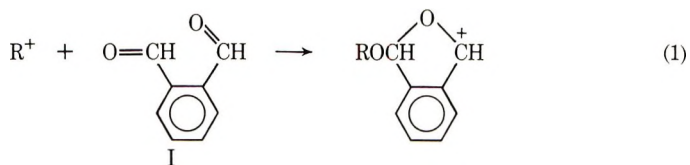
### Synopsis

Copolymerizations of three phthalaldehyde isomers ( $M_2$ ) with styrene ( $M_1$ ) were carried out in methylene chloride or in toluene with  $\text{BF}_3\text{OEt}_2$  catalyst. The monomer reactivity ratios were  $r_1 = 0.77$ ,  $r_2 = 0$  for the *meta* isomer and  $r_1 = 0.60$ ,  $r_2 = 0$  for the *para* isomer. The second aldehyde group of both isomers did not participate in polymerization and acted simply as the electron-withdrawing group, thus reducing the cationic reactivity of these monomers. Copolymerization behaviors of the *ortho* isomer (*o*-PhA) were quite different between  $0^\circ\text{C}$  and  $-78^\circ\text{C}$ . At  $-78^\circ\text{C}$ , *o*-PhA preferentially polymerized to yield "living" cyclopolymers, until an equilibrium concentration of *o*-PhA monomer was reached. Then, styrene propagated from the living terminal rather slowly. The block structure of the copolymer was confirmed by the chemical and spectroscopic means. In the copolymerization at  $0^\circ\text{C}$ , the *o*-PhA unit in copolymer consisted both of cyclized and uncyclized units. This copolymer seemed to contain short *o*-PhA sequences. The variation of the *o*-PhA-St copolymer structure with the polymerization temperature was explained on the basis of whether the polymerization was carried out above or below the ceiling temperature ( $-43^\circ\text{C}$ ) of the homopolymerization of *o*-PhA.

### INTRODUCTION

It was recently reported that the carbonyl group of benzaldehyde readily underwent addition copolymerization with styrene<sup>1-3</sup> and with conjugated dienes by cationic catalysts<sup>1</sup> although its homopolymerization was not possible. The content of the benzaldehyde unit in copolymer reached almost 50 mole-% at high benzaldehyde feeds in the monomer mixture.<sup>1</sup> Then phthalaldehyde isomers which possess two aldehyde groups conceivably give rise to interesting polymer structures such as branching, cross-linking, and intramolecular cyclization by copolymerization with vinyl compounds. Therefore, cationic copolymerizations between styrene and the three isomers of phthalaldehyde were studied in the present investigation.

It was expected in the copolymerization of *o*-phthalaldehyde that the adjacent aldehyde groups would selectively form a five-membered ring by intramolecular cyclization [eq. (1)] as was the case for some aliphatic dialdehydes.<sup>4-6</sup>



Thus, differences in polymerization behavior which would probably arise between the *ortho* isomer and the *meta* and *para* isomers were of particular interest. The results obtained in the present investigation that copolymers containing more than 50 mole-% of the *o*-phthalaldehyde unit were formed in the copolymerization with styrene led us to the finding that *o*-phthalaldehyde by itself could yield the cyclopolymer. The latter results were reported in detail in previous publications.<sup>7-9</sup>

## EXPERIMENTAL

### Materials

Phthalaldehyde (*o*-PhA), mp 54.5–55.0°C, was prepared according to the method of Bill and Tarbell.<sup>10</sup> Terephthalaldehyde (*p*-PhA), mp 112–113°C, was prepared by the method of Zimmermann et al.<sup>11</sup> Commercial isophthalaldehyde (*m*-PhA) was purified by recrystallization from ligroin mp 87–88°C. Styrene (St) was washed with dilute alkali, dried over CaCl<sub>2</sub>, and distilled over CaH<sub>2</sub> under reduced pressure. Methylene chloride was washed with dilute alkali, dried over CaCl<sub>2</sub>, refluxed over P<sub>2</sub>O<sub>5</sub>, and distilled over CaH<sub>2</sub>. Toluene was washed with concentrated sulfuric acid and with dilute alkali, dried over CaCl<sub>2</sub>, refluxed over metallic sodium, and distilled. BF<sub>3</sub>OEt<sub>2</sub> was distilled under nitrogen.

### Polymerization

Given amounts of aldehydes, styrene, and solvents were placed in Schlenk-type ampoules under nitrogen and cooled to the given polymerization temperature. Catalyst (BF<sub>3</sub>OEt<sub>2</sub>) solutions were then added. After given periods, polymerization was terminated by adding pyridine. The polymer was recovered by pouring the reaction mixture into methanol and purified by reprecipitation from benzene and methanol.

### Reaction of Copolymers with 2,4-Dinitrophenylhydrazine

Copolymers were dissolved in a mixture of benzene and methanol and an acidic (H<sub>2</sub>SO<sub>4</sub>) ethanol solution of 2,4-dinitrophenylhydrazine was added. The mixture was kept at 40°C. In the case of copolymers from *m*-PhA and *p*-PhA, the precipitated polymeric products were separated and reprecipitated from THF and methanol.

In the case of the copolymer of styrene and *o*-PhA, the polymeric product presumably remained in solution and the bishydrazone of *o*-PhA precipitated. The bishydrazone was recrystallized from dimethylformamide.

### Acid Hydrolysis of *o*-PhA–St Copolymer

The copolymer (0.5 g) (run 2 in Table IV) was dissolved in dioxane and concentrated hydrochloric acid was added. Upon standing overnight, the

reaction mixture was poured into methanol and the precipitated product (0.098 g) recovered. The solution was treated with an acidic ( $\text{H}_2\text{SO}_4$ ) alcohol solution of 2,4-dinitrophenylhydrazine, and 0.745 g of the bis-hydrazone of *o*-PhA was obtained.

### Determination of the Residual Carbonyl Group in the Copolymer of *o*-Phthalaldehyde and Styrene

A calibration curve was prepared between the concentration of the aldehyde group and the intensity of its infrared peak ( $1703\text{ cm}^{-1}$ ), *o*-PhA ( $\text{CCl}_4$  solution) being used as a reference. The amount of the carbonyl group in the copolymer was determined by using the calibration curve from the intensity of the carbonyl peak of  $\text{CCl}_4$  solutions of the copolymer.

## RESULTS

### Cationic Copolymerization of Terephthalaldehyde and Isophthalaldehyde with Styrene

Methylene chloride was used as polymerization solvent. Terephthalaldehyde (*p*-PhA) and isophthalaldehyde (*m*-PhA) did not homopolymerize with  $\text{BF}_3\text{OEt}_2$  catalyst at  $0^\circ\text{C}$  and  $-78^\circ\text{C}$ , consistent with the result of benzaldehyde. On the other hand, the cationic copolymerization of these monomers with styrene proceeded easily, as shown in Table I. The copolymerizations proceeded homogeneously at any monomer feed, and the copolymers obtained were white powders which were soluble in benzene, chloroform, and carbon tetrachloride.

Infrared spectra of these copolymers (*p*-PhA-St and *m*-PhA-St) are shown in Figure 1. The absorption due to the ether linkage is observed at  $1000\text{--}1100\text{ cm}^{-1}$ , similar to that in the benzaldehyde-styrene copolymer. At the same time these copolymers possess strong carbonyl peaks in the  $1700\text{ cm}^{-1}$  region, which are assigned to the pendent aldehyde groups. They cannot be attributed to contaminating monomers because the copolymers were freed of the monomers by reprecipitation from benzene and methanol.

The amount of the aldehyde unit in copolymer obtained from 1:1 monomer mixtures was about 38 mole-% for both *m*-PhA and *p*-PhA. The content of the aldehyde unit did not exceed 50 mole-%, even at 80 mole-% feed of *p*-PhA (Table I). This implies that the monomer reactivity ratios of these phthalaldehydes were close to zero.

When the copolymers were treated with 2,4-dinitrophenylhydrazine in acidic media, the recovered products were orange powders and their softening points were higher by about  $60^\circ\text{C}$  than those of the starting copolymers. The main-chain ether linkage of the copolymer was considered to remain intact, since a benzaldehyde-styrene copolymer was stable under the same condition. Infrared spectra of the product polymers showed that on the hydrazine treatment, the absorption of the main-chain ether linkage ( $1000\text{--}1100\text{ cm}^{-1}$ ) did not change but the carbonyl peak at  $1700\text{ cm}^{-1}$  disappeared completely and new peaks appeared at  $1620$  ( $\nu_{\text{C=N}}$ ),  $3300$  ( $\nu_{\text{NH}}$ ), and  $1330\text{ cm}^{-1}$  ( $\nu_{\text{NO}_2}$ ). These infrared data indicate that the pendent alde-

TABLE I  
Copolymerization of Iso- and Terephthalaldehyde (M<sub>2</sub>) with Styrene (M<sub>1</sub>)<sup>a</sup>

No.	M <sub>2</sub> in monomers		Temp, °C	Time, hr	Conversion, %	Softening point, °C	$\bar{M}_n$	m <sub>2</sub> in copolymer		
	Type	Mole-%						I <sup>b</sup>	II <sup>c</sup>	III <sup>d</sup>
1	<i>m</i> -PhA	49.1	0	5.2	18.5	110-128	6490	37.5	32.2	26.5
2	<i>p</i> -PhA	25.0	0	13	20.7	—	1650	29.4	29.8	25.0
3	<i>p</i> -PhA	29.1	0	22.7	53.8	—	—	32.7	—	—
4	<i>p</i> -PhA	50.0	0	5.2	17.6	122-140	3510	38.9	31.8	26.7
5	<i>p</i> -PhA	80.0	0	24	7.5	—	—	50.5	—	—
6	<i>p</i> -PhA	49.9	-78	110	41.5	117-125	2040	38.5	26.8	21.1

<sup>a</sup> Catalyst, BF<sub>3</sub>OEt<sub>2</sub>; 2.5 mole-%; solvent, methylene chloride; monomer concn, 0.10 g/cc.

<sup>b</sup> Values calculated from C content of copolymers.

<sup>c,d</sup> Values calculated from C and N content of 2,4-dinitrophenylhydrazones of copolymers, respectively.



hyde group reacted quantitatively. In Table I are compared the copolymer compositions calculated from the elemental analyses of the starting copolymers and from those of the hydrazone polymers. Their agreement was not necessarily satisfactory.

Thus it can be concluded that one of the aldehyde groups in *m*-PhA and *p*-PhA remained unreacted under the polymerization conditions used. The reduced reactivity of the pendent aldehyde group is further supported by the fact that no crosslinked polymer was formed during copolymerization.

### Copolymerization of *o*-Phthalaldehyde and Styrene

Phthalaldehyde (*o*-PhA) copolymerized quite readily with styrene, as summarized in Tables II and III. The polymerization system was brown at 0°C and changed from yellowish to yellow brown at -78°C. The polymerization proceeded homogeneously in methylene chloride, and the polymer formed at 0°C was a yellowish white or white powder, and that formed at -78°C was a white powder.

**Infrared Spectra.** In Figure 1 are given infrared spectra of the copolymers obtained at 0°C (copolymer c) and at -78°C (copolymer d) from the 1:1 monomer mixture. The characteristic peaks for the styrene unit appears at 1603, 1490, 1450, and 700 cm<sup>-1</sup> in both spectra. The broad peaks at 950-1100 cm<sup>-1</sup> are ascribable to the ether linkage and are generally similar to that of poly(*o*-PhA) or its model compound, 1,3-dimethoxyphthalan.<sup>8</sup>

The copolymers obtained at 0°C were shown to contain some aldehyde groups from its infrared spectra. The amount of aldehyde, as determined by using *o*-PhA monomer as reference was 10-25 mole-% of the total *o*-PhA

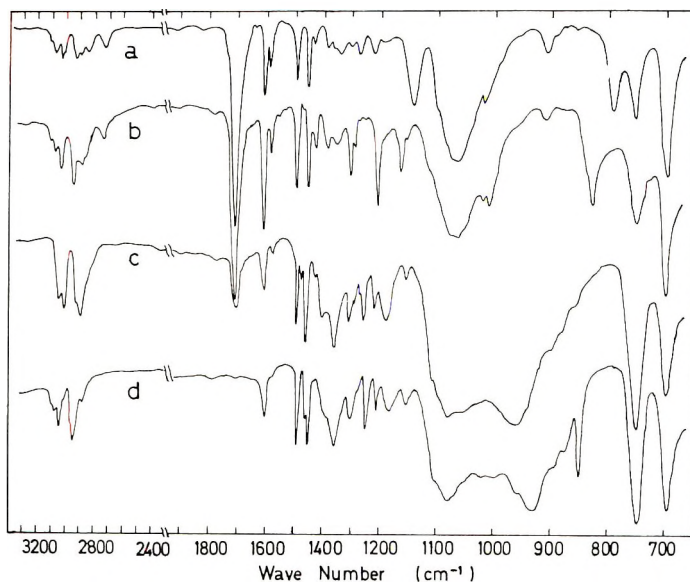


Fig. 1. Infrared spectra of PhA-St copolymers (KBr disk): (a) *m*-PhA-St; (b) *p*-PhA-St; (c) *o*-PhA-St (polymerized at 0°C); (d) *o*-PhA-St (polymerized at -78°C).

TABLE II  
 Copolymerization of *o*-Phthalaldehyde ( $M_2$ ) with Styrene ( $M_1$ ) at 0°C<sup>a</sup>

No.	$M_2$ in monomers, mole-%	Monomer concn, g/cc	Time, hr	Conversion, %	Polymer		
					$m_2$ units in copolymer, mole-%	Softening point, °C	$\bar{M}_n$
1	29.1	0.20	2.0	25.6	36.0	—	22.9
2	47.7	0.20	2.0	23.0; ins 13.1 <sup>e</sup> sol 9.9 <sup>d</sup>	50.1	137-143	21.1
3	53.7	0.40	2.0	53.7	49.9	122-128	22.9
4	54.1	0.27	0.1	46.6	51.2	—	25
5	76.6	0.18	240	11.6	49.5	130-141	10
					66.8	145-152	1040

<sup>a</sup> Solvent, toluene; catalyst,  $\text{BF}_3\text{OEt}_2$ , 5.0 mole-%.

<sup>b</sup> Residual carbonyl contents to *o*-PhA units.

<sup>c</sup> Insoluble in cyclohexane.

<sup>d</sup> Soluble in cyclohexane.

TABLE III  
 Copolymerization of *o*-Phthalaldehyde ( $M_2$ ) with Styrene ( $M_1$ ) at  $-78^\circ\text{C}^a$ 

No.	$M_2$ in monomers, mole-%	Monomer, g/cc	Catalyst, mole-%	Time, hr	Conversion, % <sup>b</sup>	$m_2$ in copolymer, mole-%	Polymer	
							Softening point, $^\circ\text{C}$	$\bar{M}_n$
1	10.4	0.16	2.3	0.3	21.1; ins 16.2 <sup>e</sup> sol 4.7 <sup>d</sup>	36.0	128-132	—
2	30.5	0.16	2.7	0.3	27.3 <sup>e</sup> (75.0)	13.1	115-120	—
3	20.7	0.16	2.7	22.7	79.6 <sup>e</sup> (81.1)	100	112-116	—
4	51.7	0.21	2.7	11.3	88.9 <sup>e</sup> (97.9)	29.5	135-143	4200
5	53.2	0.18	5.0	14.0	77.2 <sup>e</sup> (97.5)	57.8	145-153	7100
6	53.2	0.18	5.0	2.0	57.1 <sup>e</sup> (88.1)	67.4	122-124	4000
7	49.3	0.20	3.8	6.0	70.7 <sup>e</sup> (94.1)	85.4	—	2600
8	81.0	0.15	2.7	0.1	76.5 <sup>e</sup> (90.4)	69.0	—	8400
						100	—	—

<sup>a</sup> Catalyst,  $\text{BF}_3\text{OEt}_2$ ; solvent, methylene chloride.

<sup>b</sup> The values in parentheses mean conversion of phthalaldehyde per initial amount of phthalaldehyde to copolymers.

<sup>c</sup> Insoluble in cyclohexane, and soluble in carbon tetrachloride.

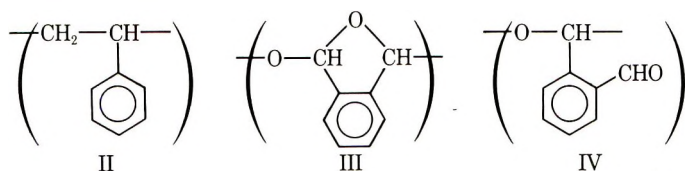
<sup>d</sup> Soluble in cyclohexane and carbon tetrachloride.

<sup>e</sup> Insoluble in cyclohexane and carbon tetrachloride.

unit in copolymer (Table II). On the other hand, the copolymers obtained at  $-78^{\circ}\text{C}$  contained less than a few per cent of the aldehyde group (not detectable in most cases).

These infrared data indicate that there are three structural units (II, III, IV) contained in the copolymer and that the *o*-PhA unit was almost completely cyclized at  $-78^{\circ}\text{C}$  while some uncyclized units (IV) were present in the copolymer obtained at  $0^{\circ}\text{C}$ .

Nuclear substitution on *o*-PhA monomers appears improbable as a cause for the presence of the aldehyde group in the copolymer on the basis of the infrared spectrum data.



**Composition of *o*-PhA-St Copolymer.** The copolymer composition changed considerably with polymerization temperature, as is apparent from Tables II and III. The *o*-PhA unit was incorporated into polymer more readily at  $-78^{\circ}\text{C}$  than at  $0^{\circ}\text{C}$ . The content of the *o*-PhA unit in copolymer could be much higher than 50 mole-%, indicating that sequences of the *o*-PhA unit, consequently the intermolecular acetal linkage, were present. This result is in marked contrast with the copolymer composition of styrene and the other isomers of phthalaldehyde, where the content of the aldehyde unit never exceeded 50 mole-%.

The copolymer composition was affected differently by the conversion at  $0^{\circ}\text{C}$  and at  $-78^{\circ}\text{C}$ . Thus, the compositions of the copolymer obtained at  $0^{\circ}\text{C}$  were close, irrespective of conversions (Table II, runs 2, 3 and 4). On the other hand, the composition changed remarkably with conversion when the copolymerization was carried out at  $-78^{\circ}\text{C}$ . Inspection of Table III indicates that the content of the *o*-PhA unit in the copolymer was quite high at low conversions but that it decreased with increasing conversions (compare runs 2 and 3, and runs 4, 5, and 6).

The variations of the copolymer composition and of the conversion with the polymerization period are shown in Figures 2 and 3 for the copolymers obtained at  $-78^{\circ}\text{C}$  from the 1:1 monomer mixture. The polymerization process was divided into two stages. In the first stage, rapid polymerization occurred, and the polymer formed was composed almost exclusively of the *o*-PhA unit. The subsequent stage was characterized by the gradual increase in the polymer yield and by the decrease in the *o*-PhA unit content of the copolymer. The molecular weight of the polymer similarly reached a certain value in the first stage and then gradually increased with time. The amount of *o*-PhA monomer incorporated into copolymer was constant during these periods (Fig. 3), being 92–94% of the initial amount of *o*-PhA. The concentration of the remaining *o*-PhA monomer (0.06 mole/l.) was close to the equilibrium concentration (0.09 mole/l. in  $\text{CH}_2\text{Cl}_2$  at  $-78^{\circ}\text{C}$ )<sup>8</sup> in the homopolymerization.

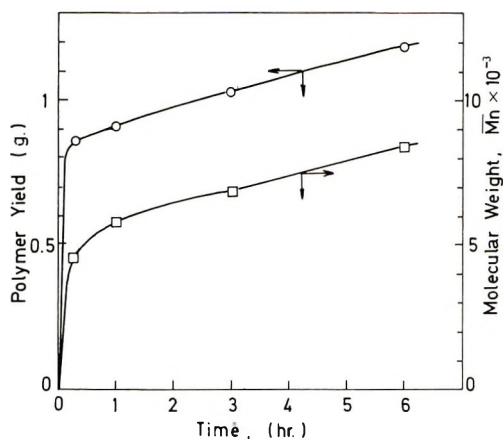


Fig. 2. Dependence of conversion and molecular weight on polymerization period. St, 0.742 g; *o*-PhA, 0.932 g;  $[M_2] = 49.3$  mole-%; monomer concn, 1.34 mole/l.; solvent,  $\text{CH}_2\text{Cl}_2$ ; catalyst,  $\text{BF}_3\text{OEt}_2$ , 3.8 mole-%; polymerization temperature,  $-78^\circ\text{C}$ .

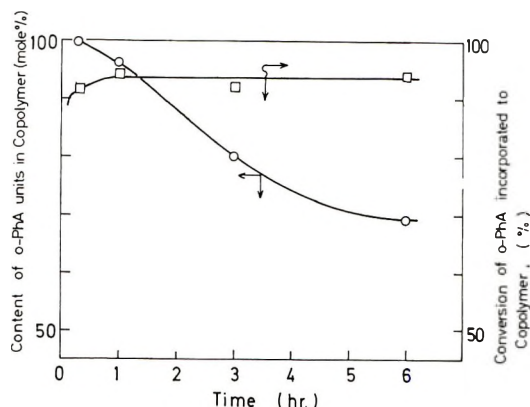


Fig. 3. Dependence of copolymer composition and *o*-PhA consumed on polymerization period. Polymerization conditions as in Fig. 2.

**Fractionation of the Copolymer.** The preceding polymerization data strongly suggest that the *o*-PhA-St copolymers obtained at  $-78^\circ\text{C}$  are not random copolymers. Therefore, some of the *o*-PhA-St copolymers were fractionated in order to see if they are true copolymers. Poly(*o*-PhA) is insoluble in  $\text{CCl}_4$  and in cyclohexane, which are good solvents for polystyrene.

The copolymers formed in the first stage of the polymerization (Table III, runs 2 and 8) were insoluble in  $\text{CCl}_4$  and cyclohexane, as can be inferred from their very high *o*-PhA content. A copolymer containing 58 mole-% of the *o*-PhA unit (Table III, run 4) was completely soluble in  $\text{CCl}_4$  and did not contain any fraction soluble in cyclohexane. Therefore, it was concluded that this copolymer was not a homopolymer mixture.

On the other hand, the copolymer obtained from a monomer mixture containing 10 mole-% of *o*-PhA (Table III, run 1) was fractionated in cy-

TABLE IV  
 Acid Hydrolysis of *o*-PhA-St Copolymers

No.	Copolymer			Conversion, %	Melting point, °C	2,4-DNP <sup>b</sup>		
	Table- run	<i>o</i> -PhA units, mole-%	Reaction conditions <sup>a</sup>			C, %	H, %	N, %
1	III-5	67.4	A	68.4	293-294	47.88	2.72	22.09
2	III-7	69.0	B	54.5 <sup>c</sup>	—	—	—	—
3	II-4	49.5	A	29.0	293.5-294	48.02	4.01	21.59

<sup>a</sup> 40°C; A, benzene-ethanol (4:1)-H<sub>2</sub>SO<sub>4</sub>; B, dioxane-HCl.

<sup>b</sup> Bis-2,4-dinitrophenylhydrazones of *o*-PhA. Calcd for C<sub>20</sub>H<sub>14</sub>N<sub>4</sub>O<sub>8</sub>: C, 48.59%; H, 2.85%; N, 22.66%.

<sup>c</sup> Recovered polystyrene: 76.3%;  $\bar{M}_n = 1700$ . Anal. Calcd for (C<sub>8</sub>H<sub>8</sub>)<sub>n</sub>: C, 92.26%; H, 7.74%. Found: C, 88.83%; H, 7.52%.

clohexane into soluble and insoluble fractions, and these fractions were found to contain 13 mole-% and 36 mole-%, respectively, of the *o*-PhA unit. The cyclohexane-soluble fraction was also a copolymer containing the *o*-PhA unit, and this solubility probably arose from the large content of the styrene unit.

A *o*-PhA-St copolymer obtained at 0°C (Table II, run 2) could be separated into cyclohexane-soluble and -insoluble fractions. However, their structural characteristics such as infrared spectra, the pendent carbonyl content, and the copolymer composition were the same. This fractionation appears to be done on the basis of the difference in their molecular weights.

**Acid Hydrolysis of *o*-PhA-St Copolymers.** When *o*-PhA-St copolymers were treated with 2,4-dinitrophenylhydrazine in acidic media, the bis-hydrazone of the *o*-PhA monomer was recovered as shown in Table IV. The extent of recovery was 68% of the PhA unit in copolymer (run 1), as against the quantitative recovery in the case of the *o*-PhA homopolymer.<sup>8</sup>

When a copolymer (content of *o*-PhA unit, 69.0 mole-%;  $M_n = 8400$ ) obtained at -78°C was hydrolyzed in a hydrochloric acid-dioxane solution (run 2), a methanol-insoluble polymer was recovered as yellowish powders. The latter polymer ( $M_n = 1700$ ) was soluble in cyclohexane, and its infrared spectrum resembled that of polystyrene. The elemental analysis indicated that it consisted of 90 mole-% of the St unit. *o*-PhA liberated by hydrolysis was recovered by treating the methanol solution with the hydrazine. The recovery of the bishydrazone was 55% of the *o*-PhA unit in copolymer. These results suggest that the *o*-PhA-St copolymers obtained at -78°C possessed long *o*-PhA blocks and shorter St blocks. The recovery of the bishydrazone was poorer for the copolymer obtained at 0°C, implying shorter *o*-PhA sequences.

## DISCUSSION

It now became clear that the polymerization behaviors of the *meta* and *para* isomers of phthalaldehyde were very much alike, but the *ortho* isomer reacted quite differently in the cationic copolymerization with styrene. The latter isomer gave rise to the phthalan ring unit in the copolymer due to cyclopolymerization. These copolymerization results are discussed below in connection with the polymerization results of some related systems.

### Copolymerization of Terephthalaldehyde and Isophthalaldehyde

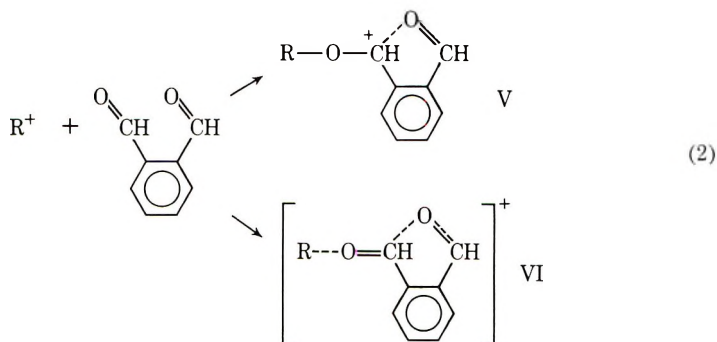
It is interesting that only one of the two aldehyde groups in these monomers was involved in the copolymerization with styrene, the other remaining unreacted. At the same time, the hydrazine treatment of these copolymers indicated that the acetal linkage derivable from the aldehyde sequence was not present. This results, together with the fact that the content of the aldehyde monomers did not exceed 50 mole-%, implies that the monomer reactivity ratios of these dialdehydes were close to zero, as was the case for benzaldehyde in the cationic copolymerization with sty-

rene. Assuming that the reactivity ratios of these aldehydes ( $M_2$ ) were zero,  $r_1$  (St) was calculated to be 0.77 and 0.60 for *m*-PhA and *p*-PhA, respectively. Since these  $r_1$  values are greater than that ( $r_1 = 0.27$ ) in the copolymerization of St ( $M_1$ ) and benzaldehyde ( $M_2$ ),<sup>1</sup> the second aldehyde group seems simply to exert an electron-withdrawing effect on the reacting aldehyde group, thus decreasing the reactivity of these monomers toward the styryl cation.

### Copolymerization of *o*-Phthalaldehyde and Influence of Polymerization Temperature

As described in the previous section, the copolymerization characteristics of *o*-PhA and St are quite different at 0°C and -78°C. The difference can be attributed to whether the polymerization temperature is above or below the ceiling temperature (-43°C) of the homopolymerization of *o*-PhA.

**Copolymerization at -78°C.** We already reported that the propagation in the cyclopolymerization of *o*-PhA was not a simple stepwise process but proceeded through an intramolecularly stabilized carbonium ion intermediate (V) or in a concerted manner (VI).



The copolymer obtained at -78°C contained solely the cyclized *o*-PhA unit. Therefore, the addition step of *o*-PhA monomer in this copolymerization presumably resembles mechanistically homopolymerization.

The cationic polymerization of *o*-PhA was shown previously to be an equilibrium polymerization and the propagating cation to be "living" under the suitable condition. In addition, the rate constant of propagation was quite large (0.18 l./mole-sec with  $\text{BF}_3\text{OEt}_2$  at -78°C in  $\text{CH}_2\text{Cl}_2$ ).<sup>8</sup>

The copolymerization data at -78°C can be interpreted in consistence with these homopolymerization results. *o*-PhA polymerizes preferentially in the presence of styrene, and the homopolymer of *o*-PhA is formed in the initial stage of the copolymerization. This stage continues until the amount of *o*-PhA monomer reaches the equilibrium concentration, and the slower addition of styrene to the living end of poly(*o*-PhA) ensues. Only a small amount of *o*-PhA is incorporated into polymer in the second stage, as clearly shown by the constancy of the concentration of the residual *o*-PhA monomer (0.06 mole/l.) over a wide polymerization period (See Fig. 3).







## Metal Coordination Polymers. III. Molecular Weights of Beryllium Phosphinate Polymers in Chloroform

N. R. FETTER\* and C. M. GRIEVE, *Chemistry Division, Naval Weapons  
Center, Corona, California 91720*

### Synopsis

Vapor-phase osmometric molecular weight measurements on beryllium di-*n*-butylphosphinate are in general agreement with the results obtained in chloroform by Ripamonti and co-workers. The degree of polymer association in anhydrous chloroform is approximately twice that obtained in reagent-grade chloroform, and the values obtained in both types of chloroform are higher than those obtained by Ripamonti. Membrane osmometric molecular weight measurements on beryllium 4-biphenyl(phenyl)phosphinate in chloroform indicate a reversible degradation exists between a number-average molecular weight of 170 000 and 30 000, with the value dependent upon the polymer concentration. Treatment of chloroform solutions of this polymer with ammonia prevents reassembly of the polymer from 30 000 to higher values. To explain this and other solution properties of this polymer, a structure is proposed which involves endgroup hydrogen bonding of phosphinate-bonded aggregates containing approximately 50 monomer units ( $\bar{M}_n = 30\,000$ ). Under certain conditions, the hydrogen-bonded aggregates may contain up to 300 monomer units, but in polar solvents such as water or chloroform they are rapidly degraded.

### INTRODUCTION

Our studies<sup>1</sup> of the molecular weights of beryllium phosphinate polymers in toluene have demonstrated the effect of traces of water on number-average molecular weights. We wished to see whether similar effects could be observed in a polar solvent, and chloroform was chosen because several beryllium phosphinates are soluble in it.

The molecular weight studies of Ripamonti and co-workers<sup>2</sup> on beryllium di-*n*-butylphosphinate in chloroform by vapor-phase osmometry showed that number-average molecular weight increased with increasing polymer concentration. This result was interpreted as a dynamic polymer chain breaking and reforming process which yielded oligomers whose degree of polymerization was dependent upon concentration.

It is the purpose of this paper to offer an explanation of this process with some supporting experimental evidence.

\* Present address: Institute of Geophysics and Geochemistry, Dept. of Geologic Sciences, University of California, Riverside, Ca 92502.

## EXPERIMENTAL

### Apparatus

Molecular weights were measured at 37°C on a Hewlett-Packard Model 301 vapor-phase osmometer or at 25°C on a Hewlett-Packard Model 502 membrane osmometer with the use of S & S 0-8 nonaqueous cellulose membranes. Sample solutions were prepared in 10-ml volumetric flasks at concentrations ranging between 2.0 and 10.0 mg/ml for the membrane osmometer, and between 1.0 and 50.0 mg/ml for the vapor-phase osmometer.

For vapor-phase osmometry, the samples were withdrawn from storage flasks into the syringes in the air, but readings were taken as quickly as possible when dry chloroform was used. Four readings were made and averaged and, in most cases, solution concentrations were made large enough to obtain  $\Delta R$  values of 2 ohms or more.

For membrane osmometry, sample solutions were transferred into the sample stack as quickly as possible. Determinations were made within 3 min, and dry chloroform was used as the reference solvent. Accuracy of both instruments was checked against ArRO polystyrene molecular weight standards, purchased from ArRO Laboratories, Inc., Joliet, Illinois.

### Solvents

Both reagent grade and chloroform which had water and ethanol inhibitor removed were used for this study. Dry chloroform was prepared by refluxing it over  $P_2O_5$  for 4 hr, followed by distillation into a 1-liter flask containing approximately 20 g of Linde molecular sieve, Type 4-A. The flask was stored in a drybox in which solutions were prepared and stored until used. Reagent grade chloroform and toluene were used without treatment, and sample solutions were prepared in air.

### Reagents

The preparation of beryllium phosphinates has been described elsewhere.<sup>1,3</sup>

The treatment of beryllium 4-biphenyl(phenyl)phosphinate with ammonia was accomplished by dissolving approximately 1 g of polymer in 50 ml of chloroform and bubbling ammonia gas through the solution for 1 hr. The chloroform was removed under vacuum. The treated polymer was dissolved in toluene and filtered to remove the insoluble ammonium phosphinate. For a 1-g sample of polymer, 60 mg (11 mole-%) of ammonium 4-biphenyl(phenyl)phosphinate was recovered. The toluene was removed by vacuum transfer, and remaining polymer was heated at 100°C under vacuum for 18 hr.

## RESULTS AND DISCUSSION

The  $\bar{M}_n$  values obtained from vapor-phase osmometry are shown in Table I and those from membrane osmometry are shown in Table II.

TABLE I  
Number-Average Molecular Weights  
of Beryllium di-*n*-butyl Phosphinate by Vapor-Phase Osmometry

Concn, mg/ml	$\bar{M}_n$	Degree of polymerization	Solvent
10.30	3120	8.6	Reagent grade chloroform
16.73	3890	10.7	"
20.84	4170	11.5	"
26.17	4760	13.1	"
40.40	5310	14.6	"
7.40	4300	11.8	Dry chloroform
11.70	4875	13.4	"
20.92	5505	15.2	"
30.26	5820	16.0	"
43.62	6510	18.0	"

Our molecular weight data and those reported by Ripamonti<sup>2</sup> for beryllium di-*n*-butylphosphinate are presented in Figure 1. Also shown are typical results for a sample of ArRO Laboratories polystyrene ( $\bar{M}_n = 3500 \pm 2\%$ ).

There is a general agreement between our results and those of Ripamonti, except that the degree of polymerization of our sample was slightly higher and is probably a reflection of different preparative methods and water content of the chloroform used to make solutions. Our results for beryllium di-*n*-butylphosphinate and for the ArRO polystyrene show an increase of  $\bar{M}_n$  with concentration in a manner analogous to Ripamonti's observations. Such behavior is a common occurrence when a colligative

TABLE II  
Number-Average Molecular Weights of Beryllium Phosphinates  
in Chloroform by Membrane Osmometry

Be phosphinate	$\bar{M}_n$	Degree of polymer- ization	Solvent	Time in solution before measurement, hr
Beryllium trifluoro methyl(phenyl) phosphinate	13 000	30	Reagent-grade chloroform	22
	11 500	27	"	120
	14 000	33	Dry chloroform	96
Beryllium 4-biphenyl- (phenyl)phosphinate	35 000	60	Reagent-grade chloroform	4
	30 000	50	"	30
	25 000	42	"	96
	30 000	50	Dry chloroform	240
	32 000	55	"	288

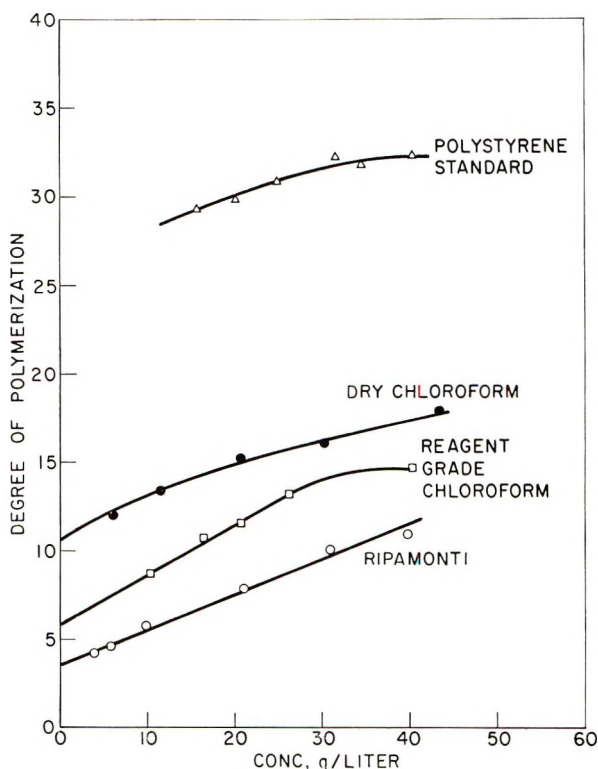


Fig. 1. Degree of polymerization vs. concentration: Beryllium di-*n*-butyl phosphinate in chloroform.

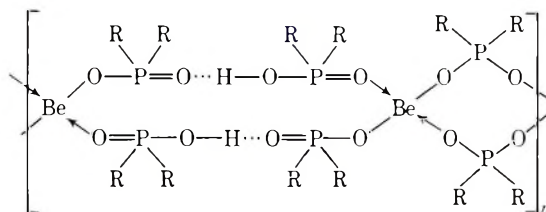
property is used to measure molecular weight<sup>4</sup> and is attributed to solution nonideality rather than dynamic polymer degradation and reformation.

The  $\bar{M}_n$  values for beryllium trifluoromethyl(phenyl)phosphinate and beryllium 4-biphenyl(phenyl)phosphinate, determined by membrane osmometry in chloroform, were found to be about the same as those obtained for the same polymers in toluene after the solutions had aged for 10 days.<sup>1</sup>

The results, obtained from samples dissolved in reagent grade chloroform for 2 hr, indicate rapid degradation occurs within, at most, a few hours, whereas in toluene, several days are required. This degradation is reversible in chloroform and irreversible in toluene. A sample of beryllium 4-biphenyl(phenyl)phosphinate ( $\bar{M}_n = 170\,000$ ) was refluxed in chloroform for 16 hr, followed by removal of the solvent under vacuum. The sample was left under pumping vacuum at 25°C for 24 hr, and  $\bar{M}_n$  was measured in toluene and found to be 121 000. A sample of the same batch of polymer, which was aged in toluene for 10 days, had an  $\bar{M}_n$  of 39 000 when dried under vacuum at 50°C for 24 hr.<sup>1</sup>

Our observation that beryllium 4-biphenyl(phenyl)phosphinate is reversibly degradable in chloroform and in the degraded state still has

number average molecular weights corresponding to approximately 50 monomer units leads us to postulate a polymer structure which is made up of units of approximately 50 monomer units ( $\bar{M}_n \approx 30\,000$ ) connected by a phosphinate backbone of the type suggested by Coates<sup>5</sup> or Ripamonti.<sup>6</sup> These units are connected by hydrogen-bonded phosphinic acid endgroups to give polymers with number-average molecular weights in non-polar solvents corresponding to 500 monomer units ( $\bar{M}_n \approx 300\,000$ ). Such a polymer may have the structure I.



I

An experiment, designed to effect permanent depolymerization by blocking the hydrogen bonding sites, was undertaken by reacting ammonia with chloroform solutions of beryllium 4-biphenyl(phenyl)phosphinate. This polymer, in chloroform, is dissociated to the 50 mer chains shown in Table II and the acid endgroups should react with a base.

The results of ammonia treatment of two different preparations of polymer are summarized in Table III.

TABLE III  
Ammonia Treatment of Beryllium 4-Biphenyl(phenyl)Phosphinate

Sample wt, g	Recovered ammonium phosphinate, mg	$\bar{M}_n$ in toluene	Nitrogen, %
1.010	60.0	41 000	0.06
1.005	not measured	38 000	0.06

The ammonium phosphinate was verified by infrared comparison with an authentic sample of ammonium 4-biphenyl(phenyl)phosphinate. The nitrogen analysis of the treated polymer, although expectedly low, agrees closely with that calculated for two ammonium ions per polymer chain of approximately 65 units ( $\bar{M}_n = 41\,000$ ; calcd N = 0.068%;  $\bar{M}_n = 38\,000$ ; calcd N = 0.074%).

Ammonia appears to be a base strong enough to neutralize the phosphinic acid endgroups without hydrolyzing the phosphinate backbone seriously. The 60 mg of ammonium phosphinate recovered from one of the treatments probably represents the extent of ammonolysis.

The possibility of hydrogen bonding through acetylacetonate end groups is also possible, and, although evidence for the presence of acetylacetonate was not observed, such bonding should not be discounted.

The authors wish to acknowledge useful discussions with Dr. Peter J. Slota of the Naval Weapons Center Corona Laboratories, Corona, California, and the financial assistance of the Naval Air Systems Command.

### References

1. P. J. Slota, C. M. Grieve, N. R. Fetter, and A. J. Bilbo, *J. Polym. Sci. A-1*, **7**, 2051 (1969).
2. F. Gemitì, V. Giancotti, and A. Ripamonti, *J. Chem. Soc. A*, **1968**, 763.
3. P. J. Slota, L. P. Freeman, and N. R. Fetter, *J. Polym. Sci. A-1*, **6**, 1975 (1968).
4. P. W. Allen, *Techniques of Polymer Characterization*, Butterworths, London, 1959, pp. 113-114.
5. G. E. Coates and D. S. Golightly, *J. Chem. Soc.*, **1962**, 2523.
6. F. Giordano, L. Randaccio, and A. Ripamonti, *Chem. Comm.*, **1967**, 19.

Received September 10, 1969



## Anionic Graft Polymerization and Homopolymerization of Phenyl Glycidyl Ether

GABRIEL EZRA and ALBERT ZILKHA, *Department of Organic Chemistry, The Hebrew University, Jerusalem, Israel*

### Synopsis

Phenyl glycidyl ether was found to react with potassium starch alkoxide in dimethyl sulfoxide (DMSO) to give graft polymers in almost quantitative yields, both the monomer and the starch being incorporated completely into the graft polymer. No transfer reactions to monomer or solvent leading to homopolymerization was found. For this reason this system was used as a model for the study of the rate of the graft polymerization of alkylene oxides on starch and other carbohydrates. Comparison of the rates of the graft polymerization of phenyl glycidyl ether on starch alkoxide with that of the homopolymerization by potassium naphthalene in DMSO under comparable conditions showed that the former reaction was much slower. Rates of the graft polymerizations on dextrin and sucrose under comparable conditions, were similar to those obtained with starch. On the other hand, the rates of polymerization on poly(ethylene oxide) alkoxides of different molecular weights were similar to those obtained in the corresponding homopolymerization by potassium naphthalene, showing that neither the molecular weight of the initiator nor the viscosity of the reaction medium were the governing factors. This suggested that the lower rates obtained by using the carbohydrate alkoxides as initiators were connected with the heterogeneity of these reaction systems, the polymeric alkoxide being insoluble in DMSO. The systematic study carried out on the homopolymerization by potassium naphthalene in DMSO showed that the effective initiator was dimethyl anion obtained by interaction of potassium naphthalene with DMSO. The reaction was bimolecular, being first order to monomer and to initiator. The molecular weights increased with increasing monomer concentration and decreasing catalyst concentration, in accordance with a "living" polymerization system.

### INTRODUCTION

Graft polymers of poly(ethylene oxide)<sup>1,2</sup> and poly(propylene oxide)<sup>3</sup> on starch were prepared by reaction of starch alkali metal alkoxide, obtained by reaction of the starch with alkali metal naphthalene, with the respective monomers in DMSO. The graft polymers had various melting points and were soluble in water and organic solvents.

In order to obtain graft polymers having even more different physical properties, the reaction of an aromatic alkylene oxide, namely styrene oxide, with starch alkoxide under the same conditions was investigated.<sup>4</sup> No graft polymerization occurred, however, and the reaction stopped at the initiation stage, due to steric hindrance of the phenyl group.

As a continuation of this work we now studied the reaction of phenyl glycidyl ether with starch alkoxide. This monomer has the aromatic nucleus further away from the epoxide ring as compared with styrene oxide and is reactive due to the phenoxy group, so that graft polymers may be obtained.

Graft polymers were in fact obtained in almost quantitative yield and there was no homopolymerization. This system was therefore found to be convenient to use as a model for studying the rate of the graft polymerization of alkylene oxides on starch and other carbohydrates. In order to obtain more information on the graft polymerization, the homopolymerization of phenyl glycidyl ether by potassium naphthalene in DMSO was also studied. The rate of the graft polymerization was found to differ considerably from that of the homopolymerization. To find out whether the polymeric nature of the initiator was the cause of this behavior, the rates of the graft polymerizations on the alkoxide derivative of lower carbohydrates, i.e., dextrin and sucrose on the one hand, and on the polyalkoxide of poly(ethylene oxide) of different molecular weights on the other were investigated.

## EXPERIMENTAL

### Materials

Soluble starch (Analar grade) and dextrin (BDH) containing 15 and 5% moisture, respectively, were used. Dry stock solutions of the carbohydrates including sucrose (BDH) were obtained by dissolving them in dimethyl sulfoxide (DMSO) (Fluka) and evaporating about 15% of the solvent *in vacuo* at 60°C. The potassium starch, dextrin, sucrose, or poly(ethylene oxide) alkoxide derivatives were conveniently prepared by reaction of the dry compounds in DMSO, with potassium naphthalene prepared in THF.<sup>5</sup> Phenyl glycidyl ether (Matheson, Coleman and Bell) was fractionally distilled *in vacuo*.

Tetrahydrofuran was dried as previously described.<sup>5</sup> DMSO was dried and distilled *in vacuo* over calcium hydride.

### Graft Polymerization of Phenyl Glycidyl Ether on Starch

The graft polymerizations were carried out in three-necked flasks fitted with a high speed stirrer, a thermometer and a self-sealing rubber cap for the introduction of reagents by syringes. The polymerization flask was flamed twice *in vacuo*, and filled with argon. A typical experiment in which the graft polymer was isolated is given below. Starch (2 g) in DMSO (50 ml) was introduced followed by potassium naphthalene in THF (22 ml, 0.845*N*, 18.6 mmole) to convert 50% of the hydroxyl groups of the starch to alkoxide. When the green color of the reagent disappeared, phenyl glycidyl ether (14 ml, 0.104 mole) was added, and the reaction mixture was stirred at room temperature until all the monomer has reacted (VPC).

The reaction mixture was neutralized with acetic acid and the graft polymer was precipitated by methanol, filtered, and dried *in vacuo*; yield, 92%.

In a duplicate experiment the graft polymer was isolated in 91% yield.

### Rate Measurements

The rate of disappearance of monomer in the graft and homopolymerization was followed by quantitative gas chromatography techniques. An Aerograph Autoprep Model A-700 instrument was used. Helium was used as the carrier gas at a flow rate of 33 ml/min and 2 m of standard 0.25-in. tubing was used to contain the packing of 5% SE 30 on chromosorb P (60–80 mesh).

The injector temperature was 180°C, the column temperature 125°C, and the detector 210°C. The monomer was quantitatively determined by injecting known volumes of the reaction mixture, and comparison of the peak areas on the chromatogram thus obtained with a calibration curve.

### Homopolymerization of Phenyl Glycidyl Ether by Potassium Naphthalene in DMSO

The polymerizations were conducted using the same apparatus and under similar conditions to those used in the graft polymerization. A typical example is given below.

Potassium naphthalene in THF (22 ml, 0.845*N*, 18.6 mmole) was added at room temperature to dry DMSO (50 ml). After an exothermic reaction, the temperature was adjusted to 25°C, and monomer (14 ml, 0.104 mole) was added in one portion. After all the monomer had polymerized (VPC), acetic acid was added to neutralization and the polymer precipitated with water. The solvents were decanted and the polymer was taken up in chloroform and steam-distilled to remove any impurities in the polymer. The water was evaporated, and the polymer was dried *in vacuo* over phosphorus pentoxide. The homopolymers were generally viscous syrups, but those obtained at low catalyst and high monomer concentrations were more or less solid.

### Determination of Number-Average Molecular Weights of the Homopolymers

Number-average molecular weights were determined from the hydroxyl endgroups of the polymers, assuming one such endgroup per polymer chain (see Discussion).

The procedure given by Sorenson and Campbell<sup>6</sup> was followed with the use of pyridine-acetic anhydride acetylation reagent prepared from acetic anhydride (10 ml) which was dissolved in dry redistilled pyridine (500 ml). Poly(phenyl glycidyl ether) (1 g) was added to 20 ml of the acetylation reagent and the solution was refluxed for 4–5 hr. Water was added and the mixture was refluxed for 10 min. The solution was cooled and titrated with 0.5*N* sodium hydroxide with phenolphthalein as indicator.

## RESULTS

Phenyl glycidyl ether was reacted with potassium starch alkoxide, prepared by reaction of starch in DMSO solution with potassium naphthalene, to give graft polymers isolated in 91–92% yield, under the conditions investigated, namely, 50% starch alkoxide and 1.21 mole/l. monomer. The graft polymers were solid, mp 60–80°C, as compared to the homopolymers of phenyl glycidyl ether, which are viscous syrups. The graft polymers were extracted with hot water in which the starch is soluble, but no free starch was extracted. Extraction with benzene in which the homopolymer is soluble gave no solute, indicating that all the monomer polymerized was incorporated into the graft polymers. The graft polymers were soluble in DMSO and pyridine and insoluble in chloroform, benzene (contrary to the homopolymer), ethanol, and water.

The rate of disappearance of monomer in the graft polymerization reaction was followed by gas-chromatographic techniques. The rate increased with increasing monomer concentration and with starch alkoxide concentration. Due to the heterogeneity of the reaction mixture (starch alkoxide is insoluble in DMSO) no attempt was made to find out the order of the reaction. The rate of the graft polymerization was relatively slow but faster than that found in the graft polymerization of propylene oxide on potassium starch alkoxide under comparable conditions.<sup>3</sup>

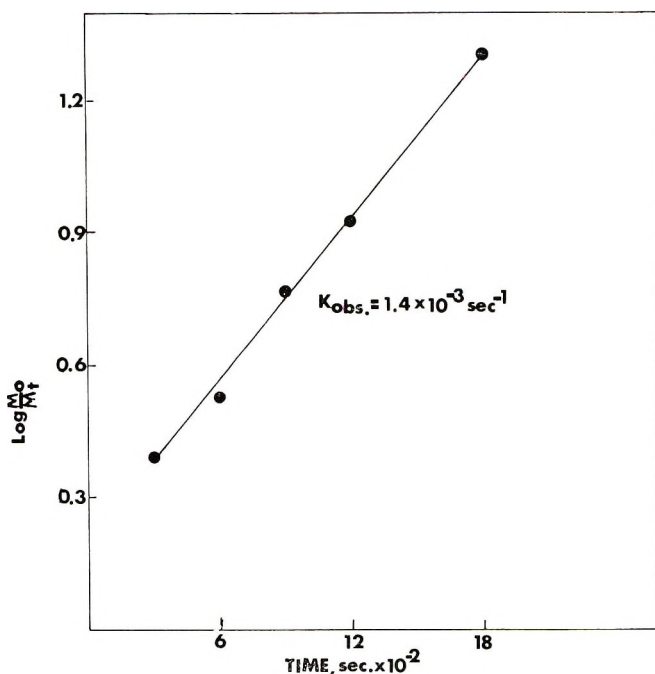


Fig. 1. Homopolymerization of phenyl glycidyl ether in DMSO. Plot of  $\log M_0/M_t$  vs. time. [Potassium naphthalene], 0.26 mole/l.; [monomer], 0.605 mole/l.

TABLE I  
Homopolymerization of Phenyl Glycidyl Ether by Potassium Naphthalene in Dimethyl Sulfoxide<sup>a</sup>

[Monomer], mole/l.	[K-naphthalene], ([C <sub>init.</sub> ]) <sub>0</sub> , mole/l.	[M] [C <sub>init.</sub> ]	DP <sub>n</sub> <sup>b</sup>	[C <sub>eff.</sub> ] <sup>c</sup>		k <sub>obs</sub> × 10 <sup>3</sup> , sec <sup>-1</sup> d	k <sub>p</sub> × 10 <sup>2</sup> , l./mole sec <sup>e</sup>
				mole/l.	% of [C <sub>init.</sub> ]		
0.605	0.260	2.8	10.6	0.069	26.0	1.40 <sup>f</sup>	2.04
1.210	0.260	5.6	20.6	0.070	27.0	1.56	2.23
1.210	0.260	5.6	22.6	0.065	25.0	—	—
0.345	0.049	7.0	9.9	0.035	71.5	0.73	2.11
0.345	0.049	7.0	9.5	0.036	73.5	—	—
0.605	0.049	12.3	16.7	0.036	73.5	0.84	2.33
0.605	0.049	12.3	15.7	0.035	78.2	—	—
1.210	0.049	24.7	33.3	0.036	74.0	0.87	2.40
1.210	0.049	24.7	31.7	0.038	78.2	—	—

<sup>a</sup> Experimental conditions: Potassium naphthalene in THF was added to DMSO, followed by monomer. The reaction was continued until disappearance of all the monomer (VPC). The polymers were isolated in 90–95% yield. Reaction temp. 25°.

<sup>b</sup> DP<sub>n</sub> calculated from  $\bar{M}_n$  determined by endgroup analysis, assuming 1 hydroxyl group per polymer chain.

<sup>c</sup> The effective catalyst concentration [C<sub>eff.</sub>] was calculated from the initial catalyst concentration [C<sub>init.</sub>] by using the equation:  $DP_n = [M]/[C_{eff}]$ .  $k_{obs}$  is the first order rate constant obtained from the slope of the plot of  $\log M_0/M_t$  vs. time.

<sup>d</sup> Calculated from  $k_p = k_{obs}/[C_{eff}]$ .

<sup>e</sup> After the polymerization was complete a second equal portion of monomer was added.  $k_{obs}$  for the rate of disappearance of newly added monomer was  $1.45 \times 10^{-3}$  sec.<sup>-1</sup>

To find out the effect of the polymeric initiator backbone on the rate of the graft polymerization, the homopolymerization by potassium naphthalene in DMSO was studied in detail.

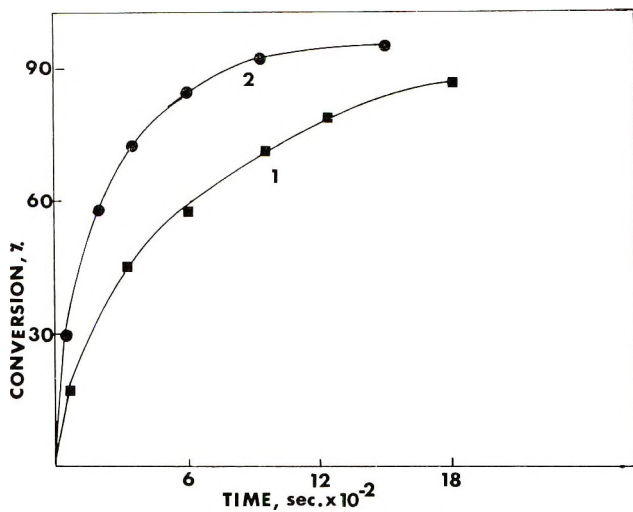


Fig. 2. Homopolymerization of phenyl glycidyl ether in DMSO. Dependence of rate of conversion on alkoxide concentration at various [potassium naphthalene]: (1) 0.049 mole/l.; (2) 0.26 mole/l. [Monomer], 1.21 mole/l.

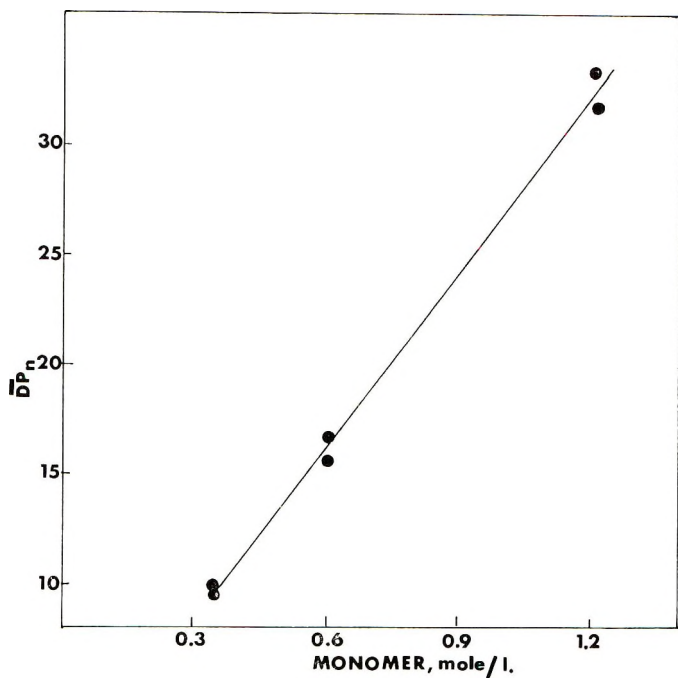


Fig. 3. Homopolymerization of phenyl glycidyl ether in DMSO. Dependence of  $\overline{DP}_n$  on monomer concentration. [Potassium naphthalene], 0.049 mole/l.

It was found that under comparable conditions of monomer and potassium naphthalene concentrations on the one hand and starch alkoxide on the other, the rate of the homopolymerization was much faster. The homopolymerization was first-order to monomer concentration, as seen from the linear plots of  $\log M_0/M_t$  versus time (Fig. 1), from the slopes of which the  $k_{\text{obs}}$  values were calculated (Table I). The rate increased with increasing potassium naphthalene concentration (Fig. 2).

The number-average molecular weights increased linearly with increasing monomer concentration (Fig. 3). In all cases they were higher than those calculated from the ratio of the concentrations [monomer]/[potassium naphthalene], possibly indicating that not all the introduced potassium

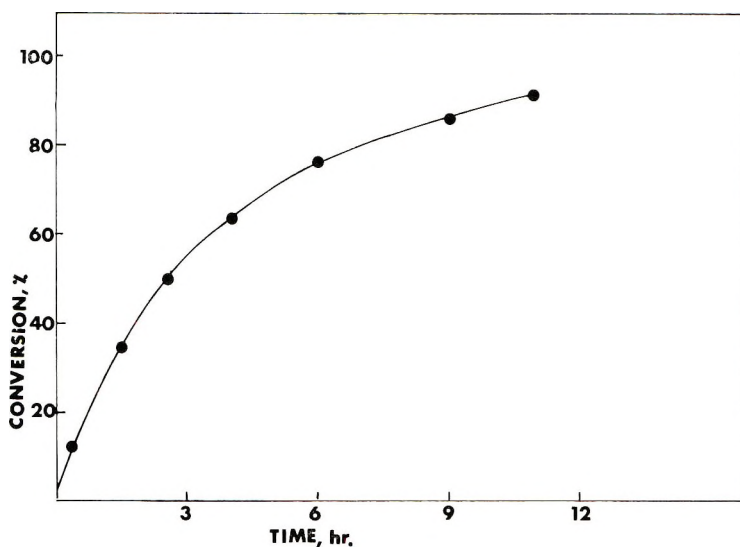


Fig. 4. Graft polymerization of phenyl glycidyl ether on sucrose potassium alkoxide. [Monomer], 1.21 mole/l.; [alkoxide], 0.26 mole/l. (50% of the hydroxyl groups converted to alkoxide).

naphthalene led to initiation of polymer chains. Furthermore the change of  $\bar{M}_n$  was not directly proportional to the potassium naphthalene concentration used.

To investigate the slower rate of the graft polymerization as compared with the corresponding homopolymerization, experiments were carried out to find out the effect of the molecular weights of the polymeric alkoxide on the graft polymerization. Experiments with the alkoxide derivatives of carbohydrates of lower molecular weight, namely, dextrin and sucrose (Fig. 4) in DMSO under comparable conditions, gave the same reaction rates as those found with soluble starch (Fig. 5). On the other hand, rate experiments on the disappearance of monomer in the polymerization of phenyl glycidyl ether initiated by the alkoxide derivatives of poly(ethylene oxide) having  $\bar{M}_n$  of 400 and 4000 (Fig. 6, Table II) showed that the rates

were not dependent on the  $\bar{M}_n$  of poly(ethylene oxide) and were of the same order as those found in the homopolymerization by potassium naphthalene in DMSO.

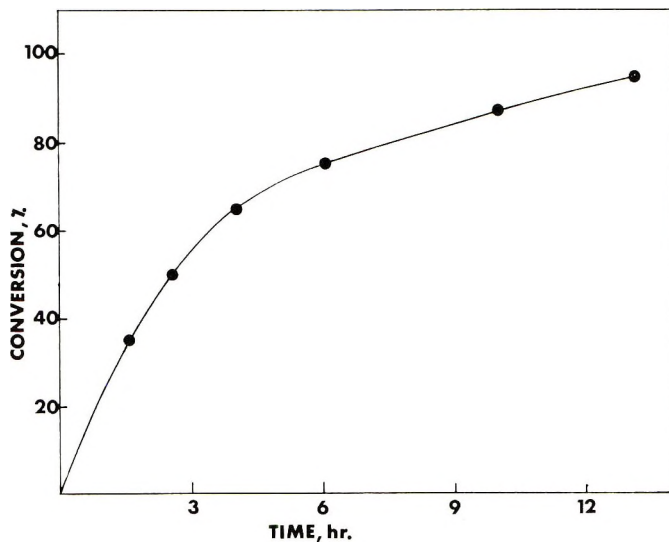


Fig. 5. Graft polymerization of phenyl glycidyl ether on starch potassium alkoxide. [Monomer], 1.21 mole/l.; [alkoxide], 0.26 mole/l. (50% of the hydroxyl groups converted to alkoxide).

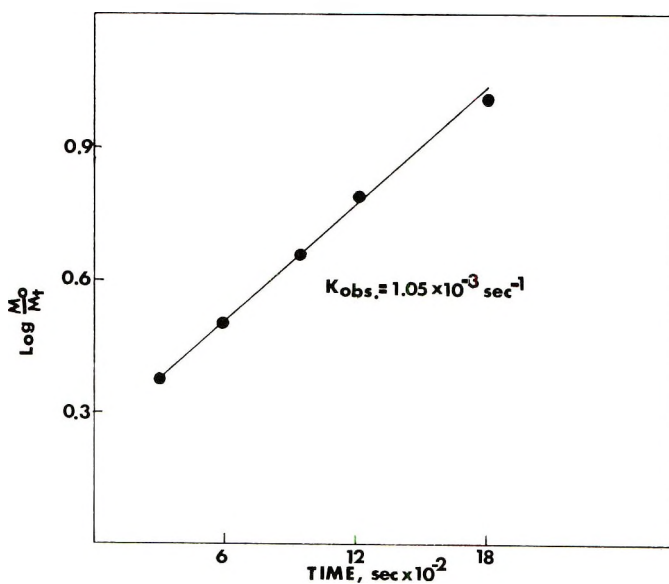


Fig. 6. Polymerization of phenyl glycidyl ether initiated by poly(ethylene oxide) ( $\bar{M}_n = 400$ ) alkoxide. Plot of  $\log M_0/M_t$  vs. time. [Monomer], 1.21 mole/l.; [alkoxide], 0.049 mole/l.



TABLE II  
 Polymerization of Phenylglycidyl Ether  
 Initiated by Poly(ethylene Oxide) (PEO) Alkoxide<sup>a</sup>

PEO		PEO alkoxide		[Monomer], mole/l.	$k_{\text{obs}} \times 10^3$ , sec <sup>-1b</sup>	$k_p \times 10^2$ l./mole-sec <sup>c</sup>
$\bar{M}_w$	Wt, g	mmole	mole/l.			
400	2 <sup>d</sup>	4.23	0.049	1.21	1.05	2.14
4000	20 <sup>d</sup>	4.23	0.049	1.21	1.15	2.35

<sup>a</sup> Experimental conditions: To a dry poly(ethylene oxide) solution in DMSO, potassium naphthalene in THF (5 ml, 0.845*N*, 4.23 mmole) was added to form the PEO alkoxide. Monomer was added and the polymerization was carried out at 25°C.

<sup>b</sup>  $k_{\text{obs}}$  is the first-order rate constant obtained from the slope of the plot of  $\log M_0/M_t$  vs. time.

<sup>c</sup>  $k_p$  was calculated from the equation,  $k_p = k_{\text{obs}}/[C]$ , where  $[C]$  is the PEO alkoxide concentration.

<sup>d</sup> This amount of poly(ethylene oxide) contained 10 mmole hydroxyl endgroups.

## DISCUSSION

The results showed that the reaction of phenyl glycidyl ether with potassium starch alkoxide led to the formation of graft polymers in almost quantitative yield with no homopolymer formation. The mechanism of the graft polymerization consists of anionic initiation on the starch alkoxide, followed by propagation. The fact that no homopolymer was formed indicates that there was no transfer to monomer, a reaction which is appreciable in the case of the graft polymerization of propylene oxide.<sup>3</sup>

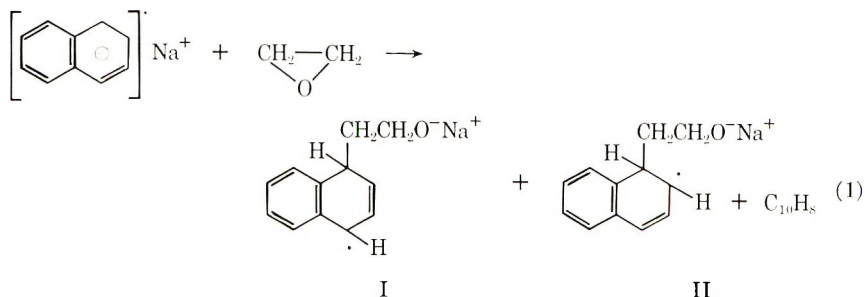
The rate of the graft polymerization on starch alkoxide was found to be much slower than that of the homopolymerization by potassium naphthalene in DMSO. The fact that the rates obtained with the alkoxide derivatives of the lower molecular weight carbohydrates were the same as those obtained with starch alkoxide indicates that the molecular weight of the initiator is not the cause of the slowing of the rate observed in the case of the graft polymerization. This is further strengthened by the fact that the rates obtained with poly(ethylene oxide) alkoxide ( $\bar{M}_n = 400$ ) were the same as those found with that having  $\bar{M}_n = 4000$ . This also indicates that the viscosity of the reaction medium is not the factor for the lower rates observed in the case of the graft polymerization. In fact, the rates observed with the poly(ethylene oxide) alkoxides were fast and of the order of those obtained in the homopolymerization and not of the graft polymerization. Close examination of the reaction media showed that while the polymerizations in the case of starch, dextrin, and sucrose were heterogeneous, due to the insolubility (swollen gel) of their alkoxide derivatives in DMSO, that of poly(ethylene oxide) alkoxide as well as the homopolymerization were homogeneous. This seems to point out clearly that the heterogeneity of the graft polymerization system is the cause of the low rates of polymerization observed. The insolubility of the starch alkoxide may lead to low alkoxide efficiency as found in the case of the graft polymerization of propylene oxide on starch.<sup>3</sup> On the other hand, however,

there may be some slowing in the rate of the propagation reaction, due to lower diffusion of the insoluble growing ends.

Homopolymerization studies on phenyl glycidyl ether by anionic initiators were reported. Sorokin et al.<sup>7-9</sup> found in the polymerization at relatively high temperature initiated by potassium or sodium hydroxides and ethoxides, that the reaction was first order to monomer and to initiator. Lebedev and Baranov<sup>10</sup> used sodium and potassium methoxides at high temperature in solvents such as chlorobenzene and found that the polymerization reaction was first order to monomer but second order to initiator. No detailed study of the anionic polymerization of phenylglycidyl ether in DMSO was carried out, although such studies of the lower alkylene oxides namely ethylene oxide and propylene oxide were carried out<sup>11,12</sup> using potassium *t*-butoxide as catalyst.

The polymerization of alkylene oxides by potassium naphthalene was studied, and the mechanism of initiation suggested consisted of the addition of alkylene oxide to the potassium naphthalene.

For ethylene oxide, initiation was formulated as shown in eq. (1).<sup>13</sup>

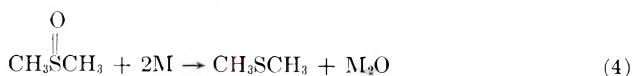
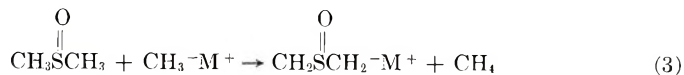
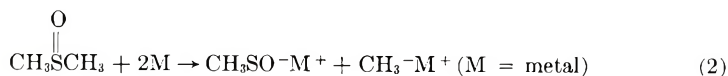


The free radicals (I,II) formed by transfer of an electron from potassium naphthalene are converted to anions which also initiate polymerization. This mechanism was confirmed by the evidence that dihydronaphthalene was detected in the polymers.

Investigation of the homopolymers of phenyl glycidyl ether obtained in the polymerization by potassium naphthalene in DMSO showed that there were no resonance peaks in the NMR for the vinyl hydrogens of 1,2- or 1,4-dihydronaphthalenes at  $\delta = 6.4$  and  $5.9$  ppm respectively. All the polymers, however, were found to contain sulfur. The percentage of the sulfur varied depending on concentration of the reactants, but due to their small values and inexactness of the analytical determination, quantitative results could not be concluded.

The possible source for the sulfur in the polymers has its origin in the DMSO. The polymerizations were carried out in such a manner that potassium naphthalene was first added to the DMSO. There was heat of reaction and after this had subsided (several minutes) the monomer was added. It seems that the potassium naphthalene reacted with DMSO.

In fact, potassium metal was found to react readily with DMSO leading to a mixture of products [eqs. (2)–(5)].<sup>14</sup>



Since potassium naphthalene may be regarded as solubilized potassium,<sup>15</sup> it is quite logical that similar reactions may have occurred with potassium naphthalene. Since the reaction with potassium naphthalene in solution is expected to be even faster than that with potassium metal, it may be quite possible that when the monomer was added no potassium naphthalene was present, and that is why no dihydronaphthalenes were found in the polymer. The presence of sulfur in the polymers points out clearly that the actual active initiator of the polymerization was an anion derived from dimethyl sulfoxide. From the possible products formed [eqs. (2)–(5)] it seems that dimethyl sulfide anion is the most probable initiator, being a very strong base. In connection with this it may be mentioned that it was recently reported that in polymerization of vinyl monomers and alkylene oxides conducted in DMSO in the presence of potassium *tert*-butoxide, the initiator was dimethyl sulfide anion.<sup>12</sup>

The anionic polymerization of alkylene oxides in aprotic solvents is characterized by being a "living" one with no termination.<sup>16–18</sup> For such a living system the rate of the polymerization may be defined as follows:<sup>19</sup>

$$-d[\text{M}]/dt = k_p[\text{M}]^a[\text{C}]^b \quad (6)$$

where  $a$  and  $b$  are the order of reaction to monomer and initiator, respectively. If the initiation is fast, the concentration of the "living" ends is identical with the initiator concentration, and in this case  $k_p$  would be the propagation rate constant, provided that sufficiently high molecular weight polymers were formed. As shown the polymerization was first order to monomer. As regards the order to initiator, it should be taken in account that the actual initiator was not potassium naphthalene but dimethyl sulfide anion, and the rates of polymerization observed should be connected with  $C_{\text{eff}}$  (dimethyl sulfide anion) and not with  $C_{\text{introd}}$ , namely, the potassium naphthalene concentration.

From eqs. (2)–(5) it is seen that only part of the potassium naphthalene leads to the formation of dimethyl sulfide anion. It is also expected that using different amounts of potassium naphthalene will lead to different amounts of dimethyl sulfide anion, but obviously a certain amount of potassium naphthalene

will lead always to the same amount of dimsyl anion under the same reaction conditions. Since the polymerization is a "living" one for which  $\overline{DP}_n = [M]/[C_{eff.}]$ ,<sup>18</sup> where  $C_{eff.}$  is the effective initiator, it follows that from the  $\overline{DP}_n$  values and the monomer concentration (the polymerizations were carried out to completion), the effective catalyst concentration can be calculated. It may be seen (Table I) that this effective catalyst concentration was the same for a certain starting concentration of potassium naphthalene and did not vary with increasing monomer concentration, indicating further that the dimsyl anion reacts completely even at low monomer concentration.

The order of reaction in effective initiator concentration,  $b$ , was calculated from the following two equations:

$$k_{obs. I} = k_p [C_{eff. I}]^b$$

$$k_{obs. II} = k_p [C_{eff. II}]^b \quad (7)$$

The average order value for effective initiator was approximately first-order ( $b = 0.90 \pm 0.12$ ) where the average was carried out on all the series of monomer concentrations investigated.

Knowing that the reaction was first order to monomer and to initiator, the  $k_p$  values [eqs. (7)] were calculated from the  $k_{obs}$  values and the effective initiator concentration by the equation,

$$k_p = k_{obs}/[C_{eff}]$$

These  $k_p$  values are actually the propagation rate constants, as seen from the fact that polymerization of a second equal portion of monomer on the living ends of one that has already been completely polymerized, gave the same  $k_{obs}$  values as those obtained in the first portion (Fig. 7, compare with Fig. 1). Obviously in the second polymerization the  $k_p$  value is actually that of propagation.

In the polymerization initiated by the potassium alkoxide derivative of poly(ethylene oxide) at an alkoxide concentration equivalent to the potassium naphthalene concentration in a parallel reaction, the  $k_{obs}$  values were found to be higher than those obtained with potassium naphthalene. The  $k_p$  values, however, calculated as above and on taking the alkoxide concentration as the effective initiator concentration, were the same as those found with potassium naphthalene on taking the effective initiator concentration into consideration. Since here also initiation on polyethylene oxide alkoxide may be looked at in a way as propagation of polymerization, this further indicates that the  $k_p$  values found were actually those of the propagation rate constants.

In view of the results of the present work in which potassium naphthalene was found to react easily with DMSO, the question arises whether in the metallation of starch in DMSO solution by alkali metal naphthalene the metallation is directly by the reagent or whether it proceeds via prior formation of dimsyl anion, which is the true metallating agent. Some

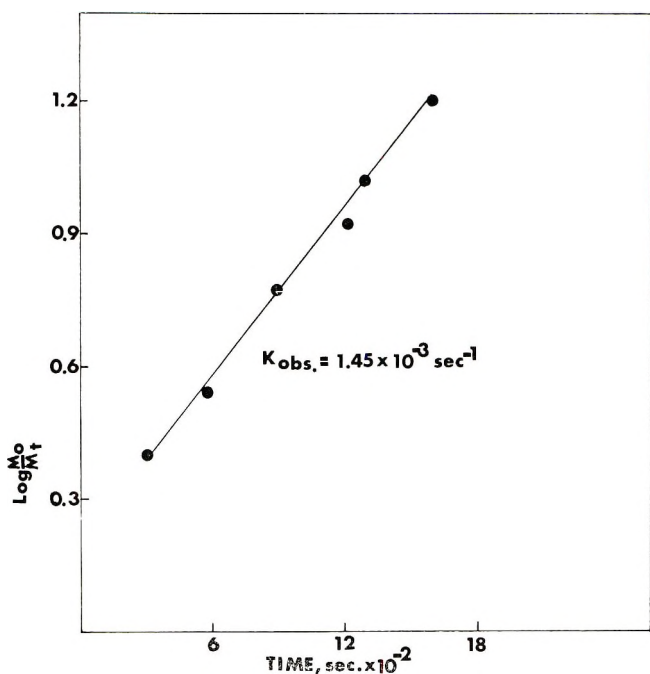


Fig. 7. Homopolymerization of phenyl glycidyl ether in DMSO initiated by "living" poly(phenyl glycidyl ether). Addition of a second equal portion of monomer (0.605 mole/l.) to one completely polymerized by using 0.26 mole/l. potassium naphthalene (compare with Fig. 1).

answer to this question may be obtained from the results of a recent work<sup>20</sup> in which we have shown that metallation of starch in DMSO solution by potassium naphthalene is quantitative, each molecule of the reagent reacting to give an alkoxide group, as seen from quantitative methylation of the product. Had the potassium naphthalene reacted first with DMSO, subsequent methylation should not have been quantitative, since as shown above part of the potassium naphthalene on reaction with DMSO gives species which are not enough basic to lead to metallation of the hydroxyl groups of the starch.

The authors are pleased to acknowledge a studentship for G. E. from the Israel National Council for Research and Development.

### References

1. M. Tahan and A. Zilkha, *J. Polym. Sci. A-1*, **7**, 1815 (1969).
2. M. Tahan and A. Zilkha, *J. Polymer Sci. A-1*, **7**, 1825 (1969).
3. G. Ezra, Ph.D. Thesis, submitted to the Senate of the Hebrew University of Jerusalem, 1969; G. Ezra and A. Zilkha, *Europ. Polym. J.*, in press.
4. G. Ezra and A. Zilkha, *Europ. Polym. J.*, in press
5. A. Zilkha and Y. Avny, *J. Polym. Sci. A*, **1**, 549 (1963).
6. W. R. Sorenson and T. W. Campbell, *Preparative Methods of Polymer Chemistry*, Interscience, New York, 1961, p. 134.

7. M. F. Sorokin and Z. A. Kochnova, *Lakokras. Materialy Primen.*, **4**, 6 (1962).
8. M. F. Sorokin, L. G. Shode, and L. S. Mikhailova, *Lakokras. Materialy Primen.*, **4**, 10 (1962).
9. M. F. Sorokin and L. G. Shode, *Vysokomol. Soedin.*, **6**, 96 (1964).
10. N. N. Lebedev and Y. I. Baranov, *Vysokomol. Soedin.*, **8**, 198 (1966); *Polym. Sci. USSR*, **8**, 211 (1966).
11. C. C. Price and D. D. Carmelite, *J. Amer. Chem. Soc.*, **88**, 4039 (1966).
12. C. E. H. Bawn, A. Ledwith, and N. McFarlane, *Polymer*, **8**, 484 (1967).
13. M. Szwarc and D. H. Richards, *Trans. Faraday Soc.*, **55**, 1644 (1959).
14. D. E. O'Connor and W. L. Lyness, *J. Org. Chem.*, **30**, 1620 (1965).
15. J. J. Eisch, *The Chemistry of Organo-Metallic Compounds (The Main Group Elements)*, McMillan, New York, 1967, p. 19.
16. P. J. Flory, *Principles of Polymer Chemistry*, Cornell Univ. Press, Ithaca, N. Y., 1953, pp. 56-61, 331.
17. P. J. Flory, *J. Amer. Chem. Soc.*, **62**, 1561 (1946).
18. R. Waack, A. Rembaum, J. D. Coombes, and M. Szwarc, *J. Amer. Chem. Soc.*, **79**, 2026 (1957).
19. M. Szwarc and Y. Smid, in *Progress in Reaction Kinetics*, Vol. 2, G. Porter, Ed., Pergamon Press, London, 1964, p. 250.
20. G. Ezra and A. Zilkha, *J. Macromolec. Sci. Chem.*, **A3**, 1589 (1979).

Received September 25, 1969

## Calorimetric Investigation of Polymerization Reactions. III. Curing Reaction of Epoxides with Amines

K. HORIE, H. HIURA, M. SAWADA, I. MITA, and H. KAMBE,  
*Institute of Space and Aeronautical Science, University of Tokyo,  
Komaba, Tokyo, Japan*

### Synopsis

The curing reactions of epoxy resin with aliphatic diamines and the reaction of phenyl glycidyl ether with butylamine as a model for the curing reactions were investigated with a differential scanning calorimeter (DSC) operated isothermally. The heat of reaction of phenyl glycidyl ether with butylamine is equal to  $24.5 \pm 0.6$  kcal/mole. The rate of reaction was followed over the whole range of conversion for both model and curing reactions. The reactions are accelerated by the hydrogen-bond donor produced in the system. The rate constants based on the third-order kinetics were determined and discussed for the model reaction and for the chemically controlled region of curing reactions. The activation energies for these rate constants are 13–14 kcal/mole. At a later stage of conversion, the curing reactions become controlled by diffusion of functional groups. The final extent of conversion is short of completion for most isothermally cured and even for postcured samples because of crosslinking. It was quantitatively indicated that the final conversion of isothermal cure corresponds to the transition of the system from a viscous liquid to a glass on the basis of the theory of glass transition temperature of crosslinked polymer systems.

### INTRODUCTION

The investigation of the curing mechanism of thermosetting resins has been restricted by the insolubility in any solvent of the resulting network polymers. The curing reaction of epoxy resin is not exceptional.

In order to discuss the curing mechanism of epoxy resin with amines, it is necessary to know final conversion and rate of cure for the crosslinked polymer system. The change in physical properties of the system, such as refractive index,<sup>1</sup> electrical resistivity,<sup>2,3</sup> and viscosity,<sup>4</sup> has been proposed as a relative indication of the extent of conversion of monomer to polymer. Infrared analysis<sup>5</sup> has also been applied to determine the conversion for the cure of epoxy resin. However, an accurate and continuous measurement of the rate of cure has not been attained by these methods.

Calorimetry is a powerful method for the direct measurement of the rate of exothermic polymerization. In our previous works, the rate of polymerization of methyl methacrylate and styrene<sup>6</sup> and the rate of copolymer-

ization of diethyl fumarate with styrene<sup>7</sup> have been measured directly, continuously, and over the whole range of conversion by the isothermal operation of a differential scanning calorimeter (DSC). The relative conversion for a thermosetting polymer has been determined by the differential thermal analysis (DTA).<sup>8</sup> This method is based on the exothermic peak during the temperature scanning. In contrast to DTA, DSC measures the absolute conversion over the whole range of process, and in particular, it can be used in a strictly isothermal condition. Recently, Fava<sup>9</sup> has reported an application of DSC to the curing reaction of epoxy resin system. His emphasis has been placed on the techniques of differential scanning calorimetry, and an important feature of DSC which is capable of absolute measurements of conversion and rate of cure has not been utilized.

The reaction of a primary amine with an epoxide usually affords a secondary amine, which reacts with another epoxide resulting in a tertiary amine. The reaction of monofunctional epoxide with amines has been studied by many investigators<sup>10-14</sup> as a model reaction for the curing process of epoxy resin. Shechter et al.<sup>10</sup> as well as Kakurai and Noguchi<sup>11</sup> have shown that the addition of amine to epoxide can be accelerated by the presence of alcohol, water, or other hydrogen donor in the system and suggested a mechanism involving opening of the epoxide ring with the aid of hydrogen bonding in the transition state. Smith<sup>13</sup> has proposed the third-order kinetics for the reaction of epoxide with secondary amine accelerated by the hydrogen-bond donor and indicated that the third-order kinetics tends towards a pseudo-second-order one in a large excess of the hydrogen-donating solvent.

Our preliminary results for the reaction of phenyl glycidyl ether with butylamine have already been reported.<sup>15</sup> In the present paper, the curing reaction of epoxy resin with aliphatic diamines as well as its model reaction, i.e., the reaction of phenyl glycidyl ether with butylamine, is investigated by DSC. The heat of reaction and the rate constants based on the third-order kinetics were determined for the model reaction. The absolute extent of conversion and the rate constants for the curing reaction were measured and discussed in relation to the structure of diamines and the glass transition phenomena of the system.

## EXPERIMENTAL

### Materials

Phenyl glycidyl ether was dried and purified by fractional distillation under nitrogen at a reduced pressure. Dow DER 332/LC regarded as a pure diglycidyl ether of bisphenol A (DGEBA) was used as an epoxy resin. Butylamine was dried over potassium hydroxide. Ethylenediamine, trimethylenediamine, and hexamethylenediamine were dried in the same way as with butylamine. *n*-Butyl alcohol was dried and purified by fractional distillation.

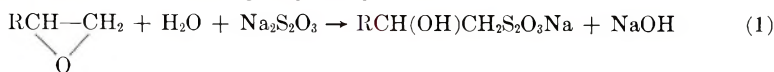


### Procedure

The reaction of phenyl glycidyl ether with various amounts of butylamine was carried out at 50, 60, and 70°C. In some cases *n*-butyl alcohol was added to the system as a hydrogen-donating accelerator. The epoxy resin (DGEBA) was cured isothermally with ethylenediamine, trimethylenediamine, and hexamethylenediamine at 50, 60, and 70°C. Both model and curing reactions were carried out in a modified closed sample pan of a Perkin-Elmer differential scanning calorimeter (DSC-1) operated isothermally. Details of the procedure with the DSC are similar to those described previously.<sup>6</sup> The factor converting the peak area to the thermal energy was obtained from heats of fusion of eight nonvolatile compounds measured between 40 and 150°C.<sup>15</sup>

### Measurements of Residual Reactants for Model Reaction

An epoxide reacts quantitatively with sodium thiosulfate in an acetone-water mixed solvent liberating a hydroxyl ion.<sup>16</sup>



This reaction was applied for determining the residual content of epoxide in the model reaction. Residual amine was determined by titration with acetic acid. It was ascertained that the solution of primary butylamine and that of secondary amine formed by the addition of epoxide were colored in the presence of phenolphthalein, whereas the solution of tertiary amine (reaction product of butylamine with a large excess of phenyl glycidyl ether) was not colored by this indicator.

After reaction in the DSC, the sample (40–80 mg) was dissolved in 1 ml acetone, mixed with 5 ml of water, and titrated with 0.5*N* acetic acid solution with phenolphthalein in order to determine the residual amine content. Then, 5 ml of 0.2*M* sodium thiosulfate solution in acetone–water (4:1) mixed solvent was added to the sample solution. When residual epoxide was present, the solution became red, and was titrated with 0.5*N* acetic acid solution over a 2-hr period.

### Glass Transition Temperature for Cured Epoxy Resins

DSC thermograms of postcured DGEBA with diamines, unreacted DGEBA, and linear copolymer of DGEBA with butylamine were obtained by temperature scanning at the rate of 8°C/min. The glass transition temperature was defined at the low temperature end of the transition region. Temperature calibration of DSC was made with melting temperatures of fourteen organic compounds between –45 and 150°C.<sup>15</sup>

## RESULTS AND DISCUSSION

### Heat of Reaction of Phenyl Glycidyl Ether with Butylamine

Typical DSC curves for the reaction of phenyl glycidyl ether with butylamine at 70°C are shown in Figure 1. The feed composition and residual

TABLE I  
Heat of Reaction of Phenyl Glycidyl Ether (PGE) with Butylamine (BA)

Sample weight, mg	Weight loss, mg	Composition in feed				Residual reactant			Reacted PGE, mmole	Exothermic energy, cal	Heat of reaction, kcal/mole
		PGE, mmole	BA, mmole	mole fraction of BA	PGE, mmole	primary and secondary amines, mmole	PGE, mmole				
48.5	0.5	0.288	0.066	0.19	0.138	0	0.132	3.30	25.0		
83.6	1.1	0.495	0.113	0.19	0.250	0	0.226	5.45	24.1		
41.7	1.7	0.222	0.091	0.29	0.024	0	0.182	4.34	23.9		
77.4	0.5	0.427	0.176	0.29	0.065	0	0.352	8.93	25.4		
62.2	0.8	0.333	0.156	0.32	0.010	0	0.312	7.43	23.8		
54.6	1.7	0.287	0.134	0.32	0.016	0	0.268	6.53	24.4		
56.3	0.7	0.300	0.145	0.33	0.014	0	0.286	6.90	24.1		
61.5	0.6	0.293	0.232	0.44	0	0.115	0.293	7.02	24.0		
41.6	0.7	0.186	0.177	0.49	0	0.108	0.186	4.67	25.1		
46.8	0.2	0.209	0.208	0.50	0	0.130	0.209	5.14	24.6		
51.5	0	0.231	0.230	0.50	0	0.132	0.231	5.62	24.3		
55.6	0.6	0.245	0.249	0.50	0	0.107	0.245	6.12	25.0		
50.1	1.4	0.175	0.307	0.64	0	0.264	0.175	4.37	25.0		

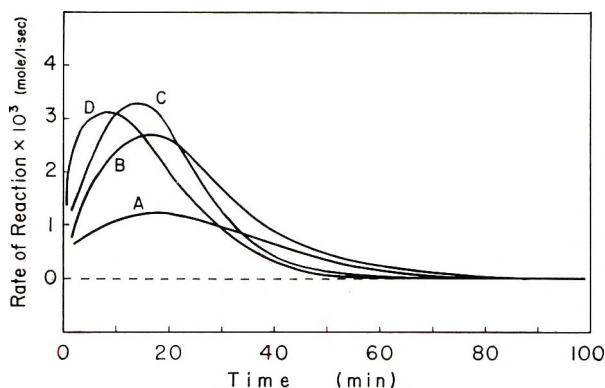


Fig. 1. DSC curves for reaction of Phenyl glycidyl ether with butylamine (BA) at 70°C. Mole fractions of BA are (A) 0.19; (B) 0.32; (C) 0.50; (D) 0.64.

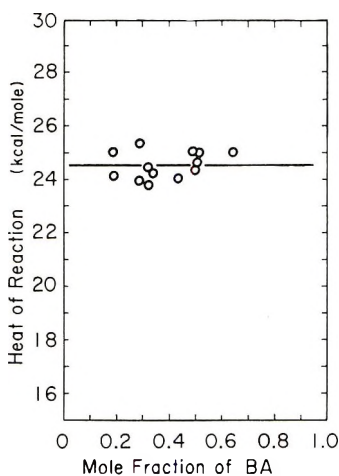


Fig. 2. Heat of reaction of phenyl glycidyl ether with butylamine (BA) against mole fraction of BA.

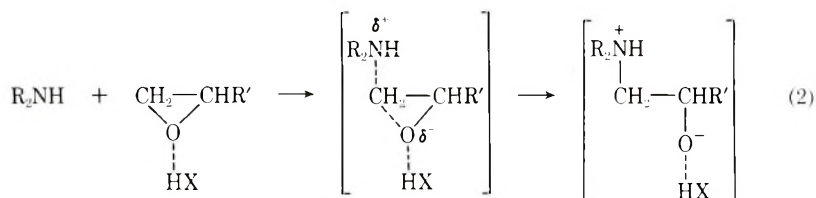
contents of epoxide and amine, determined by titration, are summarized in Table I. When the molar ratio of epoxide to amine is about 2-4, primary and secondary amines were thoroughly converted to tertiary amine, while in the case of equimolar or amine-rich composition phenyl glycidyl ether reacted completely.

The average heat of reaction of phenyl glycidyl ether with butylamine was determined as the ratio of the total heat evolved to the epoxide consumption and is listed also in Table I. The average heat of reaction consists of heats of two different reactions, that is, the reaction of epoxide with primary amine and that with secondary amine. Since the average heat of reaction is independent of the feed composition and seems to be constant, as is shown in Figure 2, the difference between heats of the two reactions would be negligibly small. The heat of reaction of phenyl glycidyl ether

with butylamine was determined to be  $24.5 \pm 0.6$  kcal/mole, which shows a fairly good agreement with the results of Klute and Viehmann<sup>17</sup> for epoxide with primary amines (26 kcal/mole).

### Kinetics of Epoxide Reaction with Primary Amines

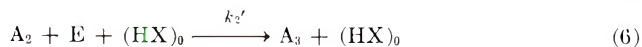
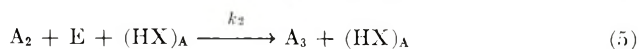
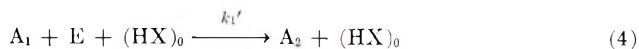
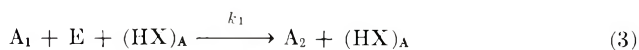
Smith<sup>13</sup> has assumed that the rate-controlling step for the reaction between a secondary amine and an epoxide may be represented by eq. (2), where HX is any hydrogen-bond donor molecule,



and proposed the third-order kinetics which is consistent with reasonable accuracy with the results of Shechter et al.<sup>10</sup>

In order to investigate the epoxide reaction with primary amines, the third-order kinetics by Smith must be extended to the case in which epoxide reaction with primary amine as well as that with the resulting secondary amine is to be considered.

A reaction scheme [eqs. (3)–(6)] will be set forth, assuming that the molecule  $(HX)_0$  initially present in the system and the reaction products having hydroxyl group  $(HX)_A$  act as true catalysts and are not consumed in any side reactions:



Here E,  $A_1$ ,  $A_2$ , and  $A_3$  represent epoxide, primary amine, secondary amine produced by addition of an epoxide, and tertiary amine as a final product, respectively.

Let  $e$ ,  $a_1$ , and  $a_2$  be the concentrations of E,  $A_1$ , and  $A_2$  at time  $t$ , respectively,  $e_0$  and  $a_0$  the initial concentrations of E and  $A_1$ , respectively,  $c_0$  concentration of  $(HX)_0$ ,  $x$  the epoxide consumed after time  $t$ . As the concentration of  $(HX)_A$  is equal to  $x$ , the rate of consumption of epoxide at time  $t$  is given by

$$dx/dt = k_1 a_1 e x + k_1' a_1 e c_0 + k_2 a_2 e x + k_2' a_2 e c_0 \quad (7)$$

Assuming

$$k_2/k_1 = k_2'/k_1' = n \quad (8)$$

eq. (7) can be written

$$dx/dt = (e_0 - x)(k_1x + k_1'c_0)(a_1 + na_2) \quad (9)$$

Since  $n$  becomes 0.5 when the reactivity of each hydrogen atom attached to the nitrogen atom in  $A_1$  is equal to the reactivity of a hydrogen atom in  $A_2$ , it is reasonable to assume the value of  $n$  close to 0.5, and  $n$  is set as eq. (10).

$$n = 0.5 + \Delta n \quad (10)$$

The relation between  $a_1$  and  $a_2$  at time  $t$  will be given stoichiometrically by eq. (11).

$$a_1 + (a_2/2) = a_0 - (x/2) \quad (11)$$

Substitution of eqs. (10) and (11) into eq. (9) and subsequent transformation result in eq. (12).

$$(dx/dt)/[(e_0 - x)(a_0 - x/2)] = (k_1x + k_1'c_0)\{1 + 2a_2\Delta n/(2a_1 + a_2)\} \quad (12)$$

The value of  $2a_2\Delta n/(2a_1 + a_2)$  in right-hand side of eq. (12) would be neglected compared to unity, since it is zero at the onset of the reaction, nearly equal to  $1.2\Delta n$  at 60% conversion and close to  $2\Delta n$  at the complete conversion. A DSC curve of the reaction and its integration provide  $dx/dt$  and  $x$  over the whole range of conversion, and the left-hand side of eq. (12) can be plotted against  $x$ .

Typical change of the left-hand side of eq. (12) with  $x$  for the reaction of phenyl glycidyl ether with various amounts of butylamine at 70°C are

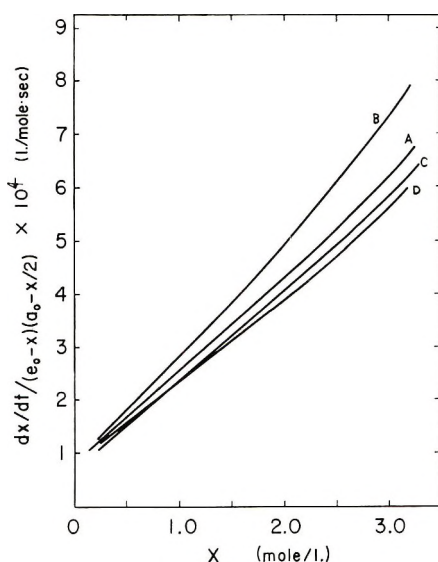


Fig. 3. Reduced rate curves for the reaction of phenyl glycidyl ether with butylamine (BA) at 70°C. Mole fractions of BA are (A) 0.19; (B) 0.32; (C) 0.50; (D) 0.64.

shown in Figure 3. Straight lines were obtained at the first half of the conversion. Deviation of intercepts of the curves from the origin suggests the existence of traces of impurity accelerating the reaction in the system. The reaction of phenyl glycidyl ether with equimolar amount of butylamine was carried out at 50 and 60°C with DSC and similar reduced rate curves were obtained.

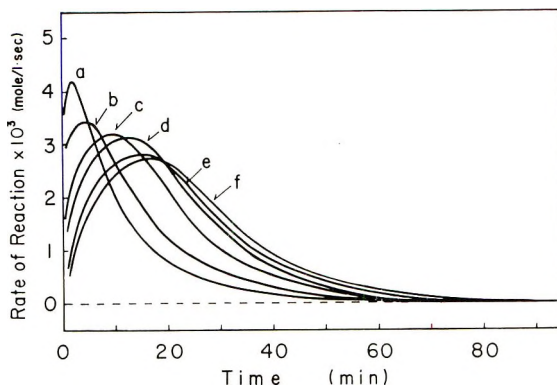


Fig. 4. DSC curves for reaction of phenyl glycidyl ether with butylamine at 70°C in the presence of various contents of *n*-butyl alcohol: (a) 50 mole-%; (b) 25 mole-%; (c) 10 mole-%; (d) 5.0 mole-%; (e) 2.0 mole-%; (f) 0.

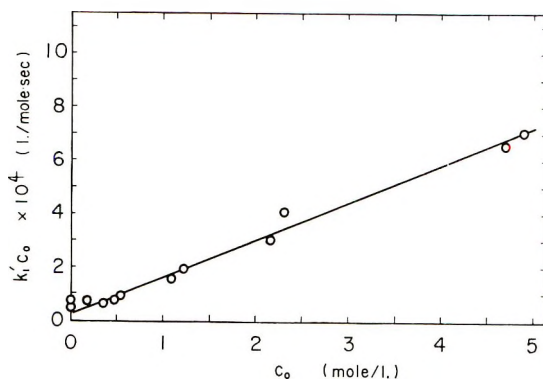


Fig. 5. Determination of  $k_1'$  for reaction of phenyl glycidyl ether with butylamine at 70°C by the addition of *n*-butyl alcohol.

From the slopes of the straight part of curves the values of  $k_1$  were determined,  $\Delta n$  and hence  $k_2$  were evaluated from the slopes at 60% conversion.

In order to get values for rate constants  $k_1'$  and  $k_2'$ , the reaction of phenyl glycidyl ether with an equivalent amount of butylamine was carried out at 70°C in the presence of *n*-butyl alcohol as an accelerator.

DSC curves of the reaction are shown in Figure 4. The peak in DSC curves appears in earlier time with increasing concentration of *n*-butyl alcohol in the system, which supports the suggestion that the pseudo-

second-order kinetics may be observed in systems with a large excess of hydrogen-bond donor.

The plot of the intercept  $k_1'c_0$  of reduced rate curves according to eq. (12) against the concentration of *n*-butyl alcohol  $c_0$  is shown in Figure 5. A linear relationship was attained between them, which gave the value of  $k_1'$ . The value of  $k_2'$  was determined with the use of a value of 0.61 for  $n$ .

Rate constants for the reaction of phenyl glycidyl ether with butylamine are summarized in Table II. The value of  $k_2$  at 50°C is in good accord with that reported by Smith<sup>13</sup> for the reaction of phenyl glycidyl ether with diethylamine ( $2.6 \times 10^{-5}$  l.<sup>2</sup>/mole<sup>2</sup>-sec).

TABLE II  
Rate Constants for the Reaction of Phenyl Glycidyl Ether with Butylamine

Reaction temperature, °C	$k_1 \times 10^4$ , l. <sup>2</sup> /mole <sup>2</sup> -sec	$n$	$k_2 \times 10^4$ , l. <sup>2</sup> /mole <sup>2</sup> -sec	$k_1' \times 10^4$ , l. <sup>2</sup> /mole <sup>2</sup> -sec	$k_2' \times 10^4$ , l. <sup>2</sup> /mole <sup>2</sup> -sec
50	$0.45 \pm 0.09$	$0.65 \pm 0.08$	$0.29 \pm 0.06$	—	—
60	$0.85 \pm 0.1$	$0.64 \pm 0.09$	$0.54 \pm 0.06$	—	—
70	$1.9 \pm 0.3$	$0.61 \pm 0.03$	$1.2 \pm 0.1$	$1.5 \pm 0.1$	$0.91 \pm 0.06$

The Arrhenius plot of  $k_1$  and  $k_2$  gave the activation energies of 13.9 and 13.4 kcal/mole for the autoaccelerated reactions of epoxide with primary and secondary amines, respectively. Though overall apparent activation energy for the curing reaction of epoxide with amines has been obtained by measurements of gel time (14–16 kcal/mole),<sup>13,18</sup> viscosity measurements (12–13 kcal/mole),<sup>4</sup> and resistivity techniques (14 kcal/mole),<sup>2,3</sup> the activation energy for elementary reaction of epoxide with amine has not been reported.

Fairly good agreement between activation energies for elementary rate constants and overall apparent activation energy suggests that there may be little differences between activation energies of four rate constants, and that the curing reaction would proceed in the same mechanism as the model reaction and is not controlled by diffusion in the early stage of conversion, in spite of the high viscosity of the system.

### Curing Reaction of Epoxy Resin with Aliphatic Diamines

The curing reaction of epoxy resin (DGEBA) with ethylenediamine, trimethylenediamine, and hexamethylenediamine was carried out at 50, 60, and 70°C.

DSC curves for the isothermal cure of DGEBA with ethylenediamine are shown in Figure 6. Autoacceleration in rate of cure was also observed in these cases. After an isothermal cure in DSC had been completed, a temperature scanning at 4°C/min was carried out on the same sample up to 200°C. As is shown in Figure 7, an exothermic peak due to the postcure of

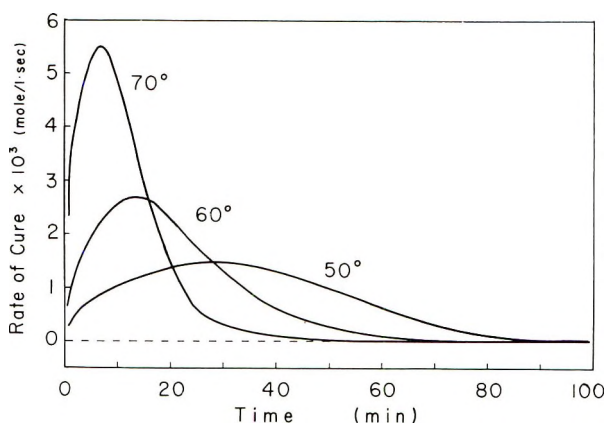


Fig. 6. DSC curves for isothermal cure of DGEBA with ethylenediamine. Reaction temperatures are as indicated.

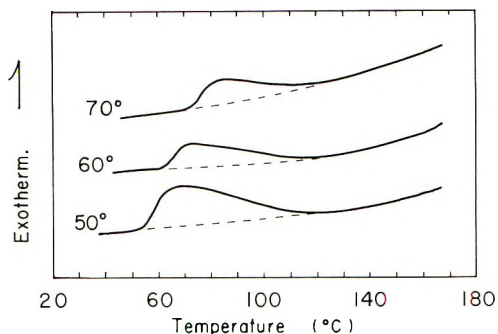


Fig. 7. DSC curves for the postcure by temperature scanning of DGEBA with ethylenediamine. Temperatures of preceding isothermal cure are as indicated.

unreacted functional groups began just at the temperature of isothermal cure. DSC curves with similar tendencies were obtained for isothermal cure and temperature scanning of DGEBA with trimethylenediamine and hexamethylenediamine.

The existence of a peak in each rate curve of isothermal cure suggests the catalytic effect of the reaction products having hydroxyl groups and the third-order kinetics being predominant in the curing reaction of DGEBA with aliphatic diamines.

The reduced rate curves according to eq. (12) for the cure of DGEBA with almost equivalent amount of aliphatic diamines at 50 and 70°C are illustrated in Figure 8, where all parameters representing concentration are expressed in concentration of each functional group instead of molecule. Similar reduced rate curves were obtained for the reactions at 60°C. Straight lines were observed at the first half of conversion for all cases. A sudden decrease in reduced rate at 55–75% conversion is caused by the onset of rate control by the diffusion process of the reactants due to the in-



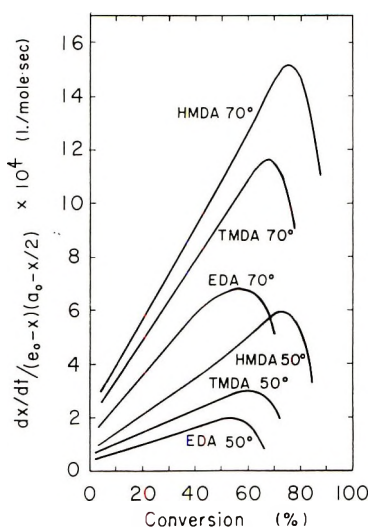


Fig. 8. Reduced rate curves for isothermal cure of DGEBA with ethylenediamine (EDA), trimethylenediamine (TMDA) and hexamethylenediamine (HMDA) at 50 and 70°C. Diamines and reaction temperatures are as indicated.

creased viscosity of the system. The critical conversion for the formation of infinite network is supposed to be 58% for the polycondensation of a bifunctional unit with an equivalent amount of tetrafunctional unit.<sup>19</sup> The curing reaction of DGEBA with ethylenediamine begins to be controlled by diffusion at a conversion corresponding to the formation of infinite net-

TABLE III  
Curing Reaction of DGEBA with Ethylenediamine (EDA),  
Trimethylenediamine (TMDA), and Hexamethylenediamine (HMDA)

Diamine	Mole fraction of diamine	Isothermal cure			Conversion added by temperature scanning, %	Total conversion, %
		Temperature, °C	$k_1 \times 10^4$ , l. <sup>2</sup> /mole <sup>2</sup> -sec	Final conversion, %		
EDA	0.36	50	0.52	67.3	13.5	80.8
EDA	0.38	50	0.57	74.5	—	—
EDA	0.36	60	1.10	77.2	7.1	84.3
EDA	0.38	70	1.90	82.8	4.6	87.4
TMDA	0.35	50	0.71	78.7	13.2	91.9
TMDA	0.36	60	1.56	83.5	10.0	93.5
TMDA	0.33	60	2.06	86.6	—	—
TMDA	0.36	70	2.75	89.2	5.0	94.2
TMDA	0.36	70	2.70	90.7	—	—
HMDA	0.37	50	1.06	90.9	9.1	100
HMDA	0.36	60	2.00	95.1	3.1	98.2
HMDA	0.37	60	2.04	89.2	—	—
HMDA	0.37	70	3.42	100	0	100
HMDA	0.36	70	2.96	94.5	—	—

work. For the cure of DGEBA with more flexible trimethylenediamine or hexamethylenediamine, however, the onset of diffusion control is delayed in comparison with the formation of infinite network.

The values of rate constant  $k_1$  for the chemically controlled region of the curing reaction were determined from the slope of straight lines in Figure 8 and listed in Table III. The rate constant  $k_1$  increases with the increase in the reaction temperature and also in the number of methylene units in diamines.

Activation energies for the reaction of epoxide group in DGEBA with primary amino group in ethylenediamine, trimethylenediamine, and hexamethylenediamine were determined to be 13.2, 13.7, and 12.9 kcal/mole, respectively. These values are considered to be equal to each other and to the values of model reaction of phenyl glycidyl ether with butylamine by taking account of the accuracy of the experiments. Then, the difference in  $k_1$  should be caused by the difference in the preexponential factor.

It is supposed that the steric hindrance by the DGEBA molecule attached to one end of diamine may affect the reactivity of amino group at the another end, and if this should be the case, the influence of the steric hindrance would be greater for diamine with shorter methylene units. The fact that values of  $k_1$  for the cure of DGEBA with diamines are not smaller than those for model reaction would also be explained by the frequent presence of hydroxyl groups belonging to DGEBA in the neighborhood of the reacting amino group.

### Final Conversion of Curing Reaction

The final conversion of the isothermal cure of DGEBA with aliphatic diamines and the conversion added by the temperature scanning were calculated from the area of exothermic peak in DSC curves divided by the heat of epoxide reaction with amine, determined for the model reaction. The results are summarized in Table III and plotted against temperature in Figure 9. The final conversion of isothermal cure increases with the temperature. The increase in the number of methylene units in diamines also provides in increase in the final conversion.

The temperature scanning of isothermally cured samples of DGEBA with ethylenediamine and trimethylenediamine did not force the reaction to completion, although the scanned temperature was raised well beyond the glass transition temperature of the crosslinked system. The isothermal postcure of the samples at 100°C in 2 hr and successively at 160°C in 24 hr gave almost the same results (total conversion of 80–90%) as the postcure by temperature scanning. Hence, it was ascertained that the curing reaction of DGEBA with ethylenediamine and trimethylenediamine does not reach 100% conversion, even by the postcure at elevated temperatures above the glass transition temperature of the system. This fact would be due to the restriction of segmental mobility of main chains and the suppression of segmental diffusion of functional groups by crosslinking. The effect of flexibility of hexamethylene chains seems to have overcome the

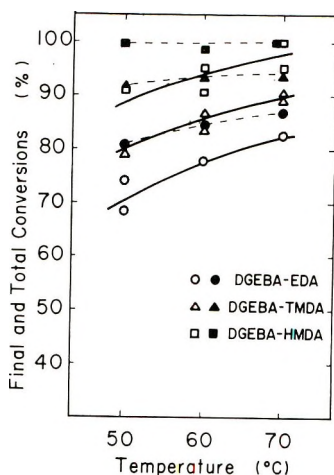


Fig. 9. Final conversion of isothermal cure ( $\circ, \triangle, \square$ ) and total conversion added by temperature scanning ( $\bullet, \blacktriangle, \blacksquare$ ) for the cure of DGEBA with diamines against the temperature of isothermal cure.

effect of the suppression of segmental diffusion by crosslinking in the curing reaction of DGEBA with hexamethylenediamine, where 100% conversion is attained by the temperature scanning of the isothermally cured sample.

The final conversion of isothermal polymerization is considered to be closely related to the transition of the polymer-monomer system from a viscous liquid to a glassy state. This has been confirmed quantitatively for the diffusion-controlled polymerization of methyl methacrylate.<sup>6</sup> In the present paper it is extended to the crosslinked system.

The crosslinking density was evaluated from the concentration of tertiary amino group in the system.

The mole fraction of reacted primary amino group in total amino group ( $q_1$ ) is related to the mole fraction of reacted secondary amino group in total amino group ( $q_2$ ) by eq. (13) and hence eq. (14) according to Kakurai and Noguchi.<sup>20</sup>

$$dq_2/dq_1 = n(q_1 - q_2)/(1 - q_1) \quad (13)$$

$$q_2 = 1 + (1 - q_1)n/(1 - n) - (1 - q_1)^n/(1 - n) \quad (14)$$

The extent of conversion of epoxide group ( $X$ ) is expressed by

$$X = (a_0/e_0)(q_1 + q_2) \quad (15)$$

where  $n$ ,  $a_0$ , and  $e_0$  have the same definitions as in eqs. (7) and (8). On setting  $X$  in eq. (15) equal to the total conversion in Table III and by using eqs. (14) and (15) with  $n = 0.61$  and  $a_0/e_0 = 0.55$ , the value of  $q_2$  and hence the crosslinking density  $\nu$  of the postcured DGEBA were calculated and shown in Table IV.

The glass transition temperatures ( $T_g$ ) of the postcured DGEBA with diamines were measured with DSC. Typical DSC thermograms are shown

TABLE IV  
Glass Transition of DGEBA-Diamine Systems  
Related to the Final Conversion ( $X_f$ )

Diamine	Temperature of isothermal cure, °C	Postcured system		$K$ , g-°C/mmole	Isothermal cure		
		$\nu$ , mmole/g	$T_g$ , °C		$\nu_{T_g}$ , mmole/g	$X_{T_g}$ , %	$(X_f)_{obs.}$ , %
EDA	50	1.62	74		1.22	71	68, 74
EDA	60	1.74	78	52.3	1.41	76	77
EDA	70	1.86	79		1.61	81	83
TMDA	50	2.02	82		1.39	76	79
TMDA	60	2.07	83	46.1	1.61	82	84, 87
TMDA	70	2.10	77		1.82	87	89, 91
HMDA	50	2.20	74		1.62	85	91
HMDA	60	2.15	71	39.5	1.87	91	89, 95
HMDA	70	2.20	72		2.13	98	95, 100

in Figure 10 and values of  $T_g$  are listed in Table IV. Kwei<sup>21</sup> has reported the little lower values of  $T_g$  than ours for the cured DGEBA with ethylenediamine and hexamethylenediamine. By taking account of his curing condition of samples, the difference in  $T_g$  would be caused by the difference in the crosslinking density in both samples. The glass transition temperature of unreacted DGEBA and that of linear copolymer of DGEBA with butylamine prepared from their equimolar mixture were also determined by DSC and found to be  $-32$  and  $-14$ °C, respectively.

As the glass transition temperature of crosslinked polymer ( $T_g$ ) increases with the increase in molecular weight and crosslinking density, it would be reasonable to express  $T_g$  by eq. (16),

$$T_g = T_{g0} + (\Delta T_g)_M + (\Delta T_g)_\nu \quad (16)$$

where  $T_{g0}$  is the  $T_g$  of the unreacted monomer mixture,  $(\Delta T_g)_M$  and  $(\Delta T_g)_\nu$  are the increases in  $T_g$  resulting from an increase in molecular weight and

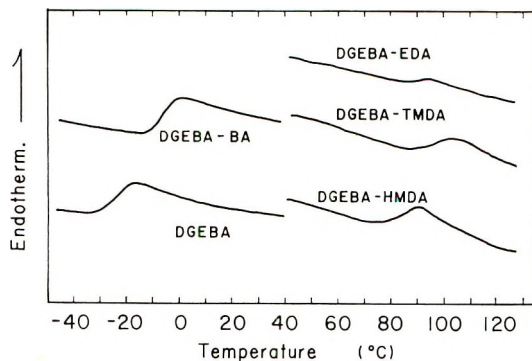


Fig. 10. DSC thermograms of postcured DGEBA with diamines, unreacted DGEBA, and linear copolymer of DGEBA with butylamine (scan rate 8°C/min, range 4).

crosslinking density, respectively. Equation (16) can be transformed to eq. (17), since the linear relationship of  $(\Delta T_g)_\nu$  with  $\nu$  has been established by Fox and Loshaek<sup>22</sup> with the assumption that the volume shrinkage accompanying the formation of each crosslink is constant.

$$T_g = T_{g0} + (\Delta T_g)_M + K\nu \quad (17)$$

Shibayama<sup>23</sup> has proposed the logarithmic relationship between  $(\Delta T_g)_\nu$  and  $\nu$  which is consistent with the linear relationship by Fox and Loshaek for the range of low crosslinking density as appeared in Table IV. Employing the values of  $\nu$  and  $T_g$  for the postcured DGEBA with diamines and taking the sum of  $T_{g0}$  and  $(\Delta T_g)_M$  as  $-14^\circ\text{C}$ , the value of  $K$  was calculated for each DGEBA-diamine system. The assumption that the change in conversion of epoxide is related only to the change in crosslinking density would be reasonable for the later stage of curing reaction where infinite network has already been formed.

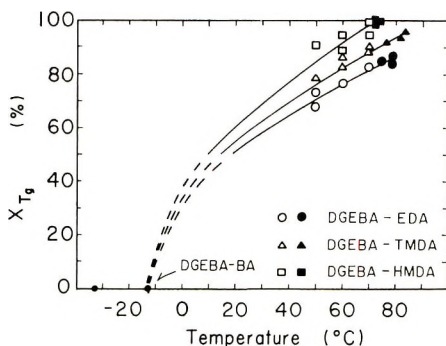


Fig. 11. Calculated relations between  $X_{T_g}$  and the reaction temperature of isothermal cure (solid lines). The experimental results of final conversion ( $\circ, \triangle, \square$ ) and  $T_g$  ( $\bullet, \blacktriangle, \blacksquare$ ) are also illustrated.

The critical crosslinking density at which the system shows a transition from viscous liquid to glass ( $\nu_{T_g}$ ) was then calculated from eq. (17) by setting  $T_g$  in eq. (17) equal to the temperature of isothermal cure and by using the above-indicated values for  $T_{g0} + (\Delta T_g)_M$ , and  $K$ . On introducing the values of  $\nu_{T_g}$  into eqs. (14) and (15), the critical conversion corresponding to the transition of the system from viscous liquid to glass ( $X_{T_g}$ ) was obtained. The calculated values of  $X_{T_g}$  agree well with the final conversion values of isothermal cure ( $X_f$ ) observed from the DSC data, as is shown in Table IV. These results are visualized in Figure 11, where filled symbols are experimental values of  $T_g$ , solid lines represent the change in  $X_{T_g}$  against reaction temperature calculated from eqs. (14), (15), and (17), and open symbols are the experimental results of final conversion. Thus, it would be possible to predict the final conversion for the isothermal cure of epoxy resin with diamines at any reaction temperatures as long as the infinite network is formed.

It is concluded from the above results that the curing reaction of DGEBA with aliphatic diamines proceeds through the third-order mechanism, which is followed by the diffusion-controlled mechanism at the later stage of conversion, and the reaction ceases at a conversion where any segmental diffusion of functional groups is suppressed because of the glass transition of the system. This final conversion will be predicted by calculation based on the theory on the glass transition temperature of crosslinked polymer systems.

### References

1. H. Dannenberg, *SPE J.*, **15**, 875 (1959).
2. J. A. Aukward, R. W. Warfield, and M. C. Petree, *J. Polym. Sci.*, **27**, 199 (1958).
3. B. Miller, *J. Appl. Polym. Sci.*, **10**, 217 (1966).
4. T. Kakurai and T. Noguchi, *Kobunshi Kagaku*, **19**, 547 (1962).
5. H. Dannenberg, *SPE Trans.*, **3**, 78 (1963).
6. K. Horie, I. Mita, and H. Kambe, *J. Polym. Sci. A-1*, **6**, 2663 (1968).
7. K. Horie, I. Mita, and H. Kambe, *J. Polym. Sci. A-1*, **7**, 2561 (1969).
8. G. B. Johnson, P. H. Hess, and R. R. Miron, *J. Appl. Polym. Sci.*, **6**, S19 (1962).
9. R. A. Fava, *Polymer*, **9**, 137 (1968).
10. L. Shechter, J. Wynstra, and R. P. Kurkijy, *Ind. Eng. Chem.*, **48**, 94 (1956).
11. T. Kakurai and T. Noguchi, *Kogyo Kagaku Zasshi*, **63**, 294 (1960).
12. N. S. Isaacs and R. E. Parker, *J. Chem. Soc.*, **1960**, 3497.
13. I. T. Smith, *Polymer*, **2**, 95 (1961).
14. J. F. Harrod, *J. Appl. Polym. Sci.*, **6**, S63 (1962).
15. I. Mita, H. Hiura, K. Horie, and H. Kambe, *Rept. Inst. Space Aeronaut. Sci., Univ. Tokyo*, **4**, 401 (1968).
16. W. C. J. Ross, *J. Chem. Soc.*, **1950**, 2257.
17. C. H. Klute and W. Viehmann, *J. Appl. Polym. Sci.*, **5**, 86 (1961).
18. L. J. Gough and I. T. Smith, *J. Appl. Polym. Sci.*, **3**, 362 (1960).
19. P. J. Flory, *Principles of Polymer Chemistry*, Cornell Univ. Press, Ithaca, N. Y., 1953, p. 348.
20. T. Kakurai and T. Noguchi, *Kogyo Kagaku Zasshi*, **64**, 398 (1961).
21. T. K. Kwei, *J. Polym. Sci. A-2*, **4**, 943 (1966).
22. T. G. Fox and S. Loshaek, *J. Polym. Sci.*, **15**, 371 (1955).
23. K. Shibayama, *Kobunshi Kagaku*, **18**, 181 (1961).

Received October 2, 1969

## Representation of Terpolymer Kinetics on Triangular Coordinates

D. R. CRUISE and R. G. LACOMBE, *Naval Weapons Center, China Lake,  
California 93555*

### Synopsis

The ideal steady-state kinetics of polymer formation from two or more monomeric species can be derived from basic rate equations by using the theory of discrete parameter Markov chains. Advantages are: (1) steady-state assumptions are not required; and (2) a particularly lucid graphical visualization is possible for the case where there are three monomeric species.

### INTRODUCTION

Early work leading to the derivation of the kinetics of polymerization from two or more monomeric species<sup>1</sup> is well known. This derivation usually begins with very sophisticated steady-state assumptions. Indeed, understanding such a process depends more upon an intuitive grasp of these assumptions than upon the derivation.

A derivation leading to the same classic results can be obtained from basic rate equations by using the theory of discrete parameter Markov chains.<sup>2</sup> With the aid of this theory it can be shown that a three-component (terpolymer) process can be represented on a triangular graph in a way that promotes visualization of both the kinetics and the mathematical theory. This representation is possible because of the unique properties of triangular coordinates which have been a subject of recent interest.<sup>3-5</sup>

It will be assumed here that only the end group of a polymer will affect the probability that another specified group will be added to the chain. It will also be assumed that all possible polymerization reactions occur with a finite rate. Otherwise, special considerations beyond the scope of this work would have to be made.

### THEORY

Let the monomeric building blocks be denoted  $M_1$ ,  $M_2$ , and  $M_3$ , and let the polymers be denoted  $\cdot M_1$ ,  $\cdot M_2$ , and  $\cdot M_3$ , where only the terminal unit is identified. A link is added to a chain by one of nine possible reactions.<sup>6</sup>



The reaction rates of these equations are taken to be

$$\xi_{ji} = k_{ji}[\text{M}_i][\cdot\text{M}_j] \quad (2)$$

where  $k_{ji}$  is the rate constant and brackets denote concentration.

The conditional probability that a polymer,  $\cdot\text{M}_j$ , will add a monomer,  $\text{M}_i$ , is equal to the rate at which  $\cdot\text{M}_j$  reacts with  $\text{M}_i$  divided by the total rate at which  $\cdot\text{M}_j$  reacts with all monomers.

$$p(i|j) = \xi_{ji}/(\xi_{j1} + \xi_{j2} + \xi_{j3}) \quad (3)$$

Combining eqs. (2) and (3) yields

$$p(i|j) = k_{ji}[\text{M}_i][\cdot\text{M}_j]/(k_{j1}[\text{M}_1][\cdot\text{M}_j] + k_{j2}[\text{M}_2][\cdot\text{M}_j] + k_{j3}[\text{M}_3][\cdot\text{M}_j]) \quad (4)$$

This may be rewritten

$$p(i|j) = k_{ji}g_i/(k_{j1}g_1 + k_{j2}g_2 + k_{j3}g_3) \quad (5)$$

where  $g_i$  is the monomer mole fraction,

$$g_i = [\text{M}_i]/\sum_{i=1}^3 [\text{M}_i]$$

In certain important cases  $g_i$ , and therefore  $p(i|j)$ , may be considered to be constant. One such case is in the early stages of polymerization, where there is only an insignificant depletion of the monomer feed; another case is where the monomer influx is deliberately controlled; and a third case is the azeotropic situation, where the monomers add to the polymers in proportion to their concentrations. Because these cases include most situations of practical importance,  $p(i|j)$  will be regarded as a constant in the development that follows.

If  $f_i^{(n)}$  is the mole fraction of chains ending in  $\text{M}_i$  after  $n$  steps (superscripts in parentheses are to be distinguished from exponents), then the mole fractions after  $n + 1$  steps are

$$f_1^{(n+1)} = p(1|1)f_1^{(n)} + p(1|2)f_2^{(n)} + p(1|3)f_3^{(n)} \quad (6)$$

$$f_2^{(n+1)} = p(2|1)f_1^{(n)} + p(2|2)f_2^{(n)} + p(2|3)f_3^{(n)} \quad (7)$$

$$f_3^{(n+1)} = p(3|1)f_1^{(n)} + p(3|2)f_2^{(n)} + p(3|3)f_3^{(n)} \quad (8)$$

from a basic rule of conditional probabilities.<sup>7</sup> These may be rewritten in matrix notation

$$\begin{bmatrix} f_1^{(n+1)} \\ f_2^{(n+1)} \\ f_3^{(n+1)} \end{bmatrix} = \begin{bmatrix} p(1|1) & p(1|2) & p(1|3) \\ p(2|1) & p(2|2) & p(2|3) \\ p(3|1) & p(3|2) & p(3|3) \end{bmatrix} \begin{bmatrix} f_1^{(n)} \\ f_2^{(n)} \\ f_3^{(n)} \end{bmatrix} \quad (9)$$

or

$$\mathbf{F}^{(n+1)} = \mathbf{PF}^{(n)} \quad (10)$$

This is the basic equation for a discrete parameter Markov chain, and shows the probable change in composition ( $\mathbf{F}$ ) after one chain-linking step.



The columns of the  $\mathbf{P}$  matrix may be considered the composition trends for the polymer type given by that column. For instance, the first column

$$\begin{array}{l} p(1|1) \\ p(2|1) \\ p(3|1) \end{array}$$

contains the proportions in which polymer type  $\cdot M_1$  tends to add  $M_1$ ,  $M_2$ , and  $M_3$  to the chain. It is only a trend because it must compete with the trends for  $\cdot M_2$  and  $\cdot M_3$ , which are given by the other two columns of the  $\mathbf{P}$  matrix.

The columns of the  $\mathbf{P}$  matrix each sum to one. This may be established from eq. (5) by summing over the index,  $i$ . Therefore, each column may be plotted as a single point on a triangular graph. For example, the columns of the following  $\mathbf{P}$  matrix are plotted at the vertices of the small shaded triangle in Figure 1.

$$\mathbf{P} = \begin{bmatrix} 0.70 & 0.60 & 0.50 \\ 0.20 & 0.35 & 0.25 \\ 0.10 & 0.05 & 0.25 \end{bmatrix}$$

Similarly, any three-by-three matrix will plot as a triangle if its columns sum to one.

Since they are mole fractions, the entries in the column matrix  $\mathbf{F}^{(n)}$  also sum to one and may be plotted as a single point on triangular coordinates.

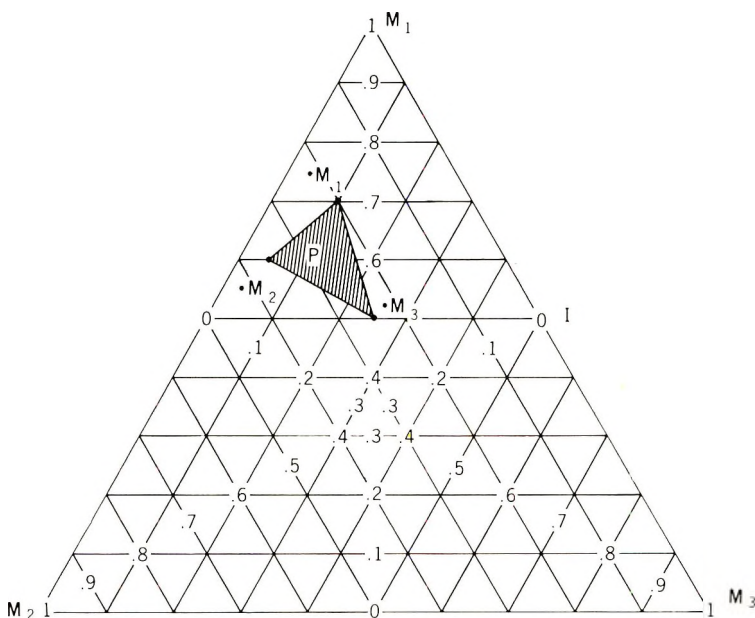


Fig. 1. Matrix  $\mathbf{P}$  on triangular coordinates showing the composition trends due to polymer types  $\cdot M_1$ ,  $\cdot M_2$ , and  $\cdot M_3$ .

It will be shown that many of the properties of  $\mathbf{P}$  and  $\mathbf{F}$  can be graphically depicted to provide an insight into a polymerization process.

The entire triangular grid on which  $\mathbf{P}$  is plotted may be called  $\mathbf{I}$  because it is the representation of the identity matrix

$$\begin{bmatrix} 1 & 0 & 0 \\ 0 & 1 & 0 \\ 0 & 0 & 1 \end{bmatrix} = \mathbf{I} \quad (11)$$

Note that the columns of this matrix are plotted at the vertices of the triangular grid.

A composition point,  $\mathbf{F}^{(n)}$ , can be expressed as the product of itself with the identity matrix.

$$\mathbf{F}^{(n)} = \begin{bmatrix} 1 & 0 & 0 \\ 0 & 1 & 0 \\ 0 & 0 & 1 \end{bmatrix} \begin{bmatrix} f_1^{(n)} \\ f_2^{(n)} \\ f_3^{(n)} \end{bmatrix}$$

In expanded form, this product is

$$\mathbf{F}^{(n)} = f_1^{(n)} \begin{bmatrix} 1 \\ 0 \\ 0 \end{bmatrix} + f_2^{(n)} \begin{bmatrix} 0 \\ 1 \\ 0 \end{bmatrix} + f_3^{(n)} \begin{bmatrix} 0 \\ 0 \\ 1 \end{bmatrix} \quad (12)$$

which is more simply written

$$\mathbf{F}^{(n)} = f_1^{(n)} \mathbf{V}_1 + f_2^{(n)} \mathbf{V}_2 + f_3^{(n)} \mathbf{V}_3 \quad (13)$$

where  $\mathbf{V}_i$  (for vertex) denotes the columns of  $\mathbf{I}$ . Equation (13) may be multiplied on both sides by  $\mathbf{P}$  to obtain

$$\mathbf{F}^{(n+1)} = f_1^{(n)} \begin{bmatrix} 0.70 \\ 0.20 \\ 0.10 \end{bmatrix} + f_2^{(n)} \begin{bmatrix} 0.60 \\ 0.35 \\ 0.05 \end{bmatrix} + f_3^{(n)} \begin{bmatrix} 0.50 \\ 0.25 \\ 0.25 \end{bmatrix}$$

or

$$\mathbf{F}^{(n+1)} = f_1^{(n)} \mathbf{V}_1' + f_2^{(n)} \mathbf{V}_2' + f_3^{(n)} \mathbf{V}_3' \quad (14)$$

where the  $\mathbf{V}_i'$  are the columns of the matrix  $\mathbf{P}$ . It is apparent—note the similarity of eqs. (13) and (14)—that the point  $\mathbf{F}^{(n+1)}$  has the same relationship to the vertices of the triangle  $\mathbf{P}$  that the point  $\mathbf{F}^{(n)}$  has to the triangle  $\mathbf{I}$ . Geometrically,  $\mathbf{F}^{(n+1)}$  occupies the same position within the triangle  $\mathbf{P}$  that  $\mathbf{F}^{(n)}$  occupies within the triangle  $\mathbf{I}$ , as shown in Figure 2.

Equation (10) may be repeated for successive steps

$$\mathbf{F}^{(n+1)} = \mathbf{P}\mathbf{F}^{(n)}$$

$$\mathbf{F}^{(n+2)} = \mathbf{P}\mathbf{F}^{(n+1)}$$

Combining these

$$\mathbf{F}^{(n+2)} = \mathbf{P}^2\mathbf{F}^{(n)} \quad (15)$$

Proceeding further, eq. (15) may be generalized to

$$\mathbf{F}^{(n)} = \mathbf{P}^n \mathbf{F}^{(0)} \quad (16)$$

where  $\mathbf{F}^{(0)}$  denotes the mole fractions of active monomers which initiate the chain building processes. (Here, the exponent of  $\mathbf{P}$  denotes raising that matrix to the power of  $n$ .)

The second and higher powers of a matrix also may be represented on triangular coordinates. The matrix  $\mathbf{P}^2$  is simply the matrix  $\mathbf{P}$  plotted on the coordinate system of  $\mathbf{P}$ . The matrix  $\mathbf{P}^3$  is the matrix  $\mathbf{P}$  plotted on the

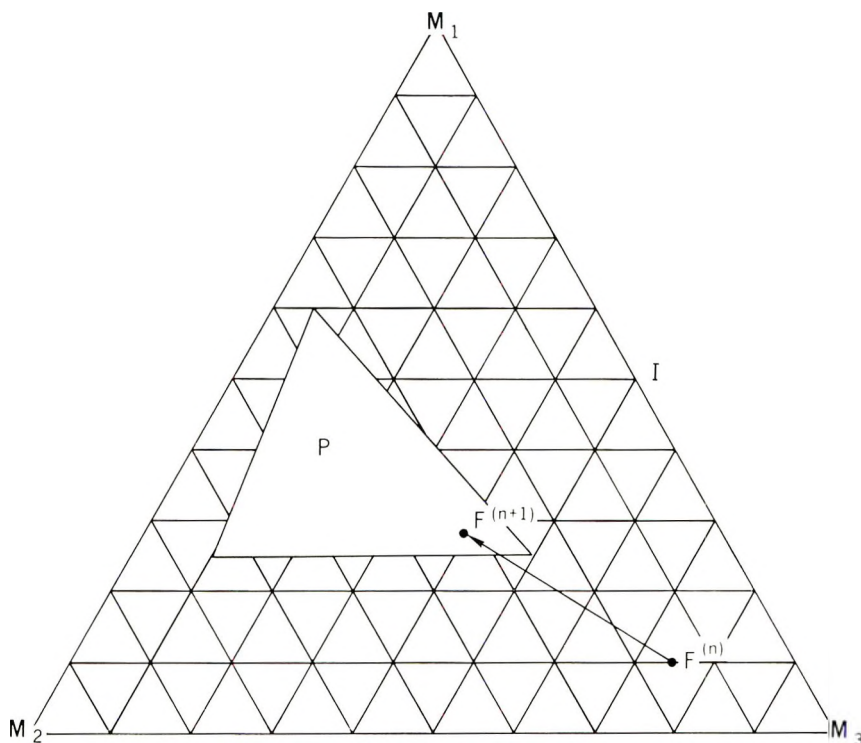


Fig. 2. Matrix relationship  $\mathbf{P}\mathbf{F}^{(n)} = \mathbf{F}^{(n+1)}$  showing the probable change in composition due to a single chain linking step.

coordinate system of  $\mathbf{P}^2$ , and so on. Figure 3 graphically illustrates that  $\mathbf{P}^2$  is oriented within  $\mathbf{P}$  as  $\mathbf{P}$  is oriented within  $\mathbf{I}$ .

Except for some special cases which will be discussed later, Figure 3 shows how terpolymerization approaches a steady-state condition. It can be seen that  $\mathbf{P}^n$  and the point  $\mathbf{F}^{(n)}$  within it converge to a single point; this is the steady state, or equilibrium point, and is the point that will describe the composition of a polymer after a large number of steps have occurred. Obviously, the smaller  $\mathbf{P}$  is with respect to  $\mathbf{I}$ , the fewer the steps required to approach steady state.

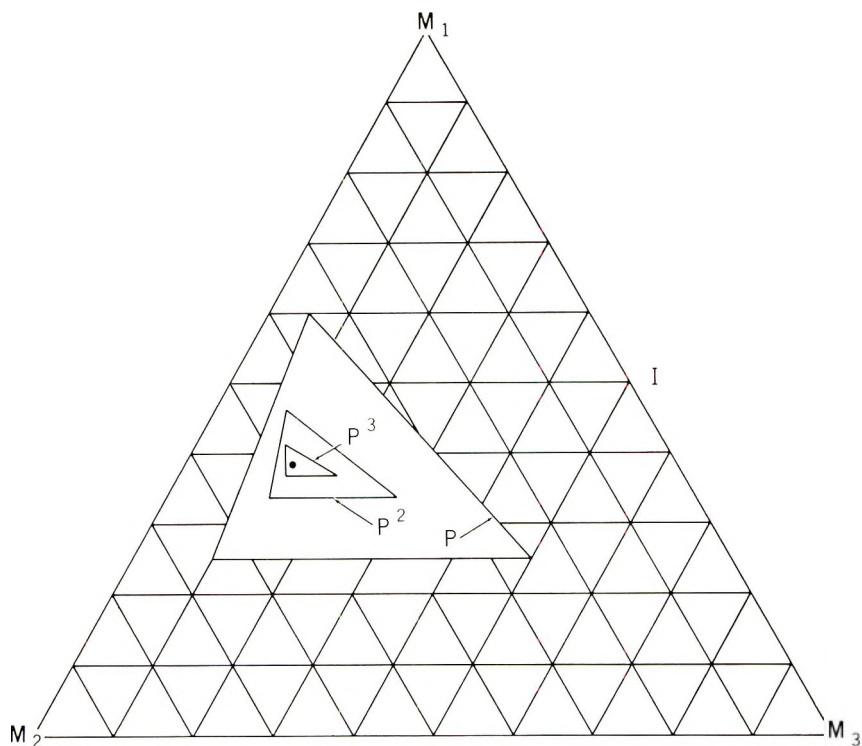


Fig. 3. The powers of a matrix showing convergence toward a single composition point.

Because of the convergence of  $\mathbf{P}^n$  and  $\mathbf{F}^{(n)}$ , the value of  $\mathbf{F}^{(n)}$  approaches that of  $\mathbf{F}^{(n+1)}$  as  $n$  becomes large.

$$\lim_{(n \rightarrow \infty)} \mathbf{P}\mathbf{F}^{(n)} = \lim_{(n \rightarrow \infty)} \mathbf{F}^{(n)} \quad (17)$$

or

$$\mathbf{P}\mathbf{F}^{(\infty)} = \mathbf{F}^{(\infty)} \quad (18)$$

Equation (18) may be considered a basic equation for steady-state terpolymer formation (its relation to better known forms of the terpolymer equation will be presented in the Discussion section).

Whenever the relation  $\mathbf{P}\mathbf{F}^{(\infty)} = \lambda\mathbf{F}^{(\infty)}$  holds, where  $\lambda$  is a scalar constant (here equal to one),  $\mathbf{F}^{(\infty)}$  is called an eigenvector. Graphically, an eigenvector is a single point having the same coordinates in both  $\mathbf{P}$  and  $\mathbf{I}$  (Fig. 4).

The certain special cases of steady state terpolymer formation mentioned previously deserve brief discussion. Consider the situation where a polymer,  $\cdot M_1$ , will add only a like monomer,  $M_1$ . The  $\mathbf{P}$  matrix in this case will be

$$\begin{bmatrix} 1 & p(1|2) & p(1|3) \\ 0 & p(2|2) & p(2|3) \\ 0 & p(3|2) & p(3|3) \end{bmatrix}$$

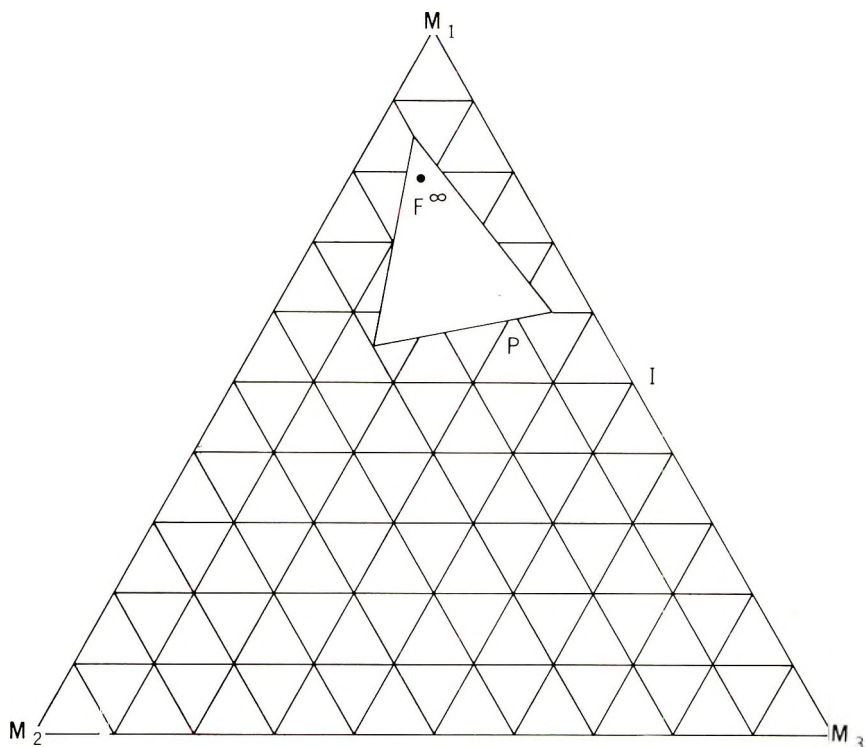


Fig. 4. The eigenvector property; the steady-state composition,  $F^\infty$ , has the same geometric relationship to both  $\mathbf{P}$  and  $\mathbf{I}$ .

Note that the first vertex of  $\mathbf{P}$  corresponds to the first vertex of  $\mathbf{I}$  (Fig. 5). In this case,  $\cdot M_1$  is an absorption state,<sup>2</sup> or "sink." Once a chain acquires an  $M_1$  link, it will always end in  $M_1$ . Except for negligibly few  $M_2$  and  $M_3$  links near the start, the polymer formed will consist entirely of  $M_1$ .

There also exists the possibility of two sinks (e.g., if  $\cdot M_1$  adds only  $M_1$ , and  $\cdot M_2$  adds only  $M_2$ ). Here  $\mathbf{P}$  is

$$\begin{bmatrix} 1 & 0 & p(1|3) \\ 0 & 1 & p(2|3) \\ 0 & 0 & p(3|3) \end{bmatrix}$$

and two  $\mathbf{P}$  vertices coincide with their corresponding  $\mathbf{I}$  vertices (Fig. 6). In this case, the  $\mathbf{P}^n$  triangle never approaches a single point because one side never shrinks. Some polymers consisting almost entirely of  $M_1$ , and some consisting almost entirely of  $M_2$  will be formed. The amounts of each type of polymer formed depend upon the number of active monomers ( $f_1^{(0)}, f_2^{(0)}, f_3^{(0)}$ ) that form the first link of a chain. This is a departure from the cases previously cited, where the steady state is completely independent of  $f_1^{(0)}, f_2^{(0)}$ , and  $f_3^{(0)}$ . When two or more sinks exist, eq. (18) is not valid.

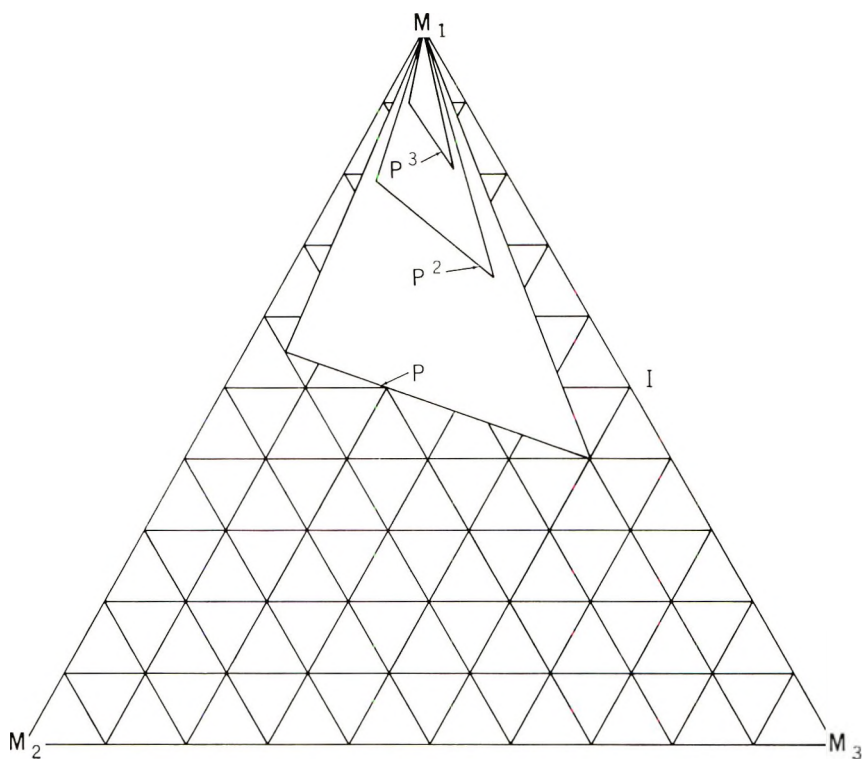


Fig. 5. Relationship of **I**, **P**, and **P**<sup>2</sup> when a common vertex exists ( $\cdot$   $M_1$  adds only  $M_1$ ) showing convergence toward the vertex point, which represents a polymer of pure  $M_1$ .

Another special case is that for which the area of the triangle approaches zero (Fig. 7). The steady-state result is still that of eq. (18), but visualization is difficult because the triangle has collapsed.

### DISCUSSION

Monomer reactivity ratios are generally defined in terms of rate constants:

$$\begin{aligned}
 r_{12} &= k_{11}/k_{12} \\
 r_{21} &= k_{22}/k_{21} \\
 r_{31} &= k_{33}/k_{31} \\
 r_{11} &= r_{22} = r_{33} = 1 \\
 r_{13} &= k_{11}/k_{13} \\
 r_{23} &= k_{22}/k_{23} \\
 r_{32} &= k_{33}/k_{32}
 \end{aligned}$$

In terms of these ratios and the monomer mole fractions  $g_i$ , the probability equation (5) becomes

$$p(i|j) = \frac{(g_i/r_{ji})}{(g_1/r_{j1}) + (g_2/r_{j2}) + (g_3/r_{j3})} \quad \begin{matrix} 1 \leq i \leq 3 \\ 1 \leq j \leq 3 \end{matrix} \quad (19)$$

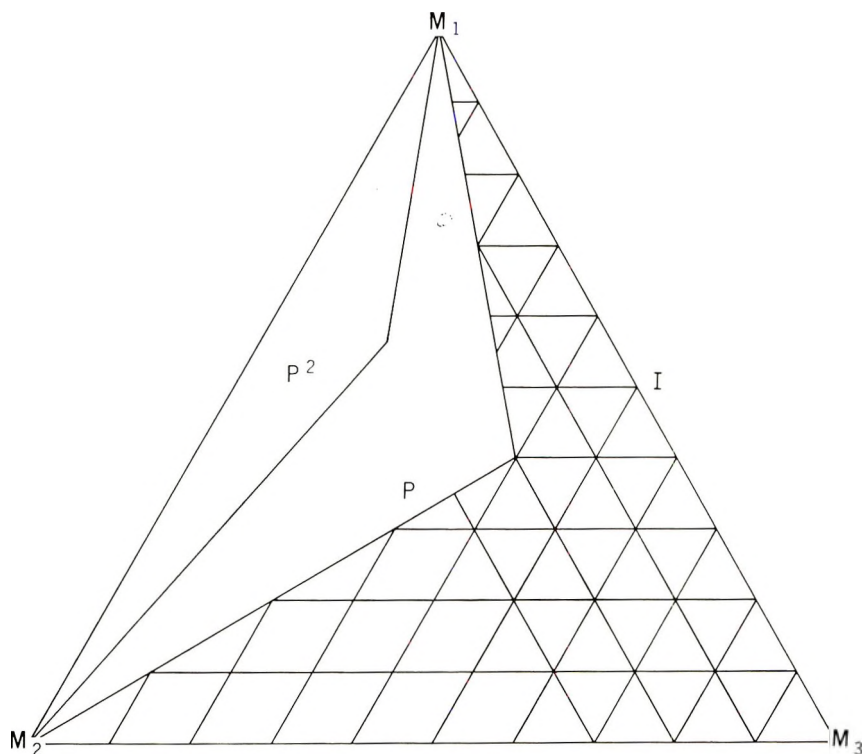


Fig. 6. Relationship of **I**, **P**, and **P<sup>2</sup>** when two vertices are common to each triangle ( $\cdot M_1$  adds only  $M_1$  and  $\cdot M_2$  adds only  $M_2$ ). The steady-state composition cannot be determined.

Equation (19) may be combined with eq. (18), the steady-state condition, to obtain the usual forms of the copolymer and terpolymer equations. Equation (18) is expanded

$$p(1|1)f_1 + p(1|2)f_2 + p(1|3)f_3 = f_1 \quad (20)$$

$$p(2|1)f_1 + p(2|2)f_2 + p(2|3)f_3 = f_2 \quad (21)$$

$$p(3|1)f_1 + p(3|2)f_2 + p(3|3)f_3 = f_3 \quad (22)$$

By using the relation  $p[1|j] + p[2|j] + p[3|j] = 1$ , these equations may be rewritten

$$[-p(2|1) - p(3|1)]f_1 + p(1|2)f_2 + p(1|3)f_3 = 0 \quad (23)$$

$$p(2|1)f_1 + [-p(1|2) - p(3|2)]f_2 + p(2|3)f_3 = 0 \quad (24)$$

$$p(3|1)f_1 + p(3|2)f_2 + [-p(1|3) - p(2|3)]f_3 = 0 \quad (25)$$

In the copolymer case—where  $g_3$  is zero and therefore  $f_3$ ,  $p(3|1)$ , and  $p(3|2)$  are zero—eqs. (23) and (24) both reduce to

$$p(2|1)f_1 = p(1|2)f_2 \quad (26)$$

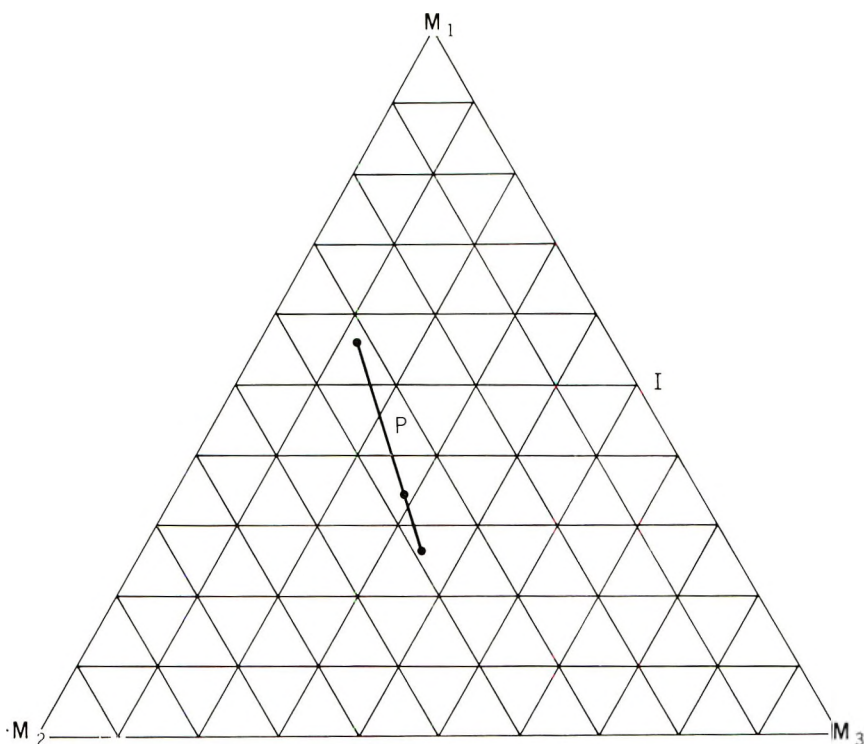


Fig. 7. A case where the **P** triangle has no area.

into which eq. (19) may be substituted

$$g_2 f_1 / (r_{12} g_1 + g_2) = g_1 f_2 / (g_1 + r_{21} g_2) \quad (27)$$

Finally, the polymer mole fractions may be related to the monomer mole fractions

$$\frac{f_1}{f_2} = \frac{r_{12}(g_1/g_2) + 1}{r_{21}(g_2/g_1) + 1} \quad (28)$$

This familiar form of the copolymer equation, with information from two or more copolymer experiments, allows one to obtain numerical values for  $r_{12}$  and  $r_{21}$ .<sup>8</sup>

Returning to the more general terpolymer case, eqs. (20) and (21) can be combined to eliminate  $f_3$ .

$$\frac{f_1}{f_2} = \frac{p(1|2)p(1|3) + p(2|3)p(1|2) + p(3|2)p(1|3)}{p(2|1)p(2|3) + p(1|3)p(2|1) + p(3|1)p(2|3)} \quad (29)$$

A similar manipulation of eqs. (23) and (25) to eliminate  $f_2$  gives

$$\frac{f_1}{f_3} = \frac{p(1|2)p(1|3) + p(2|3)p(1|2) + p(3|2)p(1|3)}{p(3|1)p(3|2) + p(1|2)p(3|1) + p(2|1)p(3|2)} \quad (30)$$

These are the terpolymer equations presented by Ham.<sup>9</sup>

This document has been approved for public release.



### References

1. T. Alfrey, Jr., and G. Goldfinger, *J. Chem. Phys.*, **12**, 205 (1944).
2. E. E. Parzen, *Stochastic Processes*, Holden-Day, San Francisco, 1967, Chap. 6.
3. H. Scheffé, *J. Roy. Statist. Soc.*, **B20**, 344 (1958).
4. I. S. Kurotori, *Ind. Quality Control*, **22**, 592 (May 1966).
5. D. R. Cruise, *J. Chem. Ed.*, **43**, 30 (January 1966).
6. T. Alfrey, Jr., and G. Goldfinger, *J. Chem. Phys.*, **12**, 322 (1944).
7. E. Parzen, *Modern Probability Theory and Its Application*, Wiley, New York, 1960, p. 137.
8. F. W. Billmeyer, Jr., *Textbook of Polymer Science*, Interscience, New York, 1962, pp. 314-315.
9. G. E. Ham, *Copolymerization*, Interscience, New York, 1964, p. 38.

Received July 28, 1969

Revised October 28, 1969

## Quinone Copolymerization. I. Reactions of *p*-Chloranil, *p*-Benzoquinone, and 2,5-Dimethyl-*p*-benzoquinone with Vinyl Monomers under Free-Radical Initiation

C. F. HAUSER\* and NATHAN L. ZUTTY, *Union Carbide Corporation, Chemicals and Plastics, South Charleston, West Virginia 25303*

### Synopsis

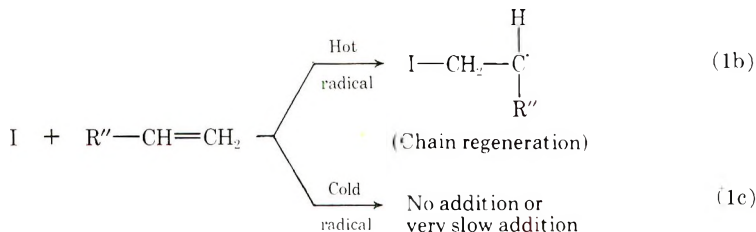
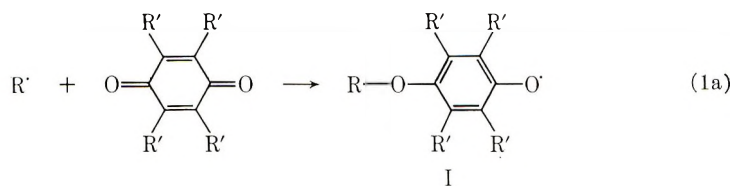
The free-radical copolymerization reactions of *p*-chloranil, *p*-benzoquinone, and 2,5-dimethyl-*p*-benzoquinone with vinyl monomers were studied. Reactions of *p*-chloranil with styrene yielded copolymers of approximately 1:1 composition under a variety of reaction conditions. A copolymer containing a block of 1:1 of styrene:*p*-chloranil and a block of polystyrene was prepared. Several styrene-like monomers copolymerized with *p*-chloranil to yield copolymers possessing considerable amounts of incorporated quinone. *p*-Benzoquinone copolymerized with 1,3-butadiene and 2-vinyl-pyridine to yield copolymers of significant molecular weights. Reactions of 2,5-dimethyl-*p*-benzoquinone with vinyl monomers did not yield any isolable polymeric products.

### INTRODUCTION

Quinones have long been associated with polymer chemistry as retarders or inhibitors to free radical vinyl polymerization. Consensus has been that quinones retard by addition to radicals, forming relatively stable semiquinones (I) which do not add to vinyl monomer [eq. (1a)]. Some recent publications on the inhibition of vinyl polymerization by quinones, however, have demonstrated that semiquinones (I) once formed do not always assume a passive role. Indeed, some of these species were active enough to add to certain vinyl monomers and to a very limited extent, regenerate polymer chains.<sup>1-4</sup> Although the quinone/monomer ratios in the regenerated chains were minute, the quinones were incorporated within the chains and not present solely as endgroups.

More recently, Tudos<sup>5</sup> studied the inhibition to vinyl polymerization by certain quinones and observed the occasional incorporation of quinone into the polymer products. As an explanation for the incorporation phenomenon, Tudos invoked the hypothesis of "hot radicals" in solution. In this hypothesis, a vibrationally-hot semiquinone [I, of eq. (1a)], generated via

\* To whom inquiries should be addressed.



reaction of quinone with radical, may use its excess energy either for reaction with vinyl monomer and generation of the polymer chain [eq. (1b)] or transfer that energy to the medium and yield an inactive (cold) radical [eq. (1c)].

Whatever the exact nature of chain propagation, the above facts and hypothesis implies that under the proper conditions considerably larger concentrations of quinones could be incorporated into polymer backbones than have been observed to date. Indeed, the proper combination of quinones, vinyl monomers, and reaction conditions might bring about a high degree of copolymerization and, as a primary goal, the direct formation of aromatic-aliphatic polyethers,  $\left[ \text{O}-\text{C}_x\text{H}_y-\text{CH}_2-\underset{\text{Z}}{\text{CH}} \right]_n$ . We have re-

acted a number of quinones with selected vinyl monomers under free-radical, vinyl polymerization conditions and are reporting some of our observations in this paper.

## EXPERIMENTAL

### Materials

The quinones were purchased and purified by threefold recrystallization from dry toluene or benzene, followed by two vacuum sublimations. The vinyl monomers were purified by distillation through a spinning band distillation column or by repeated recrystallization from dry solvents. The solvents were dried over 4-A molecular sieves (product of Union Carbide Corporation) and distilled through a spinning band column.

### Polymerization Procedures

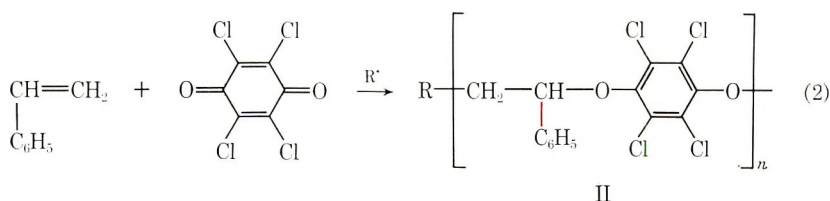
While under a nitrogen atmosphere, pressure tubes were charged with reactants, solvent (if other than vinyl monomer), and catalyst. The tubes were capped and placed in a rotating, constant temperature bath. Upon completion of the desired reaction periods, the contents of each tube were

mixed with enough benzene (dimethyl sulfoxide or *N,N*-dimethylformamide if the polymer was insoluble in benzene) to give a pourable solution, and insoluble quinone was removed by filtration. The benzene filtrate was poured with stirring into a large excess of methanol, and the precipitated product, if any, collected by filtration. Final purification was accomplished by solution and precipitation (3 times) from benzene (or DMF)/methanol, whereupon the product was dried *in vacuo* at 40°C for 24 hr. Reduced viscosities were measured in a Ubbelohde viscometer at 25°C.

## RESULTS

### Reactions of *p*-Chloranil with Styrene

Some years ago Breitenbach<sup>6</sup> reported the bulk copolymerization of *p*-chloranil with styrene to yield a copolymer of 21 000 number-average molecular weight and a structure approximating a 1:1 alternating styrene:*p*-chloranil (II). Breitenbach postulated that the quinone entered the polymer *via* its carbonyl groups to afford the aromatic-aliphatic polyether II [eq. (2)].



We have attempted, by variation of reaction conditions, to prepare copolymers of the type II of higher molecular weight than reported in the above reference. In this attempt, we were unsuccessful. We did show, however, that copolymers of approximate 1:1 structures could be prepared from styrene and *p*-chloranil under a variety of reaction conditions. The data for these experiments are recorded in Table I, wherein styrene was utilized both as reactant and solvent by being present in 4:1 molar excess to the quinone.

The effect of *p*-chloranil purity upon the copolymer yield and reduced viscosity is demonstrated by experiments 1 and 2. With the exception of the latter experiment, the *p*-chloranil utilized in this paper was purified by threefold recrystallization from dry toluene, followed by two vacuum sublimations. The sublimations were necessary because the last traces of 2,3,5,6-tetrachlorohydroquinone could not be removed by recrystallization, as evidenced by the presence of minute amounts of the fluffy material always present in the recrystallized quinone.

Recrystallized and sublimed *p*-chloranil was utilized in experiment 1, wherein after 18 hr at 70°C (benzoyl peroxide initiator) a copolymer of reduced viscosity 0.19 (benzene) was obtained in 61% yield. Under similar conditions threefold recrystallized, but unsublimed, *p*-chloranil provided a

TABLE I  
 Copolymerization Reactions of *p*-Chloranil with Styrene under Free-Radical Conditions<sup>a</sup>

Expt. no.	Temp, °C	Time, hr	Initiator		Yield, % <sup>e</sup>	Reduced viscosity (benzene)	Chlorine, % <sup>d</sup>	Copolymer composition <sup>f</sup>
			Type	Concn, mole-% <sup>b</sup>				
1	70	18	BzO <sub>2</sub>	2.2	61	0.19	38.11	1.22
2	70	18	BzO <sub>2</sub>	2.2	6	0.08	37.16	1.32
3	70	18	BzO <sub>2</sub>	1.3	48	0.10	38.00	1.23
4	70	18	BzO <sub>2</sub>	0.25	3	0.10	37.38	1.29
5	50	44	AIBN	1.3	23	0.14	39.71	1.08
6	60	44	AIBN	1.3	41	0.14	39.47	1.10
7	40	110	Ac peroxide	1.3	6	0.10	37.92	1.24
8	110	52	<i>t</i> -Bu peroxide	1.3	4	0.04	34.62	1.59
9	40	110	Lupersol 11 <sup>e</sup>	1.3	41	0.19	37.57	1.27
10	70	88	BzO <sub>2</sub>	1.3	99	0.33	20.64	4.23

<sup>a</sup> Unless otherwise noted, *p*-chloranil recrystallized three times from dry toluene and sublimed twice, and styrene used in 4:1 molar ratio to *p*-chloranil.

<sup>b</sup> Catalysts concentrations in mol % based upon moles of *p*-chloranil.

<sup>c</sup> Yields based upon *p*-chloranil.

<sup>d</sup> Elemental analyses conducted at Union Carbide.

<sup>e</sup> *tert*-Butyl peroxyvalate.

<sup>f</sup> Calculated from elemental analysis as molar ratio of styrene:*p*-chloranil.

copolymer of reduced viscosity 0.08 in only 6% yield. Apparently, the small quantity of hydroquinone present in the second experiment was sufficient to retard the copolymerization reaction and significantly reduce the chain length of the resulting copolymer. On the basis of Tudos' postulate,<sup>5</sup> hydrogen atom transfer from the hydroquinone to "hot" semiquinone (I, R' = Cl) could have reduced the number and length of growing polymer chains.

The copolymer of reduced viscosity of 0.19 (expt. 1) was shown by osmotic pressure (chlorobenzene solution) to possess a molecular weight of 15 900 or a DP of about 45 (based upon an alternating structure). Elemental analysis for chlorine corresponded to an incorporation of 1.22 equivalents of styrene per equivalent of *p*-chloranil.

A comparison of experiment 1 with experiments 3 and 4 shows the influence of initiator concentration (benzoyl peroxide) upon the yields and properties of the copolymers. In contrast to the 2.2 mole-% utilized in the first experiment, a concentration of 1.3 mole-% (expt. 3) afforded a copolymer of reduced viscosity 0.10 in 48% yield. Further reduction of initiator concentration to 0.25 mole-% (expt. 4) provided a copolymer in only 3% yield, but of similar reduced viscosity (R.V. = 0.10). Although the yields diminished directly with decreasing initiator concentration, the copolymer molecule weights fell to a minimum value corresponding to a reduced viscosity of 0.10 and remained at that point. It is interesting to note that throughout the range of initiator concentrations, the compositions of the resulting copolymers remained nearly constant. Concentrations of 2.2, 1.3, and 0.25 mole-% afforded copolymers of 1.22, 1.23, and 1.29 equivalents of styrene per equivalent of *p*-chloranil, respectively.

Experiments 5-9 show the reactions of styrene with *p*-chloranil under initiation by free-radical generators other than benzoyl peroxide. In experiments 5 and 6, azoisobutyronitrile (AIBN) was used at 50 and 60°C, respectively, to afford copolymers of reduced viscosity 0.14 and of similar composition. The only apparent difference in the two reaction products was the 2-fold increase in yield accompanying the increase in reaction temperature from 50°C to 60°C. Interestingly, chlorine analysis indicates more nearly 1:1 copolymer structure than was obtained with benzoyl peroxide as initiator.

Initiation by acetyl peroxide (expt. 7) and *tert*-butyl peroxide (expt. 8) provided copolymer products in only 6% and 4% yields, respectively. The acetyl peroxide product (R.V. = 0.10) contained styrene and *p*-chloranil in 1.24 mole ratio, whereas the product from *tert*-butyl peroxide (RV = 0.4) possessed a ratio of 1.59. The latter product contained a somewhat larger amount of incorporated styrene than was provided by prior initiators. The low yield of relatively low molecular weight copolymer may be indicative of a ceiling temperature in the vicinity of the reaction temperature (110°C) which in the process of chain propagation and "un-zipping" could have allowed the preferential build-up of styrene at the expense of *p*-chloranil.

Lupersol 11 (*tert*-butyl peroxyvalate) was used as initiator in experiment 9 to afford a copolymer of reduced viscosity 0.19 in 41% yield. Elemental analysis for chlorine showed this copolymer to have a similar composition to those prepared under initiation by benzoyl peroxide. From a preparative viewpoint, therefore, Lupersol 11 at 40°C, AIBN at 60°C, and benzoyl peroxide at 70°C are suitable initiator types and reaction temperatures for the bulk copolymerization of styrene with *p*-chloranil.

The final experiment in Table I was carried out at 70°C in the presence of benzoyl peroxide with a 16:1 molar excess of styrene:*p*-chloranil (experiments 1-9 utilized a 4:1 molar excess). Unlike the previous experiments, wherein some quinone remained undissolved even at 70°C, complete solution was effected by this concentration of styrene at the reaction temperature. During the 88-hr reaction period, the reaction material underwent a change from a bright orange-colored, nonviscous solution to a pale yellow-colored, viscous solution. The disappearance of the initial orange color, the color of *p*-chloranil in solution, indicated that all the free quinone had been consumed. In experiments 1-9, the reaction products still possessed bright orange colors. Workup of the reaction product from Experiment 10 afforded a 99% yield (based on *p*-chloranil and 4.23 equivalents of styrene per equivalent of *p*-chloranil) of polymer of reduced viscosity 0.33. The high concentration of incorporated styrene probably means that the product was a mixture of styrene/*p*-chloranil copolymer plus polystyrene. Styrene and *p*-chloranil copolymerized in a ratio of 1.2 (1.3):1.0, respectively, in a 4-fold molar excess of styrene, and a similar copolymerization ratio would seem logical with a 16-fold excess. One would assume, therefore, that the two monomers copolymerized in an alternating fashion until most or all of the *p*-chloranil had been consumed, whereupon styrene homopolymerization prevailed. In such a reaction sequence, a block polymer would have been formed which contained blocks of 1.2(1.3):1.0 of styrene:*p*-chloranil and blocks composed largely of polystyrene. The dilution effect by styrene provided a somewhat less brittle product than is characteristic of the alternating copolymer, but considerably more brittle than polystyrene of similar reduced viscosity. Indeed, the copolymer product was too brittle to be shaped into a plaque and subjected to a stiffness-temperature determination.

It is of interest to note that all the polymer products of Table I possessed a strong, broad absorption in the infrared from 9.4 to 10.4  $\mu$  with an apex at 10.1  $\mu$ .<sup>7</sup> This similarity indicates a uniformity in product structure. The absorption was somewhat weaker for the product from experiment 10 (high styrene incorporation) than for the other copolymers, but nevertheless that product possessed a definite apex at 10.1  $\mu$ . This absorption arises most probably from the aliphatic-aromatic ether linkage but is seen at a somewhat longer wavelength than expected. The influence of four nuclear chlorine atoms of the *p*-chloranil residue may account for the longer wavelength.<sup>7</sup>

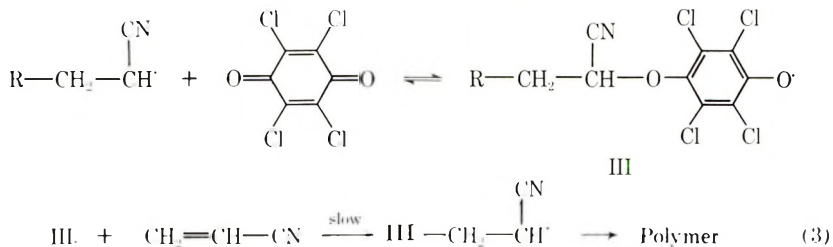
### Reactions of *p*-Chloranil with Vinyl Monomers Other than Styrene

The copolymerization reactions of *p*-chloranil with a number of vinyl monomers are recorded in Table II. In experiments 1, 2, and 3, acrylonitrile was reacted in 4:1 molar excess to quinone at 40, 70, and 110°C, respectively, to yield products containing small amounts of incorporated quinone. The intrinsic viscosities of these products diminished progressively from 4.07 to 1.18 to 0.34 with increasing reaction temperatures. Apparently the quinone became a better polymerization retarder at higher temperature, due at least in part to its increased solubility in acrylonitrile.

The copolymer from the 70°C reaction,  $[\eta] = 1.18$ , was analyzed for incorporated *p*-chloranil by use of the Mark-Houwink relationship<sup>8</sup> (calculations based upon polyacrylonitrile). The analysis indicated a weight-average molecular weight of 86,970, corresponding to a DP of about 1,640, which in consideration of the chlorine analysis shows that nine *p*-chloranil molecules had been incorporated into an average polymer chain. Although nine molecules per chain represents only a 0.6 mole-% copolymerization, it does provide evidence that the *p*-chloranil actually was incorporated into the polymer backbone rather than functioning solely as an inhibitor and being present only as end groups.

The weight-average molecular weights were also calculated for the products from the 40°C and 110°C experiments. Molecular weights of 453,200 and 16,500 were obtained, respectively, which correspond to degree of polymerizations of 8550 and 300. These data, together with the elemental chlorine analyses, indicates that 21 molecules of *p*-chloranil were incorporated per average chain at 40°C and 17 molecules per average chain at 110°C.

*p*-Chloranil could have been incorporated into the acrylonitrile chain by way of its carbonyl groups to form a polyether linkage. We surmise that the acrylonitrile underwent homopolymerization until the growing chain reacted with a *p*-chloranil molecule to interrupt the homopolymer sequence and form the semiquinone III. This oxygen radical could have unzipped to yield the growing chain of the homopolymer and *p*-chloranil, or it



could have undergone a slow addition with acrylonitrile [eq. (3)]. The latter route would have led again to a carbon radical and a relatively rapid chain growth of the homopolymer.

A random incorporation of *p*-chloranil appears to have taken place over the temperature range of 40–110°C. The lowest number of incorporated



TABLE II  
Reactions of *p*-Chloranil with Vinyl Monomers other than Styrene<sup>a</sup>

Expt. no.	Monomer	Temp, °C	Time, hr	Solvent <sup>b</sup>	Initiator <sup>c</sup>	Yield, %	R.V. (solvent)	Chlorine, % <sup>d</sup>
1	Acrylonitrile	40	90	Monomer	Ac peroxide	24 <sup>e</sup>	4.07(DMF) <sup>f</sup>	0.68
2	Acrylonitrile	70	18	Monomer	BzO <sub>2</sub>	80 <sup>e</sup>	1.18(DMF) <sup>f</sup>	1.59
3	Acrylonitrile	110	52	Monomer	<i>t</i> -Bu peroxide	23 <sup>e</sup>	0.34(DMF) <sup>f</sup>	12.54
4	Ethyl acrylate	40	112	Monomer	Ac peroxide	N.R.		
5	Vinyl acetate	40	112	Monomer	Ac peroxide	N.R.		
6	1,3-Butadiene	40	112	Monomer	Ac peroxide	N.R.		
7	Maleic anhydride	40	72	DMF	Lupersol 11	N.R.		
8	2-Vinylpyridine	40	112	THF	Ac peroxide	14 <sup>e</sup>	0.25(DMF)	2.68 <sup>b</sup>
9	N-Vinylcarbazole	40	72	THF	Lupersol 11	14 <sup>e</sup>	0.05(benzene)	1.56
10	Ethyl acrylate	70	90	Monomer	BzO <sub>2</sub>	N.R.		
11	Maleic anhydride	70	90	Monomer	BzO <sub>2</sub>	N.R.		
12	Vinylidene chloride	70	37	Monomer	BzO <sub>2</sub>	N.R.		
13	1,1-Diphenylethylene	70	28	Monomer	BzO <sub>2</sub>	N.R.		
14	2-Chloroacrylonitrile	70	42	Monomer	BzO <sub>2</sub>	N.R.		
15	Vinyl isobutyl ether	70	42	Monomer	BzO <sub>2</sub>	N.R.		

16	Bicycloheptene	70	90	Monomer	BzO <sub>2</sub>	N.R.	
17	Vinyltriphenylsilane	70	72	Chlorobenzene	BzO <sub>2</sub>	N.R.	
18	<i>p</i> -Methoxystyrene	70	37	Monomer	BzO <sub>2</sub>	43*	0.15(benzene)
19	Vinyltoluene	70	42	Monomer	BzO <sub>2</sub>	43*	0.14(benzene)
20	<i>o</i> -Chlorostyrene	70	42	Monomer	BzO <sub>2</sub>	41*	0.05(benzene)
21	<i>p</i> -Chlorostyrene	70	42	Monomer	BzO <sub>2</sub>	50*	0.32(benzene)
22	1,1-Bis( <i>p</i> -methoxyphenyl)- ethylene	70	88	Chlorobenzene	BzO <sub>2</sub>	10*	0.02(benzene)
23	<i>N</i> -Vinylcarbazole	70	37	Benzene	BzO <sub>2</sub>	36*	0.17(benzene)
24	Methyl $\alpha$ -chloroacrylate	70	16	Monomer	BzO <sub>2</sub>	34*	2.02(DMSO)
25	2-Vinylpyridine	70	18	Monomer	BzO <sub>2</sub>	112*	0.29(DMF)

<sup>a</sup> *p*-Chloranil purified by thrice recrystallization from dry toluene and twice vacuum sublimed.

<sup>b</sup> When monomer is referred to as solvent, 4 equivalents of monomer per equivalent of *p*-chloranil are employed. When a special solvent is used, *p*-chloranil and monomer are used in 1:1 molar ratio and the solvent is present in 10 ml per 0.012 mole *p*-chloranil.

<sup>c</sup> Initiators used in 1.3 mole-% based upon *p*-chloranil.

<sup>d</sup> Analyses conducted at Union Carbide.

<sup>e</sup> Yield based upon homopolymer of vinyl monomer.

<sup>f</sup> Tabulated as intrinsic viscosity.

<sup>g</sup> Yield based upon stoichiometry of 1:1 copolymers.

<sup>h</sup> Tabulated as elemental nitrogen analysis.

quinones was 9 for the 70°C experiment and differed by a factor of 2.3 from the highest number (21) for the 40°C experiment. However, the number of incorporated *p*-chloranils per acrylonitrile increased by some 22 times within the same temperature limits. The temperature increase facilitated the ability of the quinone to react with a growing chain, but it changed little the reactivity of the resulting radical toward monomer and chain regeneration. Within the limits of experimental error, therefore, the reactivity of radical III with acrylonitrile monomer appears to be temperature-independent.

Six monomers, in addition to acrylonitrile, were reacted with *p*-chloranil at 40°C, and the data for these reactions are tabulated in experiments 4-9 of Table II. Ethyl acrylate, vinyl acetate, and 1,3-butadiene when reacted in bulk (4:1 molar excess of monomer:quinone), and maleic anhydride when reacted in DMF solution, all failed to produce isolable polymer products. Indeed, the reaction mixtures, once the initial mixing was complete, did not appear to undergo any change in color or consistency during the reaction period.

However, reactions at 40°C with 2-vinylpyridine (expt. 8) and with *N*-vinylcarbazole (expt. 9), both in the presence of tetrahydrofuran solvent, afforded low yields of polymeric materials. The material derived from the 2-vinylpyridine experiment analyzed for 2.68 wt.-% nitrogen, an analysis somewhat below that expected for 1:1 stoichiometry (3.99%), and possessed a reduced viscosity of 0.25 in DMF. The infrared spectrum of the jet-black product showed a strong, broad absorption with an apex at 3.0  $\mu$  and strong, sharp absorptions at 5.9  $\mu$  and 9.0  $\mu$ . However, the material was quite brittle and a stiffness-temperature relationship could not be obtained. The product derived from *N*-vinylcarbazole was of low molecular weight (RV = 0.05) and composed largely of poly-*N*-vinylcarbazole, as indicated by infrared data and elemental analysis for chlorine.

Sixteen monomers were reacted with *p*-chloranil at 70°C. Bulk reactions (4:1 molar ratio of monomer:quinone) with ethyl acrylate, maleic anhydride, vinylidene chloride, 1,1-diphenylethylene, 2-chloroacrylonitrile, vinyl isobutylether and bicycloheptene all failed to yield isolable polymer products (expts. 10-16). A chlorobenzene solution reaction of vinyl-triphenylsilane (expt. 17) also failed to provide an isolable product. None of these reaction mixtures, once initial mixing was complete, appeared to undergo any change in color or consistency during the reaction periods.

A number of styrene derivatives reacted with *p*-chloranil. *p*-Methoxystyrene (expt. 18), vinyltoluene (expt. 19), *o*-chlorostyrene (expt. 20), and *p*-chlorostyrene (expt. 21) all reacted in bulk to yield polymeric products. The *p*-methoxystyrene reaction provided a good yield of a material of reduced viscosity 0.15, but which contained only 6 wt.-% of incorporated *p*-chloranil as indicated by elemental chlorine analysis. An infrared spectrum of the product was similar to that of polymethoxystyrene.

The reaction with vinyltoluene (composed largely of the *para* isomer) resulted in a good yield of a copolymer of reduced viscosity 0.14. Ele-

mental analysis for chlorine showed the presence of 1.3 equivalents of vinyltoluene per equivalent of quinone. A strong, broad absorbance was observed in the infrared between 9.4 and 10.4  $\mu$  with an apex at 10.1  $\mu$ , but no carbonyl absorbance was seen. The former absorptions were of similar shape and position to absorptions noted for the styrene/*p*-chloranil copolymer, both probably resulting from the aliphatic-aromatic ether linkage.

Reactions with *o*- and *p*-chlorostyrenes resulted in good yields of polymeric products. However, infrared and elemental analyses showed these products to be quite different. The product from *p*-chlorostyrene was a copolymer of reduced viscosity 0.32 which, according to elemental chlorine analysis, contained 1.75 equivalents of monomer per equivalent of *p*-chloranil. An infrared spectrum showed considerable similarity to the styrene/*p*-chloranil copolymer, particularly to the broad, strong absorbances between 9.4 and 10.4  $\mu$ . The copolymer could be pressed into a plaque at 185°C but was so brittle that it fell apart during removal from the mold. The product derived from *o*-chlorostyrene, however, was of considerably lower molecular weight. That product possessed a reduced viscosity of 0.05 and elemental chlorine analysis showed a 7:1 molar relationship between monomer and quinone. Infrared absorbances were seen at 9.65 and 10.15  $\mu$ , but were of different shapes from those of the *p*-chlorostyrene/*p*-chloranil copolymer.

The location of nuclear chlorine appeared to have a marked influence upon the copolymerizabilities of *o*-chloro- and *p*-chlorostyrene with *p*-chloranil. Chlorine in the *ortho* position considerably reduced the styrene reactivity and was relatively effective in short-stopping the copolymer chain growth. A *para* chlorine, however, seemed to enhance the styrene reactivity as determined by the reduced viscosities of *p*-chloranil copolymers with *p*-chlorostyrene versus that with styrene (0.32 and 0.19, respectively). One could surmise that steric factors were the major cause of disparity between the *o*- and *p*-chlorostyrenes, but electronic factors (charge-transfer complexing) probably were responsible for the disparity between styrene and *p*-chlorostyrene.

1,1-Bis(*p*-Methoxyphenyl)ethylene reacted with *p*-chloranil in the presence of chlorobenzene (expt. 22) to afford a low yield of polymeric material of reduced viscosity 0.02. Elemental chlorine analysis showed the presence of 2.5 equivalents of monomer per equivalence of quinone.

*N*-Vinylcarbazole in benzene (expt. 23) and methyl  $\alpha$ -chloroacrylate in bulk (expt. 24) polymerized in the presence of *p*-chloroanil to afford polymeric products possessing little incorporated quinone. Reaction with *N*-vinylcarbazole gave a fair yield of a brown material of reduced viscosity 0.17, whose infrared spectrum and elemental chlorine analysis generally agreed with those for poly(*N*-vinylcarbazole). Reaction with methyl  $\alpha$ -chloroacrylate gave a fair yield of polymer of reduced viscosity 2.02. However, infrared and elemental analysis showed the polymer consisted largely of poly(methyl  $\alpha$ -chloroacrylate).

2-Vinylpyridine reacted with *p*-chloranil at 70°C in bulk, as it did at

TABLE III  
 Reactions of *p*-Benzoquinone with Vinyl Monomers<sup>a</sup>

Expt. no.	Monomer	Temp, °C	Time, hr	Solvent <sup>b</sup>	Initiator <sup>c</sup>	Yield, %	R. V. $\bar{M}_n$ (solvent)	Carbon, % <sup>d</sup>	Copolymer composition <sup>e</sup>
1	Styrene	40	72	Monomer	Lupersol 11	N.R.			
2	Acrylonitrile	40	72	Monomer	Lupersol 11	N.R.			
3	Ethyl acrylate	40	72	Monomer	Lupersol 11	N.R.			
4	Vinyl acetate	40	72	Monomer	Lupersol 11	N.R.			
5	N-Vinylcarbazole	40	72	THF	Lupersol 11	N.R.			
6	Bicycloheptene	40	72	THF	Lupersol 11	N.R.			
7	Maleic anhydride	40	72	THF	Lupersol 11	N.R.			
8	2-Vinylpyridine	40	72	Monomer	Lupersol 11	N.R.			
9	Isobutylene	40	48	Monomer	Lupersol 11	N.R.			
10	Vinylidene chloride	40	48	Monomer	Lupersol 11	N.R.			
11	Sulfur dioxide	40	48	Monomer	Lupersol 11	N.R.			
12	1,3-Butadiene	40	48	Monomer	Lupersol 11	19 <sup>f</sup>	0.10(benzene)	74.91	1.2
13	Styrene	70	44	Monomer	BzO <sub>2</sub>	N.R.			
14	Acrylonitrile	70	44	Monomer	BzO <sub>2</sub>	N.R.			

15	Ethyl acrylate	70	44	Monomer	BzO <sub>2</sub>	N.R.	
16	Vinyl acetate	70	44	Monomer	BzO <sub>2</sub>	N.R.	
17	<i>N</i> -Vinylcarbazole	70	44	<i>l</i> -Butanol	BzO <sub>2</sub>	N.R.	
18	Bicycloheptene	70	44	Monomer	BzO <sub>2</sub>	N.R.	
19	Maleic anhydride	70	44	Monomer	BzO <sub>2</sub>	N.R.	
20	Vinylidene chloride	70	44	Monomer	BzO <sub>2</sub>	N.R.	
21	1,3-Butadiene	70	44	Monomer	BzO <sub>2</sub>	13 <sup>f</sup>	0.03(benzene)
22	2-Vinylpyridine	70	44	Monomer	BzO <sub>2</sub>	22 <sup>f</sup>	1.16(DMF)
23	Styrene	110	17	Chlorobenzene	<i>l</i> -Bu peroxide	N.R.	77.80
24	Acrylonitrile	110	17	Monomer	<i>l</i> -Bu peroxide	N.R.	67.32(3.30) <sup>g</sup>

<sup>a</sup> *p*-Benzoquinone purified by recrystallization three times from benzene and vacuum sublimed twice.

<sup>b</sup> When monomer is referred to as solvent, 4 equivalents of monomer per equivalent of quinone are employed. When a special solvent is used, the quinone and monomer are used in 1:1 molar ratio and the solvent is present in 10 ml per 0.012 mole of quinone.

<sup>c</sup> Initiators used in 1.3 mole-% based upon *p*-benzoquinone.

<sup>d</sup> Analyses conducted at Union Carbide.

<sup>e</sup> Copolymer compositions listed as molar ratios of monomers: *p*-benzoquinone.

<sup>f</sup> Yield based upon 1:1 copolymer of monomer:quinone.

<sup>g</sup> Per cent nitrogen as averaged from duplicate analyses.

40°C in THF, to provide an excellent yield of copolymer product (expt. 25). The copolymer was a jet-black material resembling carbon in appearance, and possessed a 4.1:1 molar ratio of monomer:quinone as based upon elemental chlorine analysis and the molecular weights of the reactants. Series of broad, strong absorbances were observed in the infrared between 2.7–4.4  $\mu$  and 12.3–13.7  $\mu$ , together with sharp, strong absorbances at 6.15, 6.3, and 6.98  $\mu$ . The copolymer possessed a reduced viscosity of 0.29, and could be drawn from a melt into short, but distinct fibers. At this time, however, the structure of the polymer is unknown.

### Reactions of *p*-Benzoquinone with Vinyl Monomers

*p*-Benzoquinone was reacted with a series of vinyl monomers and the results of these reactions recorded in Table III. Most of the experiments at 40°C and 70°C, and neither of the two experiments at 110°C, provided evidence for any significant degree of copolymerization. In most cases the reaction mixtures, once initial mixing was complete, did not vary in color or consistency over the course of reaction periods of 2–3 days.

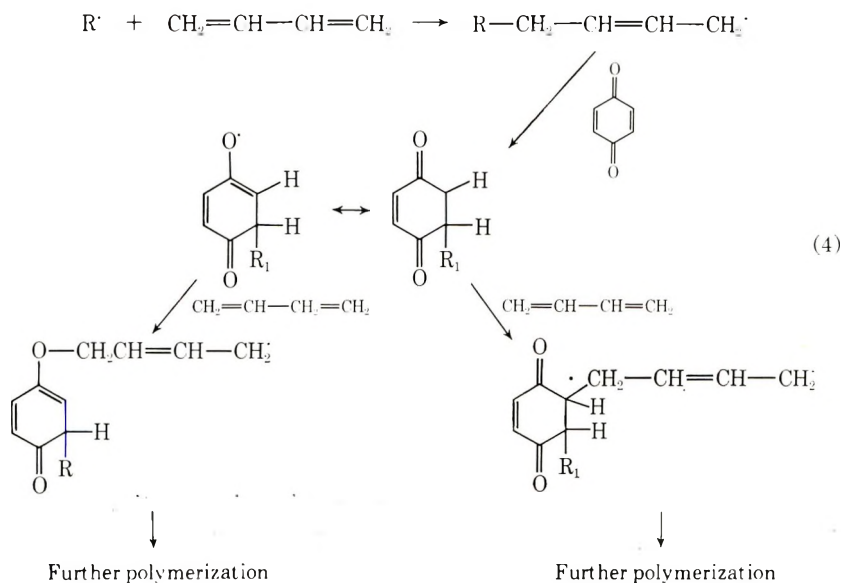
The reactions with styrene at 70 and 110°C (expts. 13 and 23, respectively) provided low yields of quinhydrone, a 1:1 molecular complex of quinone with hydroquinone. The degree of quinhydrone formation, previously observed during the polymerization of styrene inhibited by minute quantities of *p*-benzoquinone,<sup>9</sup> was temperature-dependent, with a larger quantity being isolated from the 110°C experiment. Hydroquinone could have arisen by hydrogen atom abstraction by quinone, possibly via a charge-transfer complex, from very low molecular weight polystyrene or quinone-styrene copolymers. The fate of the radicals resulting from such hydrogen abstraction is unknown, although the removal of solvent from the quinhydrone-free reaction mixtures resulted in isolation of tacky residues. It would seem that if the system were capable of transferring hydrogen atoms to quinone or semiquinone, the addition of these same species to styrene monomer would also occur. However, no significant degree of polymerization was observed under the utilized conditions.

One copolymer of significant molecular weight was isolated from the 40°C reaction series. 1,3-Butadiene reacted with *p*-benzoquinone (expt. 12) to provide a copolymer of reduced viscosity 0.10 in fair yield. Elemental analysis for carbon established a 1.2:1 molar relationship between 1,3-butadiene and quinone. A strong infrared absorption was observed at 5.9  $\mu$ , implying that part or all of the quinone carbonyl groups were intact in the copolymer and that the quinone copolymerized by some means other than *via* its carbonyls. A mechanism which could give the above results is shown in eqs. (4). The butadiene is expected to have polymerized 1,4, and the proposed mechanism would maintain intact part or all of the carbonyls. The presence of carbonyl groups in the polymer chain might enable use of this material as a redox polymer.<sup>10</sup>

1,3-Butadiene and 2-vinylpyridine were the only monomers in the 70°C reaction series which reacted with *p*-benzoquinone to yield isolable polymer

products. Reaction with 1,3-butadiene (expt. 21) afforded a 13% yield of copolymer of reduced viscosity 0.03. The product possessed a 2:1 molar relationship between diene and quinone, as established by elemental carbon analysis, and exhibited a strong infrared absorption at  $5.9 \mu$ . Interestingly, the increase in reaction temperature from  $40^\circ\text{C}$  to  $70^\circ\text{C}$  had a marked effect upon the molecular weights of the butadiene copolymers, resulting in decreased reduced viscosities from 0.10 to 0.03, respectively.

Reaction with 2-vinylpyridine (expt. 22) afforded a high molecular weight copolymer in fair yield. The product possessed a reduced viscosity of 1.16 and a strong, broad carbonyl absorbance in the infrared. However, elemental analysis for both carbon and nitrogen were considerably lower than expected for a 1:1 copolymer or for any other simple combination of monomers. The infrared spectrum and carbon analysis for the reaction product were quite different from those of poly-2-vinylpyridine, but the presence of nitrogen established that at least part of the 2-vinylpyridine residue was present in the product. At present, the structure of this material is unknown.



### Reactions of 2,5-Dimethyl-*p*-benzoquinone with Vinyl Monomers

2,5-Dimethyl-*p*-benzoquinone was reacted with a series of monomers and the results of these experiments are tabulated in Table IV. No polymer products could be isolated from any of the reactions. Indeed, 2,5-dimethyl-*p*-benzoquinone acted as a very efficient inhibitor, in spite of the fact that the utilized monomers encompassed a wide range of double bond reactivities.



TABLE IV  
Reactions of 2,5-Dimethyl-*p*-benzoquinone with Vinyl Monomers<sup>a</sup>

Expt. no.	Monomer	Temp, Time,		Solvent <sup>b</sup>	Initiator <sup>c</sup>	Yield, %
		°C	hr			
1	Styrene	40	48	Monomer	Lupersol 11	N.R.
2	Acrylonitrile	40	48	Monomer	Lupersol 11	N.R.
3	Vinyl acetate	40	48	Monomer	Lupersol 11	N.R.
4	Ethyl acrylate	40	48	Monomer	Lupersol 11	N.R.
5	Isobutylene	40	48	Monomer	Lupersol 11	N.R.
6	1,3-Butadiene	40	48	Monomer	Lupersol 11	N.R.
7	<i>N</i> -Vinylcarbazole	40	48	THF	Lupersol 11	N.R.
8	<i>p</i> -Methoxystyrene	70	37	Monomer	BzO <sub>2</sub>	N.R.
9	Styrene	70	37	Monomer	BzO <sub>2</sub>	N.R.
10	1,1-Diphenylethylene	70	28	Monomer	BzO <sub>2</sub>	N.R.
11	Acrylonitrile	70	28	Monomer	BzO <sub>2</sub>	N.R.
12	Vinylidene chloride	70	28	Monomer	BzO <sub>2</sub>	N.R.
13	Vinyl acetate	70	28	Monomer	BzO <sub>2</sub>	N.R.
14	<i>N</i> -Vinylcarbazole	70	28	Benzene	BzO <sub>2</sub>	N.R.
15	Bicycloheptene	70	28	Benzene	BzO <sub>2</sub>	N.R.

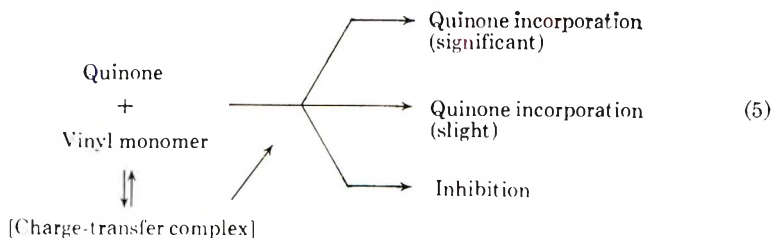
<sup>a</sup> Quinone purified by recrystallization three times from toluene and vacuum sublimed twice.

<sup>b</sup> When monomer is referred to as solvent, 4 equivalent of monomer per equivalent of quinone are employed. When a special solvent is used, the quinone and monomer are used in 1:1 molar ratio and the solvent is present in 10 mls. per 0.012 mole of quinone.

<sup>c</sup> Initiators used in 1.3 mole-% based upon the quinone.

## CONCLUSION

We have established that both *p*-chloranil and *p*-benzoquinone, but not 2,5-dimethyl-*p*-benzoquinone, can be made to undergo copolymerization reactions with certain vinyl monomers under specific experimental conditions. Charge-transfer complexes may have played definitive roles in these reactions, or as more often the case, in the non-polymerization reactions. Indeed, highly colored mixtures were observed in almost all of the experiments upon admixture of reactants. A general classification of these reactions is shown in eqs. (5).



With *p*-chloranil, a number of "significant" and "slight" quinone incorporation reactions was observed. With *p*-benzoquinone, two "significant" incorporations were observed, whereas only inhibition was noted with 2,5-dimethyl-*p*-benzoquinone.

### References

1. J. C. Bevington et al., *Trans. Faraday Soc.*, **51**, 946 (1955).
2. J. C. Bevington et al., *J. Chem. Soc.*, **37**, 2822 (1955).
3. J. C. Bevington and H. W. Melville, *Usp. Khim.*, **25**, 1336 (1956).
4. B. L. Funt and F. D. Williams, *J. Polym. Sci.*, **46**, 139 (1960); *ibid.*, **57**, 711 (1962).
5. F. Tudos, *Acta. Chim. Acad. Sci. Hung.*, **44**, 403 (1965).
6. J. W. Breitenbach, *Can. J. Res.*, **28B**, 507 (1950), and references therein.
7. L. J. Bellamy, *Infra-red Spectra of Complex Molecules*, Wiley, New York, pp. 114-131.
8. R. L. Cleland and W. H. Stockmayer, *J. Polym. Sci.*, **17**, 473 (1955).
9. J. C. Bevington, *J. Chem. Soc.*, **1955**, 2822.
10. H. G. Cassidy and K. A. Kun, *Oxidation-Reduction Polymers*, Interscience, New York, 1965.

Received August 4, 1969

Revised October 30, 1969

## The Reactive Intermediate in Acetylene Polymerization: Results of Quantum Chemical Calculations on Charge Delocalization and Its Consequences

JOOST MANASSEN, *Plastics Research Laboratory, The Weizmann Institute of Science, Rehovot, Israel*, and ROBERT REIN, *Roswell Park Memorial Institute and State University of New York at Buffalo, 666 Elm St. Buffalo New York 14203*

### Synopsis

The charge delocalization in the conjugated vinyl intermediates, which are assumed to be the reactive intermediates in acetylene polymerization, is calculated, taking into account  $\sigma$  as well as  $\pi$  electrons. Delocalization is shown to exist, but it is of a different kind for cations and anions. In the anion, the  $\sigma$  charge is localized at the reactive center and the  $\pi$  charge is displaced into the system. In the cations, the  $\sigma$  charge flows towards the reactive center and the  $\pi$  charge is more or less unaffected.  $\pi$ -overlap charges between the carbon atoms are much less affected than in the case of the corresponding allyl type anion and cation. The calculated charge delocalizations are compared with the little experimental evidence there is, and possible implications of  $\sigma$  and  $\pi$  delocalizations on reactivity and specificity of reaction are discussed.

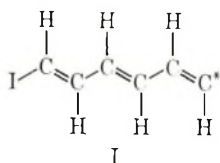
### INTRODUCTION

It is a long-established practice in the study of polymerization kinetics to assume that the rate of propagation is independent of the length of the propagating species. This assumption has generally led to consistent results in the case of polymerization of vinyl monomers. In the relatively few cases in which the polymerization of acetylenic monomers into linear polymers has been studied, it has mostly been assumed, on the other hand, that an interaction between the reactive center and the conjugated backbone exists, which may be dependent on the length of the conjugated chain.

In this paper we want to discuss why it is very difficult to understand this interaction without the use of extended calculations taking into account both  $\sigma$ - and  $\pi$ -electrons, what conclusions may be reached after having done the calculations, and how these apply to the special phenomena encountered in acetylene polymerization. The conclusions will be mainly of a qualitative or semiquantitative nature; the more quantitative aspects, which have much wider implications than the polymerization aspects alone, will be discussed in subsequent publications.

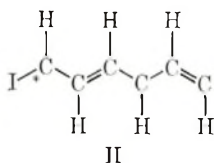
The reactive intermediate in acetylene polymerization, initiated by either a cation, an anion or a free radical, will have the form of a vinyl-intermediate, which is either a cation, an anion or a free radical, and we shall use the asterisk (\*) to indicate a reactive center, being one of the three cases mentioned. We do not consider the polymerization initiated by metal complex catalysts, as not enough is known about the nature of the reactive intermediate.

Using the initiator  $I^*$  on acetylene we can sketch the intermediate schematically as structure I:

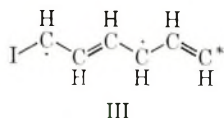


The organic chemist, using the terminology of classical  $\pi$ -electron molecular orbital theory, will look at such a structure as follows.

If we place the conjugated system in the plane of the paper, the lobes of the  $\pi$  orbitals will be at a right angle to this plane. At the reactive center, in the case of the anion, the free electron pair will occupy a  $\sigma$  orbital within the plane of the paper; in the free radical this orbital will have one electron, and in the case of the cation, it will be empty. The  $\pi$  electron theory which considers explicitly only orbitals of  $\pi$  symmetry, will assume that the charge at the reactive center is localized. Using resonance structures, which are the terminology of valence-bond calculations, will lead to approximately the same conclusion. The only structures that can be drawn are for carbene resonance (II)



or excited structures like III.



As both types of structures cannot be considered to contribute a great deal to charge delocalization, the terminology of the valence bond method too leads us to conclude that the charge is mainly localized.

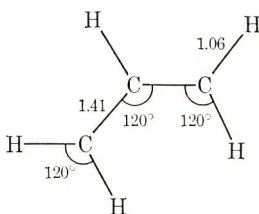
In the discussion section of this paper we shall describe some chemical evidence that suggests charge delocalization in the intermediate during acetylene polymerization does occur. Therefore we decided to do some

calculations taking into account explicitly both  $\sigma$  and  $\pi$  electrons. The molecular orbitals are then formed as linear combinations of  $1s$  hydrogen, and  $2s$  and  $2p$  carbon orbitals. For this the iterative extended Hückel method has been used.

This method has been described elsewhere.<sup>1</sup> It is optimized to be self-consistent in the charge distribution, and all our conclusions will be based on charge considerations and not those of energy. We want to stress a few points here.

The assumed geometry is not entirely realistic; all carbon-carbon distances in the conjugated system are taken as  $1.41 \text{ \AA}$ , and all carbon-hydrogen distances  $1.06 \text{ \AA}$ . All angles in the conjugated system, be they

$\text{C}-\text{C}-\text{C}$  or  $\text{C}-\text{C}-\text{H}$ , have been taken as  $120^\circ$ :



In reality, angles deviate a few degrees from  $120^\circ$ , and the carbon-carbon distances alternate between  $1.36$  and  $1.44 \text{ \AA}$ .

In energy calculations such an unrealistic model would lead to erroneous results, because the total energy is of the order of thousands of kilocalories and small deviations in the assumed geometry may cause errors larger than the effect we are looking for. If we look at charge distribution, however, an error of a few per cent will give a quantitatively slightly distorted picture, but for the qualitative aspects of charge delocalization we are interested in, the method is adequate. We have verified this in several cases by repeating the calculation with a variation in geometry. The reason for taking an idealized geometry is the fact that the bond distances in the reactive intermediate are not known anyway, and by standardizing the distances in all models studied, it is easier to follow the consequences of changes made by removal of protons or electrons. The principle will be understood when the results given in the next section are studied. It has to be stressed again however, that the numbers given are not to be taken as quantitative calculated charge densities, but as an illustration of  $\sigma$ - and  $\pi$ -electron flow in the molecule, and as such they are interesting enough. We shall consider three calculated quantities: the atomic  $\sigma$  and  $\pi$  charges; the overlap charge density; and the net atomic charge.

The atomic  $\pi$  charges are the diagonal elements of the charge bond-order matrix referring to  $\pi$  orbitals and the atomic  $\sigma$  charges are the sums of the diagonal charge bond-order elements referring to  $\sigma$  orbitals at the atom under consideration.

The overlap charge density gives the electron density in the overlap region between two atoms and can be considered as a measure of bonding between two atoms; it, too, can be separated into a  $\sigma$  and a  $\pi$  component.

Net atomic charge is the deviation from neutrality at a certain atom, and is obtained in the point-charge approximation by combining the diagonal densities with the appropriate fraction of the overlap charge and the effective core charge. As the calculation method can only be applied to a closed-shell electronic structure, we calculated only cations and anions. We hope to be able to publish results on free radicals at a later stage. Counterions were not taken into account for practical reasons, and this has to be taken into consideration when comparing the calculated values with experiment.

## RESULTS

To get an idea what we are looking for, we shall first consider the ionic structure obtained by removing a proton and electrons from the propylene molecule. Figure 1 gives the calculated charge densities and overlap charge densities in propylene. When  $\sigma$  or  $\pi$  is not indicated we are concerned only with  $\sigma$  densities. Large circles indicate a carbon atom and small circles a hydrogen atom.

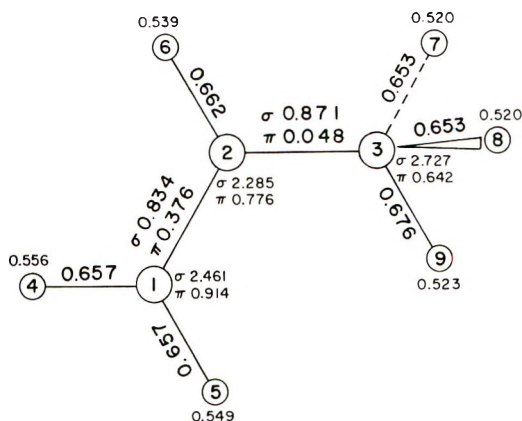
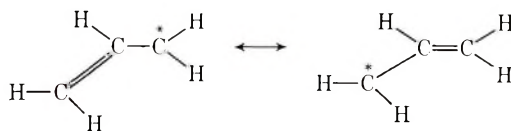


Fig. 1. Electron densities (values in small print), overlap charge densities (large print), in the propylene molecule.

We see that the double bond between C<sub>1</sub> and C<sub>2</sub> corresponds to a  $\pi$ -overlap charge density of 0.376. The double-bond character of the bond between C<sub>2</sub> and C<sub>3</sub> is smaller almost by a factor of ten.

In Figure 2 are pictured the electronic charges that occur when we remove H<sub>7</sub> from propylene, by which we obtain a familiar structure, the allylic cation or anion, depending on whether we remove H<sub>7</sub> with or without two electrons.

As we would predict from the simple resonance structures,



$\pi$ -overlap charges between  $C_1$  and  $C_2$ , and  $C_2$  and  $C_3$  are equal, and show an appreciable double-bond character, while the  $\sigma$ -overlap charge is much less affected. Some features we could not foresee are the decrease of charge density on the hydrogens in the cation, and its increase in the anion. How this delocalization influences the net atomic charges we see in Figure 3.

We see that the delocalization causes a spreading out of charge, which we know from chemical experience and can approach intuitively by con-

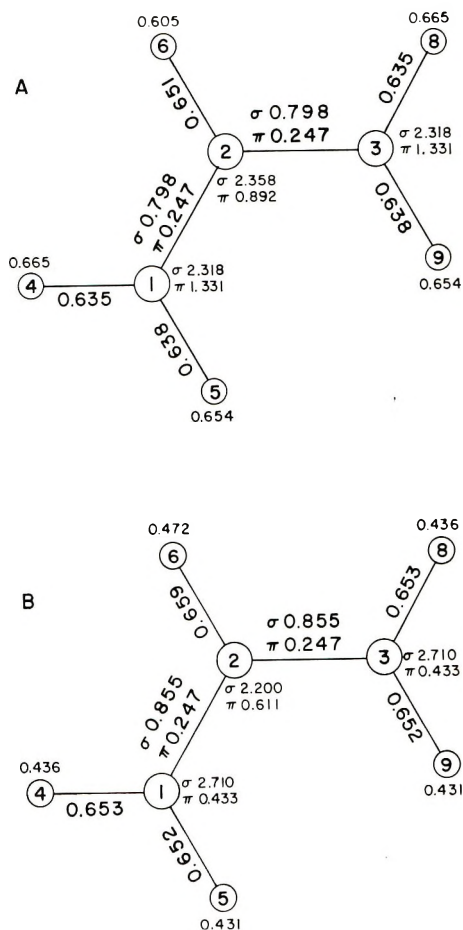


Fig. 2. Electron densities (small print) and overlap charge densities (large print) in the allylic structures, obtained by removing  $H_7$  (A) or  $H_7$  and two electrons (B) from propylene.

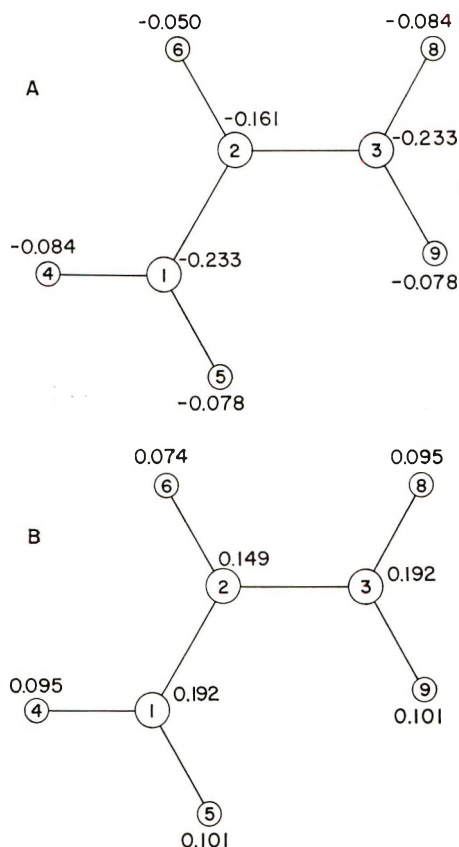


Fig. 3. Atomic charges in the allylic structures obtained by removing  $H_7$  (A) or  $H_7$  and two electrons (B) from propylene.

sidering resonance structures. If, however, we remove  $H_1$  instead of  $H_7$  from propylene, which gives a vinyl species as sketched in Figure 4, we see that again charge delocalization occurs, but according to a different picture. In the anion the  $\sigma$  charge density at  $C_1$  has increased by more than one unit; in other words, after removal of the proton the  $\sigma$  electrons stayed where they were. The  $\pi$  charge density at  $C_1$ , on the other hand, has decreased to half its value, and at  $C_2$  increased by about the same amount. The  $\pi$ -overlap charge densities between the carbons are much less affected than in the case of the allyl ion. We see here the first example of a phenomenon we shall encounter in all the conjugated vinyl anions to be studied, namely, increase in  $\sigma$  charge at the site of proton removal and flowing out of  $\pi$  charge into the conjugated system. Part of the charge is again taken up by the hydrogens.

In the cation, on the other hand, we do not find the expected localized hole, caused by the removal of two electrons and a proton from  $C_1$ . The whole molecule has given up some  $\sigma$  charge to fill the hole, and we find here an entirely new phenomenon, that of  $\sigma$  delocalization. The  $\pi$  charge



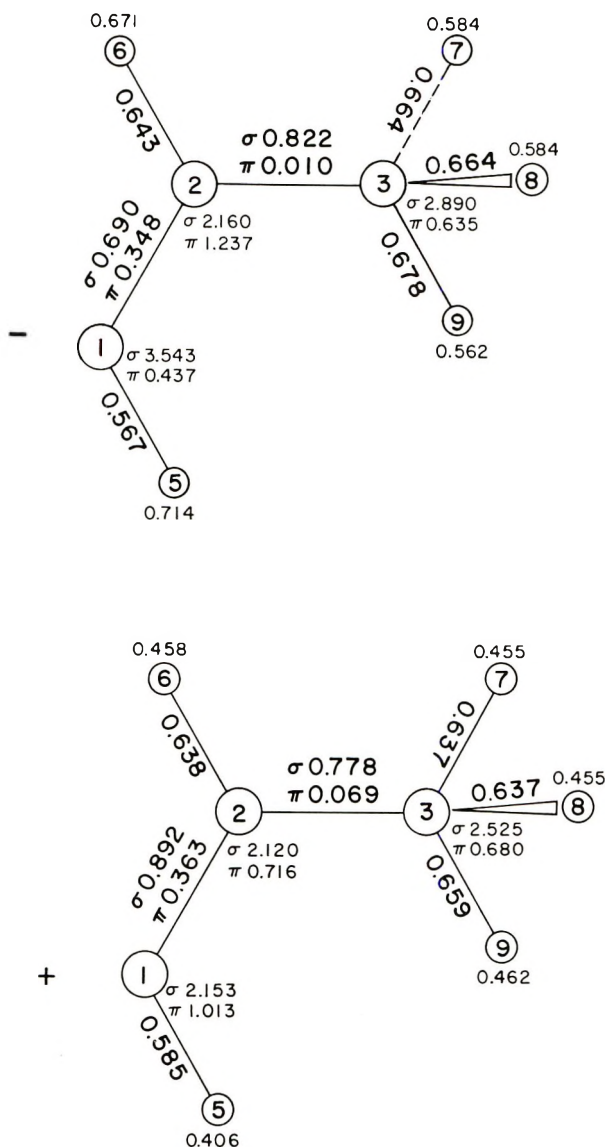


Fig. 4. Electron densities (small print) and overlap charge densities (large print) in the vinylic structures, obtained by removing  $H_4$  or  $H_4$  and two electrons from propylene.

densities are not much affected; neither are the  $\sigma$  and  $\pi$  charge overlap densities between the carbon atoms. That such a  $\sigma$  delocalization can cause the same kind of charge distribution as  $\pi$  delocalization we see in Figure 5, where the net atomic charges are given for the propylene vinyl cation. We are now in a position to distinguish three kinds of charge delocalization: (1) in the allyl type (the kind of delocalization we are familiar with,  $\sigma$  charge is more or less unaffected;  $\pi$  charge is delocalized, affecting

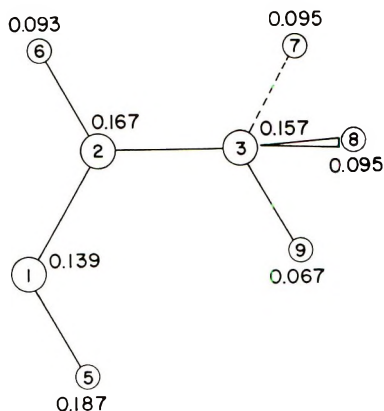


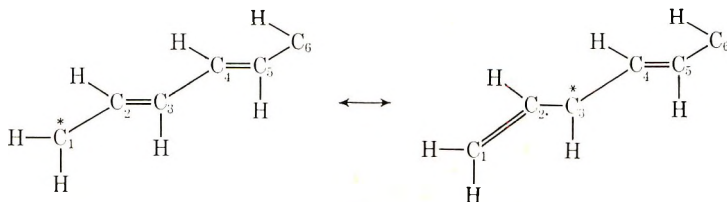
Fig. 5. Net atomic charges in the propylene vinyl cation.

$\pi$ -overlap charge densities in a manner predictable from resonance structures; (2) in the vinyl anion type,  $\sigma$  charge is localized at the ionic site, but  $\pi$  charge is displaced into the conjugated system; (3) in the vinyl cation type,  $\pi$  charge is more or less unaffected, but  $\sigma$  charge is displaced from almost all atoms present to equalize the charge developed at the ionic site.

We shall encounter types (2) and (3) in the longer conjugated systems; we shall describe these now so as to understand them in somewhat more detail.

In Figure 6 charge distributions are shown for butadiene and hexatriene. Figure 7 shows the respective anions.

We recognize the same phenomenon as indicated with the propylene vinyl anions: localized  $\sigma$  charge at the anionic site and displacement of  $\pi$  charge into the conjugated system. In the hexatriene anion the  $\pi$  charge at  $C_6$  is lower than that at  $C_4$  in the butadiene anion, and this suggests that the larger the conjugated system, the more  $\pi$  charge is drained from the anionic site. The  $\pi$  charge is concentrated on the uneven atoms and especially at  $C_1$ . Moreover the  $\pi$  overlap charge density between  $C_4$  and  $C_5$  and  $C_2$  and  $C_3$  in the hexatriene anion has increased, and between  $C_1$  and  $C_2$ ,  $C_3$  and  $C_4$ , and  $C_5$  and  $C_6$  it has decreased. There seems, then, to be some contribution from carbene resonance, if we want to use that language:



All the hydrogen atoms have again taken up part of the charge. Figure 8 shows the charge distribution for the cation case. Here, too, we see our

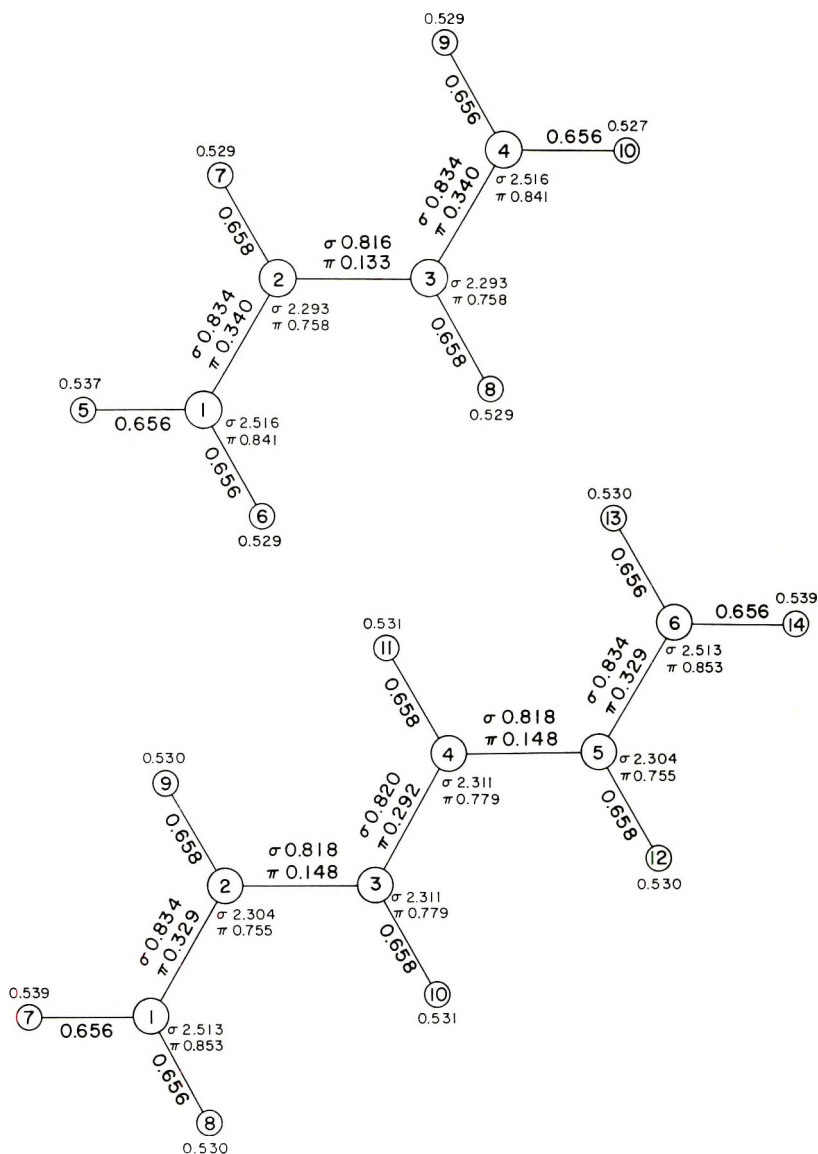


Fig. 6. Electron densities (small print) and overlap charge densities (large print) in the butadiene and hexatriene molecule.

previous observations confirmed, but we also see that the  $\sigma$  delocalization levels off with distance from the positive center;  $\sigma$  charge at  $C_1$  is barely affected in the hexatriene cation.  $\pi$  charge is displaced in the direction of the positive center somewhat more in the hexatriene case than in the butadiene case.

In summary, in the vinyl anions  $\sigma$  charge is localized at the negative center,  $\pi$  charge is displaced into the conjugated system and concentrates

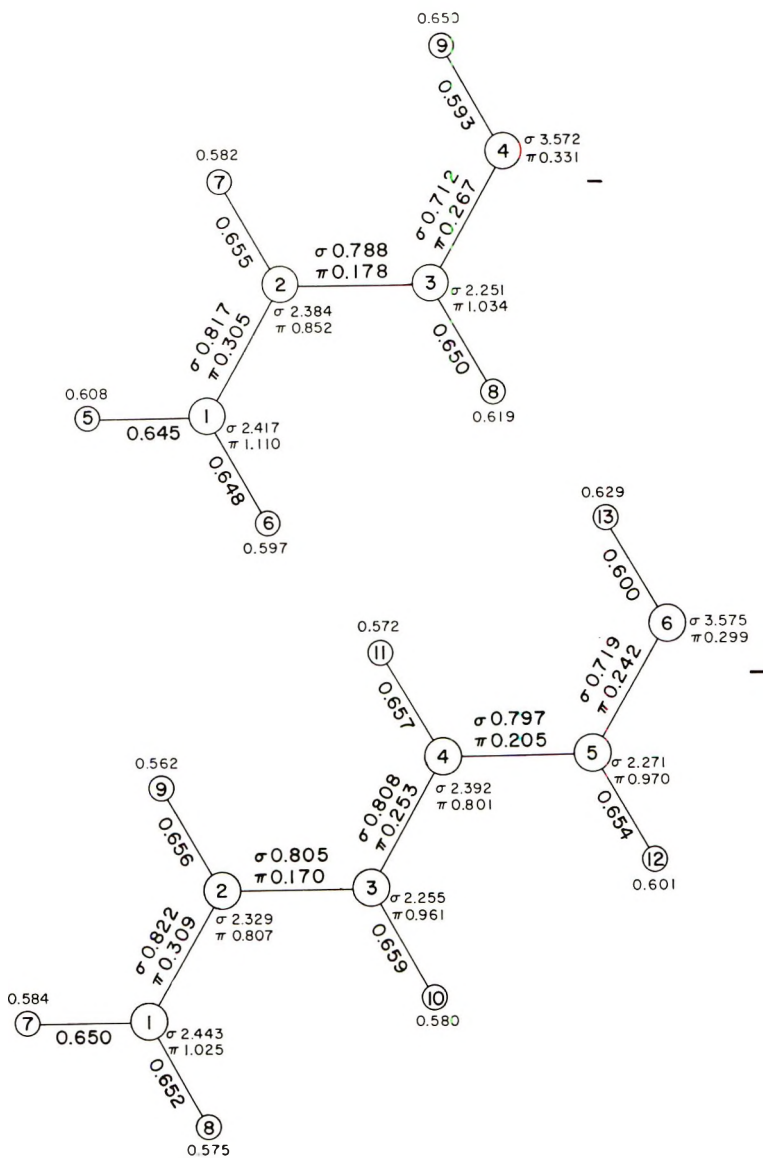


Fig. 7. Electron densities (small print) and overlap charge densities (large print) in the vinylic anions, obtained by removing  $H_{10}$  from butadiene and  $H_{14}$  from hexatriene.

at the uneven atoms, especially at  $C_1$ , the  $\pi$  bond orders are affected in the way we would expect from carbene resonance. The longer the molecule, the more  $\pi$  displacement we find. In the vinyl cation the positive charge is equalized by  $\sigma$  displacement, but in the longer molecule the flow of  $\pi$  charge increases while  $\sigma$  displacement works at shorter range. In both cases the hydrogens take part in the charge delocalization, but in the cation this effect levels off more with distance than in the anion.

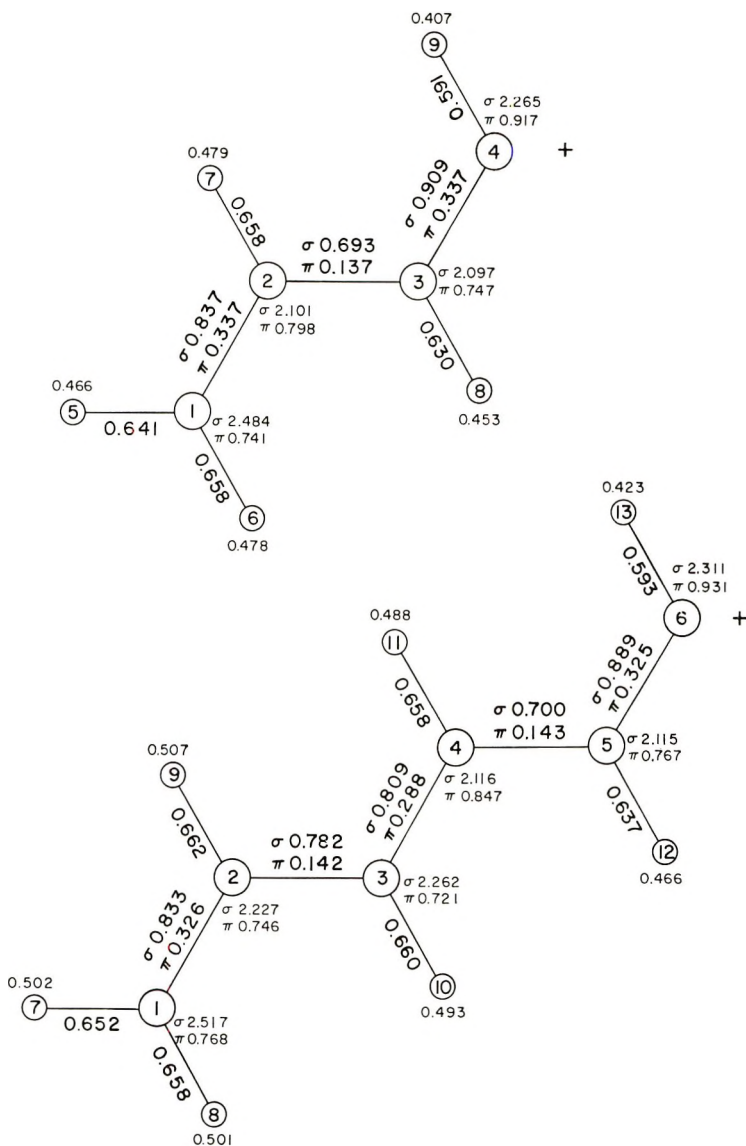


Fig. 8. Electron densities (small print) and overlap charge densities (large print) in the vinylic cations, obtained by removing  $H_{10}$  and two electrons from butadiene and  $H_{14}$  and two electrons from hexatriene.

How these electron displacements influence the atomic charges in the molecule we illustrate in Figures 9 and 10, where the atomic charges for the different species are given. From the different figures given here it is clear that the vinyl intermediate in acetylene polymerization is strongly delocalized, but that the delocalization works according to a different mechanism in cation and anion. Both mechanisms are again different from that

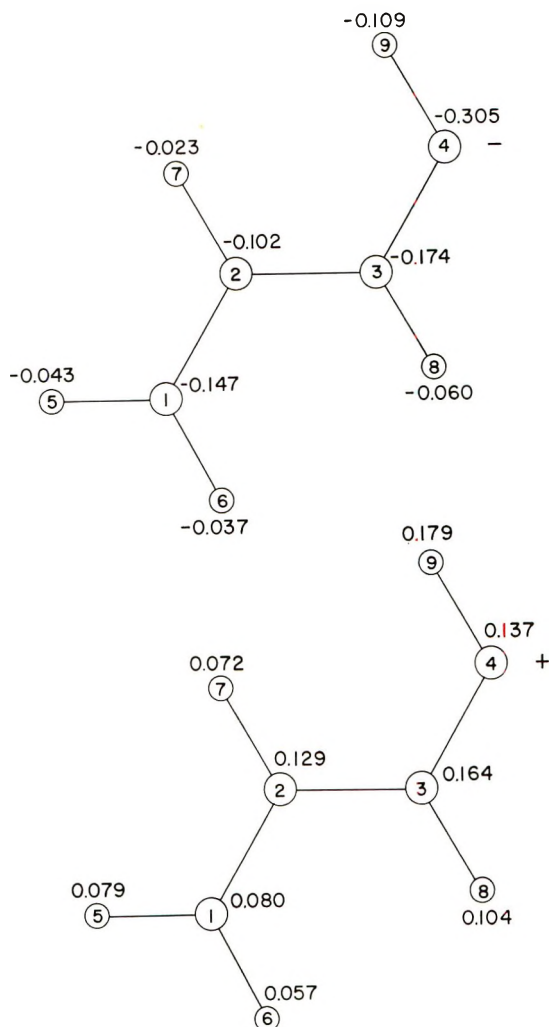


Fig. 9. Net atomic charges in the butadiene vinyl anion and cation.

found in an allyl species. We shall now have to find out how these calculated charge delocalizations agree with experimental evidence.

## DISCUSSION

We have found a significant difference in delocalization mechanism for cations and anions. A qualitative explanation of this phenomenon may be, that in the cation a low-lying  $\sigma$  orbital is vacant, and thus a reorganization of  $\sigma$  charge is energetically favorable. In the anion, on the other hand, usually there are no available  $\sigma$  atomic orbitals in the energetically favorable range which could participate in the reorganization of  $\sigma$  charge.

As mentioned in the introduction, we were not able to calculate the structures with unpaired electrons, and we shall have to speculate about

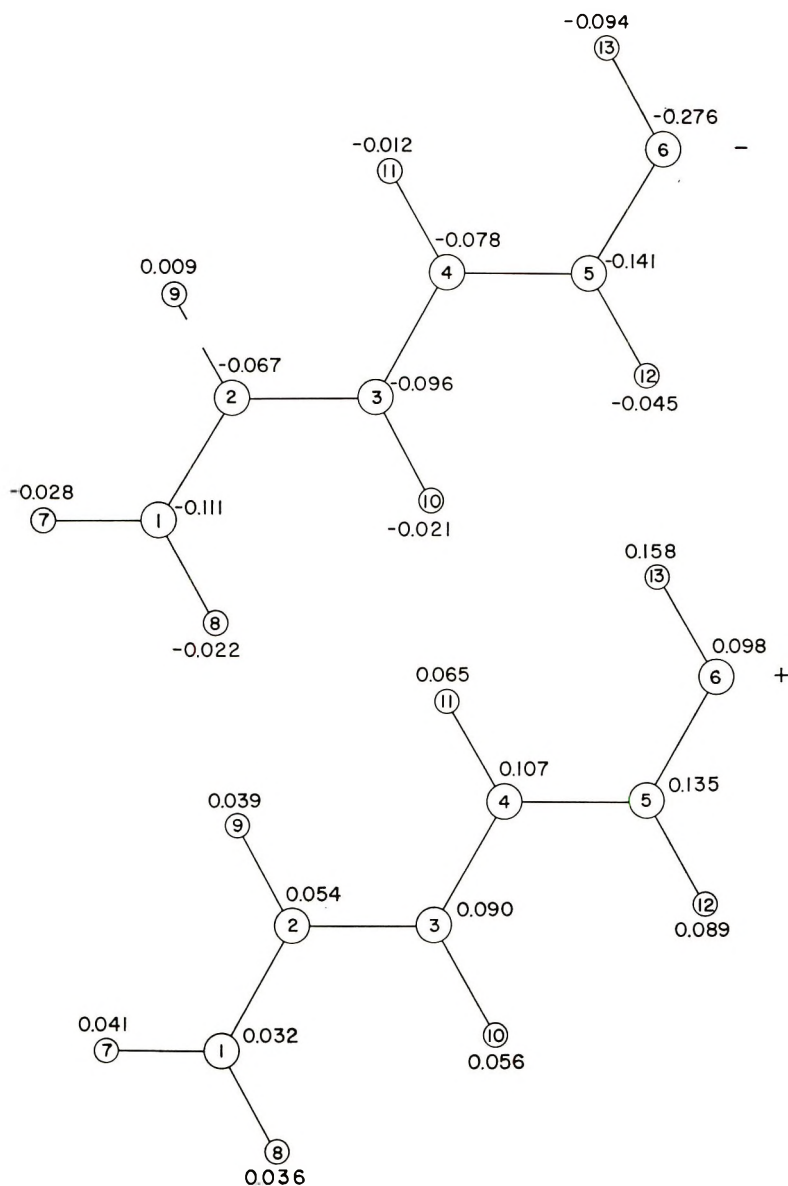


Fig. 10. Net atomic charges in the hexatriene vinyl anion and cation.

what kind of delocalization will occur in the conjugated vinyl radical. As in a free radical, a low-lying  $\sigma$  orbital would be half filled, without excess charge being present, a reorganization of  $\sigma$  charge is still plausible, while  $\pi$  delocalization, which in the anion seems to be caused by the excess charge at the reactive center, is less liable to occur.

Some features in acetylene polymerization that have been explained by a growing chain that is gradually inactivated by delocalization, are: (1) low

molecular weight in comparison with the corresponding vinyl monomer under identical polymerization conditions;<sup>2-5</sup> (2) a yield of polymer linearly proportional to the initiator concentration;<sup>4,6,7</sup> (3) a molecular weight independent of the monomer: initiator ratio;<sup>4,6,7</sup> (4) for radiation initiation, a linear dependence of polymerization rate on the radiation dose rate, which was taken by the authors as a sign of monomolecular termination<sup>8</sup> and (5) polymerization rate independent of the presence of oxygen;<sup>8</sup> (6) for anionic polymerization: the anionic polymerization of acrylonitrile can be terminated by chain transfer,<sup>9</sup> the anionic polymerization of the much more acidic cyanoacetylene seems not to be terminated by chain transfer and is not sensitive to the presence of methanol.<sup>10</sup>

Features (1)–(4) have generally been explained by the assumption that the propagating reactive species in acetylene polymerization gets more and more deactivation as it grows by electron delocalization into the conjugated chain,<sup>2</sup> in such a way that in the end it ceases to react, which causes monomolecular chain termination. We have shown that this delocalization could not be expected *a priori* to occur on the basis of classical  $\pi$ -electron theory. By taking into account  $\sigma$  as well as  $\pi$  electrons, we have seen that in conjugated anions delocalization occurs by  $\pi$ -electron flow, and in conjugated cations by  $\sigma$ -electron flow. Both types of delocalization can be distinguished from the allyl type delocalization we are familiar with. We know from chemical experience that allyl-type delocalization influences reactivity as well as the reaction site in an intermediate: the allyl intermediate  $C_1=C_2-C_3^*$  is known to be less reactive than the corresponding propyl intermediate  $C-C-C^*$  and is known to react at  $C_1$  as well as  $C_3$ , which is in accordance with the symmetrical electron distribution found in the calculations.

About the place of attack in the conjugated vinyl intermediate we know nothing, but about the reactivity of the anion some experimental material has been published.<sup>4</sup> By polymerizing acetylene in dimethyl sulfoxide solution with anionic initiators, it is possible to produce living anions of different degrees of polymerization, depending on the reaction conditions. These anions are capable of initiating the polymerization of styrene or acrylonitrile. It could be shown, however, that the longer the conjugated chain, the less active the anion is to serve as initiator. This is good evidence that the  $\pi$  delocalization in conjugated anions described here decreases its activity towards addition to a double bond. Much of the evidence given in features (1)–(4) has been collected on free-radical polymerization of acetylenes, not much is known about cationic polymerization, so we are not yet in a position to check whether the  $\sigma$  delocalization found here influences reactivity, although the low molecular weights found during cationic polymerization of acetylenes<sup>5</sup> suggest it does.

Features (5) and (6) suggest that conjugated vinyl free radicals are unreactive towards oxygen and conjugated vinyl anions unreactive towards protons, while they are able to attack the triple bond and sustain the polymerization. We mention this, because it suggests an interesting



phenomenon, namely, that of the influence of charge delocalization on the specificity of the reaction.

The authors are indebted to the Weizmann Institute of Science, Roswell Park Memorial Institute and the State University of New York at Buffalo for granting mutual visits that made this work possible.

This research has been supported in part by a grant from the National Aeronautics and Space Administration (Grant NGR-3-015-016) and by a grant from the National Institutes of Health (Grant GM-11-603).

### References

1. R. Rein, N. Fukuda, H. Win, G. A. Clarke, and F. E. Harris, *J. Chem. Phys.*, **45**, 4743 (1966).
2. A. A. Berlin, *J. Polym. Sci.*, **55**, 621 (1961).
3. J. Manassen and J. Wallach, *J. Amer. Chem. Soc.*, **87**, 2671 (1965).
4. M. Benesh, J. Peska, and O. Wichterle, in *Macromolecular Chemistry, Paris, 1963* (*J. Polym. Sci. C*, **4**), M. Magat, Ed., Interscience, New York, 1963, p. 1377.
5. B. E. Lee and A. M. North, *Makromol. Chem.*, **79**, 135 (1964).
6. I. M. Barkalov, A. A. Berlin, V. S. Gulganskii, and G. O. Min Gao, *Vysokomol. Soedin.*, **5**, 368 (1963).
7. J. Kriz, M. J. Benes, and J. Peska, *Coll. Czech. Chem. Commun.*, **32**, 4043 (1967).
8. I. M. Barkalov, A. A. Berlin, V. S. Gulganskii, and B. G. Drantiev, *Vysokomol. Soedin.*, **3**, 1103 (1960).
9. A. Zilkha, B. Fiet, and M. Frankel *J. Polym. Sci.*, **49**, 231 (1961).
10. J. Wallach and J. Manassen, *J. Polym. Sci., A-1*, **7**, 1983 (1969).

Received August 16, 1968

Revised November 5, 1969

## Reduction of Pendent Ester Groups in Polycarbonates by Use of Diborane

R. E. WHITE and Z. G. GARDLUND, *General Motors Research  
Laboratories, Warren, Michigan 48090*

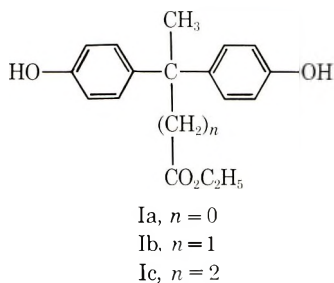
### Synopsis

A series of polycarbonates with pendent ester groups have been synthesized. These ester groups have been converted to hydroxyl functionalities by reduction with diborane in tetrahydrofuran. The number of methylene groups in the pendent chain has a large effect on the reducibility of the ester.

### INTRODUCTION

Interest in the synthesis of hydroxylated polycarbonates, i.e., polycarbonates containing one pendent hydroxyl group in every monomeric unit, led to the exploration of reductive hydroboration. The only previous study of reductive hydroboration in polymer systems was reported by Hecht and Marvel,<sup>1</sup> who successfully reduced carboxylic acid end groups in polysiloxanes without attacking the Si—O linkages.

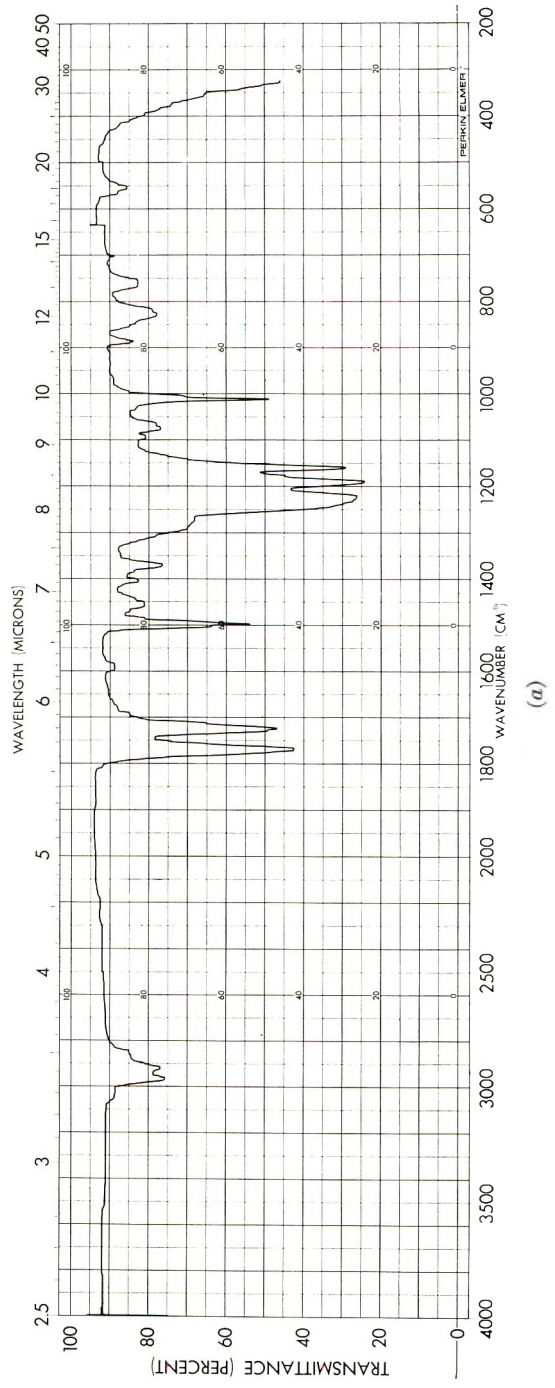
The polycarbonates in the work reported here were prepared from a series of esters (I) with varying methylene chain lengths. Copolymers of Ic with bisphenol A were also



prepared and studied. Under the proper conditions, the pendent ester group in the polycarbonates prepared from Ic are readily reduced to the alcohol by diborane in tetrahydrofuran. Molecular weight degradation is moderate, and excellent yields of the desired product are obtained.

### DISCUSSION

Diborane in tetrahydrofuran is a very effective reducing agent for the ester groups in these polymers. This is clearly shown in Figure 1. The in-



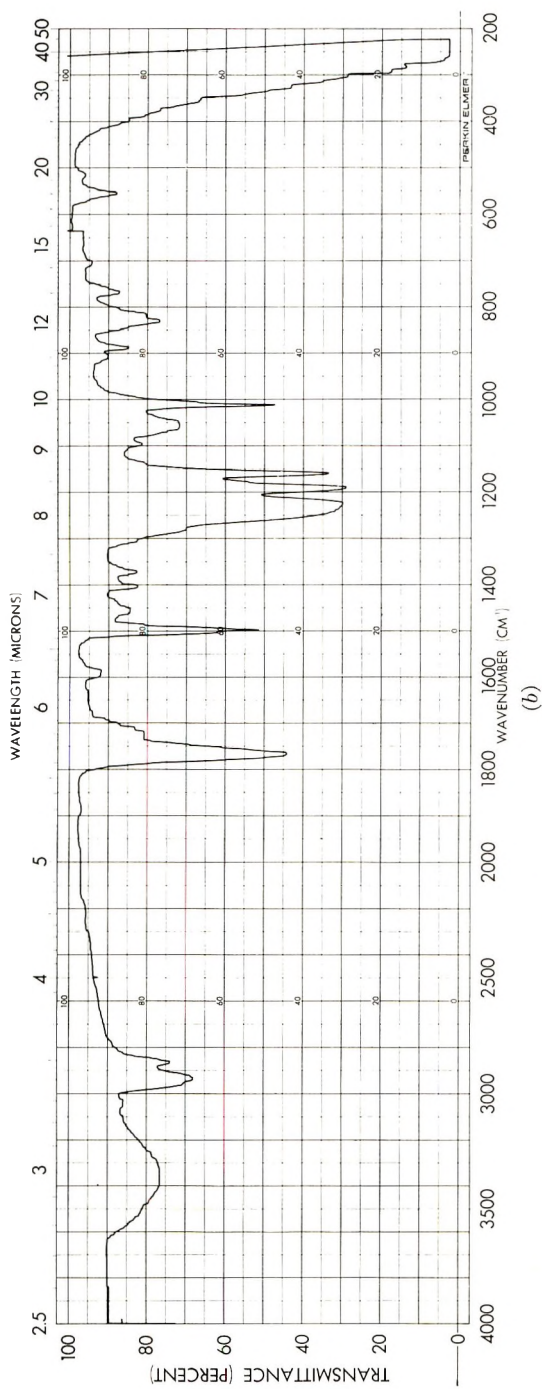


Fig. 1. Infrared spectra of polycarbonate from ethyl 4,4-bis(*p*-hydroxyphenyl)pentanoate (Ic) (a) before and (b) after reduction with diborane-tetrahydrofuran. Polymer films were cast from tetrachloroethane onto KBr plates.

TABLE I  
Experimental Data on Polycarbonates Before and After Reduction

Polycarbonate of	Polycarbonate before reduction			Polycarbonate after reduction		
	$\bar{M}_n$	$\eta_{inh}$	Analysis Calcd, %	$\bar{M}_n$	$\eta_{inh}$	Analysis found, %
Ethyl 2,2-bis( <i>p</i> -hydroxyphenyl)propanoate (Ia)	17 500	—	C, 69.1 H, 5.1	6 000	—	C, 68.7 H, 5.2
Ethyl 3,3-bis( <i>p</i> -hydroxyphenyl)butanoate (Ib)	16 500	—	C, 70.0 H, 5.5	9 500	—	C, 69.7 H, 5.6
Ethyl 4,4-bis( <i>p</i> -hydroxyphenyl)pentanoate (Ic)	13 000	—	C, 70.6 H, 5.9	6 500	—	C, 81.5 H, 6.1
2,2-Bis( <i>p</i> -hydroxyphenyl)propane (bisphenol A)	13 500	0.4	C, 75.6 H, 5.5	12 000	0.3	C, 74.2 H, 5.2
Copolymer of Ic and bisphenol A (4:1 mole ratio)	16 700	0.7	C, 71.7 H, 5.9	9 500	0.2	C, 72.4 H, 6.0
Copolymer of Ic and bisphenol A (1:1 mole ratio)	35 000	1.3	C, 72.5 H, 5.7	12 000	0.2	C, 73.2 H, 6.0
Copolymer of Ic and bisphenol A (1:4 mole ratio)	18 800	0.9	C, 74.3 H, 5.6	5 600	0.1	C, 74.0 H, 5.7

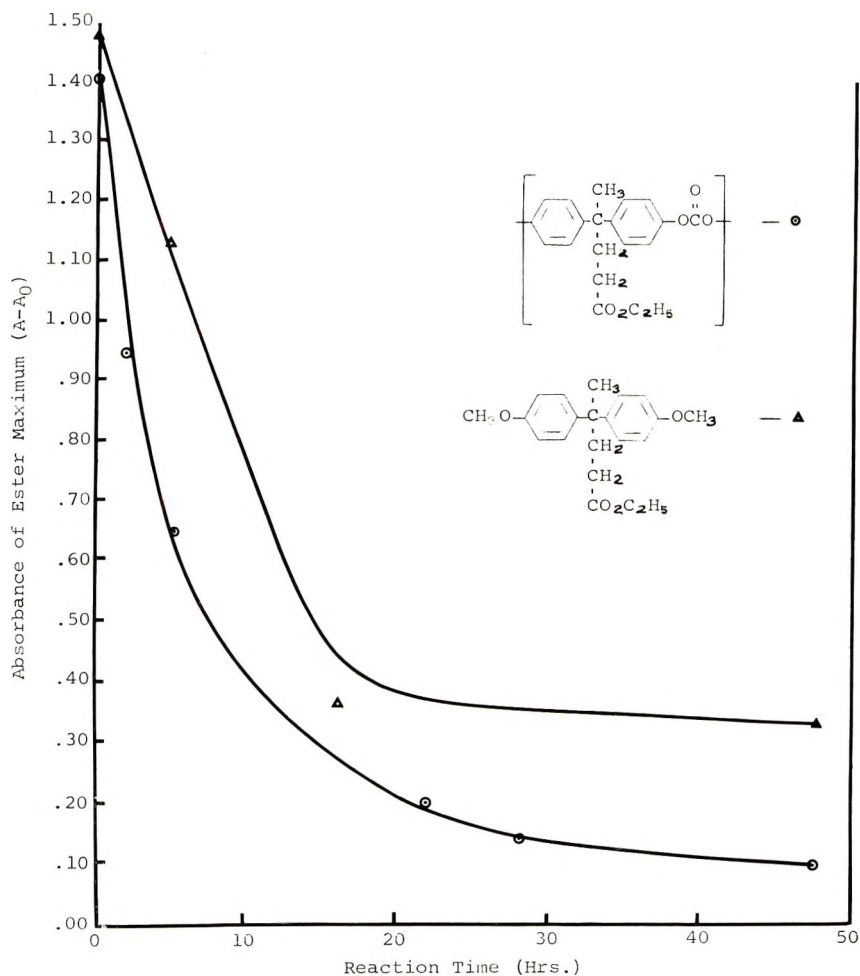


Fig. 2. Disappearance of ester as a function of reaction time.

frared spectrum of the polycarbonate from ethyl 4,4-bis(*p*-hydroxyphenyl)pentanoate (Ic) exhibits characteristic maxima at  $1765$  and  $1725$   $\text{cm}^{-1}$  due to the carbonate linkage and ester group, respectively. After reaction with diborane, the ester group is reduced, while a new infrared maximum appears at  $3350$   $\text{cm}^{-1}$  due to the hydroxyl group. Quantitative infrared and elemental analyses show that the ester group is 80% reduced.

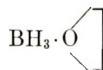
A plot of absorption at  $1725$   $\text{cm}^{-1}$  (corrected for baseline and using the aromatic maximum at  $1500$   $\text{cm}^{-1}$  as a standard) versus time in Figure 2 shows that reaction beyond 16 hr does not increase ester reduction significantly. Reduction of the model compound ethyl 4,4-bis(*p*-dimethoxyphenyl)pentanoate under identical conditions yields a similar plot. Again, the disappearance of the ester absorbance (corrected) is plotted against reaction time. The reduction is 32% complete after 2 hr, 54% after 5 hr.

and 90% complete after 28 hr. An additional reaction time of 20 hr results in an increase to 92% reduction.

Whereas lithium aluminum hydride under the same conditions not only reduces the ester but also severely degrades the polycarbonate, the diborane-tetrahydrofuran system does not attack the carbonate linkages significantly. This is illustrated in Table I where the results of diborane reductions of a series of polycarbonates are summarized. An 80% reduction in ester functionality would result in an approximately 10% reduction of molecular weight. For the polycarbonate of Ic, for example, if only ester reduction took place, the recovered polymer should have a number-average molecular weight of about  $11700 \pm 1100$ , not the  $6500 \pm 650$  observed. This indicates that some polymer degradation does take place. Acetylation of the reduced polycarbonate with acetyl chloride in pyridine yielded a polymer with a very strong maximum at  $1725 \text{ cm}^{-1}$  and no absorbance at  $3350 \text{ cm}^{-1}$ . The number-average molecular weight increased to  $7000 \pm 700$ . This increase in molecular weight is further proof that 80% of the ester moieties had been reduced to hydroxyl groups.

With the polymers from Ia and Ib, which have essentially identical elemental analyses before and after reduction and almost unchanged infrared spectra, little or no ester reduction is taking place. For Ib, the slight decrease in ester absorption shows that about 10% of the ester is reduced, while in Ia there is no decrease in the maximum at  $1725 \text{ cm}^{-1}$  after reaction. Thus, the changes in molecular weight for these two polymers are due to polymer degradation.

The question arises, why is the ester group in the polycarbonate from Ic reduced so readily, while in Ib it undergoes only a small amount of reduction and is unaffected in Ia? This may be answered in terms of steric hindrance. In the polycarbonate prepared from ethyl 2,2-bis(*p*-hydroxyphenyl) propionate (Ia), the ester group is attached directly to the backbone of the polymer. The bulkiness of the phenyl rings inhibits attack by the complex,



The steric quality of the carbonate linkages has not been changed. These are still attacked by the reducing agent with resulting polymer degradation.

## EXPERIMENTAL

### Materials

All solvents were purified by stirring with the appropriate drying agent followed by distillation. Tetrahydrofuran was distilled from lithium aluminum hydride, pyridine from barium oxide and diglyme from calcium hydride. Diborane was purchased from Alfa Inorganics as a 1*M* solution in tetrahydrofuran. Diborane was also generated in the laboratory using the method of Zweifel and Brown.<sup>2</sup>

### Synthesis of Bisphenol Esters

Published procedures were used in the preparation of ethyl 4,4-bis(*p*-hydroxyphenyl)pentanoate<sup>3</sup> (Ic) and ethyl 3,3-bis(*p*-hydroxyphenyl)butanoate<sup>4</sup> (Ib). In a similar manner, the previously unreported ethyl 2,2-bis(*p*-hydroxyphenyl)propionate was synthesized by condensing ethyl pyruvate with excess phenol in the presence of anhydrous calcium chloride and concentrated hydrochloric acid. The ester (mp 61–63°C uncorr.) was obtained in 17.5% yield.

ANAL. Calcd for C<sub>17</sub>H<sub>18</sub>O<sub>4</sub>: C, 71.4%; H, 6.3%. Found: C, 71.2%; H, 6.2%.

### Preparation of Polycarbonates

The polycarbonates were prepared by dissolving the recrystallized esters (0.1 mole) in anhydrous pyridine (250 ml) under a nitrogen atmosphere and bubbling phosgene (10% molar excess) through the rapidly stirred solution. The polymers were precipitated into water, washed with hot water and vacuum dried. Reprecipitation from chloroform into methanol afforded the desired polycarbonates in 95 wt-% yields (Table I). The polycarbonate of bisphenol A, as well as several copolymers of ethyl 4,4-bis(*p*-hydroxyphenyl)pentanoate and bisphenol A, were synthesized in a similar manner. Number-average molecular weights were determined by membrane osmometry at 45.0°C in *sym*-tetrachloroethane. Inherent viscosities were determined in *sym*-tetrachloroethane at 29.5°C.

### Reductive Hydroborations of Polycarbonates

All reductions were carried out in a manner similar to that described below for the polycarbonate of ethyl 4,4-bis(*p*-hydroxyphenyl)pentanoate (Ic). A solution of polycarbonate (3.0 g) in dry tetrahydrofuran (250 ml) under a nitrogen atmosphere was cooled to 0°C and treated dropwise with a diborane solution (55 ml, 0.055 mole) during 1 hr. After the required reaction time at 0–5°C, the unreacted diborane was destroyed with a 50:50 methanol–tetrahydrofuran solution (100 ml). The total volume was reduced to 100 ml, and the polymer was precipitated into 5% aqueous hydrochloric acid. Reprecipitation from pyridine into water and drying gave 2.6 g (86 wt-%) of polymer.

### Acetylation of Reduced Polymer

The hydroxyl groups of reduced polymers were acetylated as follows. The reduced polycarbonate of Ic (2.0 g) was dissolved in dry pyridine (60 ml). Acetyl chloride (3.3 ml, tenfold molar excess) was added dropwise, and after 2 hr stirring, the solution was precipitated into cold water (800 ml). The polymer was washed three times with hot water, dried and reprecipitated from tetrahydrofuran into methanol. The yield of dry tan polymer was 1.9 g.

ANAL. Calcd for C<sub>20</sub>H<sub>20</sub>O<sub>5</sub>: C, 70.50%; H, 5.92%. Found: C, 69.61%; H, 5.92%.



### Synthesis of Ethyl 4,4-Bis(*p*-methoxyphenyl)pentanoate

Dimethyl sulfate (13.5 g, 0.107 mole) was added dropwise to a solution of ethyl 4,4-bis(*p*-hydroxyphenyl)pentanoate (Ic) (20 g, 0.067 mole, mp 128–129°C) in aqueous sodium hydroxide (8 g in 150 ml of water) while the temperature remained about 40°C. A total of 83 g of dimethyl sulfate and 26 g. of sodium hydroxide in 450 ml of water was added while the pH was maintained at 9–10. An off-white oil formed which after 2 hr of vigorous stirring was dissolved in ethyl ether. The basic aqueous layer was extracted twice with ether. The ether solutions were combined, dried and reduced to a cloudy white oil. Distillation yielded 15 ml of clear, colorless, viscous oil (65% yield, bp 205–210°C/0.005 mm, no infrared absorption at 3500 cm<sup>-1</sup>).

ANAL. Calcd. for C<sub>21</sub>H<sub>26</sub>O<sub>4</sub>: C, 73.66%; H, 7.66%; molecular weight, 342.42. Found: C, 73.30%; H, 7.30%; molecular weight, 316.

### References

1. J. K. Hecht and C. S. Marvel, *J. Polym. Sci. A-1*, **5**, 685 (1967).
2. G. Zweifel and H. C. Brown, *Org. Reactions*, **13**, 1 (1963).
3. R. P. Fischer, G. R. Hartranft, and J. S. Heckles, *J. Appl. Polym. Sci.*, **10**, 245 (1966).
4. A. J. Yu and A. R. Day, *J. Org. Chem.*, **23**, 1004 (1958).

Received November 6, 1969

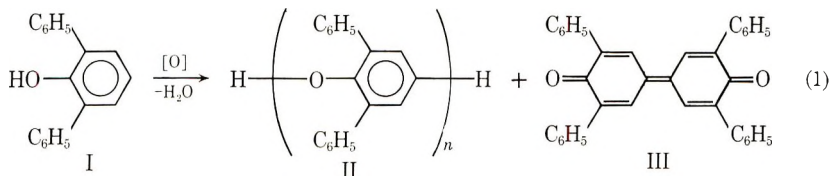
## Polymerization by Oxidation Coupling. I. A Study of the Oxidation of 2,6-Diphenylphenol to Poly(2,6-diphenyl-1,4-phenylene ether)

DWAIN M. WHITE and HOWARD J. KLOPFER, *General Electric Research and Development Center, Schenectady, New York 12301*

### Synopsis

The synthesis of poly(2,6-diphenyl-1,4-phenylene ether), by the oxidative coupling of 2,6-diphenylphenol has been studied. Procedures were found which demonstrated that polymers of very high molecular weight ( $\bar{M}_n > 200\,000$ ;  $[\eta]_{\text{CHCl}_3}^{25^\circ\text{C}} > 1.1$  dl/g) could be made with a copper-amine catalyst system. A low nitrogen-to-copper ratio (1 N atom/Cu atom) was necessary to obtain the very high molecular weights under the conditions of these reactions. A variety of amines formed active catalysts; the effectiveness of mono- and bis- primary, secondary, and tertiary amines were compared. Effects of the type of copper halide, reaction temperature, desiccants, addition rates of 2,6-diphenylphenol, and solvents were also examined. Samples of polymer were isolated at different times during the polymerization. Measurements of viscosity, osmotic pressure, light scattering, gel permeation, phenolic hydroxyl groups, and nitrogen content were made on various samples over a range of intrinsic viscosities of 0.05–0.59 dl/g. A very narrow molecular weight distribution was found for all samples. Hydroxyl endgroup analyses indicated that the concentration of phenolic endgroups per mole of polymer does not change during the polymerization. The presence of some side reactions is indicated by nitrogen analyses. The relationships between the intrinsic viscosity in chloroform at 25°C and  $\bar{M}_n$  and  $\bar{M}_w$  are:  $\log [\eta] = -3.97 + 0.72 \log \bar{M}_n$  and  $\log [\eta] = -3.56 + 0.62 \log \bar{M}_w$ .

The oxidative coupling of 2,6-diphenylphenol (I) with a copper halide-amine catalyst and oxygen was reported by Hay<sup>1-3</sup> to produce a high yield of poly(2,6-diphenyl-1,4-phenylene ether) (II) and small amounts of 3,3',5,5'-tetraphenyl-4,4'-diphenoquinone (III). The general characteris-



tics of the oxidative coupling of 2,6-diphenylphenol were found to be similar to coupling reactions of 2,6-dimethylphenol and other 2,6-disubstituted phenols which form analogous poly(phenylene ethers) and diphenoquinones.<sup>1-4</sup> One major difference, however, in the case of 2,6-diphenylphenol

oxidation was that the intrinsic viscosities of the polymers were never very high under the conditions for the oxidation of other 2,6-disubstituted phenols to high polymers. A second difference was that the high temperatures which were required to produce polymers of moderately high intrinsic viscosity did not produce large quantities of the diphenoquinone. This report describes reaction conditions for the synthesis of II whereby polymers with high intrinsic viscosities (over 1.1 dl/g;  $\bar{M}_n > 200\,000$ ) can be made. The characterization of polymers between the molecular weight range of  $\bar{M}_n \approx 5000$  to 135 000 is reported.

### EXPERIMENTAL

The 2,6-diphenylphenol, mp 104°C, was recrystallized three times from a mixture of isopropanol and toluene. The solvents, monoamines, *N,N,N',N'*-tetramethyl-1,3-butanediamine, and *N,N,N',N'*-tetramethylethylenediamine were either reagent-grade or redistilled. The other alkanediamines were used directly as obtained from the Ames Laboratory, Inc. (Milford, Conn.). The cuprous chloride was reprecipitated from concentrated hydrochloric acid solution with methanol. All desiccants were taken from newly opened bottles.

TABLE I

Reaction no.	[CuBr]:[nitrogen]:[DPP] ratio <sup>a</sup>	Polymer I		Yield of III, %
		[ $\eta$ ], dl/g <sup>b</sup>	Yield, %	
1	2:1:40	0.78 <sup>c</sup>	94	3.9
2	1:1:40	0.80 <sup>d</sup>	92	4.6
3	1:1:20	0.72	96	2.7
4	1:1.5:40	0.64	94	4.2
5	1:2:40	0.47 <sup>e</sup>	90	3.6
6	1:3:40	0.39	92	3.2
7 <sup>f</sup>	1:10:40	0.14	87	5.0
8 <sup>g</sup>	1:1:40	0.86	92	3.7
9	1:1:80	0.76	92	5.8
10	1:1:160	<0.05 <sup>h</sup>	h	6.5 <sup>h</sup>
11	1:2:160	0.32 <sup>i</sup>	91	

<sup>a</sup> Catalyst ratios for a CuBr-TMBD catalyst with 6.43 g MgSO<sub>4</sub> in 125 ml benzene and a 5-hr reaction time at 60° and 12.3 g 2,6-diphenylphenol (DPP) added over an 18-min period, unless noted otherwise.

<sup>b</sup> Intrinsic viscosity in CHCl<sub>3</sub> at 25°C.

<sup>c</sup> After 24-hr reaction: [ $\eta$ ] = 0.80 dl/g.

<sup>d</sup> After 23-hr reaction: [ $\eta$ ] = 0.90 dl/g.

<sup>e</sup> After a reaction time of 4 hr.

<sup>f</sup> All of the DPP was added at the start of the reaction; the reaction time was 3 hr.

<sup>g</sup> The DPP concentration was 20%.

<sup>h</sup> After 24 hr, DPP was still present and only traces of polymer precipitated when the solution was added to methanol. At 25 hr, the catalyst ratio was changed to 1:0.5:80. After 55 hr, [ $\eta$ ] 0.87 dl/g. The yield of III was measured after 31 hr.

<sup>i</sup> After a reaction time of 19 hr.

Viscosities were measured in chloroform at 25°C unless noted otherwise. A description of the techniques for the light-scattering and osmotic measurements has appeared elsewhere.<sup>5</sup>

### General Method for Polymerization (Reaction 2, Table I)

A 250-ml wide-mouth Erlenmeyer flask was fitted with a Vibromixer, a thermometer, a dropping funnel, and an oxygen inlet tube and was partially immersed in a large stirred oil bath at 60°C. To the flask materials were added in the order listed: benzene (100 ml), *N,N,N',N'*-tetramethyl-1,3-butanediamine (0.11 ml, 0.00063 mole), cuprous bromide (0.179 g, 0.00125 mole), and anhydrous magnesium sulfate (6.3 g). Oxygen was passed through the solution at 0.15 ft<sup>3</sup>/hr and 2,6-diphenylphenol (12.3 g, 0.050 mole) in benzene (25 ml) at 60°C was added dropwise over an 18-min period. The viscosity of the reaction mixture was measured by the flow time through a calibrated 4-ml pipet. Flow times during the course of the reaction were: 5.0 sec (at 0 min reaction time), 8.4 sec (60 min), 23.2 sec

TABLE II  
Effect of Amine<sup>a</sup>

Amine	Cu:N	II		Yield of III, %
		[ $\eta$ ], dl/g	Yield, %	
Monoamines				
<i>n</i> -Butylamine	1:1	0.37	87%	7.3
<i>n</i> -Butylamine	1:2	0.31	87	4.3
Di- <i>n</i> -butylamine	1:1	0.36, 0.39	88	5.0
Di- <i>n</i> -butylamine	1:2	0.19	90	4.6
Dimethylstearylamine	1:1	0.26	92	5.2
Ditertiary amines				
Me <sub>2</sub> N—CH <sub>2</sub> —NMe <sub>2</sub>	1:1	0.06	44	<0.01
Me <sub>2</sub> N—(CH <sub>2</sub> ) <sub>2</sub> NMe <sub>2</sub>	1:1	0.86	90	3.7
Me <sub>2</sub> N—(CH <sub>2</sub> ) <sub>2</sub> NMe <sub>2</sub>	1:1 <sup>b</sup>	0.86	88	7.5
TMBD	1:1 <sup>c</sup>	0.80	92	4.6
Me <sub>2</sub> N—(CH <sub>2</sub> ) <sub>4</sub> —NMe <sub>2</sub>	1:1	0.06	63	0.1
Me <sub>2</sub> N—(CH <sub>2</sub> ) <sub>6</sub> —NMe <sub>2</sub>	1:1	0.06	82	0.3
Other diamines				
NH <sub>2</sub> —(CH <sub>2</sub> ) <sub>2</sub> —NH <sub>2</sub>	1:1	—	0	0
EtNH—(CH <sub>2</sub> ) <sub>2</sub> —NH <sub>2</sub> Et	1:1	—	0	8.6
MeNH(CH <sub>2</sub> ) <sub>3</sub> NHMe	1:1	1.13	90	
MeNH(CH <sub>2</sub> ) <sub>3</sub> NHMe	1:1 <sup>d</sup>	0.05	91	
MeNH(CH <sub>2</sub> ) <sub>3</sub> NHMe	1:1 <sup>e</sup>	0.90	91	
MeNH(CH <sub>2</sub> ) <sub>3</sub> NHMe	1:2	0.04	42	

<sup>a</sup> In all runs monomer was added over a period of ca. 18 min. The components and conditions were: MgSO<sub>4</sub> (6.3g), 2,6-diphenylphenol (12.6 g), CuBr, benzene, at 60°C for 22 hr unless specifically noted.

<sup>b</sup> CuCl instead of CuBr.

<sup>c</sup> Reaction time: 5 hr.

<sup>d</sup> Reaction temperature: 50°C.

<sup>e</sup> Reaction temperature: 70°C.

TABLE III  
Description of Products from the First Large-Scale Polymerization

Reaction time, min	Weight, g <sup>a</sup>	Intrinsic viscosity, dl/g	Functional group analyses		Gel-permeation data			
			Hydroxyl absorbance	Nitrogen, ppm	$\bar{M}_n$	$\bar{M}_w$	$\bar{M}_w/\bar{M}_n$	
139	28.6	0.09		55				
155	26.3	0.11	0.64	90	9 700	15 100	1.55	
164	29.7	0.13	0.47	125	15 400	24 400	1.59	
173	30.4	0.18	0.34	100	25 700	41 000	1.59	
176	30.4	0.19	0.3	110	31 900	50 100	1.57	
185	31.9	0.23	0.21	140	43 400	67 700	1.56	
190	33.2	0.24	0.178	160	56 200	93 300	1.66	
195	30.5	0.30	0.153	160	66 400	108 000	1.63	
201	27.4	0.35	0.137	220	96 600	145 000	1.49	
205	30.6	0.39	0.118	185	94 600	152 000	1.61	
214	28.4	0.41	0.091	185	105 000	176 000	1.67	

<sup>a</sup> Average sample weight is calculated to be 33 g. The overall yield was 94%.

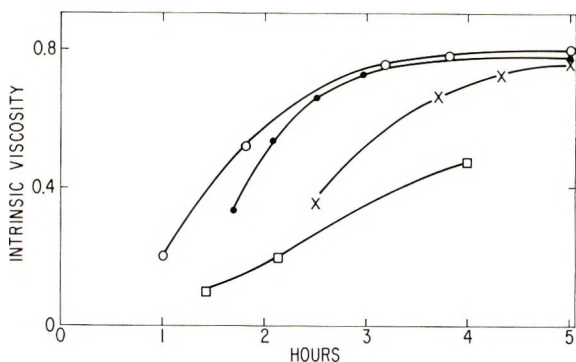


Fig. 1. Polymerization rates for reactions in Table I with Cu:N:monomer ratios of (O) 1:1:40; (●) 2:1:40; (X) 1:1:80; (□) 1:2:40.

(108 min), 51.2 sec (186 min), and 59 sec (232 min). At 257 min, a 1.00-ml sample was removed for determination of III (see below for analytical method). At 300 min, concentrated hydrochloric acid (2.0 ml) was added to the reaction mixture. The reaction mixture was filtered and the filtrate was added dropwise to methanol (1000 ml) which was being stirred vigorously with a Polytron homogenizer. The precipitate was collected on a filter and washed thoroughly three times by stirring with hot acetone (1000 ml). After drying overnight at 45°C/12 mm, the white solid polymer II weighed 11.2 g (92%). The intrinsic viscosity in  $\text{CHCl}_3$  at 25°C was 0.80 dl/g. The yield of III was 4.6%.

The polymerization reactions described in Tables I and II were carried out under similar conditions. In some cases, small samples were withdrawn at the 5-hr point and the reaction was continued for longer periods. Viscosity measurements during polymerization (for rate data in Fig. 1) were made by measuring the flow time of the reaction mixture from a 4-ml pipet. The pipet had been calibrated with solutions of the polymer of known viscosity. Although additional solvent was added before measuring the flow time to replace solvent lost by evaporation, some variations in concentration resulted, and these values are approximate.

### Preparation of Polymers with Varying Molecular Weights

**First Large-Scale Reaction (Table III).** The polymerization was carried out at 60°C. Oxygen (4.4 ft<sup>3</sup>-hr) was bubbled through a mixture of cuprous bromide (5.24 g, 0.0364 mole), *N,N,N',N'*-tetramethyl-1,3-butanediamine (3.20 ml, 0.0182 mole), and anhydrous magnesium sulfate (180 g) in benzene (2880 ml). 2,6-Diphenylphenol (360 g, 1.46 mole) in benzene (720 ml) was added over a period of 6 min, and the change in viscosity of the reaction mixture was determined by the flow time from a calibrated 4-ml pipet. After 139 min, a 350-ml sample was removed, acidified with concentrated hydrochloric acid (6 ml), and precipitated by rapid dropwise addition to methanol which was being stirred vigorously

TABLE IV  
Description of Products from the Second Large-Scale Polymerization

Polymerization time, min	Weight, g <sup>a</sup>	Intrinsic viscosity, dl/g	Osmotic pressure and light-scattering data		
			$\bar{M}_n$	$\bar{M}_w$	$\bar{M}_w/\bar{M}_n$
38	1.9 <sup>b</sup>	0.05			
56	3.1	0.05			
159	9.7	0.24	39 000	50 500	1.30
174	9.8	0.32	59 200 <sup>c</sup>	89 000	1.50
178	10.0	0.37	80 500	99 000	1.23
181	9.6	0.41			
198	9.8	0.50	110 000	185 000	1.68
220	59.6	0.59	134 000	220 000	1.64

<sup>a</sup> Except for the last sample, the calculated yields are  $10 \pm 0.5$  g.

<sup>b</sup> A gas chromatograph of the filtrate after precipitation showed considerable monomer and some dimer present.

<sup>c</sup> The sample displayed abnormal behavior; the osmotic pressure increased with time.

with a Polytron homogenizer. Additional samples were removed at intervals of 5–15 min. The precipitated polymers were dissolved in benzene, decolorized by dropwise addition of hydrazine, reprecipitated into methanol, washed with methanol, and dried at 80°C overnight in a vacuum oven.

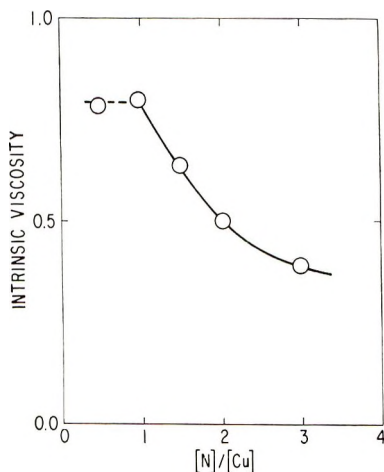


Fig. 2. Effect of the ratio of nitrogen atoms to copper atoms on the intrinsic viscosity of polymer II for polymerizations with a TMBD-CuBr catalyst at 60°C for 5 hr.

**Second Large-Scale Reaction (Table IV).** The polymerization was carried out in a similar manner to the first reaction, except it was on a smaller scale (140 g, 2,6-diphenylphenol in 1400 ml benzene) and the hydrazine treatment was omitted. The oxygen flow rate was 1.75 ft<sup>3</sup>/min.

### Determination of III

Benzene was added to the polymerization reaction mixture to replace that removed by entrainment and bring the volume to 150 ml (for a polymerization with 0.05 mole 2,6-diphenylphenol). A 1.00-ml aliquot of reaction mixture was diluted with benzene to 500 ml in a volumetric flask, and the absorbance was measured at 490  $m\mu$ . The quantity of III was calculated from the expression:

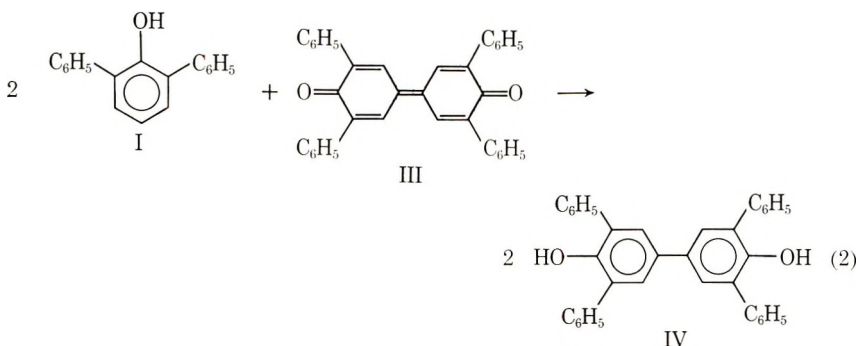
$$\text{III} = (\text{absorbance}) \times \frac{488 \times 500 \times 150}{53\,000} \text{ mg}$$

where 488 = molecular weight of III, 500 is a dilution factor, 150 is the volume of the reaction mixture, and 53 000 =  $E_{490}$  of III in benzene.

## RESULTS AND DISCUSSION

### Polymerization

**Copper-Nitrogen Ratios.** Two principal reasons for the lower reactivity of 2,6-diphenylphenol compared to 2,6-dimethylphenol in oxidative coupling reactions appear to be the increased steric hindrance of the phenyl groups adjacent to the hydroxyl group and the higher oxidation potential when there are no electron-donating *o*-methyl groups. To attain a more active polymerization system, the oxidation was run at temperatures which are higher than used for 2,6-dimethylphenol oxidation. At the higher temperatures, two side reactions could predominate. One side reaction is the oxidation of the amine in the catalyst. The other is the amine-catalyzed oxidation of 2,6-diphenylphenol (I) to 3,3',5,5'-tetraphenyl-4,4'-dihydroxybiphenyl (IV) by the diphenoquinone (II):\*



Oxygen and the copper-amine catalyst can convert IV to III, and then further oxidation of I to IV by reaction (2) can occur. To minimize side reactions due to the free amine, polymerizations were carried out under conditions where all of the amine should be strongly chelated to the copper. To attain this, the amine-to-copper ratios were low, and tertiary diamines

\* By analogy with the reaction between 2,6-dimethylphenol and 3,3',5,5'-tetramethyl-4,4'-diphenoquinone.<sup>6</sup>



which were capable of forming five- or six-membered ring chelates with copper were used.

Several examples of combinations of *N,N,N',N'*-tetramethyl-1,3-butane-diamine (TMBD) and cuprous bromide and a description of the products are presented in Table I. The rate of viscosity increase is presented in Figure 1 for several reaction conditions. These data indicate that the ratio of nitrogen atoms to copper atoms in the catalyst has a pronounced effect on the rate of polymerization and on the intrinsic viscosity of the polymeric product. In Figure 2, the maximum intrinsic viscosity attained is plotted against the ratio of copper atoms to nitrogen atoms in the catalyst. Under the conditions of these experiments, a ratio of 1:1 produced the highest intrinsic viscosity. Lower ratios also yielded high polymers, but the reaction rates were proportionately slower (Fig. 1).

The requirement of one nitrogen atom per copper atom for optimum results, appears unusual, since normal coordination of copper would be expected to involve two nitrogen atoms. Yet, the possibility that only half the copper is being used and the remainder is not in solution seems unlikely, since the reaction with a 1:1 Cu:N ratio proceeded at a faster rate than the reaction with a 1:2 Cu:N ratio. If half of the copper in the 1:1 reaction were in a 1:2 Cu:N ratio and the remainder was uncomplexed, the reaction with the 1:1 ratio should have proceeded instead at less than half the rate of the 1:2 reaction. With the 2:1 ratio the reaction proceeded at the same rate as with the 1:1 ratio, which indicates that in this case only half of the copper is being utilized, again, in a 1:1 ratio. Possibly, a more active catalyst species is present at the 1:1 ratio than in the 1:2 ratio and is either deactivated by additional amine or converted to a less active species when additional amine is present. If amine is present in a nonchelated form, i.e., when the N:Cu ratio is greater than two, the side reactions described above could occur. Lower molecular weight polymers were formed with the higher N:Cu ratios.

A decrease in catalyst concentration causes a proportionately slower rate of polymerization, but the polymer eventually builds up to the same high molecular weight as with higher concentrations (reaction 9, Table I). When the catalyst concentration is as low as Cu:I equals 1:160, no polymerization is detected; addition of an equal quantity of catalyst to the reaction mixture which changes the ratio to 1:80 produces polymer with a high viscosity ( $[\eta] = 0.87$  dl/g; Table I, reaction 11). Thus, there appears to be a minimum catalyst requirement under these conditions.

The yields of the C-C coupled product III are presented in Table I. No appreciable change in the ratio of C-C to C-O coupling occurs as the Cu:N ratio is decreased. Thus, amine catalysis of reaction (2) is not an important side reaction under these conditions. The overall catalyst concentration does affect the C-C to C-O ratio slightly, since the quantity of III increases from 3% to 6% as the ratio of monomer to copper is increased from 20 to 80.

In one case (Table I, reaction 8) the catalyst and monomer concentrations were increased (20% monomer instead of 10%) although the ratio of

Cu:TMBD:monomer was 1:1:40. As in reaction 2, the intrinsic viscosity of the product after 5 hr (0.86 dl/g) was greater than for the 10% reaction after 5 hr, but less than the value for the 10% reaction after 24 hr. The higher concentration enhanced the rate slightly. The yield of III decreased with the higher catalyst concentrations, which again indicates the formation of III is concentration-dependent.

**Effect of Amine Structure.** The highly effective 1:1 Cu:N ratio (see preceding section) was used in an examination of a variety of mono- and bis- primary, secondary, and tertiary amines. In several instances a 1:2 ratio was also employed in order to determine whether the 1:1 ratio was specific only for the bis-tertiary amines. The results are summarized in Table II.

Monoamines, whether primary, secondary, or tertiary, polymerized 2,6-diphenylphenol to polymers with moderately high molecular weights. With the Cu:N ratio of 1:1 for butylamine and dibutylamine, intrinsic viscosities were higher than with the 1:2 ratio ( $\sim 0.4$  dl/g compared to  $\sim 0.3$  and  $0.2$  dl/g). Yields of III were also higher for the 1:1 ratio (particularly in the case of butylamine, in which there was a 7% conversion of monomer to III).

Bis-tertiary amines did not produce high polymer unless the two nitrogen atoms were separated by either two or three carbon atoms. In the cases where the number of carbon atoms linking the nitrogen atoms was only one or was either four or more, very low polymers resulted. The intrinsic viscosities of these products were 0.06 dl/g, which was even well below the value of 0.26 dl/g from the mono-tertiary amine. The quantities of III were also low for the less active amines, indicating that C-C coupling was also retarded. A possible explanation for the behavior of the bis-tertiary amines is that amines that cannot form stable five- or six-membered cyclic chelates with the copper tend to form polymeric complexes which are much less soluble than the cyclic species and that the complexes precipitate from solution.

Examples of the effectiveness of other bis-amines are presented at the bottom of Table II. Ethylenediamine and its *N,N'*-diethyl derivative, were completely unreactive for polymerization. This was not the case for C-C coupling with the latter amine, however, since it produced the largest quantity of III of all the amines which were examined. A bis-secondary amine, *N,N'*-dimethyl-1,3-propanediamine (DMPD), formed a very active catalyst. This catalyst was very sensitive to the Cu:N ratio ( $[\eta] = 0.04$  dl/g at 1:2 ratio,  $[\eta] = 1.13$  dl/g at 1:1 ratio) and temperature ( $[\eta] = 0.05$  dl/g at 50°C,  $[\eta] = 1.13$  dl/g at 60°C, and  $[\eta] = 0.90$  dl/g at 70°C).

TABLE V

Reaction	Catalyst	$[\eta]$ , dl/g
A	CuBr· $\frac{1}{2}$ TMBD	0.90
B	CuBr· $\frac{1}{2}$ TMED	0.86
C	CuCl· $\frac{1}{2}$ TMBD	0.78
D	CuCl· $\frac{1}{2}$ TMED	0.86

**Copper Halide.** Both cuprous bromide and cuprous chloride produce high polymer when used with active amines. This is illustrated in Table V for four reactions run at 60°C with identical concentrations and with a 5-hr reaction time for reaction B and 22 hr for the others.

The rates of polymerization for the first 3 hr of reaction were in the order  $k_A > k_B > k_C > k_D$ .

**Drying Agents.** A variety of desiccants were used to determine the importance of water removal during polymerization. Polymerization does occur if a desiccant is not present, although the rate is less than when magnesium sulfate is present. Calcium chloride interfered with the reaction and gave both a very low polymer yield (8%) and a low intrinsic viscosity (0.1 dl/g). With 4 Å molecular sieves the rate of polymerization was as fast as with MgSO<sub>4</sub>, but the viscosity leveled off at a lower value (0.65 dl/g).

### Polymer Characterization

**Molecular Weight.** A series of polymers with intrinsic viscosities varying from 0.05 to 0.59 dl/g were obtained by periodically removing samples from two polymerization reactions. In both reactions, the very effective copper to nitrogen ratio of 1:1 was used. Values for the molecular weights and hydroxyl absorptions of phenolic endgroups of the purified samples are listed in Table III and Table IV.

The molecular weights were determined by several methods. Dynamic osmotic pressure measurements in benzene at 34°C provided number-average molecular weights  $\bar{M}_n$ . Light-scattering measurements in chloroform gave normal Zimm plots from which weight-average molecular weights  $\bar{M}_w$  were calculated. From gel-permeation chromatographic curves of the samples in chloroform at 25°C,  $\bar{M}_n$  and  $\bar{M}_w$  values were calculated by a computer integration method.<sup>7</sup>

The values of  $\bar{M}_n$  and  $\bar{M}_w$  from osmotic and light-scattering measurements show a linear relationship in log-log plots against intrinsic viscosity (Fig. 3). A similar set of curves is obtained from the gel-permeation data. However, the curves from gel permeation data were not superimposable with the curves from osmotic and light scattering. Apparently, the characteristics of the gel-permeation column which were calibrated for polystyrene and corrected by a size per Angstrom correction factor,<sup>7</sup> which has been done satisfactorily with other polyphenylene ethers, do not permit translation directly to polymer II without additional correction. One feature, however, for both sets of data is the narrow molecular weight dispersion. In all cases, the  $\bar{M}_w/\bar{M}_n$  ratio is well below a value of 2; the average value from the light scattering-osmotic pressure data is 1.5.

A comparison of the  $\bar{M}_n-[\eta]$  relationships of polymer II and poly(2,6-dimethyl-1,4-phenylene ether) (PPO, General Electric Company) is also shown in Figure 3. The curve for PPO polymer is based on static and dynamic measurements on a series of forty samples covering the range of intrinsic viscosities from 0.02 to 2.3 dl/g. The difference in intrinsic viscosity of II compared to PPO polymer for a given molecular weight is too

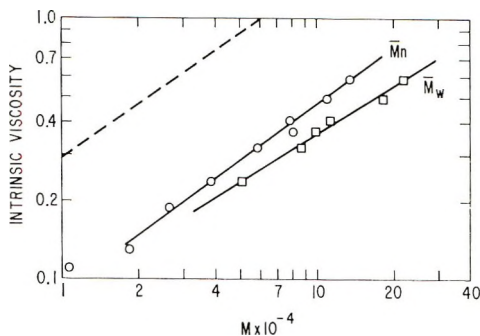


Fig. 3. Intrinsic viscosity (chloroform, 25°C) vs. molecular weight relationship for polymer II: (O)  $\bar{M}_n$ ; (□)  $\bar{M}_w$ ; (---)  $\bar{M}_n$  for PPO.

large to be attributed only to the larger weight of the monomeric unit of I (244 versus 120 in PPO polymer). Other factors, e.g., chain stiffness, appear to be important.\*

The relationships between intrinsic viscosity at 25° and molecular weight in chloroform are  $\log [\eta] = -3.97 + 0.727 \log \bar{M}_n$  and  $\log [\eta] = -3.56 + 0.624 \log \bar{M}_w$ .

**Hydroxyl Analysis.** The hydroxyl absorption in the infrared spectrum of 2,6-diphenylphenol occurs at 3543  $\text{cm}^{-1}$  and the molar extinction coefficient in carbon disulfide at 25°C is 220 when the concentration is  $2 \times 10^{-3}$  M. The value increases to ca. 223 at infinite dilution. For II, the hydroxyl absorption in carbon disulfide occurs at 3550  $\text{cm}^{-1}$ . The absorbances for a 2.5% solution with a 1-cm path length are tabulated in Table III. The baseline was determined by completely acetylating the polymer by heating in acetic anhydride and pyridine until no further change was detected at 3550  $\text{cm}^{-1}$ . The intensities are inversely proportional to the molecular weights. This is demonstrated in Figure 4, in which the absorbance of a 2.5% solution is plotted against the reciprocal of the molecular weight. Values for  $\bar{M}_n$  were taken from the viscosity- $\bar{M}_n$  relationship in Figure 3. From this plot, it appears that the number of hydroxyl groups per molecule does not change over a molecular weight range of ca. 10 000 to 100 000. If one assumes that there is one hydroxyl group per polymer molecule, the extinction coefficient for the hydroxyl absorption can be calculated to be 320. This value is 45% greater than that for diphenylphenol and is in marked contrast to the case for PPO polymer in which the extinction coefficients of the monomer and low oligomers are very similar to those of the corresponding polymers.<sup>9</sup>

The constancy of the hydroxyl absorption per molecule indicates that side reactions or termination reactions which involve the phenolic end of the polymer chain and tend to decrease the hydroxyl absorption are not occurring.

**Nitrogen Analyses.** The total nitrogen contents of some of the polymers have been measured by a Kjeldahl procedure. The values (listed in

\* The dilute solution properties have been described by Akers et al.<sup>8</sup> and Schultz.<sup>5</sup>

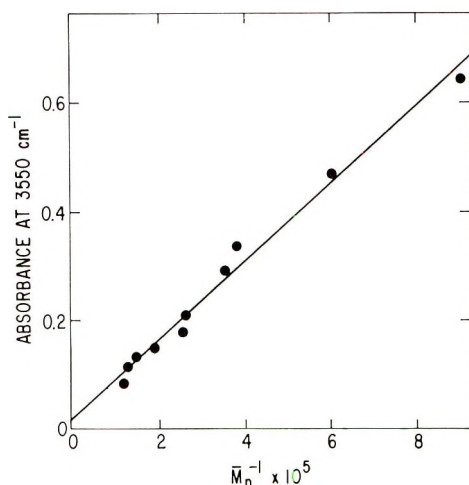


Fig. 4. Hydroxyl absorbance at  $3550 \text{ cm}^{-1}$  for polymer samples described in Table III.

Table III) in general, increase as the molecular weight increases. For the sample in Table III of highest molecular weight ( $\bar{M}_n = 83\,000$ ), the nitrogen content is equal to approximately one nitrogen atom per polymer molecule. This quantity is similar to the amounts of nitrogen found in PPO polymer when tertiary amine catalysts are used in the polymerizations.<sup>9</sup>

The gradual incorporation of nitrogen into the polymer indicates at least one type of side reaction is occurring during the synthesis.

The use of hydrazine during the workup of the polymer does not result in nitrogen incorporation. This was demonstrated in the analysis of samples for which the hydrazine step was omitted.

The authors would like to thank Drs. A. S. Hay and A. R. Shultz for helpful discussions and Mrs. D. V. Temple, Mrs. S. Woodyatt, Mrs. C. L. Symes, and Mr. W. Ruminski for analytical determinations.

### References

1. A. S. Hay, *J. Polym. Sci.*, **58**, 581 (1962); *SPE Trans.*, **2**, 108 (1962); *Adv. Polym. Sci.*, **4**, 496 (1967); U. S. Pats. 3,306,874 (1967); 3,306,875 (1967); 3,432,456 (1969).
2. A. S. Hay, *Macromolecules*, **2**, 107 (1969).
3. A. S. Hay and D. M. White, *Polymer Preprints*, **10**, No. 1, 92 (1969); paper presented at 157th ACS Meeting, Division of Polymer Chemistry, April, 1967, paper 17.
4. A. S. Hay, H. S. Blanchard, G. F. Endres, and J. W. Eustance, *J. Amer. Chem. Soc.*, **81**, 6335 (1959).
5. A. R. Shultz, paper presented at IUPAC International Symposium on Macromolecular Chemistry, Toronto, 1968, paper A2.
6. A. S. Hay, *Tetrahedron Letters*, **1965**, 4241.
7. L. E. Malay, in *Analysis and Fractionation of Polymers* (*J. Polym. Sci. C*, **8**), J. Mitchell, Jr., and F. W. Billmeyer, Jr., Eds., Interscience, New York, 1965, p. 253.
8. P. J. Akers, G. Allen and M. M. Bethell, *Polymer*, **9**, 575 (1968).
9. D. M. White and H. J. Klopfer, unpublished results.

Received October 3, 1969

Revised November 17, 1969

## Influence of Microstructure on the Tensile Behavior of Acrylic Copolymers

JOHN N. MAJERUS and ANTHONY R. PITOCHELLI, *Redstone Research Laboratories, Rohm and Haas Company, Huntsville, Alabama 35807*

### Synopsis

Uniaxial tensile properties were determined for two series of copolymers: ethyl acrylate-acrylic acid and butyl acrylate-acrylic acid. The comonomer ratio was varied from 85/15 to 95/5 and various molar ratios of a difunctional carboxylate epoxy crosslinker were used. The master modulus curves indicated that increasing the amount of crosslinker and/or increasing the number of crosslink sites per chain caused both the equilibrium modulus and the transition temperature to increase while increasing the bulk of the side groups decreased both the modulus and transition temperature. All the master ultimate strain curves exhibited a maximum value corresponding to some value of reduced time  $\tau_c$  and exhibited a shape analogous to a lognormal distribution function with nonzero asymptotes. The maximum ultimate strains were found to be a nonlinear function of the crosslink density and to occur at higher values of temperature and/or lower values of strain rate when either the amount of crosslinker or the relative frequency of the crosslink sites increased. Replacing the pendant ethyl group with a butyl group caused the maximum ultimate strains to occur at temperatures about 60°F lower than the corresponding ethyl acrylate copolymer. This replacement also decreased the magnitudes of the maximum ultimate strains associated with the same crosslink density. It was concluded that the chemical efficiency of the crosslink sites decreases with decreasing relative frequency of the crosslink sites along the prepolymer. Furthermore, the crosslink efficiency decreased as the length and flexibility of the non-reactive side groups increased. The dependency of the actual crosslink density was found to be critically influenced by the chemical crosslink efficiency. A molecular model involving both chain entanglements and chemical crosslinks is postulated which explains qualitatively the observed behavior of the master ultimate strain data.

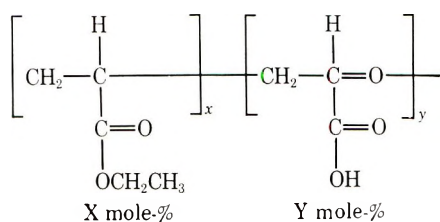
### INTRODUCTION

Although it is well known that polymeric mechanical properties such as stiffness and ultimate strain (or stress) depend in some fashion upon the microstructure of the polymeric network,<sup>1-4</sup> a knowledge of all the governing factors and their interrelationship is far from complete. This investigation was an attempt to further elucidate the microstructural influences and their interrelationships by means of a parametric study employing various crosslinkable acrylic copolymers. The actual chemical compositions and the mechanical testing procedure are outlined in the next section.

### EXPERIMENTAL

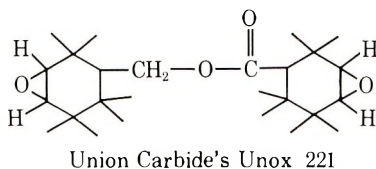
The two copolymers employed in this investigation were random copolymers of ethyl acrylate (EA) and acrylic acid (AA) and of butyl acrylate (BA) and acrylic acid. The acrylate/acrylic acid copolymers were prepared by combining the appropriate mole percentages of acrylic ester ( $X$ ) and acrylic acid ( $Y$ ) in dried ethyl acetate, adding benzyl peroxide initiator, and heating to reflux for 20 hr. This resulted in a random copolymer ( $\bar{M}_n \approx 40,000$ ) in a 50–60% polymer solution in ethyl acetate and has the average backbone composition I.

Prepolymer:



The crosslinker used in this investigation was Union Carbide's Unox 221, which is a short and stiff carboxylate diepoxide molecule.

Difunctional crosslinker:



Since this is a difunctional molecule, one molecule reacts with two carboxy hydrogens, and the stoichiometric molar ratio of Unox 221 is equal to  $Y/2$ . The crosslinker was blended with the ethyl acetate-copolymer solution, cast into a number of shallow trays, and the filled trays were placed in an air-flush box overnight to remove most of the ethyl acetate by evaporation. The resulting viscous fluid was then precured for 24 hr at 158°F to remove ethyl acetate. The trays were then placed in a 212°F oven and kept there for a period of days until the curing reaction was complete as discussed below.

In order to be sure that the mechanical properties were measured for a fully cured binder system, the surface hardness of the cast sheets was monitored as a function of time at the curing temperature. Typical results are shown in Figure 1 for three EA/AA copolymer ratios with stoichiometric levels of crosslinker. When the surface hardness reached an equilibrium value, the binder was defined to be fully cured. The acrylic acid content appeared to be the controlling factor in the rate of cure, and the copolymers took at least 12 days to cure. Each batch of copolymer was

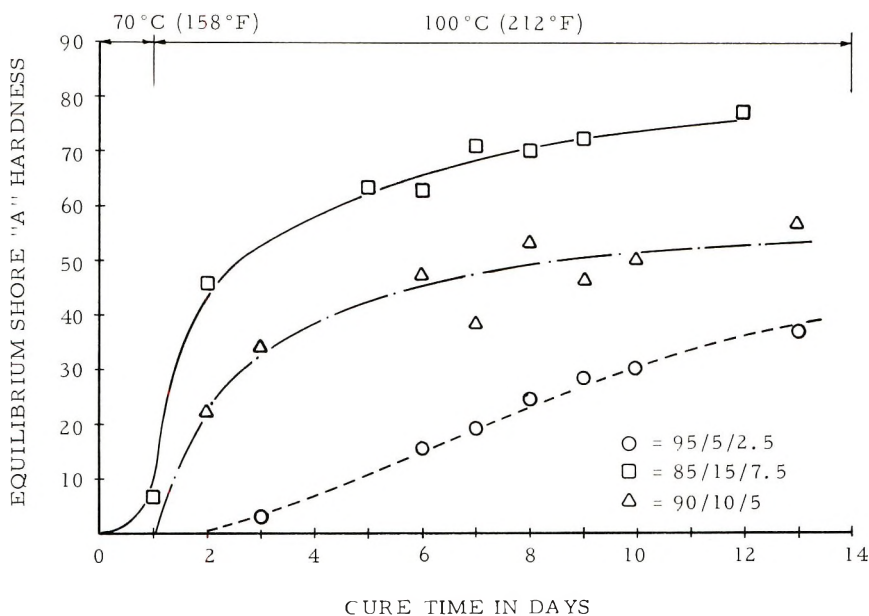


Fig. 1. Typical time dependence of surface hardness of EA/AA copolymers (with Uinox 221).

monitored separately and, when the durometer readings leveled off, the sheets were removed from the oven, and tensile test specimens were diecut from the sheets. At least eight different temperatures were employed in testing each specific formulation (except the 90/10/2.5 BA/AA copolymer), and three crosshead displacement rates, e.g., 0.1, 1, and 10 in./min, were used at each temperature. The gauge length  $L_0$  was experimentally determined for each specific formulation by means of fiducial marks and a micrometer caliper. Five specimens were tested at each combination of temperature and crosshead displacement rate  $D$ .

The initial tangent moduli and ultimate strains  $[(L_{\text{break}} - L_0)/L_0]$  were obtained from the experimental data and were plotted versus the logarithm of the reciprocal strain rate  $\dot{\epsilon}$  ( $\dot{\epsilon} \equiv D/L_0$ ). The resulting data were then shifted horizontally by an amount  $a_T$  to obtain two "master" curves for each copolymer formulation. The reference temperature for all formulations was chosen to be 78°F, and typical master ultimate strain and initial tangent modulus curves are shown for the 95/5/2.5 material in Figures 2 and 3, respectively. The test temperatures are listed in Figure 2, and the dashed curves refer to the upper and lower scatter bands which encompass almost all of the experimental data. The solid curve refers to the average behavior and the deviation between the average and the upper and lower scatter bands was on the order of  $\pm 15$ –30% for the ultimate strain data and  $\pm 20$ –40% for the initial tangent modulus for all the copolymer formulations. For comparison purposes, only the average curves will be shown for the remainder of the experimental data. Figures 4–7 show the resultant



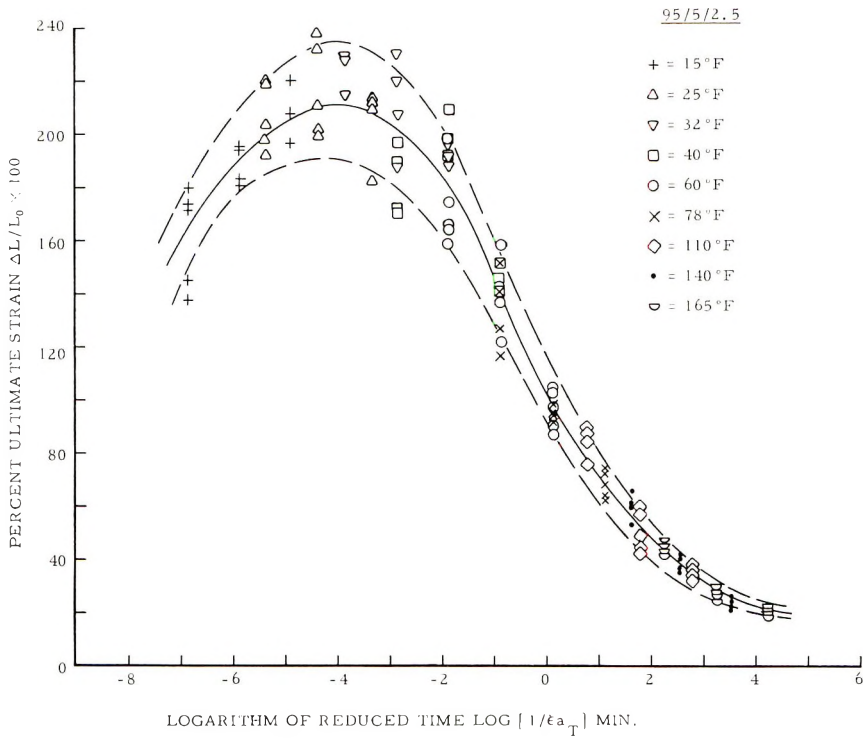


Fig. 2. Typical scatter associated with ultimate strain data.

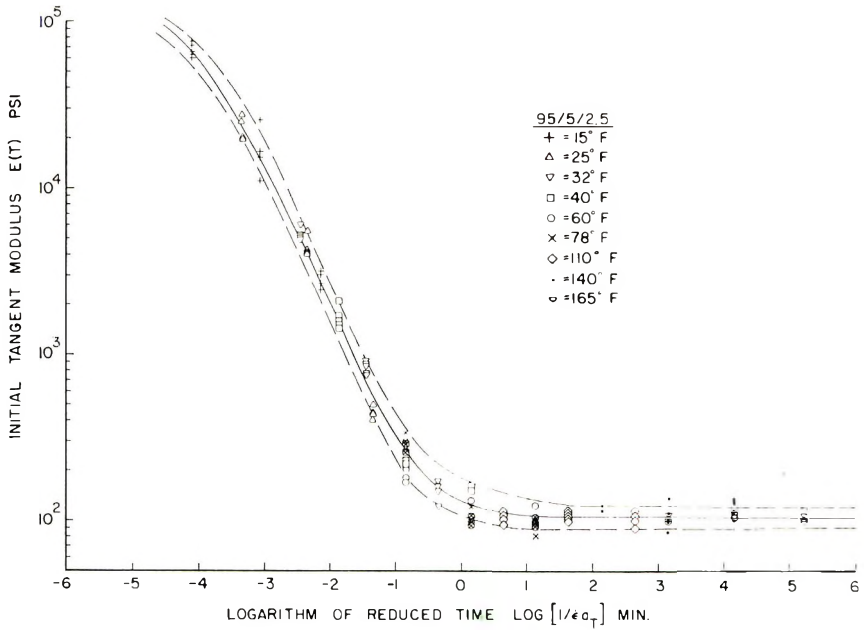


Fig. 3. Typical scatter associated with initial tangent modulus.

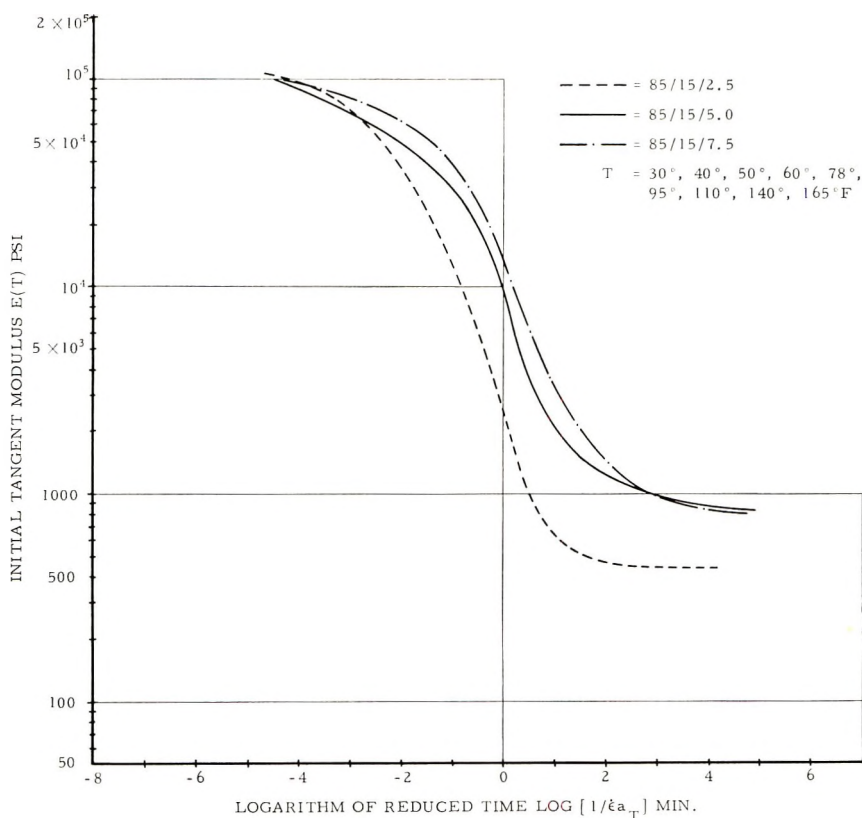


Fig. 4. Master modulus curves for 85/15 EA/AA copolymers.

average master tangent modulus curves for the EA/AA/Unox 221 copolymers, while Figures 8 and 9 contain the average curves for the BA/AA/Unox 221 copolymers. The master ultimate strain curves for the EA/AA/Unox 221 copolymers are shown in Figures 10–13, while the average curves for the BA/AA/Unox 221 copolymers are shown and compared with the corresponding EA/AA/Unox 221 curves in Figures 14 and 15. The temperatures shown in each figure refer to the test temperatures employed to obtain the experimental data.

## DISCUSSION

All the master modulus curves exhibit the usual viscoelastic type of behavior<sup>1–4</sup> involving a plateau glassy region at small values of reduced time, followed by a rapidly changing transition region which leads to another plateau known as the rubbery or equilibrium region. Although all the copolymers appear to have approximately the same “glassy” modulus ( $2\text{--}4 \times 10^5$  psi), increasing the amount of reactive hardener (Figs. 4–6, 8, 9) and/or increasing the AA content (Fig. 7) increases the equilibrium modulus (see Table I) and shifts the transition region to higher values of reduced

TABLE I  
Measured Values Associated with the Experimental Data

Case	Copolymer system	Composition	Avg. no. of monomer units between theoretical cross-link junctions	Equilibrium modulus $E_r$ , psi	Maximum ultimate strain $\epsilon_{\text{ult}}^m$ , %	Nominal temp. at $\epsilon_{\text{ult}}^m$ , °F <sup>a</sup>	Log of glassy width $\Delta\tau_g$ , min	Log of rubbery width $\Delta\tau_r$ , min	Rubbery strain capability $\epsilon_r$ , %
1	EA/AA/ -Unox 221	95/5/2.5	19	100	212	28	—	4.7	18
2		90/10/2.5	18	300	105	43	3.5	3.5	9
3		85/15/2.5	17	450	84	69	2.9	2.8	6
4		90/10/5	9	520	78	53	3.9	3.6	7
5		85/15/5	8.5	800	43	84	3.7	3.6	5
6		85/15/7.5	5.67	800	45	93	4.0	3.2	5
7		90/10/10	9	640	61	78	3.7	3.0	7
8		95/5/5	19	200	151	33	3.6	4.1	10
9	BA/AA/- Unox 221	90/10/2.5	18	190	—	—	—	—	8
10		85/15/2.5	17	240	107	13	3.0	3.6	7
11		90/10/5	9	340	75	4	3.9	4.1	6
12		85/15/5	8.5	420	61	23	3.4	3.9	6
13		85/15/7.5	5.67	630	40	33	4.2	4.0	5
14		90/10/10	9	580	47	13	5.0	5.4	5

<sup>a</sup> Associated with a strain rate of 1 in./in./min.

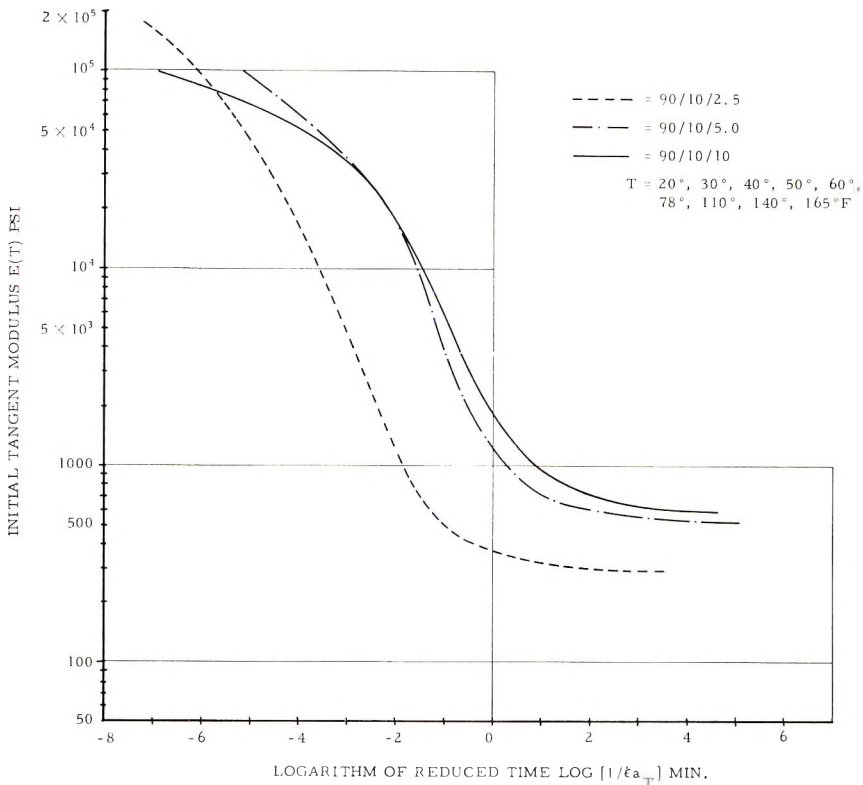


Fig. 5. Master modulus curves for 90/10 EA/AA copolymers.

time (corresponding to higher temperature). Increasing the AA content of the copolymer increases the amount of crosslinking sites. For an ideal chemical system, every crosslink site becomes a crosslink junction for stoichiometric levels of reactive hardener. The number of theoretical crosslink junctions per unit volume is the theoretical crosslink density. Thus, the theoretical crosslink density is inversely proportional to the average number of acrylate ester monomer units between the theoretical crosslink junctions; e.g., an average number of 18 corresponds to one-half the theoretical crosslink density associated with an average number of 9. However, the relative value of the equilibrium modulus  $E_r$ , depends directly upon the actual crosslink density,  $\nu;^{1-4}$  i.e., doubling the value of  $\nu$  doubles the value of  $E_r$ . Therefore, the equilibrium modulus is a relative indication of the actual crosslink density. The first 3 EA/AA copolymer formulations shown in Table I (cases 1-3) have essentially the same theoretical crosslink density. Yet, there is a large difference in equilibrium moduli. When the theoretical crosslink density is doubled compared with the previous cases (cases 4 and 5), there is still a large difference in equilibrium modulus between copolymers with the same theoretical crosslink density. The physical difference in the backbone composition between these copolymers with

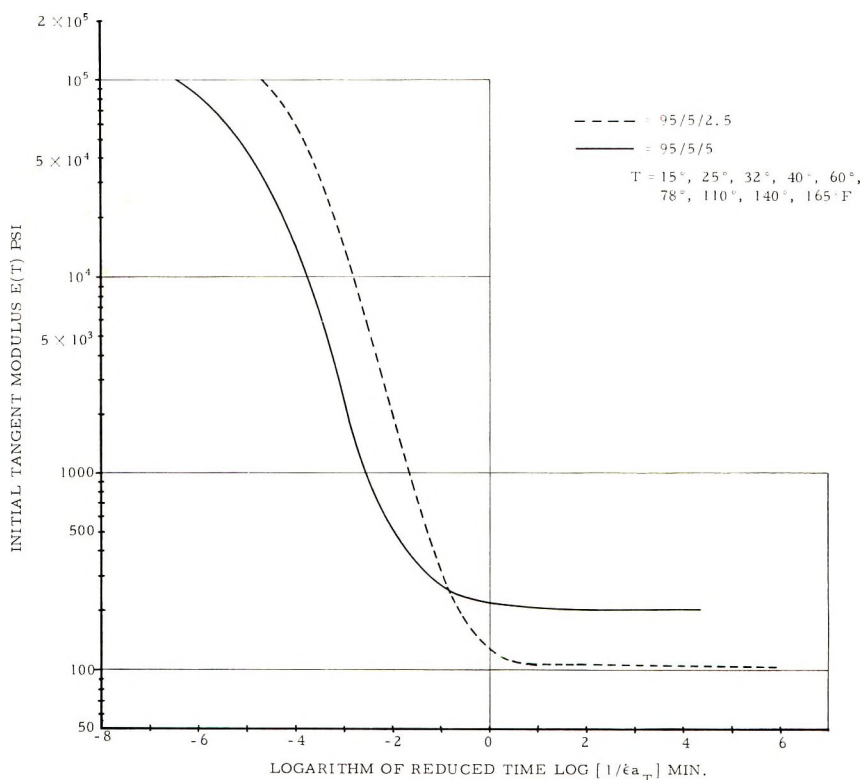


Fig. 6. Master modulus curves for 95/5 EA/AA copolymers.

the same theoretical crosslink density is the average spacing of the reactive side groups, i.e., 1 out of 20 monomers (case 1), 1 out of every 10 (cases 2 and 4), and 1 out of every 6.67 (cases 3 and 5). Hence, these moduli data indicate that as the average relative frequency of crosslink sites is decreased (decreasing the AA content) the apparent chemical efficiency (defined to be 1 when, for stoichiometric levels of crosslinker, every crosslink site becomes a crosslink junction) of the crosslink site-epoxy combination decreases. This conclusion is further substantiated by the modulus data for compositions employing twice the stoichiometric level of crosslinker. The equilibrium modulus was 520 psi for the 90/10 EA/AA copolymer with a stoichiometric level of reactive hardener (case 4). Therefore, if the chemical efficiency of the crosslink sites were 1, the crosslink level is at its maximum and additional reactive hardener should only impair the value of the modulus (due to plasticizer effect). However, doubling the level of reactive hardener (case 7) raised the equilibrium modulus to a value of 640 psi (23% change). This implies that not all the reactive sites had formed crosslink junctions for the stoichiometric level of reactive hardener, i.e., a chemical efficiency less than 1. Furthermore, in the case of the 95/5 EA/AA copolymer (cases 1 and 8), a level of crosslinker equal to twice the

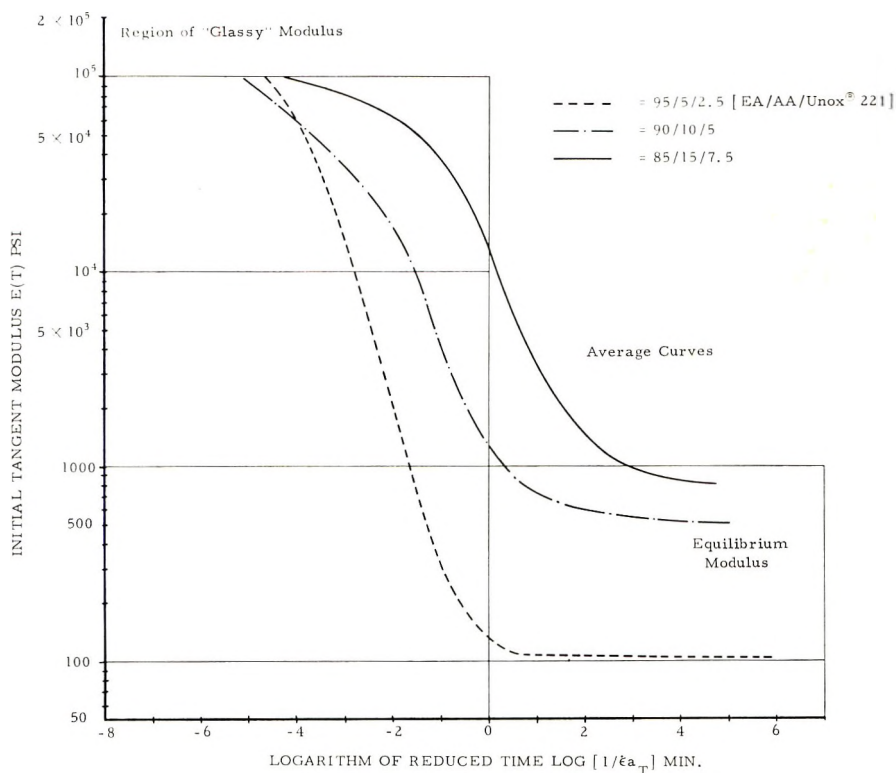


Fig. 7 Comparison of modulus behavior for EA/AA copolymers with stoichiometric levels of crosslinker.

stoichiometric amount increased the equilibrium modulus 100% over the  $E_r$  value associated with a stoichiometric level of Unox 221.

In the case of BA/AA copolymers, the formulations with the same theoretical crosslink density (cases 9 and 10; 11 and 12) exhibited the same behavior as described for the EA/AA copolymers except that the percentage difference between the moduli was not as large. Also, the equilibrium moduli for the BA/AA copolymers are less than the corresponding values for the EA/AA copolymers. This difference in the magnitude of  $E_r$  could be due to either a lower actual crosslink density and/or a more flexible chain backbone. Birshtein and Ptitsyn<sup>5</sup> have concluded that the torsional stiffness associated with a saturated chain backbone is mainly dependent upon the rigidity, size and polarity of the directly attached side groups. Hence, replacing the ethyl with the bulkier butyl group should have caused an increase in the torsional stiffness. Hence, the lower moduli cannot be due to a lower backbone flexibility. Therefore, the lower modulus may be due to a lower actual crosslink density  $\nu$ .

The percentage increase in the equilibrium moduli of the 85/15/5 versus the 85/15/2.5 formulation was the same for both the BA/AA and the EA/

AA copolymers (doubling the theoretical crosslink density produced a 75% increase in the modulus). However, a further increase (50%) in the theoretical crosslink density caused no change in the  $E_r$  value of the EA/AA copolymer (case 5 versus case 6) while increasing the BA/AA equilibrium modulus by 50%. Both the 90/10 and 85/15 BA/AA moduli appear to be approaching the corresponding EA/AA values. Therefore, the data imply that the chemical efficiency of the carboxyl groups on a backbone with butyl pendant groups is less than those associated with ethyl pendant groups. This is substantiated by the fact that increasing the amount of

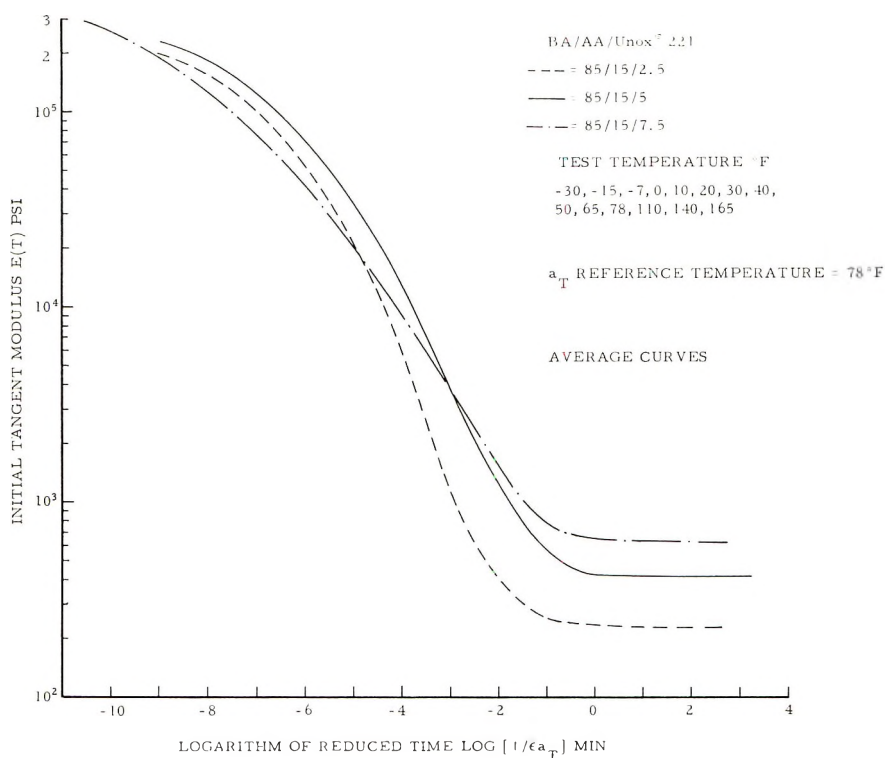


Fig. 8. Master modulus curves for 85/15 BA/AA copolymers.

Unox 221 to twice the stoichiometric level for the 90/10 compositions produced a 70% increase in the corresponding magnitude of  $E_r$  for the BA/AA copolymer (case 11 versus case 14) compared to only a 23% change for the EA/AA copolymer. The physical reasons for this decrease in crosslink efficiency can be readily seen from a Fisher-Hirschfelder molecular model. The bulk and torsional mobility of the pendant butyl groups acts as a shield to the reactive carboxyl and hence has a lower probability of reacting with an epoxide group. The probability of a reaction depends upon the number of reactive molecules available, and increases with an increasing amount of crosslinker.

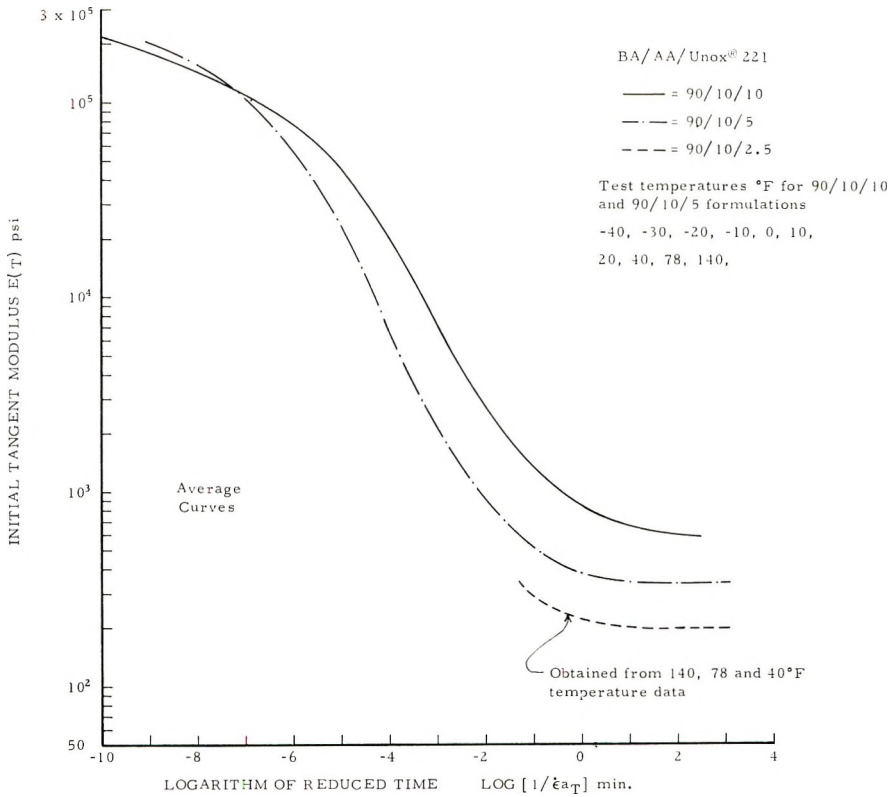


Fig. 9. Master modulus curves for 90/10 BA/AA copolymers.

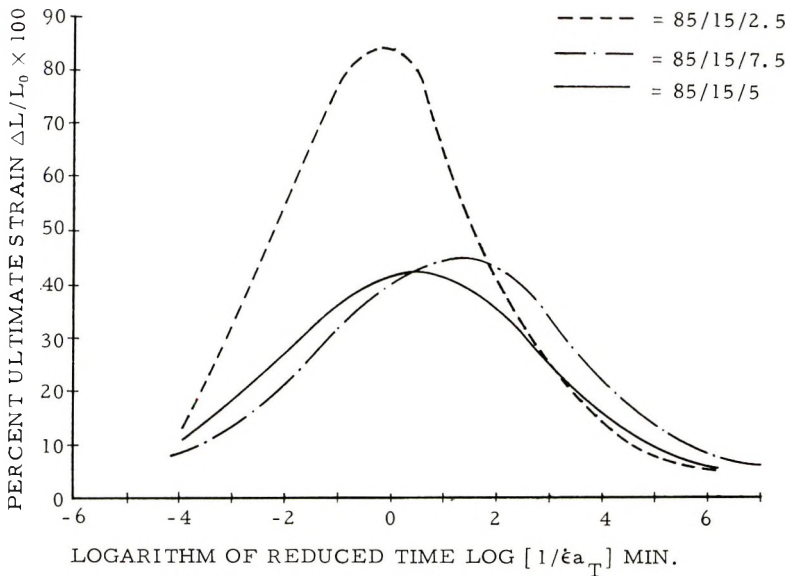


Fig. 10. Master strain curves for 85/15 EA/AA copolymers.



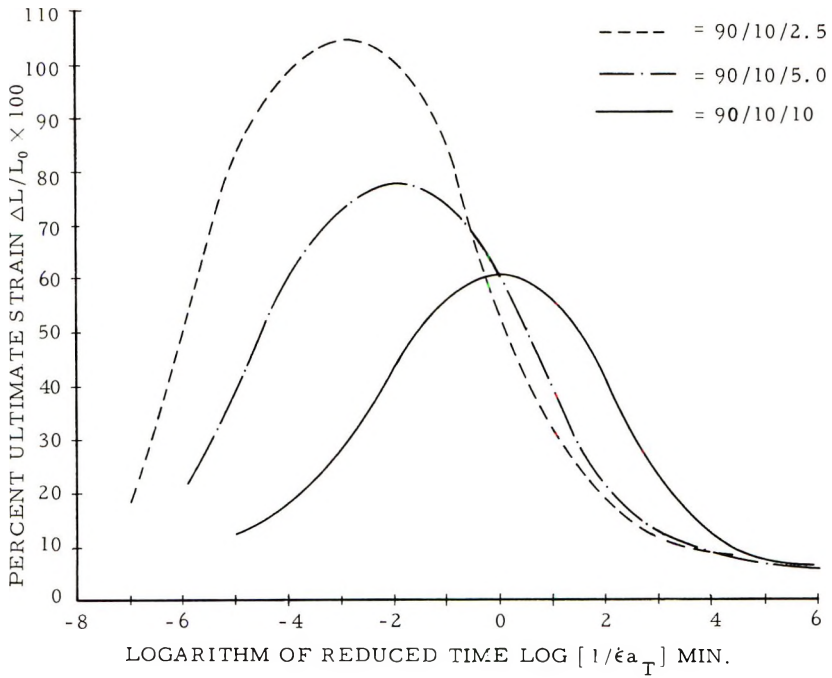


Fig. 11. Master strain curves for 90/10 EA/AA copolymers.

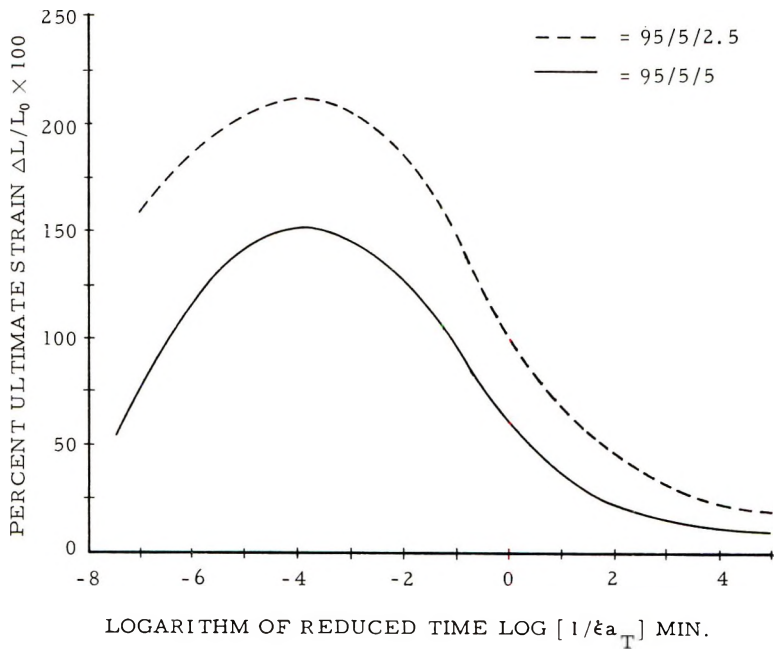


Fig. 12. Master strain curves for 91/5 EA/AA copolymers.

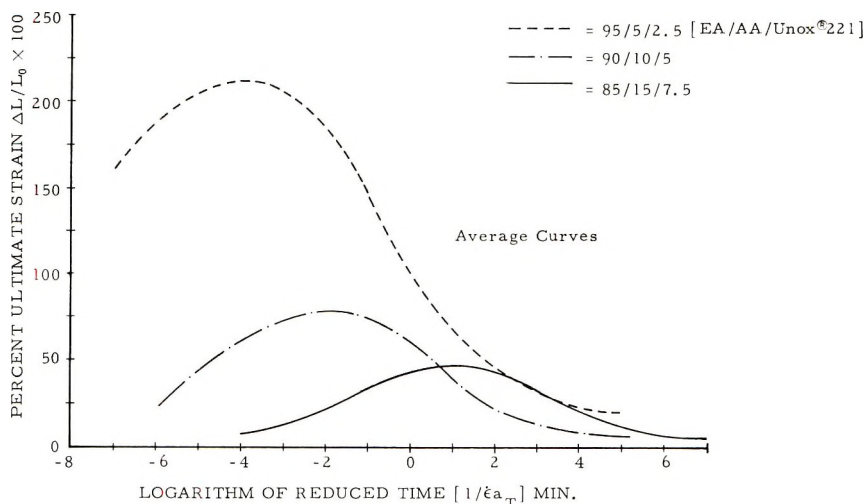


Fig. 13. Comparison of ultimate strain behavior for EA/AA copolymers with stoichiometric levels of crosslinker.

The master ultimate strain curve exhibited the same general shape for all formulations and for both the EA/AA and BA/AA copolymers (Figs. 10–15). The data for any given composition exhibits a maximum ultimate strain and, except for the asymptotes which appear to be non-zero, has a shape similar to a log normal or Pearson Type IV distribution<sup>6</sup> whose variate is replaced by the reduced time variable  $\tau$ . It appears that the master ultimate strain behavior could be described by a generalized curve such as Figure 16 which is characterized by six parameters; a maximum strain capability  $\epsilon_{ult}^m$  which occurs at some value of reduced time  $\tau_c$  (which can be associated with some particular temperature  $T_c$  for a nominal 1 in./in./min. strain rate), a rubbery strain capability  $\epsilon_r^*$  (associated with high temperatures and/or very slow strain rates), a glassy strain capability  $\epsilon_g^*$  (associated with low temperatures and/or extremely fast strain rates), and the breadth and skewness of the curve denoted by the glassy width  $\Delta\tau_g$  and the rubbery width  $\Delta\tau_r$ . The generalized curve was arbitrarily shown as skewed to the right with  $\epsilon_r^* > \epsilon_g^*$ . For a lognormal distribution function whose median or mode corresponds to  $\tau_c$ , the glassy and rubbery widths are identical. The characteristic parameters associated with the experimental ultimate strain data are listed in Table I for all the investigated copolymers. The test temperatures were not low enough to determine the glassy strain capability ( $\epsilon_g^*$ ) although in the cases of the 85/15/7.5 and 90/10/10 BA/AA copolymers (see Figs. 14 and 15) the data appear to be approaching the same limiting value as the rubbery strain capability.

The master ultimate strain curves shown in Figures 10–15 illustrate that the location of  $\epsilon_{ult}^m$  shifted to higher values of temperature and/or lower values of strain rate when either the amount of crosslinker or the relative

frequency of the reactive sites were increased. Furthermore, even when the theoretical crosslink density was held essentially constant (see Table I, cases 1, 2, 3, 8; 4, 5, 7; 11, 12, 14) the magnitude of  $\epsilon_{ult}^m$  decreased when either the relative frequency of the reactive sites or the level of crosslinker was increased. The modulus data indicated that the magnitude of the

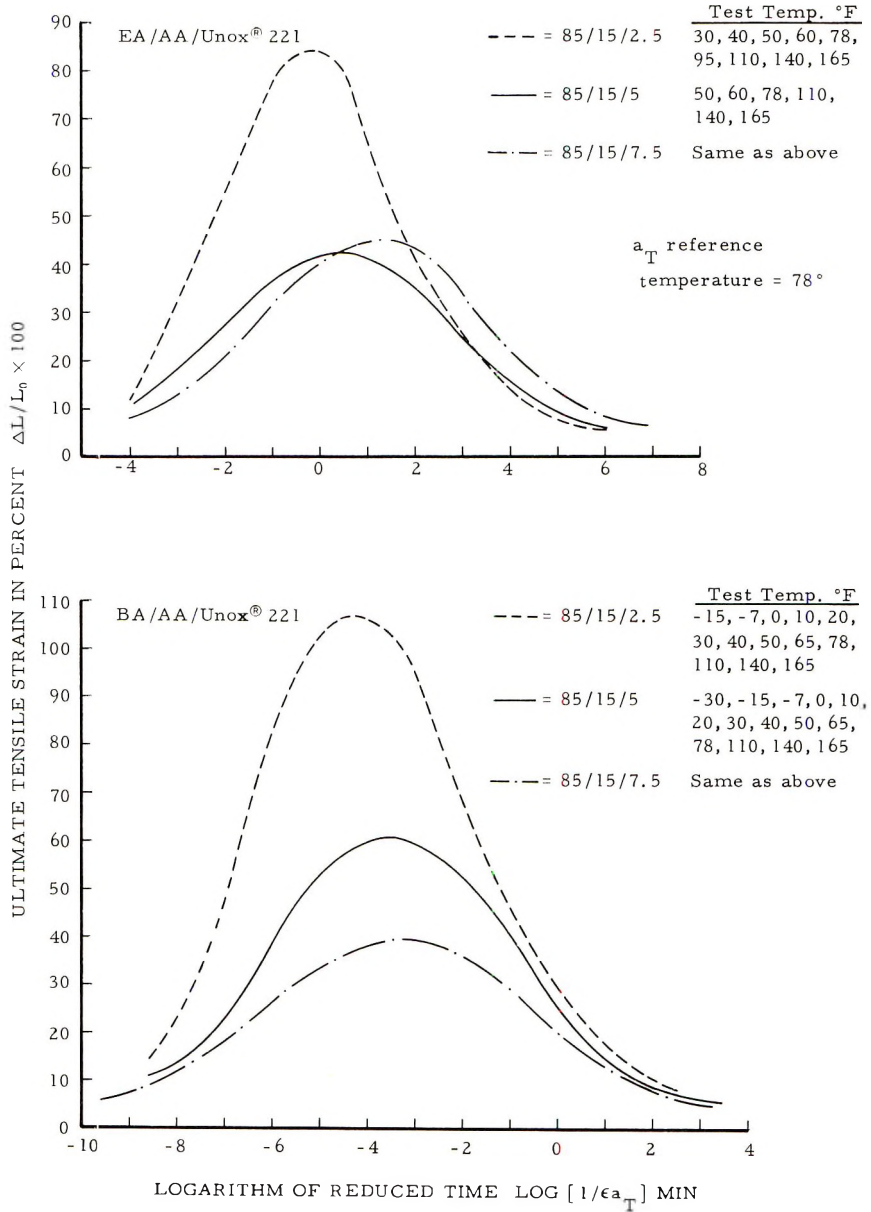


Fig. 14. Comparison of ultimate strain behavior for 85/15 EA/AA and BA/AA copolymers.

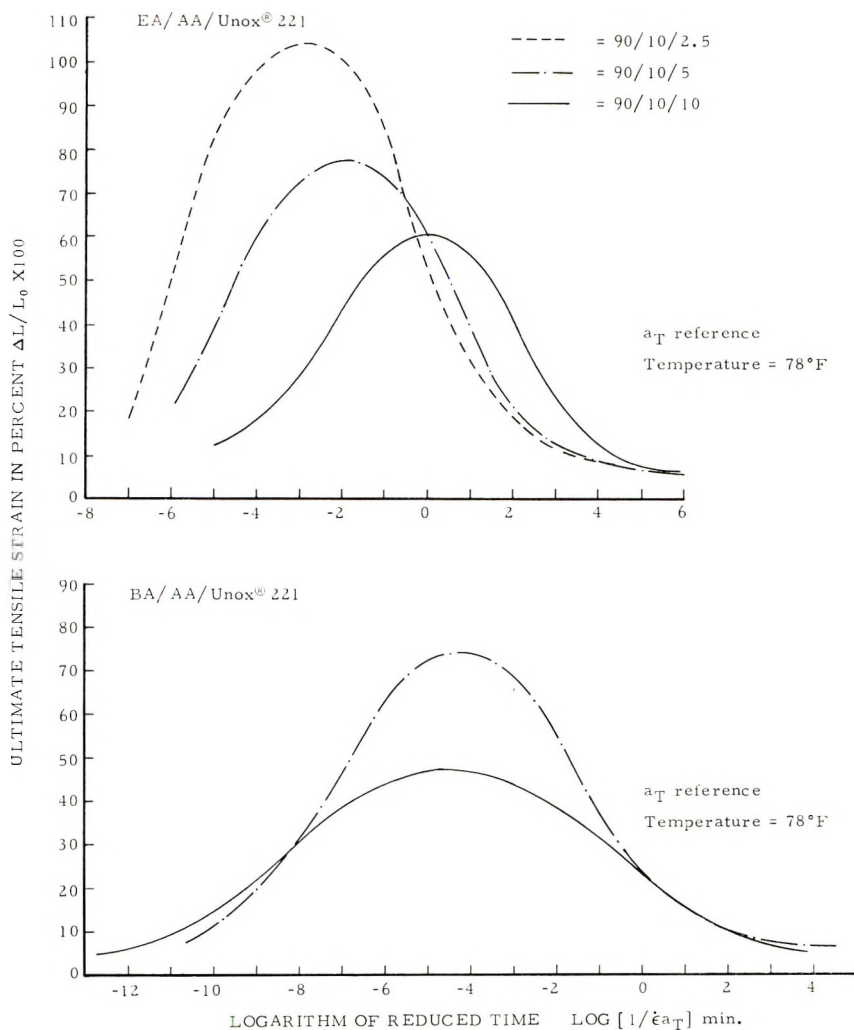


Fig. 15. Comparison of ultimate strain behavior for 90/10 EA/AA and BA/AA copolymers.

actual crosslink density was increasing for these cases, and hence, there is an interrelation between the maximum ultimate strain and the crosslink density. This is illustrated in Figure 17 where the logarithm of the maximum extension ratio ( $1 + \epsilon_{ult}^m$ ) is plotted versus the logarithm of the equilibrium modulus. The kinetic network theory,<sup>2,7,8</sup> essentially states that the maximum extension ratio is proportional to the square root of the number of monomers in a subchain between the crosslink junctions and, hence, inversely proportional to the square root of the equilibrium modulus (dash-dot line in Fig. 17). However, the experimental data seem to follow a non-linear relationship (see the two solid curves in Figure 17) while the best-fit linear relationship involves a negative slope of  $1/3$ .

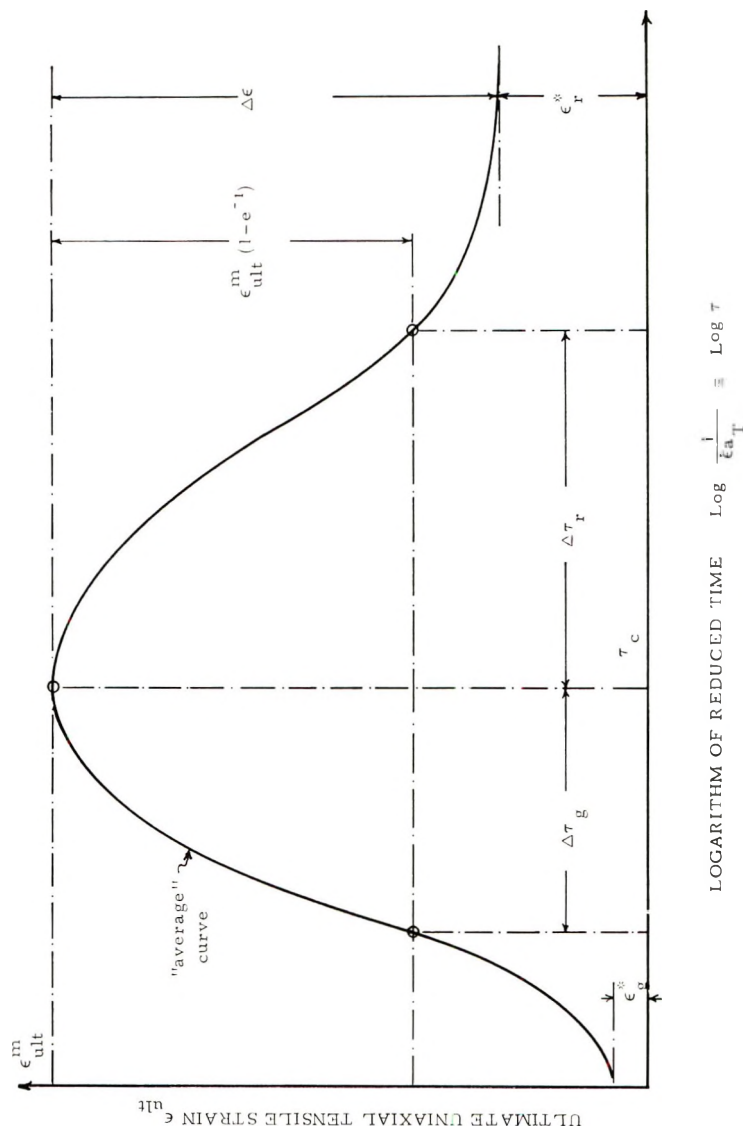


Fig. 16. Generalized ultimate strain curve.

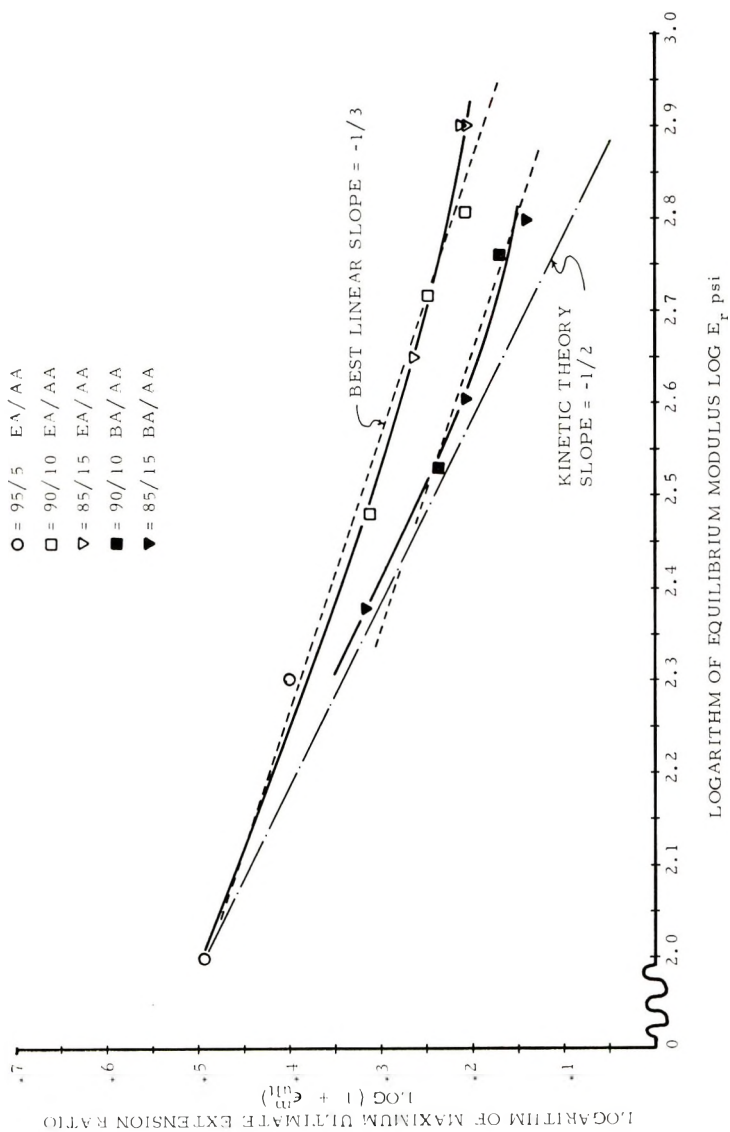


Fig. 17. Interrelationship between equilibrium modulus and maximum ultimate strain.

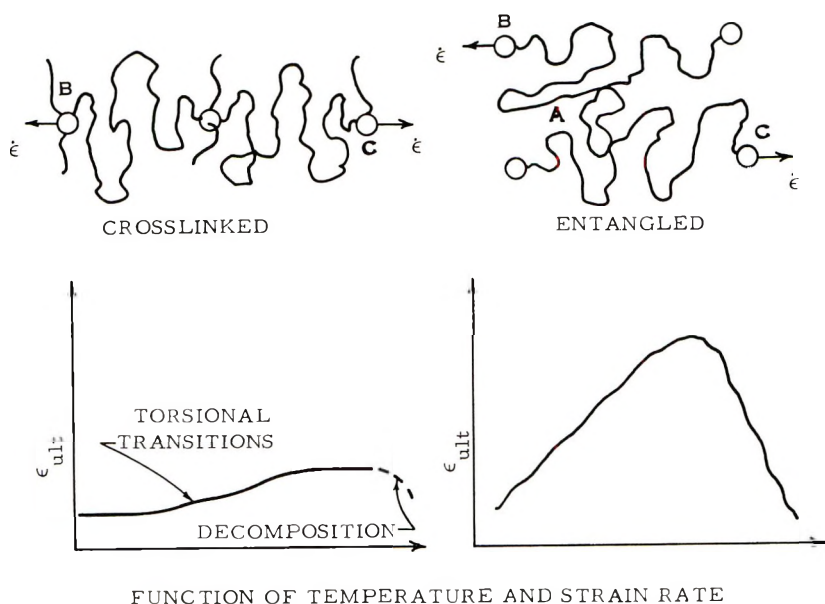


Fig. 18. Theoretical master ultimate strain curves associated with a pair of crosslink or entangled polymer chains. Point A represents the point of entanglement between the two chains.

According to the conformational theory of polymer chains<sup>4,9</sup> the extensibility of a subchain located between crosslink junctions is proportional to the square root of the number of monomers within the subchain. The proportionality constant depends upon the temperature and the backbone bond length  $l$ , backbone bond angle  $\alpha$ , and the torsional stiffness  $U(\phi)$  of the monomers within the subchain. The predominant influence of increased temperature is to increase the transitional probability to other conformational angles and, hence, the subchain length approaches the fully extended chain length,  $Nl[2(1-\cos \alpha)]^{1/2}$ . Whether or not a torsional transition can occur depends upon the time allowed for the transition. Hence, decreasing the continuum strain rate  $\dot{\epsilon}$  allows more time for a subchain torsional transition, while such transitions are less probable for more rapid strain rates. Therefore, the master ultimate strain curve for a completely crosslinked network of polymeric subchains would have the general form shown in Figure 18. Such a curve exhibits a glassy strain  $\epsilon_g^*$  region followed by a transition region to a rubbery strain  $\epsilon_r^*$  region, where  $\epsilon_r^* > \epsilon_g^*$ . It should be noted that such a curve does not exhibit a maximum such as was observed in the experimental data.

In the case of a linear, noncrystalline polymer, the chain molecules mainly interact by means of physical entanglements due to their spatial conformations. While a chain molecule within the solid possesses some set of torsional angles which gives its conformation the lowest energy state, fluctuations about these values occur due to the thermal energy of the

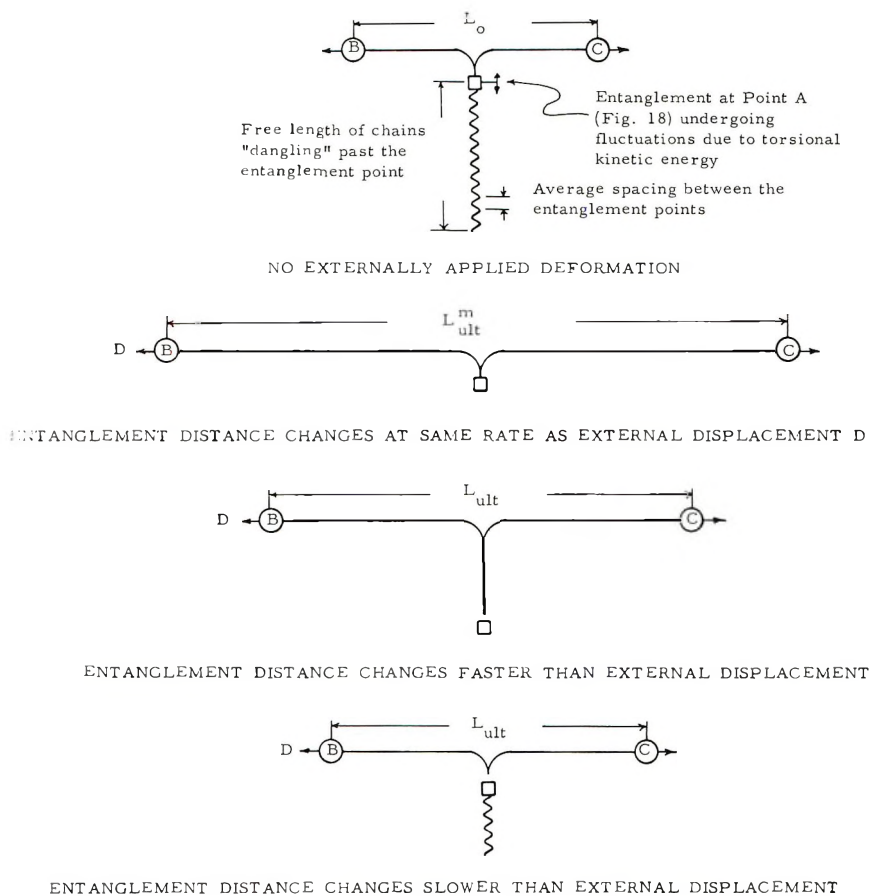


Fig. 19. "Zipper" analog of two entangled chains.

chain. Therefore, certain fluctuations in the conformations of the two entangled chains will permit the hindered side groups to glide past one another at the point of entanglement. At low temperatures (temperatures less than the glassy temperature), the entangled chains undergo small thermal fluctuations and, hence, act as if they were chemically crosslinked. Increasing the temperature increases the number of possible conformations and hence increases the possibility of an entanglement transition. As the chains undergo entanglement transitions their center-of-mass tends to move further apart with a subsequent isotropic increase in the volume. At high temperatures the conformational fluctuations cause the chains to become so flexible that the solid becomes a viscous fluid.

Due to these entanglement fluctuations there is a certain period of time during which the side groups at the point of an entanglement are not hindered. If the chains are then acted upon by some external field at that instant in time, e.g., a deformation, an entanglement transition will occur in the direction of the external field. This transition will increase the



entanglement chain distance by some amount which equals the spacing between successive entanglement points. The end-to-end chain distance (distance  $BC$  in Fig. 18) at which the two chains disassociate depends upon both the disentanglement rate and the external strain rate. The rupture process of these two entangled chains can be heuristically viewed by means of a zipper analog shown in Figure 19. The zipper tab located at point  $A$  corresponds to the point of entanglement in Figure 18. If the point of entanglement moves at the same rate as the applied strain, the two chains will not be separated until the two ends have pulled past one another (Fig. 19). However, if the disentanglement rate is faster than the strain rate, the two chains will separate prior to their "extended" length (Fig. 19). Conversely, if the disentanglement rate is less than the strain rate, backbone deformations will be induced which causes the chain to rupture prior to being untangled (Fig. 19). Therefore the ultimate strain behavior of entangled chains would exhibit a maximum such as shown in Figure 18.

Now, if the polymer contains both crosslinked and entangled chains, the master ultimate strain behavior will be a combination of the two curves

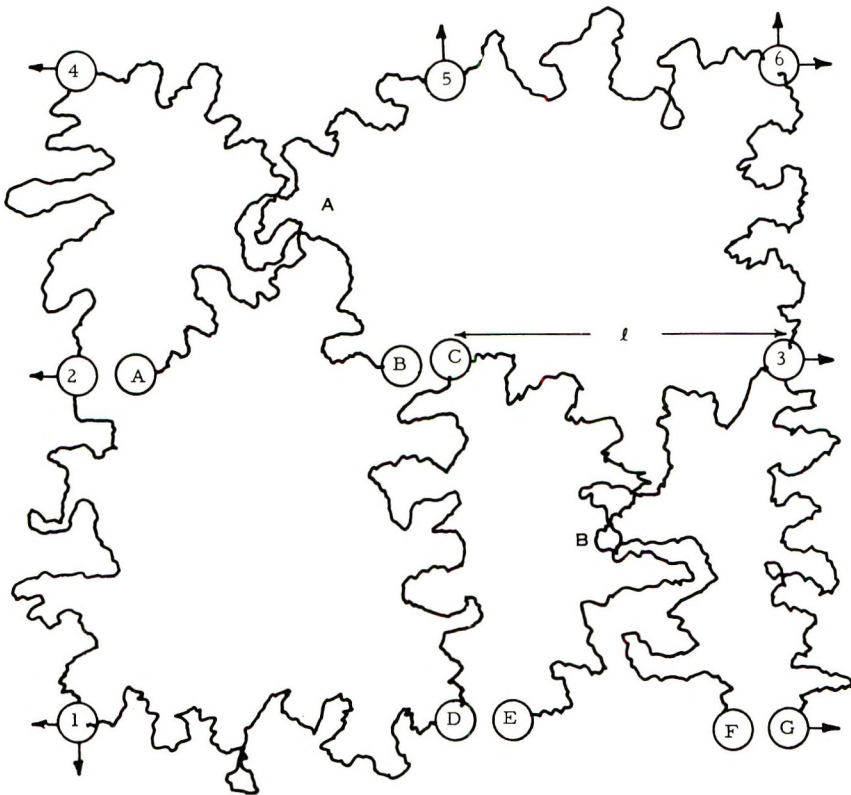


Fig. 20. A simple entanglement-crosslink model. Numbers 1-6 indicate crosslink junctions; encircled letters A-G indicate crosslink sites; A, B represent chain entanglements.

shown in Figure 18 and hence have the shape exhibited by the experimental data. Therefore, the master ultimate strain curves for the investigated acrylic copolymers depends upon both chain entanglements and the relative frequency of the actual crosslink junctions. Furthermore, by using a simple entanglement-crosslink model such as shown in Figure 20, the various characteristics of the master ultimate strain curves can be readily related to the molecular parameters associated with entanglements and chemical crosslinks.

By definition, the glassy strain capability refers to the ultimate strain when the polymer chains possess very little thermal motion so that torsional fluctuations are essentially zero. The required temperature, e.g.,  $50^{\circ}\text{C}$  below the  $T_g$ , will depend upon the chemical composition. At these low temperatures the entanglements act like a chemical crosslink and the spatial network of polymer chains is rigidly interconnected (see Fig. 20). Therefore  $\epsilon_g^*$  depends upon the subchain lengths and the deformational stiffness of the chain backbone. The subchain lengths can be increased by increasing the number of monomers between the crosslink sites (distance  $l$  in Fig. 21) and by decreasing the number of physical entanglements.

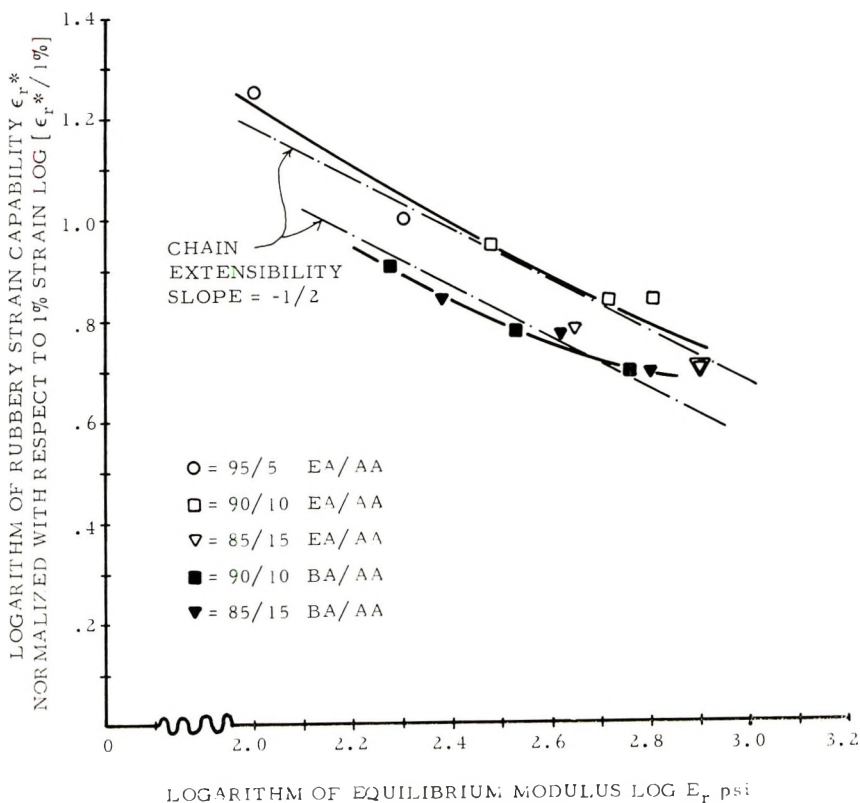


Fig. 21. Interrelationship between equilibrium modulus and normalized rubbery strain capability.

Since the experimental values of  $\epsilon_{\theta}^*$  were not obtained for the investigated acrylic copolymers no specific inferences can be made at this time.

In the case of high temperatures (but less than the chemical decomposition temperature) and/or very slow strain rates, any freely entangled chains can readily glide past one another and contribute very little to the network stiffness. The subchains located between the crosslink junctions (points 1-6 in Fig. 20) are fairly flexible due to their torsional fluctuations. The extensibility of these chains depends upon the number of monomers located between the crosslink junctions and the spatial freedom of the chain entanglements, e.g., disentanglements allow crosslink junctions 3-6 to undergo considerable displacement. Obviously if the ends of the entangled chains are located at crosslink junctions, e.g., adjoining crosslink sites *B* and *C*, *D* and *E*, and *F* and *G* in Figure 20 are joined together, the rubbery strain capability  $\epsilon_{\theta}^*$  is highly restricted. In Figure 21 the logarithm of the rubbery strain capability (normalized with respect to 1%) exhibited by the various EA/AA and BA/AA copolymers is plotted versus the logarithm of the equilibrium modulus. If the  $\epsilon_r^*$  depends only upon the chain extensibility between crosslink junctions, i.e., directly related to  $N^{1/2}$ , then the slope of  $\ln \epsilon_r^*$  versus  $\ln E_r$  should be  $-1/2$ . While the curves exhibit nonlinearity, a slope of  $-1/2$  fits the data fairly well (see dash-dot lines in Fig. 21). Furthermore, for the same value of equilibrium modulus, the  $\epsilon_r^*$  values for the BA/AA copolymers were less than the corresponding EA/AA values. This agrees with the extensibility concept since, as previously discussed, the BA/AA backbone is stiffer than the EA/AA backbone.

It is postulated that the nonlinearity of the curves in Figure 21 is due to chains which were prevented from untying by crosslink interconnections. When all crosslink sites have formed crosslink junctions, the number of entanglements which occur between crosslink junctions depends mainly on the relative frequency of the crosslink sites on the prepolymer chains. Increasing the relative frequency of the crosslink sites increases the probability of crosslinked entanglements for a given crosslink density. Such entanglements between the crosslink junctions reduce the subchain extensibility. Therefore, an increase in the crosslink density for chains with a high frequency of crosslink sites, e.g., the 85/15 copolymers, should have a less drastic effect upon the rubbery strain capability than occurs for chains with a relatively low frequency of crosslink sites, e.g., the 95/5 copolymers. This is exemplified by the EA/AA and BA/AA data shown in Figure 21, where the slope of the 95/5 data is greater than that of the 90/10 data which in turn is greater than the slope of the 85/15 data. It is these different behaviors that contribute to the nonlinearity of the curve in Figure 21.

The concept of an entangled crosslink network can also aid in understanding the microstructural influences on the observed maximum ultimate strain  $\epsilon_{ult}^m$  behavior. As previously discussed, the  $\epsilon_{ult}^m$  behavior depends upon the kinetic uncoiling of the chain entanglements. In the case of the 95/5 ethyl acrylate copolymers, the frequency of the crosslink sites is

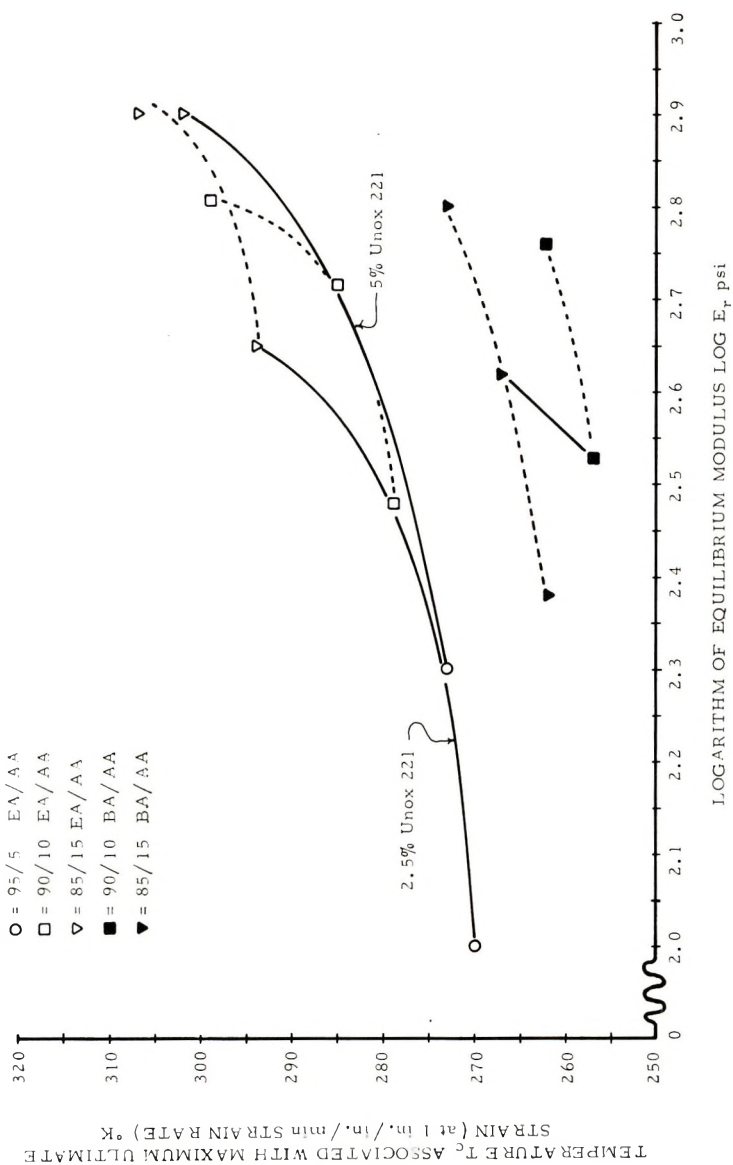


Fig. 22. Interrelationship between nominal critical temperature and equilibrium modulus: (—) square amounts of reactive hardener Unox 221; (---) same relative frequency of crosslinked sites.

relatively low and their chemical efficiency is considerably less than 1. Hence the possibility of noncrosslinked entanglements is quite high, and the subchain entanglement lengths are relatively long. This length and freedom of the entanglements allow entanglement transitions to occur at a relatively low value of thermal energy and to exhibit a large degree of extensibility prior to inter-chain dissociation. This is experimentally manifested by an  $\epsilon_{ult}^m$  value of 212% which occurs at a nominal temperature (with respect to a strain rate of 1 in./in./min.) of 28°F. Increasing the crosslink density (case 8 in Table I) caused the  $\epsilon_{ult}^m$  value to decrease by 29% and slightly increased its associated nominal temperature to 33°F. Since the modulus and rubbery strain capability indicated a nearly 100% increase in the crosslink density, the smaller change in the  $\epsilon_{ult}^m$  behavior further indicates that the 95/5 copolymer network has numerous entanglements which are not hindered by chemical crosslinks. The increase in the nominal temperature is due to the fact that more thermal energy is required for the entanglement transitions to occur since the entanglement motion is hindered by the increase in intermolecular interactions; i.e., the increase in crosslink density.

Analogously, increasing the relative frequency and the chemical efficiency of the crosslink sites will increase the probability of having entangled crosslinks and, hence, higher thermal energy will be necessary before the intermolecular interactions can be overcome. This behavior is illustrated by the experimental data shown in Figure 22 where the nominal temperatures  $T_c$  associated with the critical reduced time  $\tau_c$  are plotted as a function of the logarithm of the equilibrium modulus. For the same level of crosslinker (the solid lines), increasing the AA content (increasing the relative frequency of the crosslink sites) increased both the modulus and the temperature  $T_c$ . This increase is attributed to an increase in the crosslink chemical efficiency as the relative frequency of the crosslink sites increases. While initially, the modulus increases considerably faster than the  $T_c$  temperature, the modulus appears to be approaching a limiting value for each specific level of crosslinker which indicates a decreasing effect of increasing AA content; i.e., the relative increase in the crosslink chemical efficiency decreases with increasing frequency of the crosslink sites.

Similarly, if the backbone structure (EA/AA or BA/AA ratio) is held constant (dashed curves in Fig. 22), increasing the amount of crosslinker increases the magnitude of both  $T_c$  and the modulus. Each backbone structure exhibits its own type of  $T_c$  versus  $\log E$  behavior and increasing the relative frequency of the crosslink sites (AA content) appears to shift the behavior to higher  $T_c$  values and a higher limiting modulus. Comparing the curvature of the solid and dashed curves in Figure 22, one observes that a limiting modulus is approached faster with increasing reactive hardener level than with increasing frequency of crosslink sites. However, increasing the relative frequency of the crosslink sites for the EA/AA copolymer causes a larger increase in the modulus than a corresponding increase in the amount of reactive hardener. These EA/AA data clearly in-

dicates that the thermal energy necessary for entanglement transitions depends upon both crosslink density and backbone composition.

The compositional dependency is further demonstrated by comparing the BA/AA and EA/AA data (Figs. 17, 21, 22). The temperature data shown in Figure 22 illustrate that the BA/AA copolymers require less thermal energy than the corresponding EA/AA copolymers to undergo entanglement transitions. The data in Table I indicate that this temperature difference ranges from 49 to 65°F with an average value of 58°F. Since the pendant butyl groups increase the backbone torsional stiffness of the polymer chains, this lower thermal requirement is not due to increased backbone torsional mobility. However, increasing the length of the side group increases its torsional mobility, and torsional fluctuations can be induced at a lower temperature.<sup>10</sup> Furthermore, the bulk of the pendant butyl groups greatly increases the overall bulk of the chains and acts like an internal plasticizer.<sup>4</sup> Hence, it appears that the greater side-chain torsional mobility of the butyl copolymers decreases the intermolecular interactions which results in a lower thermal energy requirement for an entanglement transition.

The increase in backbone stiffness and the subsequent decrease in chain extensibility is exhibited by the data in Figures 17 and 21 where the  $\epsilon_{ult}^m$  and  $\epsilon_r^*$  of the BA/AA copolymer is less than the corresponding EA/AA values for the same crosslink density. Furthermore, the lower  $\epsilon_{ult}^m$  strain capability must be due to a shorter average "free" subchain length past the entanglement points (see Figs. 19 and 20). It is believed that this shorter free entanglement length is due to the fact that, for a given molecular weight, the number of reactive sites per BA/AA polymer chain is only about 75% of that corresponding to the EA/AA copolymer. Hence, for the same crosslink density, the BA/AA copolymer will involve more interconnected chains and hence a lower probability of long unhindered entanglements.

The last two characteristics associated with the master ultimate strain curve are the glassy  $\Delta\tau_g$  and rubbery  $\Delta\tau_r$  widths. As previously mentioned, these two widths are approximately the same (see Table I) with the average total width ( $\Delta\tau_g + \Delta\tau_r$ ) being 7.0 for the EA/AA copolymers and 8.1 for the BA/AA copolymers. The wider width for the BA/AA copolymers could be due to either broader distribution of entanglement lengths and/or a lower entanglement transition rate.

## CONCLUSIONS

The magnitude of the equilibrium modulus  $E_r$  was found to increase with increasing the actual crosslink density which, in turn, depends upon the amount of crosslinker and the chemical efficiency of the crosslink sites. The chemical efficiency of the investigated acrylic copolymers was found to increase as the relative frequency of the crosslink sites per chain (AA content) increased and as the bulk of the pendant side groups was decreased.

Furthermore, the equilibrium moduli appeared to be approaching a limiting value for each specific level of reactive hardener which indicates a decreasing effect of increasing AA content, i.e., the relative increase in the crosslink chemical efficiency decreases with increasing frequency of the crosslink sites.

The data also indicated that either the relative frequency of the crosslink sites or the level of crosslinker can have the greatest influence on the equilibrium modulus. It appears that when the chemical efficiency is quite low due to shielded reactive groups (the BA/AA copolymers), the modulus is more strongly dependent upon the reactive hardener content than on the AA content. When the chemical crosslink efficiency is higher (EA/AA copolymers), the crosslink density appears to depend more upon the relative frequency of the crosslink sites than on the level of crosslinker (for the range from one-half to twice the stoichiometric amount).

The temperature dependency of the modulus, i.e., its transitional behavior between the glassy and rubbery regions, was found to depend upon both the polymer chain composition and the actual crosslink density. Increasing either the torsional stiffness of the pendant side groups or the actual crosslink density increases the transition temperature. In general, increasing the crosslink density also increases the breadth of the transition region.

The ultimate strain behavior was found to be a nonlinear function of the logarithm of the reduced time ( $1/\dot{\epsilon}a_T$ ) and, as a first approximation, can be considered to be represented by a lognormal distribution function (whose variate is  $1/\dot{\epsilon}a_T$ ) with a maximum  $\epsilon_{ult}^m$  occurring at some value of reduced time  $\tau_c$  and whose asymptotes approach some nonzero value  $\epsilon_r^*$  (or  $\epsilon_g^*$ ). This behavior was interpreted in terms of a crosslinked entanglement model which attributes the maximum ultimate strain to a cooperative process involving the external rate of deformation,  $\dot{\epsilon}$ , and the chain disentanglement rate due to kinetic torsional energy.

The nominal critical temperature  $T_c$  associated with the maximum ultimate strain (for a strain rate of 1 in./in./min.) was found to be a nonlinear function of the actual crosslink density, and replacing the pendant ethyl side group with a butyl group decreased the magnitude of  $T_c$  by a value of about 58°F for any given crosslink density.

Both the rubbery strain capability,  $\epsilon_r^*$ , and the maximum ultimate strain capability,  $\epsilon_{ult}^m$ , were found to be nonlinear functions of the crosslink density. As a first approximation, the rubbery strain capability can be represented by a linear function involving  $E_r^{-1/2}$  (the kinetic theory prediction), whereas the maximum ultimate extension ratio,  $(1 + \epsilon_{ult}^m)$ , can be represented by a linear relationship involving  $E_r^{-1/2}$ . The proportionality constants depend upon the polymer microstructure and for both  $\epsilon_r^*$  and  $(1 + \epsilon_{ult}^m)$  and BA/AA copolymer exhibited lower proportionality constants than did the EA/AA copolymer.

Hence, it appears that by changing the relative frequency of the crosslink sites per molecule, modifying the bulk and torsional freedom of the

pendant side groups and altering the amount of reactive hardener, one can widely vary both the elastic moduli and the ultimate strain capability of a polymeric solid.

This work was carried out under the sponsorship of the U.S. Army Missile Command, Redstone Arsenal, Alabama, under Contract DAAH01-69-C-0772.

### References

1. S. Matsuoka, *Polym. Eng. Sci.*, **6**, 142 (1965).
2. L. R. G. Treloar, *The Physics of Rubber Elasticity*, 2nd ed., Oxford Clarendon Press, London, 1958.
3. P. Meares, *Polymers Structure and Bulk Properties*, Van Nostrand, New York, 1965.
4. N. Saito, K. Okano, S. Iwayanagi, and T. Hideshima, *Molecular Motion in Solid State Polymers, Solid State Physics*, Vol. 14, Academic Press, New York, 1963.
5. T. M. Birshtein and O. B. Ptitsyn, *Conformation of Macromolecules*, Interscience, New York, 1966, Chap. 3.
6. M. G. Kendall and A. Stuart, *The Advanced Theory of Statistics*, Vol. 1, Hafner, New York, 1958, Chap. 6.
7. T. L. Smith, *J. Appl. Phys.*, **36**, 2996 (1965).
8. F. Bueche, B. J. Kinzig, and C. J. Coven, *J. Polym. Sci. B*, **3**, 399 (1965).
9. M. V. Volkenstein, *Configurational Statistics of Polymeric Chains*, Interscience, New York-London, 1963.
10. J. Lal and K. W. Scott, in *Structure and Properties of Polymers (J. Polym. Sci. C, 9)*, A. V. Tobolsky, Ed., Interscience, New York, 1965, p. 115.

Received October 13, 1969

Revised November 26, 1969



## Copolymerization of Optically Active *N*-Bornylmaleimide with Vinyl Monomers

HIDEMASA YAMAGUCHI and YUJI MINOURA, *Department of Chemistry, Faculty of Engineering, Osaka City University, Sumiyoshi-ku, Osaka, Japan*

### Synopsis

Optically active *N*-bornylmaleimide (NBMI) was copolymerized with styrene, methyl methacrylate, and vinylidene chloride with a free-radical catalyst to obtain optically active copolymers. The monomer reactivity ratios for the radical copolymerization of NBMI ( $M_2$ ) with styrene, methyl methacrylate, and vinylidene chloride were: St-NBMI,  $r_1 = 0.13$ ,  $r_2 = 0.05$ ; MMA-NBMI,  $r_1 = 2.02$ ,  $r_2 = 0.16$ ;  $VCl_2$ -NBMI,  $r_1 = 1.15$ ,  $r_2 = 0.47$ . The  $Q-e$  values for NBMI were  $Q_2 = 0.48$  and  $e_2 = +1.47$ . The specific rotation and optical rotatory dispersion of these copolymers were measured. The correlation between the specific rotation and composition of these copolymers was not linear. The value of  $\lambda_c$  for each copolymer was independent of the copolymer composition and the comonomer, being 260  $m\mu$  for the St-NBMI system, 262  $m\mu$  for the MMA-system, and 260  $m\mu$  for the  $VCl_2$ -NBMI system. The effects of solvents and temperature on the specific rotation of these copolymers were investigated.

### INTRODUCTION

A number of studies of the preparation of optically active polymers by addition polymerization have been reported. Polymerizations of *p*-sec-butyl vinyl benzoate,<sup>1</sup> *o*-vinyl benzyl-sec-butyl sulfide,<sup>2</sup> 1,3-dimethylbutyl methacrylate,<sup>3</sup> and 1-methylbenzyl methacrylate<sup>4</sup> were carried out with the use of a radical initiator, and optically active polymers were obtained. However, after the cleavage of the asymmetric groups of side chain from the polymer, the polymers were not optically active.

After these reports, Frish *et al.*<sup>5</sup> suggested that optically active vinyl polymers would theoretically not be prepared by these methods, i.e., as the polymers of  $CH_2=CHX$ ,  $CH_2=CXY$ , and  $CHX=CHY$  have pseudo-asymmetric carbon atoms, optically active polymer could not be obtained. The random copolymerization of  $CH_2=CHX$  and  $CH_2=CHY$  also did not give optically active copolymer. In the case of alternating copolymerization of  $CH_2=CHX$  with *cis*- $CHY=CHX$ ,  $\overline{C=C-X}$ , and  $C=C-C=C$ ,

$$\begin{array}{c} \overline{C=C-X} \\ | \\ X \end{array}$$

an asymmetric structure is introduced into the polymer main chain, since

the substituted carbon atoms are converted to real asymmetric carbon atoms to give optically active copolymers. According to the above method, Schuerch<sup>4-7</sup> copolymerized (-) $\alpha$ -methyl benzyl methacrylate and (-) $\alpha$ -methylbenzyl vinyl ether with maleic anhydride to obtain optically active copolymers. After the cleavage of optically active side groups, the polymer remained optically active.

Recently, Pino et al.<sup>8</sup> reported that stereoregular copolymers of (S) 4-methyl-1-hexene and 4-methyl-1-pentene obtained in the presence of stereospecific catalyst had marked optical rotation with molecular asymmetry.

In this work, *N*-bornylmaleimide (NBMI) was prepared from *N*-bornylmaleic acid according to Searle's method<sup>9</sup> modified as described in the previous paper.<sup>10</sup> The copolymerization of NBMI ( $M_2$ ) with styrene (St), methyl methacrylate (MMA), and vinylidene chloride ( $VCl_2$ ) was carried out with the use of benzoyl peroxide (BPO) as initiator in tetrahydrofuran (THF) at 50°C, and optically active copolymers were obtained. The monomer reactivity ratios were determined, and the  $Q_2-e_2$  values of NBMI were also calculated.

The specific rotation and optical rotatory dispersion of these copolymers were measured. The effects of solvents and temperature on the specific rotation for these were also investigated. From the results of optical activity for the copolymer, the presence of the induction of asymmetric carbon atoms in polymer chain was discussed.

## EXPERIMENTAL

### Materials

As described in our previous paper,<sup>10</sup> optically active NBMI was prepared by a modification of the method of Searle.<sup>9</sup> The needlelike crystals had mp 58.5–60.5°C;  $[\alpha]_D -9.6$  ( $c = 1.0, l = 1.0$ , in ethanol).

ANAL. Calcd for  $C_{14}H_{19}O_2N$ : C, 72.1%; H, 8.2%; N, 6.0%. Found: C, 71.2%; H, 8.1%; N, 5.5%.

St, MMA, and  $VCl_2$  were commercial products purified by the usual methods and distilled over calcium hydride at a reduced pressure before use. BPO was used after two recrystallizations from chloroform. THF used was purified by the usual method.

### Copolymerization Procedure

The radical copolymerizations were carried out with BPO as initiator in THF in sealed tubes at 50°C. The required amounts of NBMI and comonomers, initiator, and solvent were placed in a tube which was degassed completely and sealed off. The tube was placed in a thermostat controlled within  $\pm 0.1^\circ\text{C}$ . After the polymerization period, the polymer solution was precipitated in a large amount of methanol, filtered, and dried

to constant weight under vacuum. The composition of the obtained copolymers was determined by elemental analysis.

### Measurements

The D-line optical rotations were measured with a Shimadzu Liebig-type polarimeter with filtered sodium light. The D-line optical rotations at various temperatures were measured with a Yanagimoto model ORD-3 polarimeter. Optical rotatory dispersion data were obtained with a Shimadzu model QV-50 polarimeter equipped with xenon source.

The intrinsic viscosity of the copolymers was measured in THF at 30°C with an Ubbelohde viscometer.

The infrared spectra of KBr pellets were measured with a Perkin-Elmer 337 photospectrometer.

The x-ray powder diffractogram were obtained with the use of Cu-K $\alpha$  as a source on a Toshiba x-ray diffractometer.

## RESULTS AND DISCUSSION

### Copolymerization of *N*-Bornylmaleimide (NBMI) with Vinyl Monomers

Optically active NBMI was copolymerized with St, MMA, and VCl<sub>2</sub> with BPO as initiator at 50°C in THF by the sealed tube method. That copolymers were obtained was confirmed from the infrared spectra (Fig. 1). The infrared spectrum for St-NBMI copolymer had absorption bands at 1700 cm<sup>-1</sup> due to the imide group and at 3030, 1600, and 1500 cm<sup>-1</sup> due to the phenyl group (Fig. 1*b*); that for MMA-NBMI copolymer had absorption bands at 1700 cm<sup>-1</sup> due to the imide group and 1735 cm<sup>-1</sup> due to the ester group (Fig. 1*c*), and that for VCl<sub>2</sub>-NBMI showed absorption at 1700 cm<sup>-1</sup> due to the imide group and at 700 cm<sup>-1</sup> due to the C-Cl bond (Fig. 1*d*).

The compositions of the copolymers were determined by elemental analysis (C, H, and N). The polymerization conditions, the compositions and the intrinsic viscosity of the copolymers are shown in Tables I-III.

The x-ray powder diffractograms for copolymers with 1:1 composition (i.e., runs 14, 24, and 34) are shown in Figure 2. It was apparent that the interplanar distance for the copolymers were 6.10 and 12.2 Å for St-NBMI copolymer, 6.10 and 13.6 Å for MMA-NBMI copolymer, and 5.75 Å for VCl<sub>2</sub>-NBMI copolymer. The values of interplanar distance for St-NBMI and MMA-NBMI were similar to those (6.0-6.1 Å, 11.4-13.6 Å) for poly-NBMI.<sup>10</sup> These values are similar also to those for copolymers of *N*-substituted maleimide and vinyl monomers reported by Cubbon.<sup>11</sup>

The relationships between  $m_2$  and  $M_2$  for each copolymerization are shown in Figure 3. The  $m_2$  values are the initial molar fractions of NBMI in the mixture of monomers, whereas the  $M_2$  values are the molar fractions of NBMI in the copolymers. The monomer reactivity ratios ( $r_1, r_2$ ) were

TABLE I  
 Copolymerization of Styrene ( $M_1$ ) and *N*-Bornylmaleimide ( $M_2$ )<sup>a</sup>

Run	Monomer		Polymer- ization time, hr	Con- version, wt-%	Rate of polymer- ization, g/hr <sup>b</sup>	<i>N</i> content, %	Copolymer				$\lambda_D$ , m $\mu$
	NBMI, g (mole)	Styrene g (mole)					NBMI molar fraction	Styrene molar fraction	$[\eta]^c$	$[\alpha]^d$	
11	0 (0)	2.73(2.62)	14	8.3	0.26	0	1.00	0	—	—	
12	1.02(0.44)	2.27(2.18)	14	39.7	0.93	3.51	0.385	0.62	0.496	+10.5	
13	2.04(0.87)	1.82(1.75)	15	30.8	0.79	3.96	0.464	0.54	0.478	+11.9	
14	3.05(1.31)	1.36(1.31)	16	26.8	0.74	4.09	0.487	0.51	0.300	+12.1	
15	4.07(1.75)	0.91(0.87)	17	17.2	0.61	4.18	0.505	0.50	0.200	+12.1	
16	5.09(2.18)	0.45(0.44)	19	20.8	0.51	4.40	0.550	0.45	0.142	+12.5	
17	6.12(2.62)	0 (0)	23	9.0	0.34	6.00	1.000	0.00	0.042	+8.1	

<sup>a</sup> Polymerized in tetrahydrofuran using with benzoyl peroxide ( $10^{-2}$  mole/l.) at 50°C.

<sup>b</sup> Calculated as  $d(M_1 + M_2)/dt$ .

<sup>c</sup> Measured in tetrahydrofuran at 30°C.

<sup>d</sup> Measured in tetrahydrofuran.

TABLE II  
 Copolymerization of Methyl Methacrylate ( $M_1$ ) and *N*-Bornylmaleimide ( $M_2$ )<sup>a</sup>

Run	Monomer		Polymer- ization time, hr	Con- version, wt-%	Rate of polymer- ization, g/hr <sup>b</sup>	N content, %	Copolymer				$\lambda_D$ m $\mu$
	NBMI, g (mole)	MMA, g (mole)					NBMI molar fraction	NBMI molar fraction	NBMI molar fraction	MMA [ $\eta$ ] <sup>c</sup>	
21	0 (0)	2.83(2.81)	25	25.2	0.028	0	0	1.00	—	0	—
22	1.08(0.45)	2.36(2.34)	25	28.2	0.038	1.04	0.083	0.92	0.503	+0.2	261
23	2.19(0.94)	1.89(1.87)	25	26.3	0.042	1.94	0.179	0.81	0.396	+0.3	262
24	3.26(1.40)	1.42(1.40)	25	26.3	0.037	2.85	0.280	0.72	0.375	+0.7	262
25	4.35(1.87)	0.94(0.94)	26	18.9	0.037	3.61	0.393	0.61	0.216	+0.7	262
26	5.45(2.34)	0.47(0.45)	30	18.0	0.035	4.50	0.563	0.44	0.126	+2.6	262
27	6.56(2.81)	0.0 (0)	53	15.6	0.022	5.90	0.980	0.02	0.050	+8.4	259

<sup>a</sup> Polymerized in tetrahydrofuran using with benzoyl peroxide ( $10^{-2}$  mole/l.) at 50°C.

<sup>b</sup> Calculated as  $d(M_1 + M_2)/dt$ .

<sup>c</sup> Measured in tetrahydrofuran at 30°C.

<sup>d</sup> Measured in tetrahydrofuran

TABLE III  
 Copolymerization of Vinylidene Chloride ( $M_1$ ) and *N*-Bormylmaleimide ( $M_2$ )<sup>a</sup>

Run	Monomer		Polymer- ization time, hr	Con- version, wt-%	Rate of polymer- ization, g/hr <sup>b</sup>	N content, %	Copolymer			$[\eta]^c$	$[\alpha]_D^{25}$	$\lambda_c$ m $\mu$
	NBMI g (mole)	VCl <sub>2</sub> , g (mole)					NBMI molar fraction	Vinyl- idene chloride molar fraction	NBMI molar fraction			
31	0 (0)	2.18(2.26)	71	31.2	0.009	0	0	1.00	0	—	—	—
32	0.88(0.38)	1.81(1.89)	71	15.8	0.006	1.35	0.105	0.90	0.062	+1.2	261	261
33	1.76(0.75)	1.45(1.51)	65	13.1	0.006	2.74	0.259	0.74	0.064	+2.3	260	260
34	2.64(1.13)	1.09(1.13)	49	6.4	0.004	3.68	0.397	0.60	0.079	+4.1	260	260
35	3.52(1.51)	0.73(0.75)	49	6.9	0.006	4.53	0.561	0.44	0.060	+6.8	261	261
36	4.40(1.89)	0.36(0.38)	49	10.0	0.011	5.26	0.747	0.25	0.085	+8.7	259	259
37	5.28(2.26)	0 (0)	44	19.8	0.027	5.90	0.980	0.02	0.058	+8.3	260	260

<sup>a</sup> Polymerized in tetrahydrofuran using with benzoyl peroxide ( $10^{-2}$  mole/l.) at 50°C.

<sup>b</sup> Calculated as  $d(M_1 + M_2)/dt$ .

<sup>c</sup> Measured in tetrahydrofuran at 30°C.

<sup>d</sup> Measured in tetrahydrofuran.

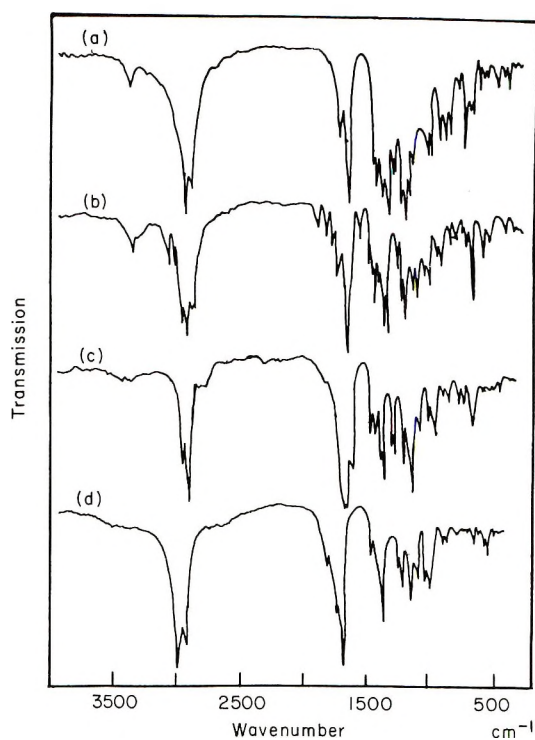


Fig. 1. Infrared spectra of (a) poly-*N*-bornylmaleimide; (b) St-*N*-bornylmaleimide (run 14); (c) MMA-*N*-bornylmaleimide (run 24); (d) VCl<sub>2</sub>-*N*-bornylmaleimide copolymer (run 34).

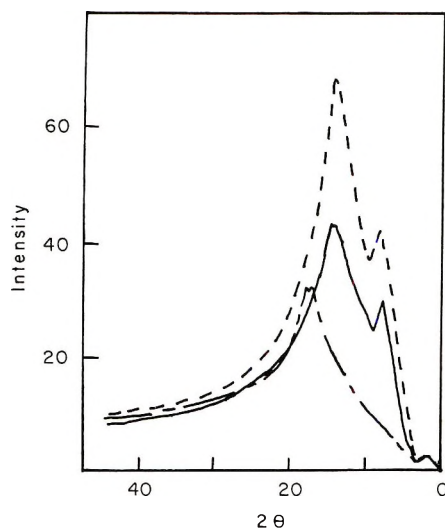


Fig. 2. X-Ray diffractometer scans of *N*-bornylmaleimide copolymers: (—) St-NBMI (run 14), (— —) MMA-NBMI (run 24); (- - -) VCl<sub>2</sub>-NBMI copolymer (run 34).

determined according to the Fineman-Ross method and the curve-fitting method.

The  $r_1$  and  $r_2$  values obtained were:  $r_1 = 0.13$  (St),  $r_2 = 0.05$  (NBMI) for the St-NBMI system;  $r_1 = 2.02$  (MMA),  $r_2 = 0.16$  (NBMI) for the MMA-NBMI system; and  $r_1 = 1.15$  (VCl<sub>2</sub>),  $r_2 = 0.47$  (NBMI) for the VCl<sub>2</sub>-NBMI system. The polymerization curves obtained from these  $r_1$ ,  $r_2$  values are shown as solid lines in Figure 3. The values of  $Q$  and  $e$  of NBMI were calculated by using the Alfrey-Price equation with the values of  $r_1$  and  $r_2$  and by assuming the values St ( $Q_1 = 1.0$   $e_1 = -0.80$ ), MMA ( $Q_1 = 0.74$   $e_1 = 0.40$ ) and VCl<sub>2</sub> ( $Q_1 = 0.22$   $e_1 = 0.36$ ). The  $Q_2$ - $e_2$  values obtained were 0.48 and +1.47, respectively.

In the calculation of the average  $Q_2$ ,  $e_2$  values, the  $Q_2$  and  $e_2$  values of NBMI from the copolymerization with St were not taken into account. These average  $Q_2$ - $e_2$  values were similar to those for  $N$ -substituted maleimide obtained by other authors,<sup>12-15</sup> as shown in Table IV. The  $Q_2$  values of these  $N$ -substituted maleimides tend to become large because of resonance effects of phenyl groups. In the case that the  $N$ -substituted group is electron-withdrawing, the  $e_2$  value becomes large. The  $Q_2$  values for the St- $N$ -substituted maleimide systems were higher than those with

TABLE IV  
Monomer Reactivity and  $Q_2$ ,  $e_2$  of NBMI ( $M_2$ )

$M_1$	$M_2$	$r_1$	$r_2$	$Q_2$	$e_2$	average		reference
						$Q_2$	$e_2$	
St	NBMI	0.13	0.05	1.09	1.44	0.48	+1.47	This paper
MMA	NBMI	2.02	0.16	0.58	1.46			
VCl <sub>2</sub>	NBMI	1.15	0.47	0.48	1.47			
St	Maleimide	0.1	0.1	1.8	1.34	0.41	+1.33	12
MMA	Maleimide	2.50	0.17	0.43	1.33			
VCl <sub>2</sub>	Maleimide	0.71	0.48	0.39	1.33			
Isobutyl vinyl ester	NPMI <sup>a</sup>	0	0.32	0.33	1.41	0.57	+1.57	13
MMA	NPMI	1.38	0.20	0.83	1.76			
Vinyl acetate	NPMI	0.03	0.66	0.56	1.53			
St	<i>N</i> - <i>n</i> -Butyl- maleimide	1.33	0.12	3.08	1.75			14
St	<i>p</i> -Chloro- phenyl- maleimide	0.01	0.05	11.6	1.89			
MMA	maleimide	1.08	0.17	1.15	1.70			15
Vinyl acetate		0.02	0.60	0.73	1.80			
St	<i>N</i> -(Carboxy <i>p</i> -phenyl) maleimide	0.02	0.1	6.3	1.19			15
MMA		1.18	0.11	1.11	1.83			
Vinyl acetate	ethyl ester	0.02	0.18	0.67	2.07			

<sup>a</sup> *N*-Phenylmaleimide.



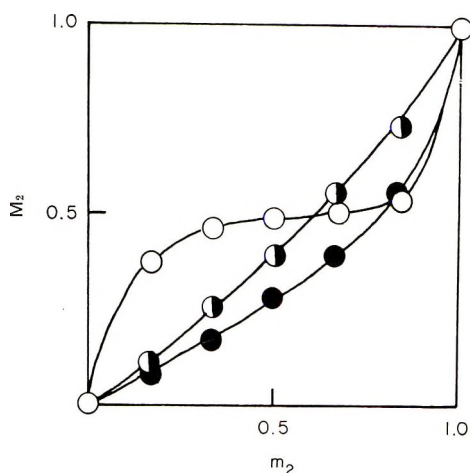
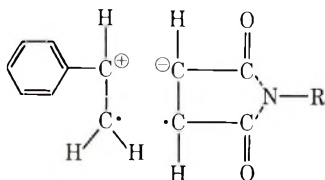


Fig. 3. Composition curves of (○) St-NBMI; (●) MMA-NBMI; (◐)  $VCl_2$ -NBMI copolymer.

other monomers (MMA,  $VCl_2$ ) and *N*-substituted maleimides (Table IV). The abnormal  $Q_2$  values for the St-NBMI system could be explained by the formation of molecular complexes in the transition state between St and NBMI as shown by Paesschen et al.<sup>12</sup> This structure formed by the transfer of an electron of the St double bond to the NBMI radical



R:bornyl

gave rise to the pronounced alternation in this copolymerization in the same way as was assumed for maleic anhydride.

### Optical Rotation

The specific rotations of the copolymers are shown in Figure 4. The value of specific rotation for poly-NBMI was estimated in a previous paper<sup>10</sup> to be +11.7 by extrapolation to eliminate the influence of polymer end group on specific rotation. The correlation between the specific rotation for the copolymers and the copolymer composition was not linear. The specific rotation for the St-NBMI copolymer increased with increasing NBMI molar fraction (from 0.0 to 0.55). On the other hand, the specific rotation for the MMA-NBMI copolymer increased gradually with increasing NBMI molar fraction from 0.0 to 0.40 and then started to increase rapidly.

The nonlinear correlation between the specific rotation and the copolymer composition seems to suggest the formation of asymmetric carbon

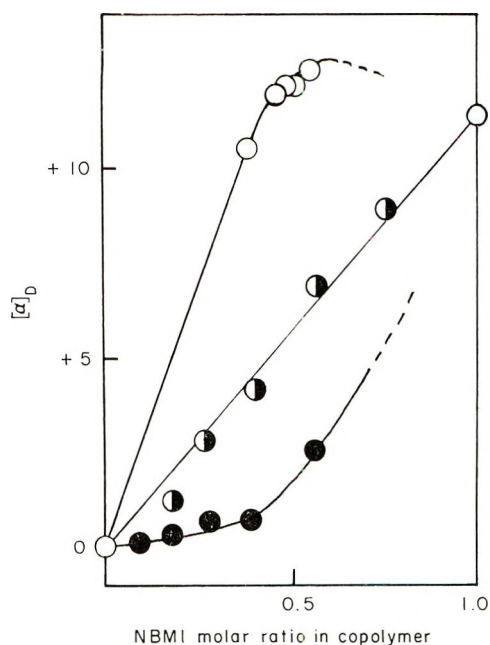


Fig. 4. Correlation between the specific rotation in THF at 25°C and NBMI molar ratio in copolymers: (○) St-NBMI; (●) MMA-NBMI; (◐) VCl<sub>2</sub>-NBMI.

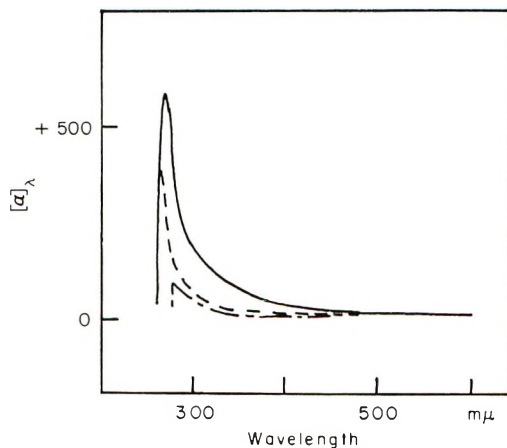


Fig. 5. Optical rotatory dispersions in THF at 25°C: (—) St-NBMI, (run 14); (---) MMA-NBMI (run 24); (- - -) VCl<sub>2</sub>-NBMI (run 34).

atoms or a helical conformation of the copolymers. As shown in Figure 5, the optically rotatory dispersion curves had positive Cotton effects. All of them were found to fit simple Drude equations over the range 270–400  $m\mu$  for St-NBMI, 266–300  $m\mu$  for MMA-NBMI, and 300–400  $m\mu$  for VCl<sub>2</sub>-NBMI copolymer (Fig. 6). In each copolymer, the  $\lambda_c$  values were independent of the composition of copolymer. The  $\lambda_c$  values for the copolymers

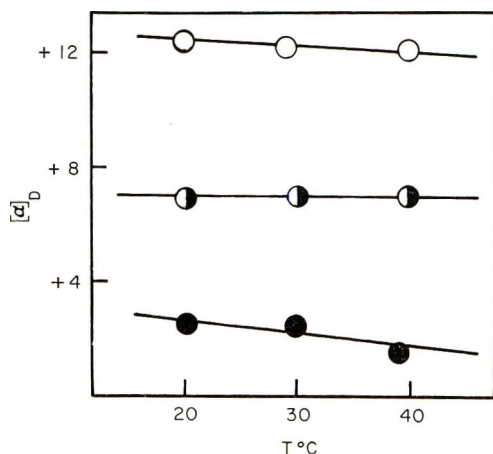


Fig. 6. Simple Drude dispersions: (○) St-NBMI (run 14); (◐) MMA-NBMI (run 24); (●) VCl<sub>2</sub>-NBMI (run 34).

of St, MMA, and VCl<sub>2</sub> were 260, 262, 260 mμ, respectively. The λ<sub>c</sub> values suggested that the chromophore causing optical activity was the carbonyl group of NBMI. The values of [α]<sub>max</sub> for each copolymer decreased in the following order: St-NBMI > MMA-NBMI > VCl<sub>2</sub>-NBMI. It was thought that the difference in the values of [α]<sub>max</sub> were caused by the newly induced asymmetric carbon atoms and chromophores.

#### Effect of Solvent and Temperature on the Specific Rotation

In addition, the temperature dependences and solvent effects on the specific rotation for the copolymers were investigated. As shown in Figure 7, a temperature dependence on the specific rotation for the copolymers was observed over the range 20–40°C. The values of the temperature coefficient ( $\Delta[\alpha]/\Delta T$ ) for St-NBMI, MMA-NBMI, and VCl<sub>2</sub>-NBMI copolymer were -0.017, -0.043, and -0.006, respectively. The values of  $\Delta[\alpha]/\Delta T$  for NBMI and poly-NBMI were +0.042 and -0.098, respectively, as reported in the previous paper.<sup>13</sup> From the result of temperature effect on the specific rotation of the copolymer, and in view of the results of Pino et al.<sup>16</sup> and Goodman et al.,<sup>17</sup> a helical conformation of the copolymers was considered not to be present.

As shown in Figure 8, the solvent dependence on the specific rotation for the copolymers was obtained. The specific rotation for the St-NBMI and VCl<sub>2</sub>-NBMI copolymer decreased with increasing the amount of ethanol (poor solvent), reached a minimum, and then increased with further increasing amounts of ethanol. On the other hand, the specific rotation for the MMA-NBMI copolymer increased with increasing amounts of ethanol, reached a maximum, and then decreased on further increasing the amounts of ethanol.

In the copolymerization of (-)- $\alpha$ -methylbenzyl methacrylate and (-)- $\alpha$ -methylbenzyl vinyl ether with maleic anhydride, Schuerch<sup>4-7</sup> reported that

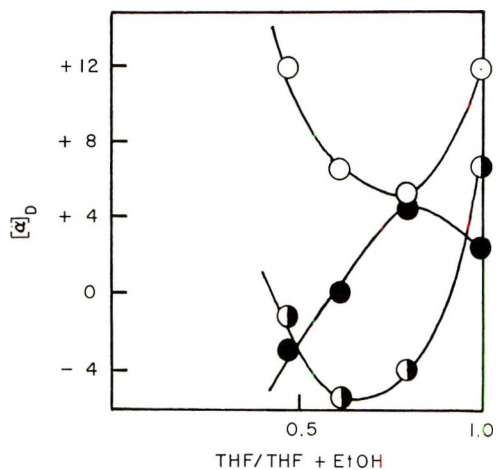


Fig. 7. Temperature dependence on the specific rotation of (○) St-NBMI (run 14); (●) MMA-NBMI (run 24); (◐) VCl<sub>2</sub>-NBMI (run 34).

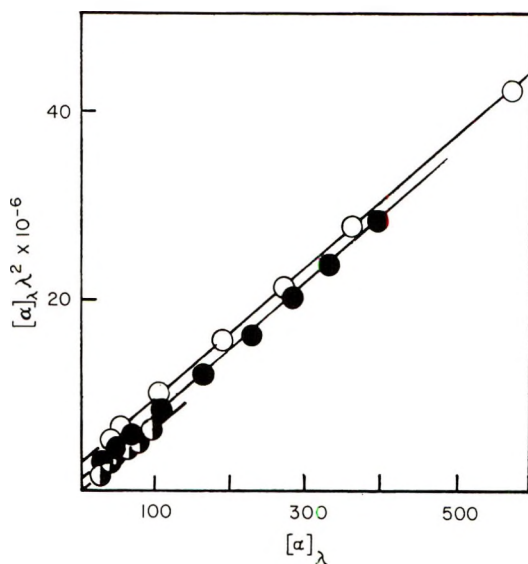


Fig. 8. Effect of solvents on the specific rotation at 25°C of (○) St-NBMI (run 14); (●) MMA-NBMI (run 24); (◐) VCl<sub>2</sub>-NBMI (run 34).

the copolymers remained optically active after the cleavage of optically active side groups from the copolymers, and the conversion of substituted carbon atoms to real asymmetric carbon atoms to give optically active copolymers because an asymmetric structure was induced into the polymer main chain.

The above results, in view of Schuerch's experimental results,<sup>4-7</sup> were considered to show that asymmetric carbon atoms were introduced in the polymer main chain under the influence of an optically active bornyl group.

Compared as the MMA-NBMI copolymer, the St-NBMI copolymer has a larger increasing effect for the specific rotation. It was thought that the probability of asymmetric induction for St-NBMI copolymer, which was an alternating copolymer, was largest, and therefore the largest increase seemed to be observed. The MMA-NBMI was not strictly an alternating copolymer, and the increasing effect for the copolymer was not so large as for St-NBMI copolymer.

ANAL. Calcd for  $C_{14}H_{19}O_2N$ : C, 72.1%; H, 8.2%; N, 6.0%. Found: C, 71.2%; H, 8.1%; N, 5.5%.

### References

1. C. L. Arcus and D. W. West, *J. Chem. Soc.*, **1959**, 2699.
2. C. G. Overberger and L. C. Palmer, *J. Amer. Chem. Soc.*, **78**, 666 (1956).
3. C. S. Marvel and C. G. Overberger, *J. Amer. Chem. Soc.*, **68**, 2106 (1946).
4. N. Beredjick and C. Schuerch, *J. Amer. Chem. Soc.*, **80**, 1933 (1958).
5. H. L. Frish, C. Schuerch, and M. Szwarc, *J. Polym. Sci.*, **11**, 559 (1953).
6. N. Beredjick and C. Schuerch, *J. Amer. Chem. Soc.*, **78**, 2646 (1956).
7. G. J. Schmitt and C. Schuerch, *J. Polym. Sci.*, **45**, 313 (1960).
8. C. Carline, F. Ciardelli and P. Pino, *Makromol. Chem.*, **119**, 244 (1968).
9. N. E. Searle, U. S. Pat. 2444536 (1948); *Chem. Abstr.*, **42**, 7340 (1948).
10. H. Yamaguchi and Y. Minoura, *J. Polym. Sci.*, in press.
11. R. C. Cubbon, *Polymer*, **6**, 419 (1965); in *Macromolecular Chemistry, Prague, 1965* (*J. Polym. Sci. C*, **16**), O. Wichterle and B. Sedlacek, Eds., Interscience, New York, 1967, p. 387.
12. G. V. Paesschen and D. Timmerman, *Makromol. Chem.*, **78**, 112 (1964).
13. Y. Minoura and Y. Suzuki, paper presented at 15th meeting of Society of Polymer Science, Japan, 1966.
14. L. E. Coleman and J. A. Conrady, *J. Polym. Sci.*, **38**, 241 (1959).
15. M. Yamada and I. Takase, *Kobunshi Kagaku*, **23**, 348 (1966); *ibid.*, **24**, 326 (1967).
16. P. Pino, F. Ciardelli, G. P. Lorenzi, and G. Montagnoli, *Makromol. Chem.*, **61**, 207 (1963).
17. M. Goodman, K. J. Clark, M. A. Stake, and A. Abe, *Makromol. Chem.*, **72**, 131 (1964).

Received September 10, 1969

Revised December 2, 1969

## Natural and Synthetic Polymers as Reagents. I. Diazonium Salt Derivatives of Polycarboxylic Resins (Insoluble Diazonium Salt Chromogens)

GIANNI LINOLI, ENZO MANNUCCI, and CARLO BERGONZI,  
*Miles Italiana S.p.A., Laboratorio di Ricerca, 22050 Garlate (CO), Italy*

### Synopsis

A method is described for the preparation of insoluble polymeric diazonium-salt chromogens which have a precise composition and well-defined specific reactivity and which are capable of undergoing coupling reactions to produce highly colored azo derivatives. The technique involves reaction of the acid chloride of an acrylic or methacrylic acid polymer crosslinked with divinylbenzene with an aromatic diamine, followed by diazotization of the free amino groups of the resultant aminoarylamido resin to give an insoluble diazonium salt. The aminoarylamido derivatives, the corresponding diazonium salts, and colors of the azo derivatives obtained in coupling reactions are tabulated.

### INTRODUCTION

Diazonium salt chromogens which are insoluble under all conditions of use and which have a well-defined composition and reactivity in coupling reactions are of value in analytical and other type reactions.<sup>1</sup> Polymers having diazonium salt groups have been prepared from polystyrene containing aminic groups,<sup>2</sup> from cellulose and its derivatives,<sup>3-5</sup> and from maleic anhydride-styrene copolymers,<sup>6</sup> but such polymers are soluble in certain solvents or reagents. Further, those methods of preparation may lead to diazonium salts with nonprecise structures, as in the reduction of randomly substituted nitro polymers followed by diazotization.<sup>2,6</sup>

It was, therefore, considered important to prepare an improved insoluble diazonium-salt chromogen with the desired characteristics.

Acrylic and methacrylic acid polymers crosslinked with about 8% divinylbenzene are insoluble under all possible use conditions. They are also macroreticular, a property which enhances reactivity with dissolved reactants. It appeared promising, therefore, to prepare diazonium salt derivatives of these copolymers for use as insoluble chromogens capable of undergoing coupling reactions to produce highly colored azo derivatives.

### RESULTS AND DISCUSSION

Initial studies involved a general evaluation of different methods of pre-

paring insoluble diazonium salt chromogens from acrylic or methacrylic acid-divinylbenzene copolymers (resin-COOH) and aromatic diamines, as shown in eq. (1). This reaction was carried out with either *N,N'*-dicyclohexylcarbodiimide (DCC) or *N*-ethyl-*N'*-(3-dimethylaminopropyl)carbodiimide (EDC) or by azeotropic distillation, but all three methods gave very low yields, as shown in Table I.

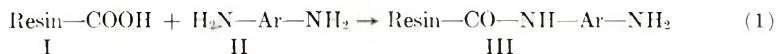


TABLE I  
Conversion of Crosslinked Methacrylic Acid Resin to Aminoarylamido Derivative

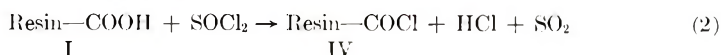
II	Condensation by	Total nitrogen, mmole/g	Conversion of I to III, %
Benzidine	Azeotropic distillation	0.018	0.18
<i>o</i> -Tolidine	Azeotropic distillation	0.010	0.10
<i>o</i> -Dianisidine	DCC	0.037	0.37
3,5 Diaminobenzene sulfonic acid	DCC	0.012	0.12
Benzidine	EDC	0.015	0.15

Similarly, the reaction of an aromatic diamine with the crosslinked polycarboxylic polymer in the form of a mixed anhydride with acetic acid gave disappointing yields of the desired product III. However, preliminary experiments demonstrated that high conversion values could be obtained if the aromatic diamine was reacted with the acid chloride of the crosslinked polycarboxylic acid resin. This latter method was adopted for further study.

### Preparation of Crosslinked Polycarboxylic Resin Acid Chlorides

Acid chloride formation in the polymer can be effected with thionyl chloride<sup>7</sup> or other agents such as phosphorus pentachloride.<sup>8</sup> Use of the former has the advantage that it has a low boiling temperature and it is converted entirely into gaseous products (HCl + SO<sub>2</sub>), thereby simplifying the purification of the resulting resin acid chloride.

Under the conditions described in the Experimental Section, conversion of the crosslinked polycarboxylic resins to the acid chlorides proceeded according to eq. (2) with the results shown in Figure 1.



The products IV, with a pre-established Cl content, were obtained by adopting a suitable reaction time. However, in spite of the continuous removal of the gaseous product formed (HCl and SO<sub>2</sub>) from the resin suspension during acid chloride formation, and in spite of the large excess of thionyl chloride used, conversion of the carboxylic acid groups remains

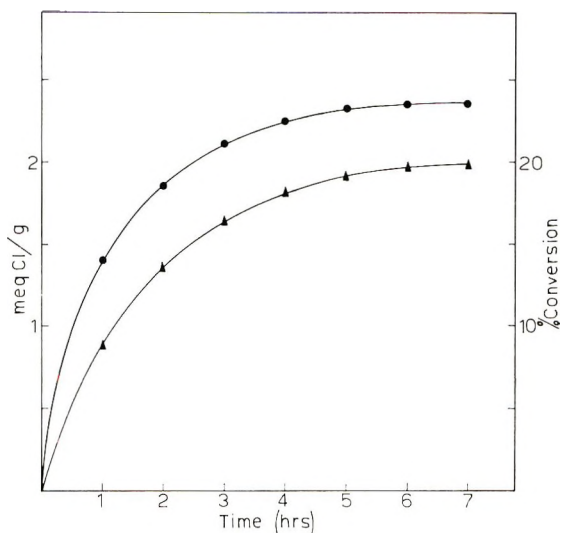
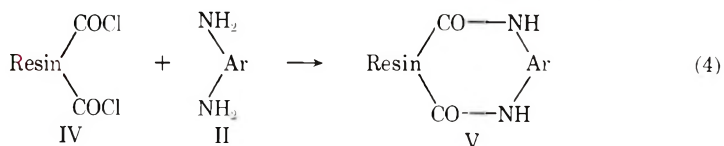
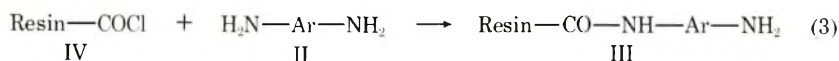


Fig. 1. Acid chloride formation from divinylbenzene-crosslinked resins: (●) acrylic and (▲) methacrylic acid resins.

incomplete. In fact, although both resins have 10 meq COOH/g, their maximum conversion to the acid chloride produced only 2.4 meq Cl/g in the product. The concurrent formation of anhydride between adjacent carboxylic groups, thereby producing a six-membered ring, might explain the incomplete conversion. Hence, the polycarboxylic resins act in a manner similar to some monomeric polycarboxylic acids.

### Reaction between Polycarboxylic Resin Acid Chlorides and Aromatic Diamines

Two possible reaction schemes may be considered, as shown in eqs. (3) and (4).



The first reaction, eq. (3), produces the polymeric compound III, an aminoarylamido derivative having amido groups and free amino groups. The amino groups can be diazotized to form diazonium salt-type structures which are insoluble and are chromogens.

Diamides V with no free amino groups could be formed by the second reaction, eq. (4). Therefore, a 50% excess of diamine was used in a stoichiometric quantity, calculated on the basis of chlorine, in order to avoid,



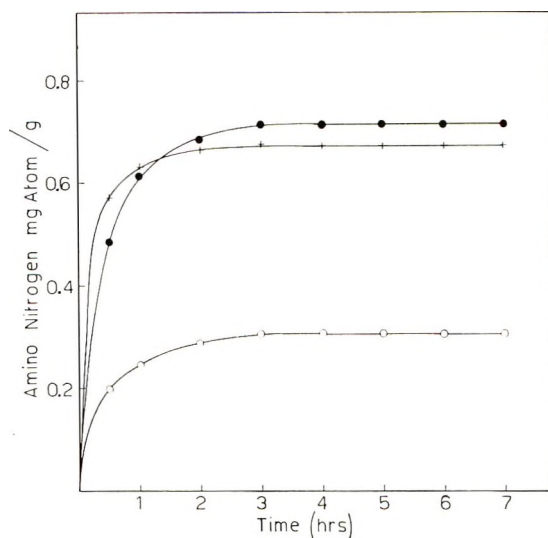


Fig. 2. Crosslinked methacrylic resin acid chloride (1.0 meq chlorine/g), amidation by: (○): *o*-dianisidine; (+) 3,6-diaminobenzensulfonic acid; (●) 2-chloro-1,4-phenylenediamine.

if possible, that reaction. If II represents an *o*-aromatic diamine, the amido groups will be *ortho* with reference to the amino group in III, and, by diazotization of III, 1-substituted benzotriazoles (VI) will be produced.<sup>9</sup>

Amidation can be carried out either in water (method A) according to the traditional Schotten-Baumann technique, or in solvents working in anhydrous conditions, either with (method B) or without (method C) an acceptor for the liberated hydrochloric acid. These methods are described in the Experimental Section and the results are reported in Table II for a reaction time of 3 hr.

The results shown in Table II indicate that the conversion of IV to III is higher for phenylenediamines than for diphenylenediamines. The ratio of total nitrogen to amino nitrogen in III gives evidence that only 1,4-phenylenediamine, of the diamines examined, underwent reaction (4) to a significant extent. Therefore, in this case, the use of 50% excess of II based on the stoichiometric quantity of IV, is insufficient to prevent such a reaction.

The amidation curves in Figure 2 show that, under the conditions adopted, a 3-hr reaction time is sufficient to reach the maximum conversion value. Consequently, the limited conversion which has been obtained for diphenylene-diamines does not appear to depend on an insufficient reaction time, but rather on another variable, such as the structure and the size of the diphenyl ring.

Another method for preparing insoluble diazonium salt chromogens involved reaction of an aromatic amine having in the aromatic nucleus a

TABLE II  
Amidation of Resin Acid Chlorides by Diamines

Crosslinked resin	Cl, meq/g	Aromatic diamines	Methods <sup>a</sup>	Conversion, %	Total nitrogen, mmole/g	Amino nitrogen, mg-atom/g	Ratio	Compound No.
Methacrylic	1.50	1,3-Phenylenediamine	C	10.78	0.168	0.159	1.06	IIIa
"	1.80	1,4-Phenylenediamine	B	79.50	1.510	1.240	1.22	IIIb
"	0.70	4-Chloro-1,3-phenylenediamine	C	45.90	0.316	0.306	1.03	IIIc
"	1.00	2,6-Dichloro-1,4-phenylenediamine	B	48.50	0.457	0.446	1.02	III d
"	1.45	2,4-Diaminobenzenesulfonic acid	A	8.03	0.120	0.114	1.05	IIIe
"	1.80	5-Amino-2-nitrobenzoic acid	B	8.16	0.143	0.143 <sup>b</sup>	1.00	III f
"	1.80	5-Amino-2-nitromethylbenzoate	B	7.72	0.135	0.135 <sup>b</sup>	1.00	III g
"	0.50	2,4-Diaminoanisole	B	76.60	0.382	0.364	1.05	III h
"	1.66	2,5-Diaminoanisole	C	36.10	0.577	0.552	1.04	III i
"	1.50	Benzidine	B	34.70	0.485	0.474	1.02	III j
"	1.20	<i>o</i> -Dianisidine	B	29.86	0.352	0.329	1.07	III k
"	0.87	4,4-Diaminodiphenylamine	B	13.30	0.121	0.113	1.07	III l
"	1.81	1,5-Diaminoanthraquinone	B	5.44	0.102	0.096	1.06	III m
"	1.45	2-Chloro-1,4-phenylenediamine	A	23.00	0.320	0.318	1.01	III n
"	1.45	3,6-Diaminobenzenesulfonic acid	A	15.60	0.219	0.217	1.01	III o
"	1.50	1,2-Phenylenediamine	C	16.50	0.241			III p
"	1.45	4-Chloro-1,2-phenylenediamine	A	15.80	0.222			III q
Acrylic	2.08	2-Nitro-1,4-phenylenediamine	B	96.00	2.310	1.530	1.01	III r
"	2.37	2-Chloro-1,4-phenylenediamine	B	84.25	1.570	1.555	1.01	III s
"	2.38	3,6-Diaminobenzenesulfonic acid	B	79.60	1.440	1.397	1.03	III t
"	2.30	3,5-Diaminobenzoic acid	B	9.10	0.219	0.203	1.03	III u
"	2.30	<i>o</i> -Tolidine	B	3.45	0.081	0.078	1.04	III v

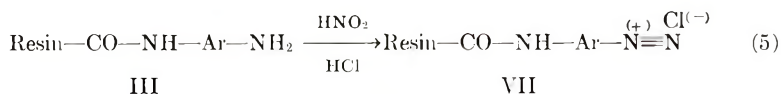
<sup>a</sup> Methods described in the Experimental Section.

<sup>b</sup> Amino nitrogen determined after reduction of the nitro group according to the method described in the Experimental Section (Method D).

substituent nitro group with an acid chloride resin according to eq. (3). The nitroarylamido resin was then reduced to an aminoarylamido resin by sodium dithionite, according to method D in the Experimental Section. Compounds IIIf and IIIg are representative examples obtained by these steps.

### Diazotization of Aminoarylamido Resins

In the preparation of soluble monomeric diazonium salts, an excess of nitrous acid exerts a very unfavorable influence on the stability of diazonium solutions.<sup>10</sup> Therefore, it is important to take the precautions of adding a stoichiometric quantity of nitrous acid based on the amino compound to be diazotized or of destroying the excess by urea or by sulfamic acid. These precautions are not required in the diazotization of the aminoarylamido resins of reaction (5).



In fact, nitrous acid can be added in excess until the reaction is completed. As shown in Figure 3, additional reaction time does not influence formation of the diazonium salt.

The excess of nitrous acid is easily removed from the insoluble diazonium salt chromogen by filtration and washing. Table III lists the insoluble diazonium salt chromogens (VII) formed by diazotization of III.

### Coupling Reactions of Insoluble Diazonium Salt Chromogens (VII)

Table III describes the colors of the azo compounds obtained in coupling reactions carried out with the insoluble diazonium-salt chromogens (VII) and selected reactants. The latter are only representative of a wide variety of known compounds which couple with diazonium salts to give colored azo products. As expected, no color was obtained if a compound produced a benzotriazole upon diazotization (IIIp and IIIq  $\rightarrow$  VIp and VIq).

The chemical structure of the insoluble diazonium salt chromogen prepared according to the method described reflects that of the aromatic diamine used in the amidation reaction. Such a structure is accompanied also by a well-defined specific reactivity.

No solvent or reagent appeared to affect the insolubility of the prepared diazonium-salt chromogens, nor was there any color bleeding observed from the azo derivatives obtained.

## EXPERIMENTAL

### Materials

Amberlite IRC-50, a methacrylic acid-divinylbenzene copolymer, and Amberlite IRC-84, an acrylic acid-divinylbenzene copolymer (Rohm & Haas Co., Philadelphia, Pa., 19105 U.S.A.) were used as starting materials.

TABLE III  
Color Reactions of Insoluble Diazonium Salt Chromogens<sup>a</sup>

No.	Coupling power CP, mg/g <sup>b</sup>	Color of azo compounds				
		$\beta$ -Naphthhol	$\beta$ -Naphthylamine	3-Methyl-1-phenyl- 5-pyrazolone	Oxalacetic acid	<i>N</i> -(1-Naphthyl) ethylenediamine
VIIa	22.8	Red	Orange	Deep yellow	Orange	Pastel violet
VIIb	176.0	High red	Orange red	Deep orange	Red orange	Pastel violet
VIIc	44.2	Red	Orange	Yellow	Red	Violet
VIIId	64.0	High red	Orange	Deep yellow	Red	Violet
VIIe	16.5	Red	Orange	Deep orange	Orange	Royal blue
VIIIf	20.6	Pastel red	Reddish orange	Yellow	Pale yellow	Pink
VIIg	19.45	Orange	Light orange	Yellow	Yellow	Pink
VIIh	52.1	Bluish red	Light orange	Orange	No color	Yellow
VIIi	79.0	Bluish red	Orange	Red	No color	Yellow
VIIj	68.0	Bluish red	Light orange	Red	Orange	Yellow
VIIk	47.1	Ruby	Reddish orange	Vivid red	No color	Deep yellow
VIIl	16.2	Red	Orange	Orange	Red orange	Pastel violet
VIIIm	13.7	Brown	Brown	Brown	No color	Brown
VIIIn	45.5	Vivid red	Orange	Deep yellow	Vivid red	Violet
VIIo	31.1	High red	Orange	Reddish orange	Red orange	Royal blue
VIIp	0.0	No color	No color	No color	No color	No color
VIIq	0.0	No color	No color	No color	No color	No color
VIIr	217.0	Deep red	Reddish brown	Deep orange	Red	Greyish violet
VIIs	220.0	Vivid red	Orange	Deep yellow	Vivid red	Violet
VIIIt	198.1	High red	Orange	Reddish orange	Red orange	Royal blue
VIIu	29.1	Orange	Pale orange	Deep yellow	Pale yellow	Pink
VIIv	11.2	Bluish red	Pale orange	Red	No color	Yellow

<sup>a</sup> Colors are evaluated and expressed according to Kornerup and Wanschel.<sup>11</sup>

<sup>b</sup> CP represents the quantity of naphthol fixed in a quantitative azo coupling reaction by 1 g insoluble diazonium salt chromogen.

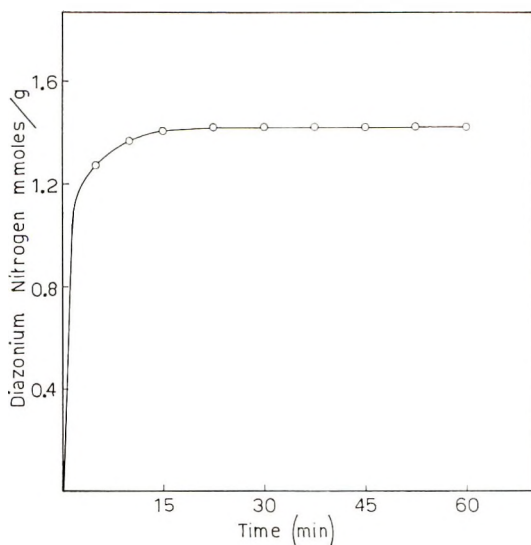


Fig. 3. Diazotization of III.

Aromatic diamines (Purum Degree) were supplied by Fluka A.G. (CH-9470, Buchs, Switzerland).

### Resin Purification

The Amberlite resins were purified from traces of residual stabilizers and from contamination products by repeated base-acid exchange with 2*N* HCl and 1*N* NaOH according to the traditional chromatographic techniques. Five exchange operations were generally required for purification.

### Preparation of Acid Chlorides of the Resin (IV)

A 250-ml three-necked round-bottomed flask suspended in an oil bath thermoregulated at 80°C was used. The flask was fitted with a well-sealed stirrer, a thermometer, and a water-cooled condenser with CaCl<sub>2</sub> trap. Reaction was carried out by refluxing dry resin (20.0 g) with a solution formed of benzene (80 ml) and thionyl chloride (80 ml) under stirring. After a pre-established time, the reaction mixture was filtered with vacuum and the resin was washed with dry benzene (three times with 25.0 ml each time). IV was maintained in high vacuum by a mechanical pump fitted with a trap until the low-boiling products were removed.

### Reaction of Polycarboxylic Resin Acid Chlorides (IV) with Aromatic Diamines (II)

Compounds IV (10.0 g) corresponding to *X* meq chlorine were reacted with  $X + X/2$  mmoles of compounds II, by three different methods, as follows.

**Method A (in Water).** The reaction was carried out at 0–5°C by slowly adding IV to the solution of the hydrochloride of II in water (100 ml). Under stirring and cooling, 5*N* NaOH was added dropwise during 30 min until the solution was alkaline (pH 10–11). Stirring and cooling were continued overnight; then the aminoarylamido resin obtained (III) was filtered off and purified from unreacted II by acid–base exchange and water washing until disappearance of II from the eluate. Compound III, in the acid form, was dried in vacuum.

**Method B (in Anhydrous Solvent with Triethylamine).** The same apparatus described in the preparation of the resin acid chloride was used. The solutions formed by compounds II in anhydrous toluene (100 ml), and triethylamine (11.0 g sufficient to saturate resin carboxylic groups and hydrochloric acid liberated by the reaction) were heated at 80°C and, under stirring, compounds IV were added. The reaction was continued for a pre-established time at constant temperature and under stirring. Compounds III were filtered off and washed according to the procedure described for method A. For the compounds IIIa, IIIb, IIIf, IIIg, IIIr, IIIs, IIIt, and IIIu, DMF was used instead of toluene.

**Method C (in anhydrous solvent, without alkaline compounds).** The procedure was the same as in Method B, except that the reaction was carried out without triethylamine.

#### Conversion of Nitroarylamido Resins to Aminoarylamido Resins (Method D)

Nitroarylamido resins (compounds IIIf and IIIg) were prepared from nitroarylamines according to method B. Reduction of nitro groups to amino groups was carried out in a 250-ml three-necked round-bottomed flask with a well-sealed stirrer, a dropping funnel and a water-cooled condenser. The flask was suspended in an oil bath. A suspension formed of nitroarylamido resin (20.0 g) in ethyl alcohol (180 ml) was heated at reflux, and a solution formed from sodium dithionite (5.0 g) and water (20 ml) was added dropwise. The suspension was stirred and refluxed for 1 hr. The deep yellow color of the nitro resin changed to light yellow. The reduced polymer was collected by filtration, washed with water, and purified by base–acid exchanges according to the general procedure for compounds III.

#### Diazotization

Compound III (5.0 g) was suspended in water (25 ml) containing 37% HCl (3.5 ml). The suspension was chilled to 0–5°C and 2*N* NaNO<sub>2</sub> (3.5 ml) was added dropwise. Stirring and cooling were continued for 30 min. The formed compound VII was collected by filtration and washed with 0.01*N* HCl until HNO<sub>2</sub> disappeared from the filtrate. Compound VII was dried in vacuum and stored in light-proof containers.

### Analytical Methods

**Chlorine Determination in Resin Acid Chlorides.** About 1 g, carefully weighed, of the resin acid chloride (IV) was poured into 15 ml 2.5*N* NaOH; the suspension was heated on a boiling water bath for 30 min and the resin filtered off and washed. The filtrate and the washing, quantitatively collected, were titrated with AgNO<sub>3</sub>, according to the Mohr method, for Cl determination. For calculating the conversion of carboxyl to acid chloride groups, the following formula was used:

$$\% \text{ Conversion} = 1000 X / (1000 - 18.45X)$$

where *X* denotes milliequivalents Cl<sup>-</sup> per gram.

**Total Nitrogen Determination in Aminoarylamido Resins (III) and Calculation of Conversion of Resin Acid Chloride (IV).** The Dumas semi-micro combustion method was used to determine total nitrogen.

Calculation of conversion of compounds IV to the hydrochlorides of III was made according to the formula:

$$\text{Conversion} = N10^5 / [X(1,000 - NM)]$$

where *N* = mmoles N<sub>2</sub>/g in III, *X* = milliequivalents Cl/g in IV, and *M* = molecular weight of the diamine used.

**Determination of Coupling Power (CP) for Compounds VII.** The method is based on the reaction between insoluble diazonium salt chromogens and β-naphthol and the determination of unreacted naphthol.

The standard solution was a solution of 2% β-naphthol in ethyl alcohol. A solution of tris(hydroxymethyl)aminomethane of pH 8.5 was obtained by dissolving 10 g Tris in 50 ml of water and addition of 5*N* HCl to give the desired pH and enough water to make the volume to 100 ml.

The test solution consisted of β-naphthol solution in Tris containing about 50% excess naphthol based on the quantity to be coupled by the resin diazonium salt.

In an amber glass beaker, 100 mg VII were added to 5 ml of the test solution. The suspension obtained was stirred for 20 min, diluted to 10 ml with 20% acetic acid, filtered, and the suspension washed with 40 ml of 20% acetic acid. The filtrate and the washings were collected and diluted to obtain a naphthol concentration of approximately 20 μg/ml. A standard solution diluted in the same way was used. The absorption of the solutions was measured by a spectrophotometer at 274 mμ. The coupling power CP was calculated from the formula:

$$\text{CP} = [A - (AD'/D)] \times 10$$

where *A* is the weight (mg) of naphthol used for 100 mg insoluble diazonium salt chromogen, *D'* is the optical density of the solution under measurement, and *D* is the optical density of the standard solution.

The CP is expressed as milligrams of naphthol coupled per gram of VII.

**Amino Nitrogen in Compounds III.** The coupling power determined for the corresponding compounds VII was used to calculate amino nitrogen in compounds III by the ratio, CP/144.16.

The data were checked further by a method based on the measurement of the nitrogen liberated by decomposition of insoluble diazonium salt chromogens. This method will be the subject of a separate paper.

### CONCLUSIONS

A new class of reagents, insoluble diazonium-salt chromogens which give colored azo compounds in coupling reactions, has been prepared from cross-linked polycarboxylic acid resins by formation of the acid chloride, amino-aryl-amidation with aromatic diamines, and diazotization of the free amino groups. These insoluble diazonium salt chromogens have a precise composition and specific reactivity.

### References

1. G. Linoli and E. Mannucci, French Pat. 1,527,628 (1968).
2. N. Grubhofer and L. Schleicht, *Naturwiss.*, **40**, No. 19, 508 (1953).
3. D. H. Campbell, H. Luescher and L. S. Lerman, *Proc. Nat. Acad. Sci. U. S.*, **37**, 575 (1951).
4. A. E. Gurevich, O. B. Kuzovleva and A. E. Tumanova, *Biokhimiya*, **26**, 934 (1961).
5. H. H. Weetal and N. Wekily, *Nature*, **204**, 896 (1964).
6. W. O. Kenyon, L. M. Minsk, and G. P. Waugh, U. S. Pat. 2,274,551 (1939).
7. H. C. Isliker, *Ann. N.Y. Acad. Sci.*, **57**, 225 (1953).
8. Rohm and Haas, private communication.
9. A. Ladenburg, *Ber.*, **9**, 219, 1524 (1876).
10. H. Gies and E. Pfeil, *Ann.*, **578**, 11 (1952).
11. A. Kornerup and J. H. Wanscher, *Methuen Handbook of Colour*, Methuen, London, 1963.

Received October 17, 1969

Revised December 3, 1969



## Role of Dimethyl Sulfoxide as a Solvent for Vinyl Polymerization

SATYENDRA NATH GUPTA and UMA SANKAR NANDI,  
*Department of Macromolecules, Indian Association for the Cultivation of  
Science, Calcutta 32, India*

### Synopsis

Dimethyl sulfoxide has been used as a solvent in the polymerization of methyl methacrylate and styrene. The chain-transfer coefficients of the solvent and the values of  $\delta$  [i.e.,  $(2k_t)^{1/2}/k_p$ ] in solvent-monomer mixtures of various compositions were determined.  $\delta$  was observed to be dependent on the solvent concentration in the case of methyl methacrylate but remained constant in case of styrene. The lowering of the values of  $\delta$  with increasing solvent concentration in case of methyl methacrylate has been attributed to an interaction between the solvent and poly(methyl methacrylate) radical resulting in lower termination rate.

The use of dimethyl sulfoxide (DMSO) as a solvent for vinyl polymerization is of comparatively recent development. Wide solubility range, high dielectric constant, and low transfer value has opened up the possibility of diverse applicability of this solvent in polymerization studies.

As DMSO adds to the limited number of solvents for polyacrylonitrile, polymerization of acrylonitrile has been followed to a great extent in this solvent. White and Zisell<sup>1</sup> observed a higher rate of polymerization and molecular weight and a low solvent transfer constant in DMSO compared to dimethylformamide (DMF). Poly(methyl methacrylate) obtained by electroinitiation has also been reported<sup>2</sup> to have a high molecular weight and enhanced rate of polymerization in DMSO. These observations rightly demand thorough and systematic study with this solvent.

We have reported here results on the polymerization of methyl methacrylate and styrene in this solvent initiated by 2,2'-azobisisobutyronitrile (AIBN).

### EXPERIMENTAL

#### Materials

Most of the water which might be present in the BDH quality DMSO used was removed by azeotropic distillation with benzene. The product was then dried over calcium hydride and fractionally distilled under reduced pressure. The middle fraction was used for polymerization studies.

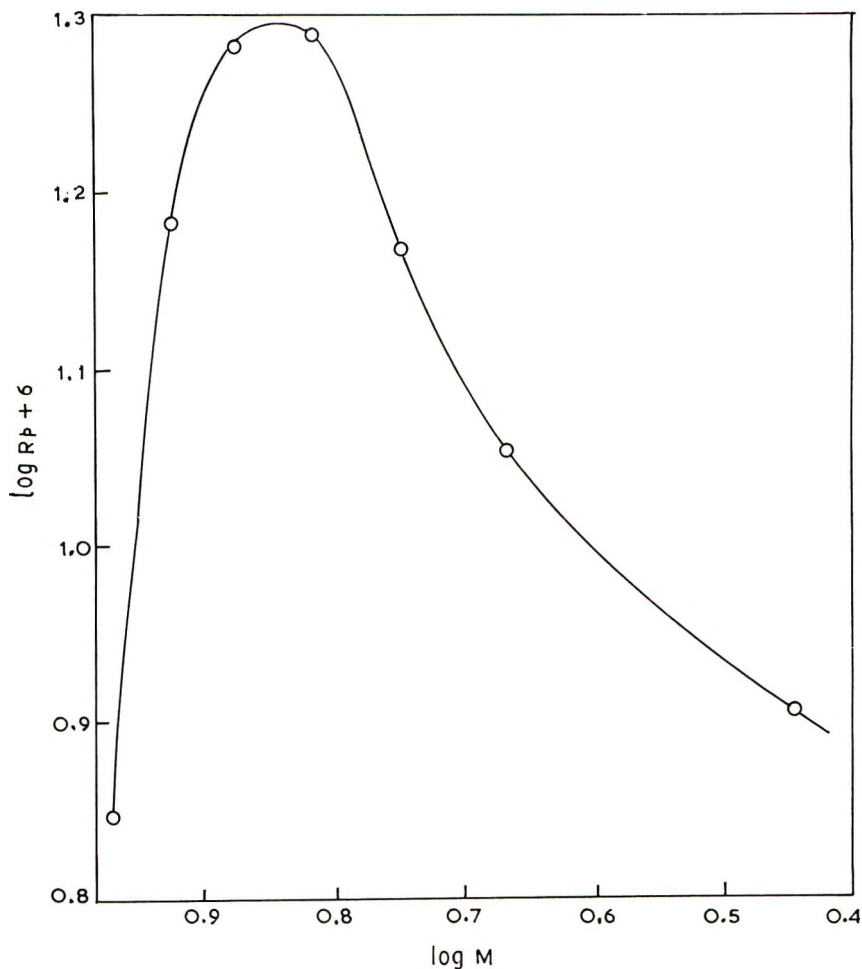


Fig. 1. Variation of  $R_p$  with monomer concentration in thermal polymerization of MMA in DMSO at 60°C.

Benzene was purified in the conventional way and dried over sodium and fractionally distilled.<sup>3</sup>

AIBN was crystallized three times from ethyl alcohol and dried under vacuum. Methyl methacrylate<sup>4</sup> and styrene<sup>5</sup> were purified in the usual way.

Polymerization studies were carried out dilatometrically at 60°C. The dilatometer with the contents was frozen, degassed, and flushed with nitrogen. This operation was repeated a number of times and finally the dilatometer was sealed under vacuum. It was then placed in a thermostat, the contraction measured by a cathetometer, and  $R_p$  calculated thereby. The number-average degree of polymerization  $\bar{P}$  was determined from viscometric measurements with the help of the equation  $\bar{P} = K[\eta]^\alpha$  where  $[\eta]$  is the intrinsic viscosity and  $K$  and  $\alpha$  are constants, the values being

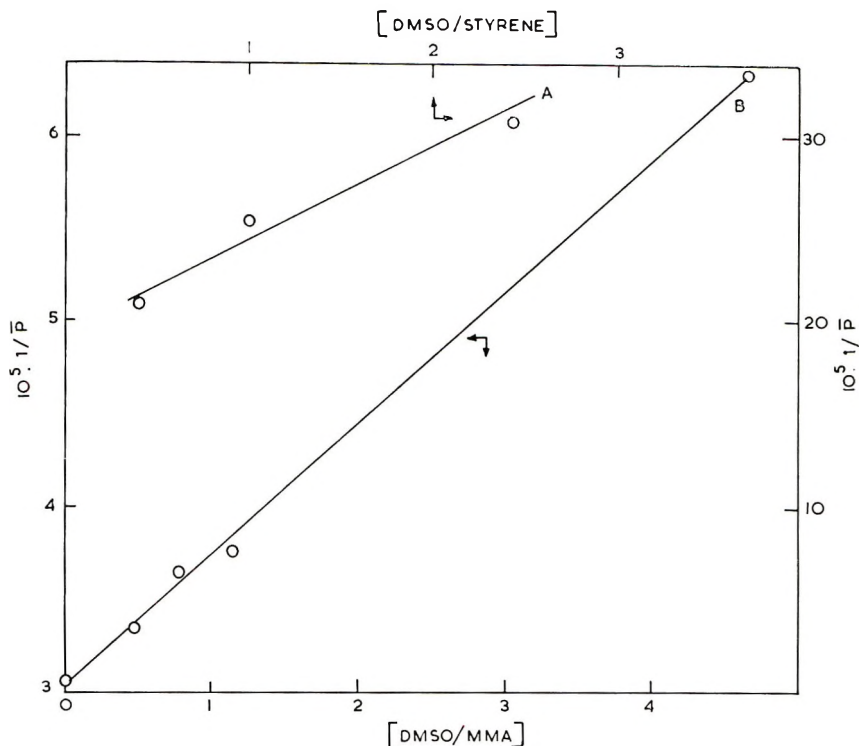


Fig. 2. Determination of the  $C_S$  of DMSO: (A) styrene; (B) methyl methacrylate.

$2.205 \times 10^3$  and 1.32, and  $1.77 \times 10^3$  and 1.40 for poly(methyl methacrylate)<sup>6</sup> and polystyrene,<sup>7</sup> respectively.

## RESULTS

### Determination of Chain Transfer to the Solvent

Methyl methacrylate and styrene were thermally polymerized at different monomer concentrations in DMSO at 60°C. The monomer concentration was varied by varying the concentration of DMSO.  $R_p$  was observed to increase with increasing concentration of DMSO, i.e., decreasing monomer concentration, and after passing through a maximum the rate decreases (Fig. 1). No such initial rise was observed in the case of styrene.

To determine the solvent-transfer coefficient, the inverse of the degree of polymerization ( $1/\bar{P}$ ) was plotted against the ratio of the concentration of the solvent to the concentration of the monomers,  $[S]/[M]$ . From the slope of the plots (Fig. 2) the values of  $C_S$  i.e., the chain-transfer coefficient to solvent were found to be  $0.71 \times 10^{-5}$  for methyl methacrylate and  $4.8 \times 10^{-5}$  for styrene.

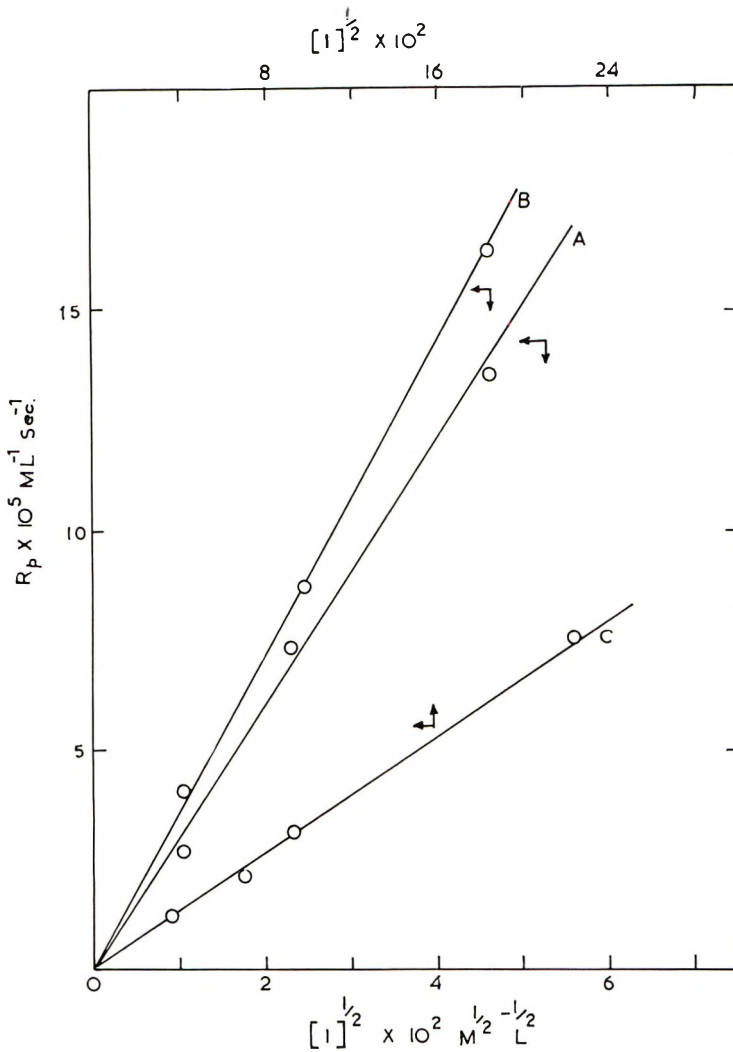


Fig. 3. Dependence of  $R_p$  on AIBN concentration at fixed monomer concentration: (A) [MMA] = 4.65 mole/l.; (B) MMA = 7.44 mole/l.; (C) [styrene] = 4.34 mole/l.

#### Effect of Initiator Concentration on the Rate of Polymerization and Evaluation of $\delta$

The rate of polymerization was found to be directly proportional to the square root of the initiator concentrations at different concentrations of the monomers (Fig. 3).

The general equation for the reciprocal degree of polymerization ( $1/\bar{P}$ ) can be easily deduced and is

$$1/\bar{P} = C_M + C_S[S]/[M] + C_I[I]/[M] + (R_p\delta^2/[M]^2) \quad (1)$$

where  $C_M$ ,  $C_S$  and  $C_I$  are chain transfer constants for monomer (M), solvent

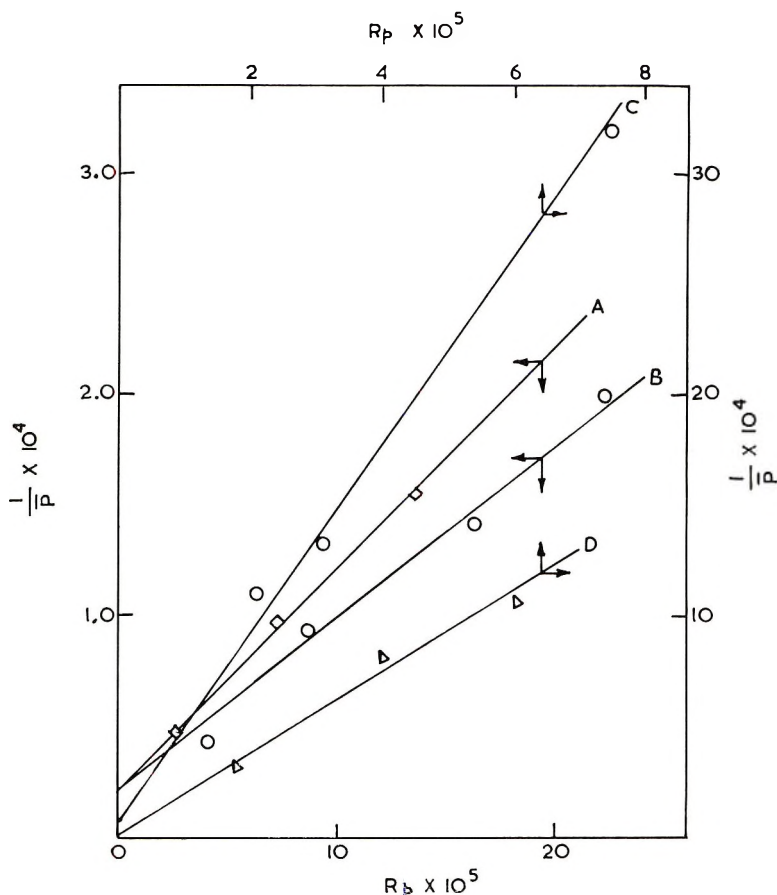


Fig. 4. Evaluation of  $\delta$  for AIBN-initiated polymerization of MMA and styrene and DMSO: (A) [MMA] = 4.65 mole/l.; (B) [MMA] = 7.44 mole/l.; (C) [styrene] = 4.31 mole/l.; (D) [styrene] = 6.89 mole/l.

(S), and initiator (I) respectively.  $R_p$  represents the rate of polymerization. For initiators whose  $C_I$  values are almost zero and at constant monomer concentration, eq. (1) can be written as

$$1/\bar{P} = \text{Constant} + R_p\delta^2/[M]^2$$

The values of  $\delta$  [i.e.,  $(2k_t)^{1/2}/k_p$ ] at different ratios of solvent to monomer were evaluated from the slopes of the plots of  $1/\bar{P}$  against  $R_p$  (Fig. 4).<sup>4</sup> The values decreased with increasing of DMSO concentration in the case of methyl methacrylate but remained virtually constant in case of styrene (Table I).

#### Dependence of the Rate of Polymerization on Monomer Concentration

The dependence of the rate of polymerization on the concentration of monomer has been studied with both the monomers in DMSO at a fixed

TABLE I  
Value of  $\delta$  at Different Monomer Concentrations

Monomer	Concentration of monomer, mole/l.	$\delta$ , mole <sup>1/2</sup> - sec <sup>1/2</sup> /l. <sup>1/2</sup>	Reference
Methyl methacrylate	Bulk	7.6	4
	7.44	6.65	Present authors
	4.65	4.65	"
Styrene	Bulk	28.62	8
	6.94	29.4	Present authors
	4.34	28.1	"

concentration of AIBN. With methyl methacrylate it was observed that  $R_p$  increased linearly with monomer concentration up to 60% monomer concentration, after which the rate virtually remained unaltered with further increase in the concentration of methyl methacrylate (Fig. 5). Styrene, on the other hand, followed a linear relationship between  $\log R_p$  and  $\log [M]$  with a monomer exponent of 1.2 which is well within the values in the literature.<sup>9-11</sup>

From what we have observed (Figs. 1 and 5) it seems that DMSO enhances the rate of polymerization of methyl methacrylate. To find out the dependency of the rate of polymerization on the DMSO concentration, polymerization was carried out in the presence of a cosolvent (benzene) in which a first-order dependence of the  $R_p$  on monomer concentration has been observed,<sup>12</sup> the chain-transfer coefficient<sup>13</sup> with poly(methyl methacrylate) radical is close to that with DMSO. In the systems studied both the initiator (AIBN) and monomer concentrations were kept constant and the ratio of benzene to DMSO varied. In the case of methyl methacrylate  $R_p$  was observed to increase with increasing concentration of DMSO but styrene showed more or less constant rate of polymerization independent of the DMSO concentration (Fig. 6). Further the molecular weight of the resulting polymer increased with increasing DMSO concentration in the case of methyl methacrylate.

## DISCUSSION

Our values of chain transfer constants for poly(methyl methacrylate) and polystyrene radicals are quite comparable with similar low transfer coefficients of this solvent observed for acrylonitrile.

The general tendency of the solvent to increase the rate of polymerization and degree of polymerization of methyl methacrylate as observed by us and also for acrylonitrile observed by many workers mentioned earlier is difficult to explain.

The possibility that DMSO produces free radicals is ruled out on the basis of its inability to initiate polymerization of other monomers which are not polymerizable thermally (e.g., acrylonitrile or vinyl acetate), and

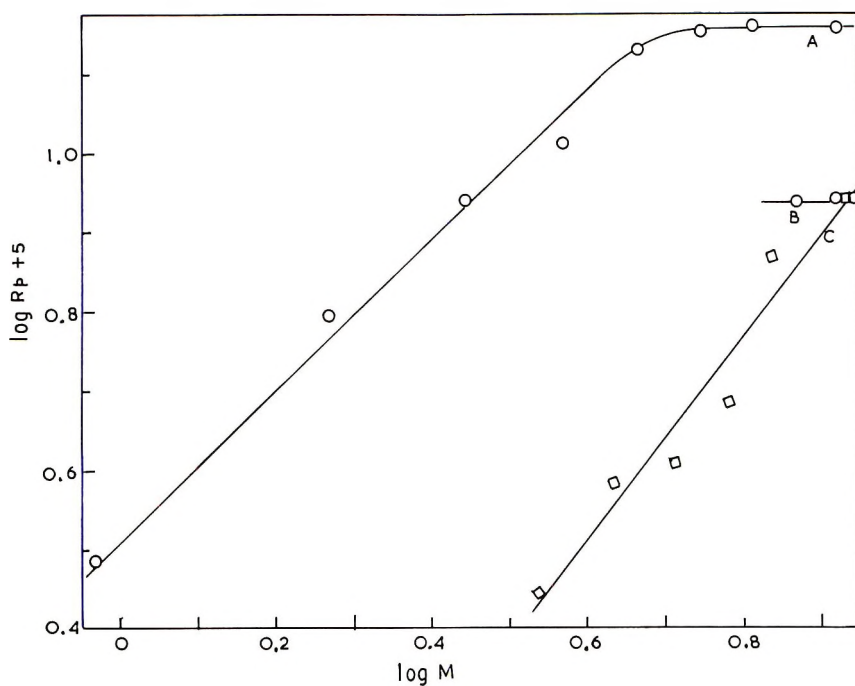


Fig. 5. Dependence of  $R_p$  on monomer concentration in DMSO at fixed AIBN concentration: (A) MMA,  $[AIBN] = 2.104 \times 10^{-3}$  mole/l.; (B) MMA,  $[AIBN] = 0.598 \times 10^{-3}$  mole/l.; (C) styrene,  $[AIBN] = 9.58 \times 10^{-3}$  mole/l.

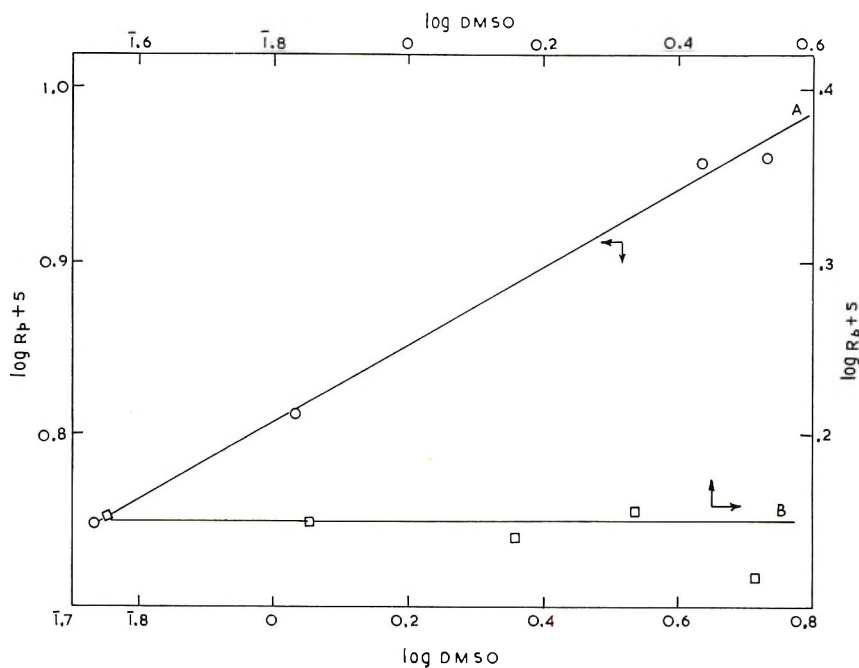


Fig. 6. Variation of  $R_p$  with DMSO concentration at fixed monomer and AIBN concentration: (A) MMA; (B) = styrene.

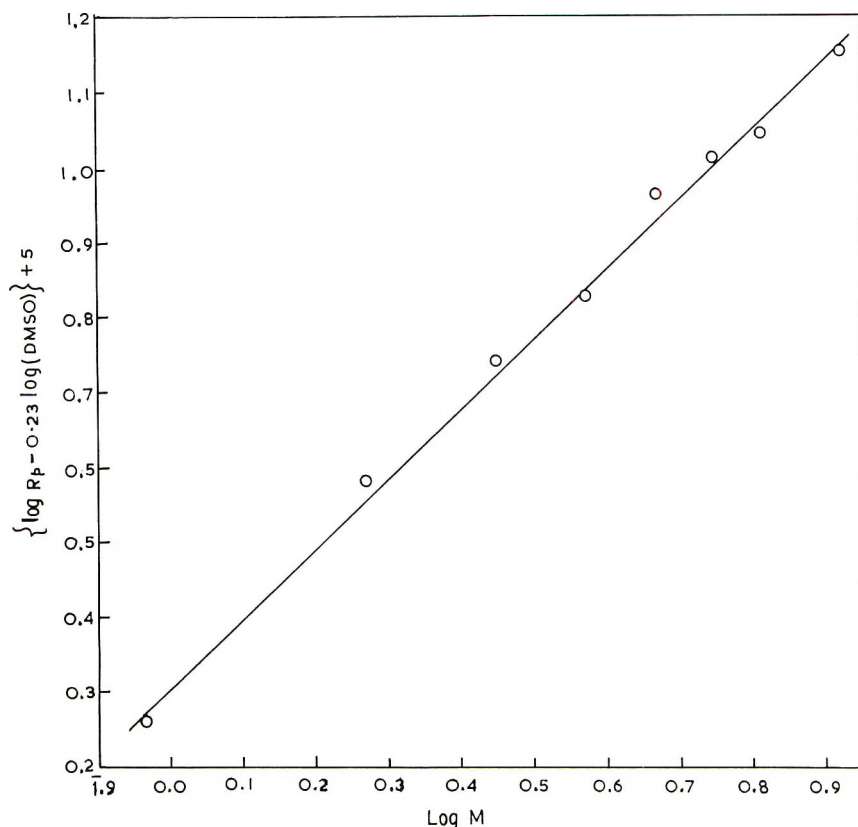


Fig. 7. Dependence of  $R_p$  on MMA concentration corrected for DMSO at fixed AIBN concentration.

also the increase of the degree of polymerization with the increase of rate of polymerization. DMSO has a higher viscosity (1.804 cP) at 30°C as compared to methyl methacrylate (0.526 cP). So it might be argued that in the presence of DMSO the termination becomes diffusion-controlled and hence the rate of polymerization as well as the degree of polymerization would increase with the increase of viscosity due to the increase in DMSO concentration. It is difficult, however, to account for the significant changes in  $R_p$  and molecular weight at low DMSO concentration where the increment in the viscosity is very small. Again DMSO was observed not to affect the  $R_p$  and molecular weight similarly if methyl methacrylate is replaced by styrene. A definite decrease in  $\delta$  is observed with increasing concentration of DMSO for methyl methacrylate but no such change was noticeable with styrene. The possibility of increased radical production due to participation of solvent in the initiation step as has been observed with halogenated benzenes<sup>14,15</sup> does not seem applicable in the present case. In such cases, the molecular weight decreases with increasing  $R_p$ . On considering all these, it seems that the effect is not due to diffusion control of



the termination; rather, the hindrance is probably the result of some interaction of DMSO with the poly(methyl methacrylate) radical. Due to the relatively active lone pair of electrons of the oxygen atom, DMSO can form a protective solvent sphere around a radical having a deficiency of negative charge due to the inductive effect of the electronegative substituents in the  $\alpha$ -position. This apparent negativity is more pronounced with methyl methacrylate and acrylonitrile than with styrene. As the radicals are thus protected from termination due to encounter with a second radical, the  $\delta$  value tends to be lower with increasing DMSO concentration.

If it is assumed that  $\delta$  and consequently  $R_p$  is a function of DMSO ( $f_n[S]$ ) concentration in the polymerization of methyl methacrylate, the rate equation may be expressed as

$$R_p = k_p[M](2k_{df}[I])^{1/2}f_n[S]$$

At constant initiator and monomer concentrations the equation can be written as

$$R_p = \text{constant } f_n[S]$$

A plot of  $\log R_p$  against  $\log [S]$  (Fig. 6) yielded a straight line of 0.23 slope.

If this treatment is valid in the polymerization of methyl methacrylate in DMSO, the correct monomer exponent could be evaluated by plotting  $(\log R_p - \log f_n[S])$  against  $\log [M]$ . A typical plot is shown in Figure 7 which is found to be linear throughout the range of monomer concentration employed. The monomer exponent is 0.95, which is very close to the theoretical value of unity.

## References

1. E. F. T. White and M. J. Zisell, *J. Polym. Sci. A*, **1**, 2189 (1963).
2. B. L. Funt and K. C. Yu, *J. Polym. Sci.*, **62**, 359 (1962).
3. A. Weissberger, Ed., *Technique of Organic Chemistry*, Vol. VII, Interscience, New York, 2nd ed., 1955.
4. N. G. Saha, U. S. Nandi, and S. R. Palit, *J. Chem. Soc.*, **1956**, 85, 427.
5. C. G. Overberger and K. Miyamichi, *J. Polym. Sci. A*, **1**, 2021 (1963).
6. T. G. Fox, *Polymer* **3**, 71 (1962).
7. A. V. Tobolsky, *J. Amer. Chem. Soc.*, **74**, 938 (1952).
8. N. G. Saha, U. S. Nandi, and S. R. Palit, *J. Chem. Soc.*, **1958**, 3, 12.
9. G. V. Schulz and E. Husemann, *Z. Physik. Chem.*, **B39**, 246 (1958).
10. J. Abere, G. Goldfinger, H. Naidus, and H. Mark, *J. Phys. Chem.*, **49**, 211 (1945).
11. C. G. Overberger, P. Fram, and T. Alfrey, *J. Polym. Sci.*, **6**, 539 (1951).
12. G. V. Schulz and G. Harborth, *Makromol. Chem.*, **1**, 106 (1947).
13. S. Basu, J. N. Sen, and S. R. Palit, *Proc. Roy. Soc. (London)*, **A202**, 485 (1950).
14. D. B. Anderson, G. M. Burnett, and A. C. Gowan, *J. Polym. Sci. A*, **1**, 1465 (1963).
15. G. M. Burnett, W. S. Daily, and J. M. Pearson, *Trans. Faraday Soc.*, **61**, 1216 (1965).

Received May 13, 1968

Revised December 4, 1969

## Comparison between Theoretical and Experimental Values of the Volume Changes Accompanying Rubber Extension

R. G. CHRISTENSEN and C. A. J. HOEVE, *Institute for Materials  
Research, National Bureau of Standards, Washington, D. C. 20234*

### Synopsis

The molecular theory of rubber elasticity assumes the free energy to consist of two parts: a liquidlike free energy that is governed by intermolecular interactions and is independent of strain at constant volume and an intramolecular interaction free energy equal to the sum of the free energies of the chains making up the network. The volume increases of rubber samples as a function of their length were found to be considerably larger than predicted by the molecular theory. Therefore, contrary to common belief, the values of  $(\partial E/\partial L)_{V,T}$  might not be related solely to changes in intramolecular interactions with extension. Also, the usual procedure to obtain values of  $(\partial E/\partial L)_{V,T}$  from measurements of  $(\partial f/\partial T)_{p,L}$  with the aid of the molecular theory is not correct.

### INTRODUCTION

For all its simplicity, the molecular theory of rubber elasticity has been remarkably successful in correlating the molecular properties of polymer chains with the stress-strain measurements on a rubberlike material.<sup>1,2</sup> Also, the theoretically calculated values of the stress-birefringence coefficient<sup>3</sup> and the degree of swelling by a solvent<sup>4</sup> are in agreement with experimental results, at least semiquantitatively. Nevertheless, important differences<sup>5-12</sup> exist between experiment and molecular theory that invite reexamination of the underlying principles of the latter. A rather bold assumption of the theory is that the free energy of the strained rubber  $\Delta F$  is given by<sup>13,14</sup>

$$\Delta F = \Delta F_{el} + \Delta F_{liq} \quad (1)$$

where  $\Delta F_{liq}$  is the free energy of interaction between chains which, as in liquids, is taken to be dependent on volume and temperature and independent of deformation at constant volume.  $\Delta F_{el}$  is the sum of the elastic free energies of the chains of the network, without taking account of interactions between them. We have for Gaussian chains<sup>13,14</sup>

$$\Delta F_{el} = \left(\frac{3}{2}\right) \nu k T \langle r^2 \rangle / \langle r^2_0 \rangle \quad (2)$$

where  $\nu$  is the number of chains,  $k$  and  $T$  are respectively Boltzmann's constant and the absolute temperature,  $\langle r^2 \rangle$  is the mean-square end-to-end distance of the polymer chains in the network, and  $\langle r^2 \rangle_0$  is the mean-square end-to-end distance of the corresponding free chains, unperturbed by excluded volume effects.

Based on eqs. (1) and (2) the following equation has been derived for the force as a function of extension<sup>13,14</sup>

$$f = (\nu kT/L_0)(V/V_0)^{2/3}(\alpha - \alpha^{-2}) \quad (3)$$

where  $f$  is the retractive force in simple extension,  $\alpha = L/L_i$ ,  $L$  and  $L_i$  are, respectively the length in the deformed and the undeformed (isotropic) state,  $V$  is the volume of the sample,  $V_0$  is the volume at which  $\langle r_i^2 \rangle = \langle r_i^2 \rangle_0$ , where  $\langle r_i^2 \rangle$  is the mean-square end-to-end distance of the chains in the isotropic network at the volume  $V$ . Although deviations from eq. (3) have been observed experimentally,<sup>5-12</sup> it is at least a first approximation.

Independent of any molecular theories, on general thermodynamic grounds, the volume change on extension of an isotropic solid for small extensions is given by<sup>15</sup>

$$\Delta V = \kappa f L / 3 \quad (4)$$

where the compressibility  $\kappa$  is given by

$$\kappa = -V^{-1}(\partial V / \partial p)_T \quad (5)$$

From thermodynamics the following expression may be derived for finite deformations

$$V^{-1}(\partial V / \partial L)_{p,T} = -\kappa_L (\partial f / \partial V)_{L,T} \quad (6)$$

where

$$\kappa_L = -V(\partial V / \partial p)_{L,T} \quad (6)$$

In order to proceed to finite deformations, a molecular theory must be used. Assuming  $\kappa_L$  to be independent of  $\alpha$ , we obtain from eqs. (3) and (6)<sup>13,16</sup>

$$\Delta V = \kappa_L \nu kT (V/V_0)^{2/3} (1 - \alpha^{-1}) \quad (8)$$

From eqs. (3) and (8) we have

$$\Delta V = \kappa_L f L (1 + \alpha + \alpha^2)^{-1} \quad (9)$$

For values of  $\alpha$  close to unity, eq. (9) reduces to eq. (4), as it should. If we determine the stress-strain relationship and take  $\kappa_L = \kappa$ , experimental and calculated values of  $\Delta V$  may be compared. Unfortunately, the volume changes to be expected are of the order of a hundredth of a per cent and are, therefore, not easily measurable. As a consequence, the error limits in the reported values<sup>17,18</sup> of  $\Delta V$  have been rather large. It is the object of this paper to report on more accurately determined volume changes and to discuss the deviation from the molecular theory.

### EXPERIMENTAL

The elastomers used were pale crepe natural (Hevea) rubber and Shell  $\delta$ 305-X11 synthetic polyisoprene. The latter is a stereospecifically polymerized polyisoprene with approximately 90% *cis* configuration. Rubber samples were compounded with approximately 3% dicumyl peroxide and cured at 140°C for 10, 15, and 40 min, in the form of sheets 15 × 15 × 0.2 cm. No antioxidants were used. Rings, approximately 3.4 cm OD and 3.0 cm ID, were cut from the sheets and stored at -30°C until used. The rings weighed 0.390-0.400 g. Additional samples of the synthetic polyisoprene were prepared by incorporating 1% by volume of small glass beads into the rubber and then curing sheets and cutting rings in the usual way. The glass beads used were approximately 40  $\mu$ m in diameter.

A drawing of the dilatometer is shown in Figure 1. The rings, usually two, were supported between a hook fixed to the top of the chamber and another one attached to a movable iron core. The rings were extended by moving the dilatometer while the iron core was held stationary by a large permanent magnet. A white background with a reference mark was affixed to the capillary near the meniscus. The positions of the rubber rings were measured with a cathetometer, to the nearest 0.01 cm. The length of a rubber ring was taken to be the distance between the inside edge at one end and the outside edge at the other. To achieve the desired sensitivity, a capillary tube of 0.0206 cm bore was used. Ordinary borosilicate glass tubing of approximately 0.1 cm wall thickness was unsuitable for the body of the dilatometer, since it was subject to sufficient deformation during manipulation of the dilatometer to cause appreciable errors. Accordingly, borosilicate boiler-gage tubing of approximately 0.2 cm wall thickness was adopted. A test with the rubber rings replaced by a coil spring showed that no significant deformation of the dilatometer occurred. The dilatometer was made ready by assembling the rings and iron core within the body, sealing off the bottom, and filling by alternately applying suction and allowing distilled water to flow in through the capillary. Residual air bubbles were expelled by warming the dilatometer. Since a dilatometer of this construction is very sensitive to temperature changes the apparatus was immersed in a water bath near 30°C. Monitoring the temperature with a thermistor bridge showed temperature variations to be less than 0.001°C during the course of an experiment.

Stress-strain curves for the samples were measured by suspending weights from the rings and measuring the lengths with a cathetometer. No difference was noted between rings cut from the same sheet. In some cases, the rings were suspended from calibrated springs in the dilatometer, and the tension was measured during the course of the experiment.

Compressibilities of some of the samples were measured by applying pressures up to three atmospheres to the top of the capillary and noting the resulting change in level. Pressures were measured with a mercury manometer. Owing to the deformation of the body of the dilatometer, this method will give only differences in compressibility. It was suitable to determine possible changes in compressibility with extension of both the

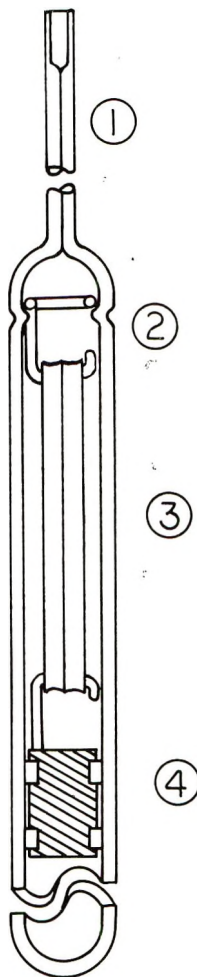


Fig. 1. Construction of dilatometer: (1) capillary 0.0206 cm bore; (2) supporting hook; (3) bands; (4) iron core with TFE bushings.

filled and unfilled rings as well as compressibilities of mixtures of xylene and rubber.

Measurements of the volume change on elongation were also made with the dilatometer under a pressure of up to 20 atm. The pressure was applied to the dilatometer by admitting nitrogen from a cylinder to a ballast tank (another cylinder) which was connected to the dilatometer by a spiral of copper tubing. This allowed free movement of the dilatometer while under pressure. The copper tubing was connected to the capillary with a Swagelok fitting, the ferrules bearing against the glass being of nylon. The meniscus was adjusted by raising the pressure nearly to the desired value and removing the excess liquid from the top to the capillary with a magnetically actuated wick.

### Results and Discussion

The observed volume changes are plotted in Figures 2-5. The force-length data for one ring of each type are given in Table I. The dotted lines

TABLE I  
Force-Length Measurements

10 min cure		15 min cure, swollen		40 min cure	
Length, cm	Force, $N \times 10^{-8}$	Length, cm	Force, $N \times 10^{-8}$	Length, cm	Force, $N \times 10^{-8}$
4.90	0	6.30	0	4.90	0
5.37	51	6.80	26	5.12	51
5.85	100	7.43	48	5.50	100
6.44	149	8.08	79	5.88	149
7.14	198	8.85	107	6.32	198
8.07	247	9.59	132	7.37	296
9.29	296	10.40	151	8.79	394
10.25	345	11.17	174	10.50	492
		11.95	187	12.42	590
		12.81	205		

are calculated with the aid of eq. (9), the data of Table I and the value<sup>19</sup>  $\kappa = \kappa_L = 5.15 \times 10^{-6} \text{ cm}^2/\text{N}$ . The value of  $\kappa$  for the rubber swollen with xylene (Fig. 4) was determined to be  $6.9 \times 10^{-6} \text{ cm}^2/\text{N}$ . This is close to the weighted average of the compressibilities of the components, taking the compressibility of xylene to be  $8.7 \times 10^{-6} \text{ cm}^2/\text{N}$ . We observe that within experimental error the initial calculated and experimental slopes are equal

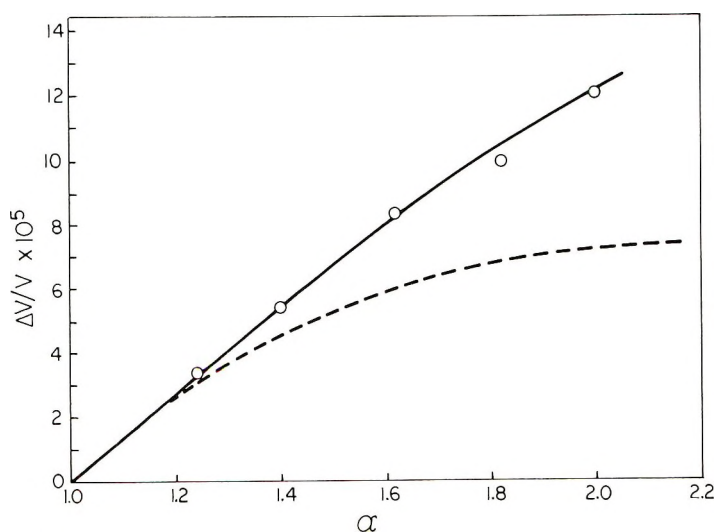


Fig. 2. Dilation of polyisoprene bands cured 10 min compared to calculated dilation as a function of  $\alpha$ . The dotted line is calculated according to eq. (9) by using data of Table I.

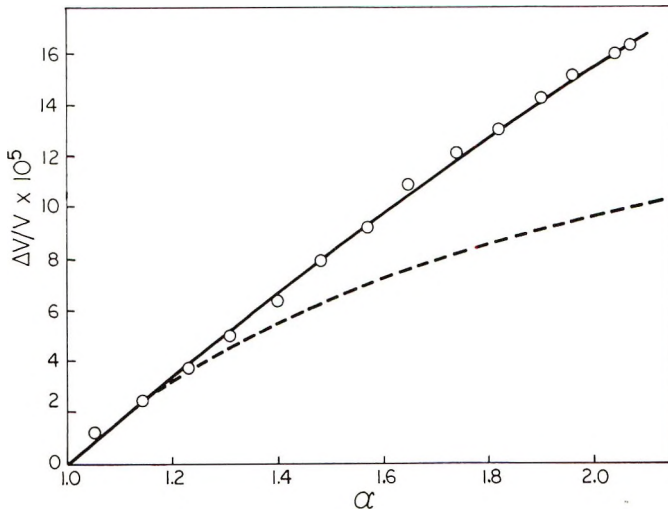


Fig. 3. Dilation of natural rubber bands cured 40 min compared to calculated dilation as a function of  $\alpha$ . The dotted line is calculated according to eq. (9) by using data of Table I.

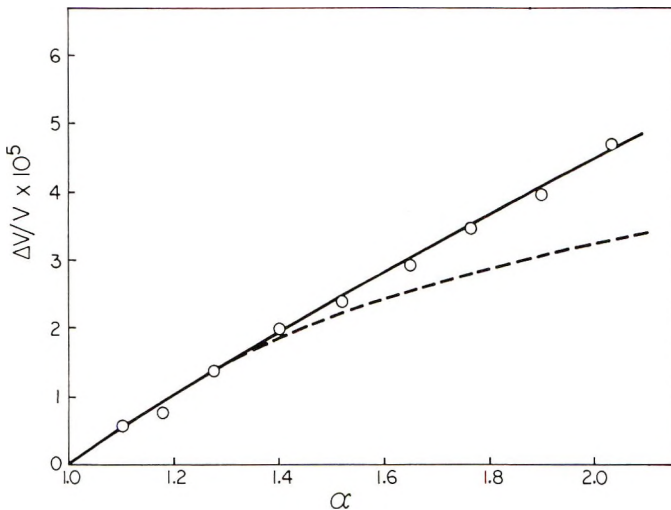


Fig. 4. Dilation as a function of  $\alpha$  for natural rubber bands cured 15 min and swollen with xylene to 212% of the original volume. The dotted line is calculated according to eq. (9) and Table I.

for all cases, except for the experiments corresponding to the open circles shown in Figure 5, which will be discussed below. It is apparent, however, that in all cases sizeable differences between experimental and theoretical results occur for higher extension. A critical examination of possible systematic experimental error is therefore in order.

The first possibility is that on extension vacuoles are formed; the apparent volume changes would then be too high. Indeed, in rubber filled with

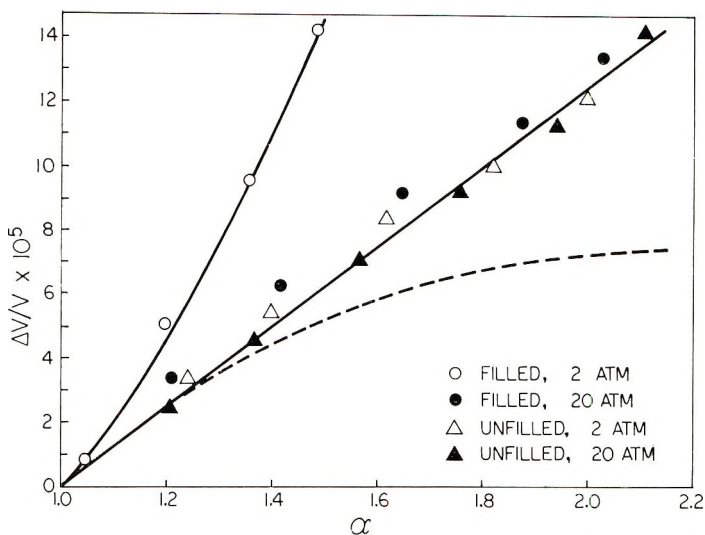


Fig. 5. Dilation as a function of  $\alpha$  for filled polyisoprene and unfilled natural rubber bands both cured for 10 min. The dotted line is calculated according to eq. (9) and Table I.

particles this effect is known to occur.<sup>20</sup> The curve with the open circles in Figure 5 for the sample filled with glass beads shows that already the initial slope deviates from the calculated value. This result confirms that on extension vacuoles are formed around the glass beads. Under the pressure of 20 atm, however, these vacuoles apparently disappear, since the same results are obtained for filled and unfilled rubber (respectively, filled circles and filled triangles in Fig. 5). In addition, these measurements are indistinguishable from those for the unfilled rubber at 2 atm. Moreover, the synthetic rubber, which is unlikely to contain the same kind of insoluble impurities as natural rubber, displays the same deviations within experimental error (Figs. 2 and 5).

A second, less likely, possibility is that on extension of the rubber a residual amount of protein may absorb some of the water used as a confining liquid. The amount of absorption could depend on extension and could then cause erroneous volume measurements. As we have remarked, however, the observed initial slopes are in accordance with theory. Furthermore, the results for synthetic and natural rubber agree (Figs. 2 and 5), whereas the former certainly contains less protein and is therefore expected to swell much less.

A third possibility is that equilibrium values may not have been obtained experimentally. Although this possibility cannot be discounted completely, we have observed that, in contrast to stress-strain measurements, volume-length measurements do not display hysteresis effects within experimental error. It is known that hysteresis effects in the stress-strain curve can be greatly suppressed by swelling of the sample.<sup>5,8,9,12</sup> The re-



sults so obtained are then believed<sup>12</sup> to be closer to the equilibrium values than those obtained for the dry state. We see in Figure 4, however, that for the volume-length measurements the deviations between theory and experiment persist at a swelling ratio of 2.12. Nevertheless, if both types of measurements would result in deviations from theory merely because of failure to attain equilibrium, these deviations would be expected to be at least of the same sign. Corresponding to a positive  $C_2$  term,<sup>6-12</sup> the experimentally determined stress-strain curve is, however, more concave, whereas according to Figures 2-5 the volume-length curve is less concave than the molecular theory predicts. We conclude that failure to attain equilibrium can not be the sole cause of both types of deviations.

It is possible that, contrary to our assumption,  $\kappa_L$  is not constant but increases with extension. Bianchi and Pedemonte<sup>21</sup> have indeed reported that  $\alpha_L \kappa_L^{-1}$  is dependent on length, where  $\alpha_L = V^{-1}(\partial V/\partial T)_{p,L}$ . This result suggests that  $\kappa_L$  is dependent on length, since Allen et al.<sup>22</sup> found no dependence of  $\alpha_L$  on  $L$ . Our measurements of the compressibility measured in the dilatometer between 0 and 3 atmospheres show, however, that to within 3%  $\kappa_L$  is independent of  $L$  for values of  $\alpha$  up to 2.

Allen et al.<sup>22</sup> measured  $(\partial f/\partial p)_{L,T}$  and reported it to be essentially in agreement with theory. According to thermodynamics this derivation equals  $(\partial V/\partial L)_{p,T}$ , which we found not to be in agreement with theory. In view of the difference in experimental procedures and also the rather large errors in the measurements by Allen et al.,<sup>22</sup> a comparison is difficult, however. Our results are in better agreement with other measurements<sup>17,18</sup> of  $(\partial V/\partial L)_{p,T}$ , but again, the experimental errors were large.

Results similar to ours for volume changes on rubber extension have been observed recently.<sup>23</sup>

We conclude from our results that the theoretical and measured volume-length relationships are at variance. At present we can only surmise how the theory should be revised. The assumption underlying the additivity of elastic and liquidlike free energies, given by eq. (1) is quite drastic. The chains are almost certainly not as unrestricted in the network as assumed. It is possible, therefore, that an additional free-energy term is required in eq. (1). Recently a modification of the elasticity equation was proposed by Tobolsky and Shen.<sup>24</sup> They introduced an *ad hoc* volume-dependent function in the term derived from the molecular theory [eq. (2)]. Better agreement between theory and experiment may be obtained by adjusting  $\gamma$ , the extra parameter introduced. It is difficult to see, however, how this parameter is to be related to a molecular theory.

Currently a wide interest<sup>1,2</sup> exists in measurements of  $f_e = (\partial E/\partial L)_{v,T}$ , the change in internal energy on deformation of rubber-like networks. Its value may be obtained from stress-temperature measurements according to the equation

$$f = f_e + T(\partial f/\partial T)_{v,L} \quad (10)$$

Also, in accordance with the spirit of eq. (1),  $f_e$  has been widely interpreted

as being determined solely by intramolecular interactions in network chains. In the light of the results obtained here, this may be true to a first approximation only.

Whatever its molecular interpretation,  $f_e$  is usually not obtained directly, since the last term on the right-hand side of eq. (10) cannot easily be measured. Instead  $(\partial f/\partial T)_{p,L}$  is usually measured and the resulting value is corrected for the effect of volume changes with the aid of the molecular theory as follows. We have the thermodynamic relation

$$(\partial f/\partial T)_{v,L} = (\partial f/\partial T)_{p,L} + \alpha_L^{-1} \alpha_L (\partial V/\partial L)_{p,T} \quad (11)$$

With the aid of the molecular theory we have from eqs. (9) and (11)

$$(\partial f/\partial T)_{v,L} = (\partial f/\partial T)_{p,L} + \alpha_L f / (\alpha^3 - 1) \quad (12)$$

Since the experimentally determined values of  $(\partial V/\partial L)_{p,T}$  are larger than given by eq. (9) the (positive) second term on the right-hand side of eq. (12) underestimates the correction term. Therefore, the values for  $f_e$  obtained from stress-temperature measurements at constant pressure and application of eqs. (10) and (12) should be reduced. By taking  $\alpha_L$  to be equal to the thermal expansion coefficient of natural rubber<sup>19</sup> of  $6.45 \times 10^{-4}$  degree<sup>-1</sup>, and by taking the measured slope of our volume-length curves at  $\alpha = 2$ , we calculate for  $f_e/f$  from eq. (11) the value of 0.06, whereas from eq. (12) the value of 0.13 has been obtained.<sup>1,2</sup>

Certain commercial equipment, instruments, or materials are identified in this paper in order to adequately specify the experimental procedure. In no case does such identification imply recommendation or endorsement by the National Bureau of Standards, nor does it imply that the material or equipment identified is necessarily the best available for the purpose.

## References

1. T. M. Birshtein and O. B. Ptitsyn, *Conformations of Macromolecules*, Interscience, New York, 1966, Chap. 8.
2. P. J. Flory, *Statistical Mechanics of Chain Molecules*, Interscience, New York, 1968, Chap. 2.
3. L. R. G. Treloar, *The Physics of Rubber Elasticity*, 2nd ed., Oxford Univ. Press, London, 1958, Chap. 4.
4. P. J. Flory, *Principles of Polymer Chemistry*, Cornell Univ. Press, Ithaca, N. Y. 1953, Chap. 13.
5. G. Gee, *Trans. Faraday Soc.*, **42**, 585 (1946).
6. M. Mooney, *J. Appl. Phys.*, **11**, 582 (1940).
7. R. S. Rivlin, *Phil. Trans.*, **A240**, 459 (1948).
8. S. M. Gumbrell, L. Mullins, and R. S. Rivlin, *Trans. Faraday Soc.*, **49**, 1495 (1953).
9. L. Mullins, *J. Appl. Polym. Sci.*, **2**, 257 (1959).
10. R. J. Roe and W. R. Krigbaum, *J. Polym. Sci.*, **61**, 167 (1962).
11. K. J. Smith, Jr., A. Greene, and A. Ciferri, *Kolloid Z.*, **194**, 49 (1964).
12. J. E. Mark and P. J. Flory, *J. Appl. Phys.*, **37**, 4635 (1966).
13. P. J. Flory, *Trans. Faraday Soc.*, **57**, 829 (1961).
14. M. V. Volkenstein, *Configurational Statistics of Polymeric Chains*, Interscience, New York, 1962, Chap. 8.

15. F. D. Murnaghan, *Finite Deformation of an Elastic Solid*, Wiley, New York, 1951, Chap. 4.
16. T. N. Khasanovich, *J. Appl. Phys.*, **30**, 948 (1959).
17. G. Gee, J. Stern, and L. R. G. Treloar, *Trans. Faraday Soc.*, **46**, 1101 (1950).
18. F. G. Hewitt and R. L. Anthony, *J. Appl. Phys.*, **29**, 1411 (1958).
19. L. A. Wood and G. M. Martin, *J. Res. Nat. Bur. Stand.*, **68A**, 259 (1964).
20. T. L. Smith, *Trans. Soc. Rheol.*, **2**, 113 (1959).
21. U. Bianchi and E. Pedemonte, *J. Polym. Sci. A*, **2**, 5039 (1964).
22. G. Allen, U. Bianchi, and C. Price, *Trans. Faraday Soc.* **59**, 2493 (1963).
23. R. W. Penn, *Trans. Soc. Rheol.*, to be published.

Received August 21, 1969

Revised December 11, 1969

## Chain Transfer in Ethylene Polymerization. IV. Additional Study at 1360 Atm and 130°C

GEORGE A. MORTIMER, *Hydrocarbons and Polymers Division,  
Monsanto Company, Texas City, Texas 77591*

### Synopsis

The previously reported chain-transfer studies were extended to include chain transfer to esters, amides, amines, phosphines, and other compounds containing functional groups. Phosphines are very reactive, amines are moderately reactive, and amides and esters are quite unreactive. Most other functional groups give moderate reactivity. Halogens and compounds containing a nitrogen-oxygen bond were all found to be inhibitors for ethylene polymerization.

### INTRODUCTION

In a previous publication on chain transfer in ethylene polymerization, the effects of the molecular structure and certain functional groups on a compound's proclivity to undergo transfer reactions were investigated.<sup>1</sup> In this paper, these topics are considered further. In particular, some functional groupings which were not thoroughly examined or not studied at all will be covered in more detail. Also, in preparation for subsequent work on the effects of pressure and temperature on the chain-transfer reaction, additional data were obtained on some of the transfer agents studied previously. These additional data and the chain-transfer constants recalculated by our improved method<sup>2</sup> are included herein for completeness.

Several compounds were screened which were found to have an inhibiting or severe retarding effect. These will also be mentioned.

### EXPERIMENTAL

All experiments were carried out in system 2 by the procedures previously described.<sup>1,2</sup> The chain-transfer data are given in Table I along with the newly calculated<sup>2</sup> chain-transfer constants,  $C_s$ .

The inhibitors or retarders allowed essentially no polymerization to take place when they were present in concentrations typical for chain-transfer agents. These data are given in Table II.

### DISCUSSION

In general, the reactivity of transfer agents in ethylene polymerization parallels their reactivity in hydrogen abstraction reactions in the liquid

TABLE I  
Chain-Transfer Data at 1360 atm, 130°C

Transfer agent	$C_s$	Feed composition, mole-% <sup>a</sup>			Melt index	$1/\bar{P}$ $\times 10^4$	Polymer- ization rate, % conversion/hr
		Ethylene	Propane	Transfer agent			
Methyl acetate	0.0031 ± 0.0004	81.86 "	14.43 "	3.56 "	3.31 3.66	8.65 8.75	9.3 10.4
<i>tert</i> -Butyl acetate	0.0040 ± 0.0005	82.78 "	" "	2.63 "	2.37 3.71	8.33 8.76	9.7 7.7
Methyl formate	0.0042 ± 0.0005	84.81 82.74 "	14.27 14.43 "	0.76 2.67 "	0.820 4.51 2.26	7.47 8.96 8.29	10.0 8.7 6.8
Ethyl acetate	0.0045 ± 0.0003	84.27 84.21 83.03 81.08 "	14.37 14.43 " " "	1.20 " 2.41 4.34 "	1.06 0.950 2.82 8.62 11.0	7.66 7.58 8.50 9.70 10.0	8.8 10.7 10.7 9.0 8.0
Triphenylphosphine	0.005 ± 0.002	84.44 81.77 81.72	14.37 " 14.43	0.18 0.65 "	0.513 0.717 1.71	7.14 7.37 8.05	6.5 3.4 5.0
Methylamine	0.0053 ± 0.0005	83.17 83.14 83.12	" " "	2.22 2.28 2.30	2.51 3.55 4.49	8.39 8.72 8.96	9.9 3.2 <sup>b</sup> 2.6 <sup>b</sup>
Methyl benzoate	0.0053 ± 0.0005	82.60 "	" "	2.82 "	5.58 4.85	9.19 9.04	3.0 2.4

Ethyl benzoate	0.0055 ± 0.0006	83.60	"	1.82	2.34	8.32	3.9
		82.94	"	2.48	4.55	8.97	3.2
<i>N,N</i> -Disopropyl- acetamide	0.0057 ± 0.0006	85.12	"	0.30	1.17	7.74	9.1
		83.64	"	1.77	2.78	8.48	6.8
		"	"	"	2.17	8.25	5.2 <sup>b</sup>
		"	"	"	2.06	8.21	2.9 <sup>b</sup>
		"	"	"	3.82	8.79	3.3 <sup>b</sup>
<i>N</i> -Methylacetamide	0.0061 ± 0.0005	82.74	"	2.03	4.69	9.01	9.7
		80.31	"	2.81	6.11	9.30	7.6
		"	"	"	5.52	9.18	9.3
		81.59	"	3.82	19.0	10.8	6.2
Isobutane	0.0072 ± 0.0003	81.40	"	4.01	13.2	10.3	6.9
		80.00	"	5.42	55.7	12.7	7.0
		81.40	"	4.02	8.73	9.72	11.9
Dimethoxymethane	0.0073 ± 0.0003	"	"	"	30.9	11.6	7.7
		"	"	"	32.8	11.7	8.3
Ethanol	0.0075 ± 0.0003	80.98	"	4.44	31.2	11.6	8.7
		"	"	"	28.3	11.4	8.9
<i>n</i> -Butyl acetate	0.0089 ± 0.0007	83.63	"	1.79	5.22	9.12	10.9
		"	"	"	5.27	9.13	10.2
		81.76	17.10	0.98	5.24	9.13	12.2
Cyclohexane	0.0095 ± 0.0003 <sup>s</sup>	"	"	"	6.13	9.30	11.5
		81.44	"	1.31	8.62	9.70	9.4
		"	"	"	8.71	9.72	8.8
<i>N</i> -Ethylacetamide	0.0115 ± 0.0006	84.14	14.43	1.27	5.49	9.18	9.2
		83.38	"	2.04	15.6	10.5	5.5 <sup>b</sup>
		"	"	"	7.65	9.56	12.2
		"	"	"	10.7	9.97	12.0
Propylene	0.0122 ± 0.0008	83.74	"	1.68	8.72	9.72	3.3
		"	"	"	8.04	9.62	5.1

(continued)

TABLE I (continued)

Transfer agent	$C_s$	Feed composition, mole-% <sup>a</sup>			Melt index	$1/\bar{P}$ $\times 10^4$	Polymer- ization rate, % conversion/hr
		Ethylene	Propane	Transfer agent			
<i>N,N</i> -Diethylacetamide	0.0125 $\pm$ 0.0006	84.75	"	0.66	3.70	8.76	12.9
		84.09	"	1.32	8.22	9.64	10.1
		82.87	"	2.55	21.0	10.9	9.4
		"	"	"	21.0	10.9	9.7
Cyclopentane	0.0126 $\pm$ 0.0005 <sup>e</sup>	83.67	14.43	1.75	12.7	10.2	5.9
	0.0130 $\pm$ 0.0005	83.78	14.32	"	10.5	9.96	6.3
Acetic anhydride		81.67	14.43	3.74	69.3	13.2	8.8
		84.49	"	0.93	3.37	8.67	4.7
<i>n</i> -Butyl benzoate	0.014 $\pm$ 0.001	"	"	"	3.62	8.74	4.2
		82.95	"	2.46	31.7	11.6	9.1
Isopropanol	0.0144 $\pm$ 0.0005	"	"	"	28.5	11.4	10.4
		83.20	"	2.21	32.2	11.7	5.6
Toluene	0.0154 $\pm$ 0.0005	"	"	"	22.6	11.1	5.6
		"	"	"	27.0	11.3	7.1
Hydrogen	0.0159 $\pm$ 0.0008 <sup>e</sup>						
	0.0168 $\pm$ 0.0005 <sup>e</sup>						
Acetone	0.0175 $\pm$ 0.0008	83.80	14.43	1.64	18.4	10.7	3.8
		"	"	"	16.1	10.5	3.5
4,4-Dimethylpentene-1		84.14	"	1.28	11.1	10.0	12.5
		"	"	"	17.8	10.7	6.3 <sup>b</sup>
<i>N,N</i> -Dimethylacetamide	0.0182 $\pm$ 0.0005	83.89	"	1.53	10.8	9.98	10.8
		"	"	"	11.3	10.2	11.3
		81.59	"	3.83	184.	15.9	13.0

<i>n</i> -Butyl isocyanate	0.0212 ± 0.0007	85.21	"	0.20	1.64	8.01	5.4
		84.80	"	0.61	3.59	8.64	8.7
		83.38	"	2.04	46.3	12.3	8.2
Methyl butyrate	0.022 ± 0.001	"	"	"	49.6	12.5	6.9
		84.17	"	1.25	13.5	10.3	8.8
		"	"	"	17.0	10.6	10.9
<i>n</i> -Butylamine	0.022 ± 0.004	85.18	"	0.24	0.899	7.54	6.1 <sup>b</sup>
		85.06	"	0.36	1.59	7.99	7.0 <sup>b</sup>
		"	"	"	2.23	8.28	4.8 <sup>b</sup>
Diethyl sulfide	0.027 ± 0.004	85.36	"	0.055	0.636	7.29	9.0
		84.98	"	0.44	2.89	8.52	9.7
Tetrahydrofuran 4-Methylpentene-1	0.0288 ± 0.0006 <sup>c</sup>	85.04	"	0.37	2.03	8.20	5.5
	0.031 ± 0.003	"	"	"	5.04	9.08	5.0
<i>p</i> -Xylene	0.0317 ± 0.0009 <sup>c</sup>	85.15	14.32	"	1.82	8.10	5.0
		82.46	17.10	0.29	5.47	9.17	10.3
		"	"	"	6.07	9.29	10.4
		82.36	"	0.38	8.10	9.63	9.6
	"	"	"	"	8.57	10.2	

(continued)



TABLE I (continued)

Transfer agent	$C_s$	Feed composition, mole-% <sup>a</sup>			Melt index	$1/\bar{P}$ $\times 10^4$	Polymer- ization rate, %/hr
		Ethylene	Propane	Transfer agent			
Trimethylamine	0.033 $\pm$ 0.001 <sup>c</sup>	85.37	14.43	0.044	0.543	7.18	7.2
		85.30	"	0.12	0.667	7.32	7.7
		82.60	"	2.82	475.	19.8	6.9
Butene-2	0.038 $\pm$ 0.004	85.25	"	0.19	1.19	7.75	4.6
		85.09	"	0.32	3.65	8.75	3.2
		85.07	"	0.34	3.36	8.67	4.7
1-Bromo-2-chloroethane	0.039 $\pm$ 0.002	85.14	"	0.28	2.56	8.41	7.5
		84.86	"	0.55	8.72	9.72	8.9
		"	"	"	8.47	9.68	8.8
Butene-1	0.047 $\pm$ 0.002 <sup>c</sup>	84.84	14.43	0.58	16.4	10.6	7.3
		"	"	"	16.7	10.6	7.0
Ethylbenzene	0.052 $\pm$ 0.002 <sup>c</sup>	"	"	"	16.4	10.6	5.9
		85.22	14.43	0.20	6.09	9.29	7.3
		"	"	"	3.57	8.73	10.1
Butanone	0.060 $\pm$ 0.005 <sup>c</sup>	83.46	"	1.96	1050.	24.9	3.1
		85.08	"	0.34	12.9	10.2	8.9
		"	"	"	13.4	10.3	8.6
<i>n</i> -Butyl isothiocyanate	0.075 $\pm$ 0.001	84.74	"	0.68	75.1	13.5	5.6
		85.32	"	0.10	1.66	8.02	9.5
		"	"	"	2.08	8.22	8.9
Methyl 3-cyano- propionate	0.079 $\pm$ 0.002	85.12	"	0.30	12.4	10.2	4.8 <sup>b</sup>
		"	"	"	8.98	9.75	6.1 <sup>b</sup>
		0.082 $\pm$ 0.004	"	"	"	"	"
Tri- <i>n</i> -butylamine	0.082 $\pm$ 0.004	85.12	"	0.30	12.4	10.2	4.8 <sup>b</sup>
		"	"	"	8.98	9.75	6.1 <sup>b</sup>
		"	"	"	"	"	"

Di- <i>n</i> -butylamine	0.107 ± 0.005	85.28 85.14 " "	" " " "	0.14 0.28 " "	4.07 16.8 24.0 13.3	8.86 10.6 11.2 10.3	7.8 3.6 <sup>b</sup> 1.5 <sup>b</sup> 4.4 <sup>b</sup>
Methyl chloroacetate	0.112 ± 0.005	85.20 85.15 "	14.37 14.43 "	0.27 " "	15.3 19.6 28.7	10.8 10.5 11.5	7.8 5.7 6.1
1,2-Dibromoethane	0.125 ± 0.004	85.25 84.98 85.44	14.32 " "	" " "	15.8 154. 27.2	10.5 15.3 11.4	8.9 2.5 3.0
1,4-Dichlorobutene-2	0.41 ± 0.01	85.31 85.46 85.32	14.43 14.37 14.43	0.11 0.010 0.096	48.7 0.711 32.0	12.4 7.37 11.6	2.7 9.9 11.0
Tri- <i>n</i> -butylphosphine	0.45 ± 0.02	" 85.36 85.35 85.40	" " " "	" 0.053 0.067 0.012	55.8 35.6 39.0 2.64	12.7 11.8 12.0 8.43	11.1 9.5 11.4 8.1
Methyl cyanoacetate	0.67 ± 0.02	" 85.51	" 14.32	" "	2.07 1.61	8.21 8.00	9.1 7.6
Bromotrichloromethane	1.0 ± 0.1	85.40 85.39	14.43 "	0.013 0.025	6.17 82.0 265.	9.31 13.6 17.2	11.2 10.5 10.2
Di- <i>n</i> -butylphosphine	3.6 ± 0.1						

<sup>a</sup> The balance of the feed, usually less than 0.2%, was benzene used as the initiator solvent.

<sup>b</sup> All rates were calculated from the grams of polymer isolated divided by the run time. In this run, there was evidence from the performance of the pump which maintained constant pressure that there was an induction period followed by a normal rate.

<sup>c</sup> In addition to the runs tabulated here, all applicable runs (system 2) given in references 1 and 10 were also included in the calculations.

TABLE II  
Summary of Data on Inhibitors

Compound	Lowest concentration used, mole-%
<i>N,N</i> -Diethylhydroxylamine	0.099
2-Nitro-2-methylpropane	2.04
1-Nitropropane	0.80
Nitrobenzene	1.82
Isoamyl nitrite	0.18
Nitrogen trioxide (N <sub>2</sub> O <sub>3</sub> )	0.031
Nitrosyl chloride	0.16
Chlorine	0.36
Iodine	0.0004
Furfural	0.14
1,4-Cyclohexadiene	0.025

phase, as might be expected.<sup>3</sup> The details in ethylene polymerization follow.

The amines studied seemed to have little or no effect on polymerization rate although ammonia itself is a retarder.<sup>4,5</sup> However, they did give long induction periods unless redistilled in vacuum under nitrogen. The water-white, oxygen-free distillates either gave no induction period or a short one. Apparently, an oxidation product of the amines is an inhibitor.

The chain-transfer activity of amines was found to be secondary > tertiary > primary > ammonia. Tertiary amines obviously transfer at a C—H bond. The C—H bond alpha to an amino nitrogen atom is activated. Secondary amines have a very reactive N—H bond which reacts in addition to the C—H bonds.<sup>6</sup> The N—H bonds in primary amines are much less reactive, so most transfer is with the hydrogen atoms alpha to the amine function.<sup>7,8</sup> It is the peculiarly high activity of the secondary N—H bond which is responsible for the high reactivity of secondary amines.

The phosphorus analogs of amines show quite a different behavior. Their reactivity order is phosphine<sup>9</sup> > secondary > phosphite > tertiary. No primary phosphines were studied. From the data at hand, it is seen that the P—H bond is more reactive than C—H bonds alpha to phosphorus, although the latter are obviously activated. The presence of oxygen on phosphorus decreases the activity of the P—H bond somewhat, but dimethyl phosphite is still a very reactive transfer agent. None of the phosphorus derivatives studied had any effect on polymerization rate: they all behaved as true chain-transfer agents.

By contrast, the unreactivity of esters and amides is truly noteworthy. They may be thought of as a structural combination of a carbonyl group and either an ether (or alcohol) linkage or amine linkage, respectively. All of these functional groups are known to activate C—H bonds alpha to them. However, amides, and more particularly esters, do not show much enhanced activity over hydrocarbons.<sup>3</sup> In fact, methyl acetate and ethyl acetate are of about the same reactivity as propane and butane, respectively.

The data for amides, which are somewhat more reactive than esters, do not present a clear picture. For the monosubstituted amides, the order of reactivity is  $C_2H_5NH > CH_3NH$ , as expected. From the low level of reactivity, it appears that the amide N—H bond is relatively unreactive.<sup>11</sup> However, for the disubstituted amides the opposite order of reactivity was found:  $(CH_3)_2N > (C_2H_5)_2N > [(CH_3)_2CH]_2N$ , and  $[(CH_3)_2CH]_2N \simeq CH_3NH$  and  $(C_2H_5)_2N \simeq C_2H_5NH$ . When these surprising results were first obtained, the amides were carefully repurified and rerun. The results were unchanged. Perhaps steric factors, which have been observed before for branched hydrocarbons,<sup>1</sup> play an important role in shielding disubstituted amides from attack, especially when the substituent itself is branched.

Returning to esters, for which more complete data are available, it appears that attaching  $\begin{array}{l} \diagup \\ \text{C}=\text{O} \\ \diagdown \end{array}$  and —O— functions together destroys much of the activating influence of each on adjacent C—H bonds.<sup>3</sup> This result may be rationalized as a manifestation of the fact that any delocalization of the odd electron involves creation of a dipole. Apparently, in esters, delocalization of the odd electron onto oxygen is opposed by the presence of the other strongly electron-withdrawing oxygen. In other words, the dipole already existing in the ester function is oppositely oriented to the dipole for delocalizing the odd electron. On the other hand, the data on benzoate esters suggests that the carbalkoxy group activates aromatic ring hydrogens where a different electron delocalization opportunity exists.

One sample each of a sulfide, an isocyanate, and an isothiocyanate were studied. Comparing oxygen and sulfur analogs, it was noted that the sulfur analogs are the more reactive.<sup>12</sup>

Several brominated compounds were studied. It is clear that bromine is a more effective activating group than chlorine.

Several compounds were studied in which one or more C—H bonds were alpha to two activating groups. Behavior ranged from no apparent extra activation due to the second group (dimethoxymethane<sup>13</sup>) to a manifold increase in reactivity (methyl cyanoacetate). Due to this range of behavior, no general rule for predicting the behavior could be formulated from the few samples studied.

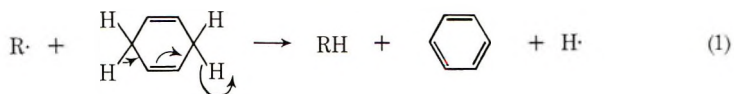
The inhibition results in Table II deserve some comment. No or essentially no polymerization took place at the concentration of reactant shown in the table. It was not possible to tell whether a trace of polymer was formed or not, so no distinction could be made between strong retarders and inhibitors. All are classified as inhibitors in this discussion.

Inasmuch as it is well known that NO and NO<sub>2</sub> are radical traps, it is not surprising to find that N<sub>2</sub>O<sub>3</sub> and NOCl are inhibitors. Nitrite esters can decompose to give NO, and this may be why they inhibit. Since nitro groups are known to be effective electron delocalizing groups, it is not too surprising to discover that nitro alkanes and aranes also do not permit polymerization to take place.

The results with iodine are particularly interesting. With the use of our standard polymerization technique, no polymerization could be detected with as little as 4 ppm iodine in the reaction feed.

Furfural was also an inhibitor. The furfural used had been specially purified and carefully redistilled under nitrogen prior to use. It is therefore unlikely that inhibition was due to oxidation products which are normally present as impurities.

1,4-Cyclohexadiene was also found to be an inhibitor. It had been thought that it might react with the growing polyethylene chain according to eq. (1), where  $R\cdot$  represents the growing polyethylene chain. It was considered that the driving force to form benzene plus the high reactivity of doubly allylic hydrogen atoms would cause cyclohexadiene to undergo the reaction shown in eq. (1), which, might make it extremely reactive. Apparently, this reaction did not take place. The reaction of hydrogen itself, as a transfer agent which shows no detectable retarding effect, is evidence that hydrogen atoms are quite efficient in regenerating new polyethylene chains. Had eq. (1) taken place, no inhibition should have resulted.



After this work had been completed, James and Stuart showed that the cyclohexadienyl radical is quite stable unless attacked by another free radical.<sup>14</sup> Thus, chain transfer to 1,4-cyclohexadiene produces a radical whose only reaction is termination.

In calculating chain-transfer constants when the transfer agent causes a rate reduction, the question of the need for a rate correction in the chain-transfer expression must be examined. This question was previously examined,<sup>1,15</sup> resulting in the conclusion that the correction would be of the order of 1% in  $1/\bar{P}$  for the most serious rate reduction experienced in Table I data. This conclusion was based on fairly well-established kinetic parameters which predict that, if there were no other molecular weight controlling reactions than combination termination,  $1/\bar{P}_0$  would be roughly  $5 \times 10^{-6}$ , or the limiting molecular weight would be roughly 5,600,000 at the conditions used in the experiments reported here. Thus, any correction required in the rate-controlled portion of  $1/\bar{P}_0$  would be approximately two orders of magnitude smaller than the  $1/\bar{P}$  values given in Table I.

However, the actual  $1/\bar{P}_0$  is not  $5 \times 10^{-6}$ , but  $2 \times 10^{-4}$  for these conditions.<sup>2</sup> Since chain transfer to monomer is known to be low<sup>1</sup> and that to initiator is probably low, the apparent discrepancy may be disturbing at first glance to those unfamiliar with the details of ethylene polymerization. The reaction which limits the maximum molecular weight in ethylene polymerization is spontaneous decomposition of a branched radical, or so-called  $\beta$ -elimination.<sup>15-18</sup> This reaction has the mathematical formalism of chain transfer to monomer, but generates vinylidene end groups rather than vinyl

endgroups. This reaction, like chain transfer, is unaffected by reaction rate. Thus,  $1/\bar{P}_0$  can be near  $1/\bar{P}$  and still not require a rate correction, a situation not found with more conventional monomers.

A limiting  $1/\bar{P}_0$  of  $1 \times 10^{-4}$  for ethylene polymerization in the absence of propane at 140°C and 1600–1800 atm has been reported.<sup>15</sup> Indeed, we have repeated this observation at our conditions with propane absent. However, since the system is heterogeneous under these conditions, the  $1 \times 10^{-4}$  value has an uncertain meaning.

### References

1. G. A. Mortimer, *J. Polym. Sci. A-1*, **4**, 881 (1966).
2. P. W. Tidwell and G. A. Mortimer, *J. Polym. Sci. A-1*, in press.
3. R. S. Davidson, *Quart. Revs.*, **21**, 249 (1967).
4. G. A. Mortimer, U. S. Pat. 3,284,432 (1966).
5. P. Gray and J. C. J. Thynne, *Trans. Faraday Soc.*, **60**, 1047 (1964).
6. P. Gray, A. Jones, and J. C. J. Thynne, *Trans. Faraday Soc.*, **61**, 474 (1965).
7. P. Gray and A. Jones, *Trans. Faraday Soc.*, **62**, 112 (1966).
8. P. Gray and A. A. Herod, *Trans. Faraday Soc.*, **63**, 2489 (1967).
9. G. A. Mortimer, U. S. Pat. 3,377,330 (1968).
10. G. A. Mortimer, *J. Polym. Sci. A-1*, **4**, 1895 (1966).
11. P. Smith and P. B. Wood, *Can. J. Chem.*, **44**, 3085 (1966).
12. G. Hardy, J. Varga, K. Nytrai, I. Tsajlik, and L. Zubonyai, *Vysokomol. Soedin.*, **6**, 758 (1964); *Polym. Sci. USSR*, **6**, 832 (1965).
13. C. L. Aldridge, J. B. Zackry, and E. A. Hunter, *J. Org. Chem.*, **27**, 47 (1962).
14. D. G. L. James and R. D. Suart, *Trans. Faraday Soc.*, **64**, 2735, 2752 (1968).
15. J. C. Woodbrey and P. Ehrlich, *J. Amer. Chem. Soc.*, **85**, 1580 (1963).
16. L. Nicolas, *J. Chim. Phys.*, **1958**, 177.
17. T. J. van der Molen, paper presented at IUPAC Conference, Budapest, 1969, Preprint 777.
18. P. Ehrlich and G. A. Mortimer, *Fortsch. Hochpolym. Forsch.*, **7**, 386 (1970).

Received October 20, 1969

Revised December 17, 1969

## Polymerization of Vinyl Chloride by Alkylolithium Compounds

V. JÍŠOVÁ, M. KOLÍNSKÝ, and D. LÍM, *Institute of Macromolecular Chemistry, Czechoslovak Academy of Sciences, Prague, Czechoslovakia*

### Synopsis

The polymerization of vinyl chloride initiated by alkylolithium compounds was investigated. The effect of temperature, initiator concentration, and monomer concentration on the conversion and the properties of the resulting polymers were studied. The optimum temperature in the investigated range (between  $-20^{\circ}\text{C}$  and  $+20^{\circ}\text{C}$ ) was  $+5^{\circ}\text{C}$ . The conversion is directly proportional to the concentration of both the initiator and the monomer. The molecular weight is inversely proportional to the initiator concentration and directly proportional to the monomer concentration. Under optimum conditions the molecular weight of the polymers is as high as 140,000. These results differ by an order from hitherto published data on the nonradical polymerization of vinyl chloride. The proportion of isotactic and syndiotactic structures resulting from the presence of *tert*-butyllithium does not differ from that obtained by radical polymerization, but the occurrence of anomalous structures is reduced to a minimum. The stability of the macromolecules is higher. A mechanism of the polymerization is suggested.

The polymerization of vinyl chloride by organometallic compounds has been discussed in several papers<sup>1-5</sup> devoted mainly to the general aspects of this process. No more profound investigation of the process occurring in the polymerization of vinyl chloride with organolithium compounds has been attempted to date. In this paper, we have been studying the reactions of vinyl chloride (VC) with an organometallic compound (RLi), and also the effect of the organometallic compound used, temperature, and concentration of the initiator, monomer, or solvents on the polymerization process.

### EXPERIMENTAL

Commercial vinyl chloride was purified and rectified on a pressure column, dried, and stored over solid potassium hydroxide. Its purity was determined by gas chromatography and by a polymerization test based on rate of polymerization.

*tert*-Butyllithium, *n*-butyllithium, and ethyllithium were used as initiators. The *tert*-butyllithium<sup>6</sup> was prepared by the reaction of lithium suspension with *tert*-butyl chloride and recrystallized three times from hexane (at least 99% purity). Ethyllithium was obtained by similar reaction

from ethyl bromide and the product was recrystallized from benzene (at least 99% purity). *n*-Butyllithium was prepared by the reaction of lithium with dibutylmercury (at least 95% purity).

Heptane and benzene solutions of *tert*-butyllithium, a heptane solution of *n*-butyllithium, and a benzene solution of ethyllithium were prepared. Their concentrations were so chosen as to make the amount of the solution negligible with respect to the total volume of the reaction mixture.

The reactions of the metal alkyl with the monomer were studied by using an equimolar mixture of vinyl chloride and initiator, in which no polymerization occurs. The gaseous products of the reaction determined by gas chromatography contained, besides the unreacted vinyl chloride, saturated hydrocarbon corresponding to the alkyl used. The reaction mixture contained also lithium acetylide, unreacted metal alkyl, and lithium chloride<sup>7</sup> (as has been proved by the formation of acetylene and of a further hydrocarbon fraction upon the decomposition by water and by the formation of acetylenedicarboxylic acid upon the action of carbon dioxide followed by hydrolysis).

The course of the reaction of the initiator with the monomer under the concentration conditions corresponding to the polymerization was investigated by the decrease of the alkaline character of the reaction mixture, and by the increase of the content of lithium chloride, acetylene, and butane in the reaction mixture with the increasing time of polymerization.

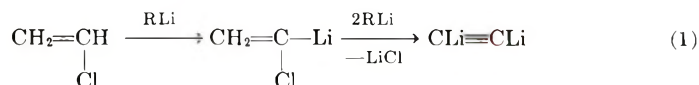
The polymerizations were carried out either in glass reactors or in glass ampoules with a pressure valve, freed from the traces of moisture and oxygen by bubbling with argon and evacuation under simultaneous heating. The last traces of oxygen were removed from the space over the liquid by several strippings of the excess of vinyl chloride.

Molecular weights were determined viscometrically and calculated from the empirical Danusso relation.<sup>8</sup>

In order to get information about the nature of the process, polymerizations initiated by azo compounds and by alkyllithium were compared; ESR signals, composition of copolymers, and also polymerization in the presence of diphenylpicrylhydrazyl were followed.

## RESULTS AND DISCUSSION

It follows from the reaction of vinyl chloride with alkyllithium that metallation of the vinyl compounds prevails in this reaction. The hydrogen atom of vinyl chloride is replaced by lithium, and a hydrocarbon corresponding to the alkyllithium used is released. The intermediate chlorovinyl lithium, which is stable only at temperatures below  $-83^{\circ}\text{C}$ ,<sup>9</sup> decomposes at higher temperatures, and lithium chloride is split off. The metallation continues until lithium acetylide is formed [eq. (1)]:





The results of the reaction of butyllithium with vinyl chloride under conditions corresponding to the polymerization are presented in Table I.

TABLE I  
Reaction of *n*-Butyllithium with Vinyl Chloride at 20°C and  $[I]/[M] = 6.7 \times 10^{-3}$

Time <i>t</i> , min	Conversion of <i>n</i> -BuLi to LiCl		Acetylene in decomposition gases after interruption of vol-% <sup>a</sup>	Conversion of <i>n</i> -BuLi to butane, <i>n</i> -BuLi, % <sup>a</sup>
	<i>n</i> -BuLi, % <sup>a</sup>	<i>n</i> -BuLi, % <sup>a</sup>		
1	8.9		0.303	
5	9.6	9.3	0.438	22.6
15	11.4	11.5	0.565	26.7
60	15.5		0.650	48.5
120			0.745	47.5
180			0.970	58.8
240		19.9		

<sup>a</sup> Based on initial *n*-BuLi content.

According to the above scheme, three molecules of alkyllithium are needed for the formation of one lithium chloride molecule; lithium chloride formed is bound in very stable complexes with unreacted alkyllithium, which leads to its deactivation.<sup>10</sup> About 7–10% of the organometallic compound is bound in the polymer. The initiator is almost completely consumed after 4 hr at 20°C, which is related with the end of the polymerization (Figs. 1 and 2). The course of the metallation reaction thus explains the very weak initiation activity of the organic lithium initiators.

The Gilman test for the presence of an organometallic compound at 20°C has shown that upon addition of alkyllithium to the monomer, 90% of active alkyllithium is consumed in 2 min, but that the increase of metallation products in the reaction mixture and of alkyls in the polymer (1.8% of the initial amount of  $12.5 \times 10^{-3}$  mole *tert*-BuLi/mole VC is bound in the polymer after 90 min, 8.7% is bound after 230 min, and 13.0% is bound after 1400 min, as determined by NMR-spectra) proves the existence of alkyllithium even after a long time. This fact can be explained by the ability of alkyllithium to form comparatively stable complexes which are inactive in the Gilman test.<sup>11</sup>

The termination reactions were studied by means of stepwise polymerization. Initiator and monomer were added successively several times in such a way that the same amount of initiator (or monomer) was added only after the preceding polymerization had been completed. The increase in the amount of polymer after the second and third addition of the initiator corresponded to the amount of alkyllithium added (Fig. 3). The molecular weights at final conversion remain practically unchanged (Fig. 4). The polymer yield did not increase upon further addition of the monomer. The existence of the final conversion and final molecular weight after each addition of the initiator proves the presence of termination reactions. The

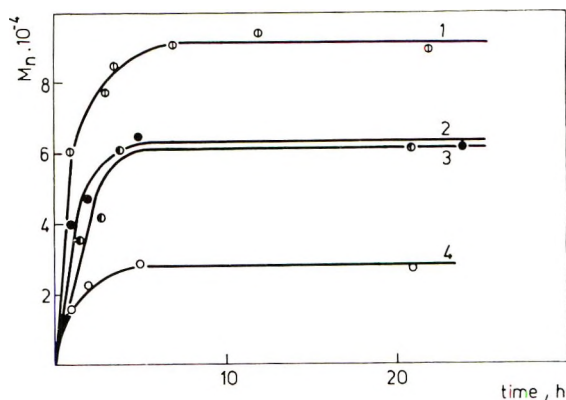


Fig. 1. Dependence of the molecular weight of poly(vinyl chloride) prepared by polymerization initiated with various alkyllithium compounds on time: (1) *t*-BuLi in heptane; (2) *t*-BuLi in benzene; (3) *n*-BuLi in heptane; (4) EtLi in benzene.  $[I] = 4.8 \times 10^{-2}$  mole/l.

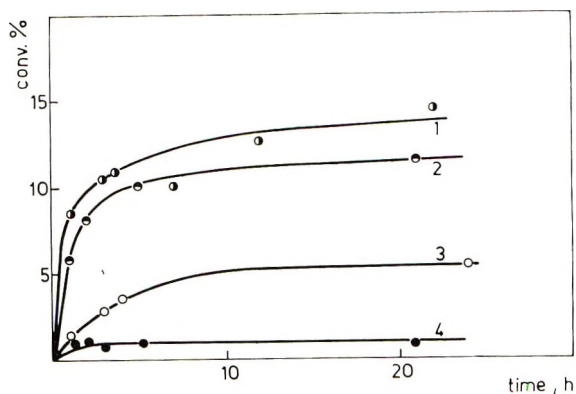


Fig. 2. Dependence of conversion in the vinyl chloride polymerization initiated with various alkyllithium compounds on time: (1) *t*-BuLi in heptane; (2) *t*-BuLi in benzene; (3) *n*-BuLi in heptane; (4) EtLi in benzene.  $[I] = 4.8 \times 10^{-2}$  mole/l.

polymerization course upon each addition of the initiator is reproducible, so that termination cannot be ascribed to the presence of impurities in the initial compounds.

The polymerizations of vinyl chloride were investigated at temperatures from  $-20^{\circ}\text{C}$  to  $+20^{\circ}\text{C}$  in the concentration range of the monomer  $[M] = 4\text{--}15$  mole/l. and initiator  $[I] = 1\text{--}200$  mmole/l.

The highest molecular weights and yields of the polymers were attained by initiation with *tert*-butyllithium. Of the two solvents used (heptane, benzene), the heptane solutions led to the higher molecular weight and yield values (Figs. 1 and 2).

In the temperature range studied, the molecular weight and conversion dependences have maxima at a constant polymerization time (Figs. 5 and 6). The conversion maxima were found at  $5^{\circ}\text{C}$ ; the molecular weight

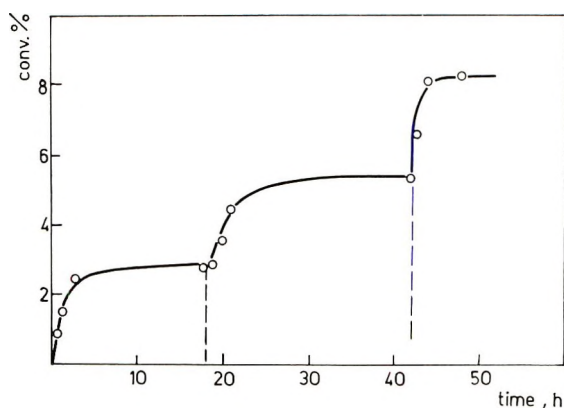


Fig. 3. Stepwise polymerization of vinyl chloride initiated with *tert*-butyllithium.  $[I]_1 = [I]_2 = [I]_3 = 5 \times 10^{-3}$  mole/l.,  $20^\circ\text{C}$ .

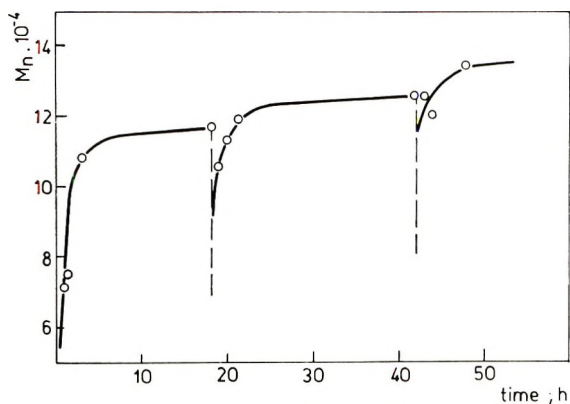


Fig. 4. Dependence of the molecular weight of poly(vinyl chloride) in the stepwise polymerization initiated with *tert*-butyllithium on time.  $[I]_1 = [I]_2 = [I]_3 = 5 \times 10^{-3}$  mole/l.,  $20^\circ\text{C}$ .

maxima are moved with increasing polymerization time from  $0^\circ\text{C}$  to  $5^\circ\text{C}$ . The molecular weights increase with time and conversion. The dependence of molecular weight on time becomes, starting from  $5^\circ\text{C}$  with decreasing temperature, less pronounced (Fig. 7).

In the concentration range studied, the polymerization rate is directly proportional to the initiator and monomer concentrations. At a constant concentration of the initiator the average degree of polymerization is proportional to the concentration of the monomer. The increase of the molecular weight with increasing monomer concentration is faster, the lower the concentration of the initiator (Fig. 8). At a constant concentration of the monomer, the molecular weight is inversely proportional to the concentration of the initiator (Fig. 9). This dependence becomes more pronounced at higher concentrations of the monomer.

The differences in polymerizations with the radical initiator and those

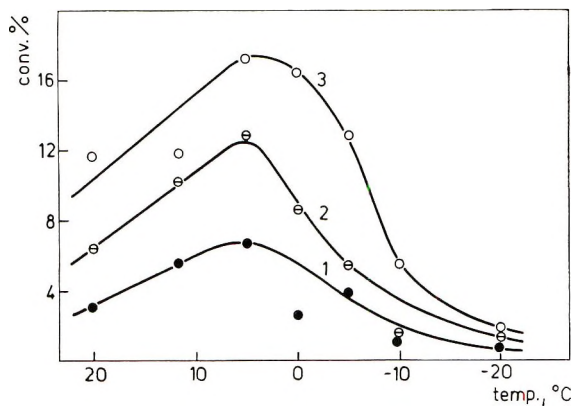


Fig. 5. Dependence of conversion in the polymerization of vinyl chloride initiated with *tert*-butyllithium on temperature: (1) 1 hr; (2) 2 hr; (3) 4 hr.  $[I] = 2.4 \times 10^{-2}$  mole/l.

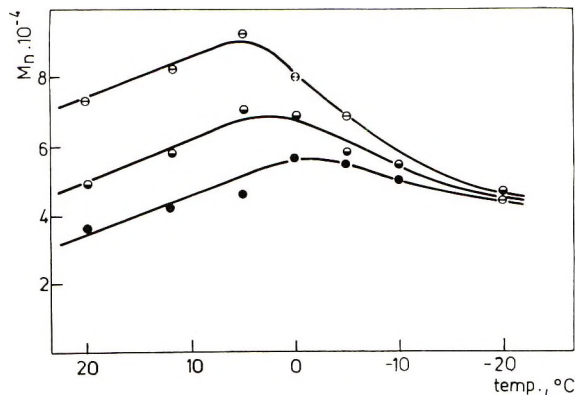


Fig. 6. Dependence of the molecular weight of poly(vinyl chloride) in the polymerization of vinyl chloride initiated with *tert*-butyllithium on temperature: (1) 1 hr; (2) 2 hr; (3) 4 hr.  $[I] = 2.4 \times 10^{-2}$  mole/l.

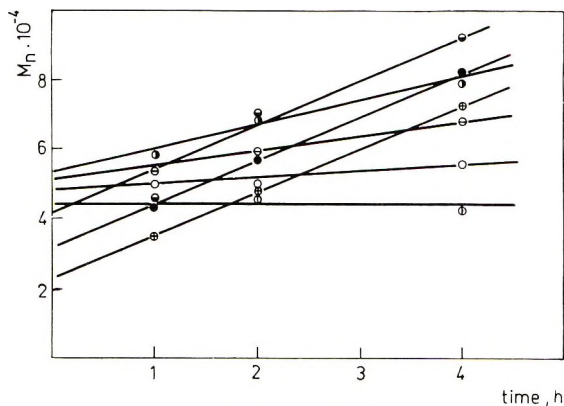


Fig. 7. Dependence of the molecular weight of poly(vinyl chloride) on time:  $\oplus$  20°C;  $\bullet$  12°C;  $\ominus$  5°C;  $\bullet$  0°C;  $\oplus$  -5°C;  $\circ$  -10°C;  $\oplus$  -20°C.

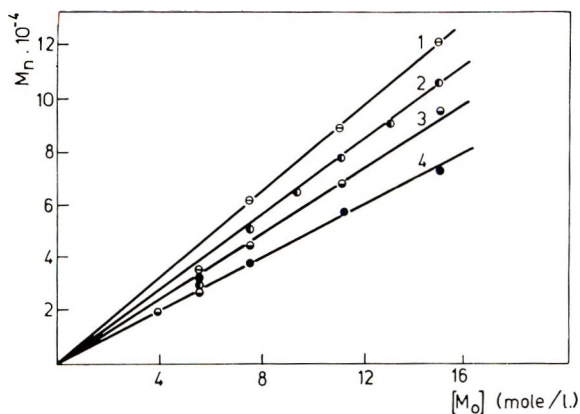


Fig. 8. Dependence of the molecular weight of poly(vinyl chloride) on the concentration of the monomer in heptane at various  $[t\text{-BuLi}]$ : (1)  $1.2 \times 10^{-2}$  mole/l.; (2)  $1.8 \times 10^{-2}$  mole/l.; (3)  $2.4 \times 10^{-2}$  mole/l.; (4)  $4.8 \times 10^{-2}$  mole/l. At  $20^\circ\text{C}$ , 2 hr.

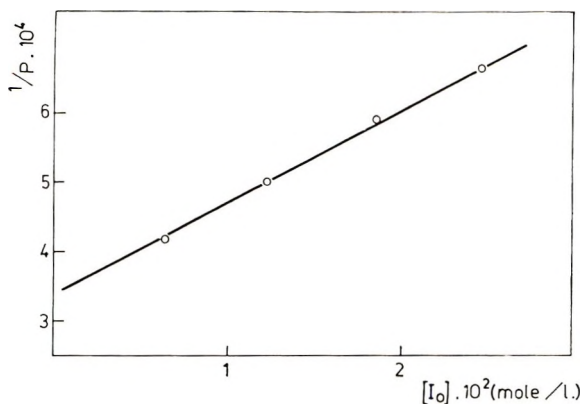


Fig. 9. Dependence of the degree of polymerization in the polymerization of vinyl chloride on the concentration of *tert*-butyllithium at  $20^\circ\text{C}$ , polymerization time 2 hr.

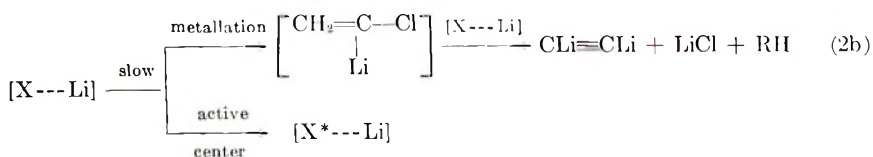
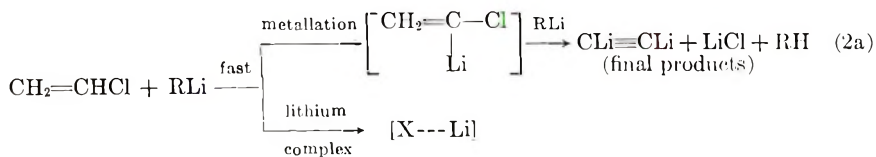
with alkylolithium support the conclusion that the character of the polymerization of vinyl chloride by alkylolithium compounds is not radical.

The structure of the polymers prepared with alkylolithium as determined by infrared spectra is similar to that of the radical polymers. The ratio of isotactic to syndiotactic bonds is practically unaffected by concentration or temperature conditions. The stability of these polymers to thermal degradation is higher than in case of unstabilized radical polymers, which is probably caused by the presence of a smaller content of defect structures. The molecular weight of these polymers varies from 60 000 to 90 000 on the average; under optimum conditions, however, it may be as high as 140 000. The degree of conversion is limited by solidification of the polymerization mixture. This is the reason that the yield in the polymerizations without

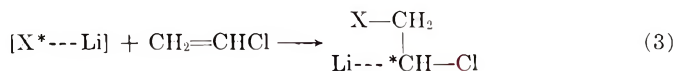
the solvents was 17.5% at the maximum, whereas in dilute solutions conversions up to 40% were possible.

For the mechanism of the polymerization of vinyl chloride with alkyl-lithium, the reaction scheme shown in eqs. (2)–(4) is suggested.

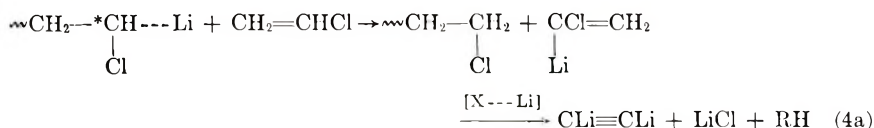
Initiation:



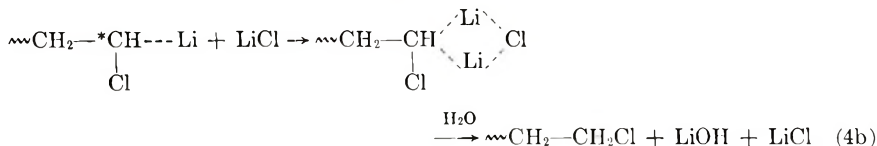
Propagation:



Termination by transfer to monomer:



Termination by formation of the complex with LiCl:



Initiation occurs without an inhibition period. A complex of alkyl-lithium with vinyl chloride is rapidly formed, and a substantial number of growth centers appear (parallel to the simultaneously occurring metallation reaction) after dissociation or rearrangement of the lithium complex formed. The addition of a further molecule of vinyl chloride to the growth center starts the propagation of the polymer. The increase of the total amount of alkyls in the polymer during polymerization proves the gradual formation of the initiation centers. The initiation with a partly metallated monomer is less probable, since the reactivity of the organolithium compounds with lithium attached to the carbon atom, from which the double bond starts is very weak in the polymerization of vinyl compounds.<sup>12</sup>

The relationships between the molecular weight and the initiator, monomer concentrations can be explained by several simultaneous parts of termination, most probably by transfer to monomer and by formation of a

complex between the growing end and lithium chloride formed in the metallation reaction. The termination by transfer is actually a metallation with polymeric organolithium compound. In the polymerization with alkyl-lithium in the presence of lithium chloride, a decrease in the yield and molecular weight of the polymers is observed, which seems to indicate a termination due to the formation of stable complexes with lithium chloride. The termination by splitting off the lithium chloride from the growing polymer end has not been proved since no other grouping has been found, even in a polymer having a molecular weight of 3000.

We wish to acknowledge the generosity of Dr. Lochmann for furnishing us with alkyl-lithium compounds. We are indebted to Dr. D. Doskočilová and Dr. J. Štokr for the spectral measurements, further to Dr. J. Pilař for the ESR measurements, and to Mrs. E. Plachetková for the gas chromatographic analyses.

### References

1. B. L. Eerusalimskii, V. V. Mazurek, I. G. Krasnoselskaya, and V. G. Gasan-Zade, paper presented at Symposium on Macromolecular Chemistry, Tokyo, 1966, Preprint 1-84.
2. V. G. Gasan-Zade and V. V. Mazurek, *Vysokomol. Soedin.*, **10**, 479 (1968).
3. A. Guyot and Pham-Quang-Tho, in *Macromolecular Chemistry, Paris 1963*, (*J. Polym. Sci. C*, **4**), M. Magat, Ed., Interscience, New York, 1963, p. 299.
4. A. Guyot and Pham-Quang-Tho, *J. Chim. Phys.*, **63**, 742 (1966).
5. A. Guyot, D. L. Trung, and R. Ribould, *C. R. Acad. Sci. (Paris)*, 266 C1139 (1968).
6. L. Lochmann, J. Pospíšil, J. Vodňanský, J. Trekoval, and D. Lím, *Coll. Czech. Chem. Commun.*, **30**, 2187 (1965).
7. O. H. Gilman and A. H. Haubein, *J. Amer. Chem. Soc.*, **67**, 1421 (1945).
8. G. Danusso, G. Moraglio, and S. Cazzera, *Chim. Ind. (Milan)*, **36**, 883 (1954).
9. G. Kolbrich and K. Flory, *Chem. Ber.*, **99**, 1773 (1966).
10. R. Waack and M. A. Doran, *Chem. Ind. (London)*, **1964**, 496.
11. V. W. Glaze and R. West, *J. Amer. Chem. Soc.*, **82**, 3337 (1960).
12. R. Waack and M. A. Doran, *J. Org. Chem.*, **32**, 3395 (1967).

Received September 24, 1969

Revised December 17, 1969

## Chain Transfer in Ethylene Polymerization. V. The Effect of Temperature

GEORGE A. MORTIMER, *Hydrocarbons and Polymers Division,  
Monsanto Company, Texas City, Texas 77591*

### Synopsis

In order to determine the effect of temperature on the chain-transfer reaction in the free-radical polymerization of ethylene, chain-transfer constants were measured for sixteen transfer agents at 130°C and 200°C at 1360 atm. The results were interpreted as  $\Delta E^*$ , the activation energy of the chain-transfer constant. This value is equal to the difference in activation energy between the transfer step (hydrogen abstraction) and the propagation step (addition to the monomer double bond):  $\Delta E^* = E_s^* - E_p^*$ . Excellent agreement was found between measured  $\Delta E^*$  values determined at 1360 atm pressure and  $(E_s^* - E_p^*)$  data for ethyl radical determined in vacuum gas-phase reactions. Apparently, the ethyl radical is a good model for polyethyl radical. The chain-transfer constant of ethylbenzene was found to be insensitive to temperature changes, indicating that  $E_p^* = E_s^*$  for this compound.

### INTRODUCTION

It has been pointed out that chain-transfer constants in the free-radical polymerization of ethylene, as calculated from the data of different authors who conducted their work at different reaction conditions, cannot be directly compared with one another because there is no published basis for recalculation of these values to a common pressure and temperature.<sup>1</sup> Thus, an otherwise valuable collection of chain-transfer data is of limited usefulness.<sup>2</sup> The purpose of the present work was to determine the effect of temperature on the chain-transfer constants of a series of representative transfer agents. As an outgrowth of the results reported herein, a method of estimating the temperature effect on chain-transfer constants by using published data in nonpolymerizing systems was found.

### EXPERIMENTAL

The experimental procedures were as previously described<sup>1</sup> with the following changes. The initiator was  $2.07 \times 10^{-4}$  mole/l. of azoisopropane. The temperature was 200°C. The ethylene was a high-purity grade containing less than 1 ppm oxygen, which gave negligible polymerization alone under the conditions of these experiments. Oxygen had to be rigorously excluded from the reaction in order for the rates and molecular weights to be reproducible because, under these conditions, oxygen is an



effective initiator. Hence, where necessary, gases were passed over a reduced copper catalyst to remove oxygen, all liquids were purged or redistilled under nitrogen, and all transfers were carried out in an inert atmosphere. The second reaction system, previously described, was used in all runs.<sup>1</sup> The pertinent data are given in Table I.

### CALCULATIONS

Chain-transfer constants were calculated as their logarithms by the non-linear least-squares method<sup>2</sup> and are listed in Table I.

The temperature effect on a chain-transfer constant  $C_s$  was interpreted as the activation energy of the Arrhenius expression (1), where subscripts p and s refer to the polymerization propagation step and the chain-transfer step respectively,  $k$  is the reaction rate constant, and  $A$  and  $E^*$  are the pre-exponential and exponential parameters of the Arrhenius expression.

$$C_s = k_s/k_p = (A_s/A_p) \exp \{ (E_p^* - E_s^*)/RT \} \quad (1)$$

On substituting  $\Delta E^*$  for the quantity  $(E_s^* - E_p^*)$ , it can readily be shown that the chain-transfer constants at two temperatures are related by equation (2).

$$C_{s2}/C_{s1} = \exp \{ (\Delta E^*/RT_1) - (\Delta E^*/RT_2) \} \quad (2)$$

An equivalent form of eq. (2) is given as eq. (3). This form is particularly useful

$$\ln C_{s2} - \ln C_{s1} = (\Delta E^*/R) [(1/T_1) - (1/T_2)] \quad (3)$$

since the value  $(\ln C_s)$  may be directly calculated, as described earlier, and thus not only  $\Delta E^*$  but also its approximate confidence limits can be readily computed.<sup>3</sup> From the  $C_s$  values at 200°C given in Table I and the corresponding values<sup>4</sup> at 130°C, the  $\Delta E^*$  values and confidence limits given in Table II were calculated.

### DISCUSSION

Some additional comment on the method of obtaining these 200°C data is appropriate. Difficulty was experienced in obtaining reproducible reactions at 1360 atm and 200°C with both propane and another transfer agent in the system, almost certainly because of oxygen contamination. It is extremely difficult to avoid adding some oxygen (as air) with each feed component. Propane is necessary at 130°C for two reasons: (1) to keep the system homogeneous, and (2) to bring the melt index of the base polymer into the measurable range. However, at 200°C, the system is homogeneous without propane and the difficulties ascribed here to oxygen were more easily circumvented if only one transfer agent was used at a time. The polymer melt index could be brought into the measurable range with a small amount of the transfer agent being studied.

TABLE I. Chain-Transfer Data at 1360 Atm, 200°C

Transfer agent	$C_s$	Feed composition, mole-% <sup>a</sup>		Melt index	$1/\bar{P} \times 10^4$
		Ethylene	Transfer agent		
None	—	99.82	0	85.1 <sup>b</sup>	3.30
		“	“	86.0 <sup>b</sup>	3.27
Propane	0.00652 ± 0.00002	88.80	11.03	27.1	11.4
		88.21	11.61	36.3	11.9
Ethyl acetate	0.0121 ± 0.0004	95.52	4.45	4.99	9.07
		“	“	3.60	8.73
Ethanol	0.0135 ± 0.0002	94.34	5.48	24.6	11.2
		“	“	22.1	11.0
Isobutane	0.0136 ± 0.0005	94.54	5.28	16.8	10.6
		“	“	27.1	11.4
Cyclohexane	0.019 ± 0.001	92.78	7.04	77.4	13.5
		98.54	1.42	0.281	6.76
		“	“	0.286	6.77
		97.72	2.25	1.62	8.00
		“	“	1.65	8.02
		96.65	3.32	14.4	10.4
		“	“	23.0	11.1
Propylene	0.0200 ± 0.0006	95.47	4.50	37.0	11.9
		“	“	46.2	12.3
		97.02	2.80	5.87	9.25
Toluene	0.022 ± 0.001	96.79	3.04	7.91	9.60
		“	“	6.32	9.33
		96.21	3.61	21.0	10.9
Cyclopentane	0.0228 ± 0.0009	“	“	38.6	12.0
		“	“	38.2	12.0
		97.08	2.74	6.82	9.42
Isopropanol	0.0234 ± 0.0005	“	“	11.4	10.1
		“	“	8.50	9.68
		97.31	2.51	6.57	9.38
Acetone	0.0282 ± 0.0006	“	“	5.15	9.11
		“	“	6.72	9.40
		97.20	2.62	18.3	10.7
Tetrahydrofuran	0.0401 ± 0.0009	“	“	22.3	11.0
		98.56	1.26	2.99	8.55
		98.25	1.58	7.52	9.54
Hydrogen	0.040 ± 0.002	“	“	9.51	9.82
		98.34	1.49	8.15	9.63
		“	“	5.19	9.11
<i>p</i> -Xylene	0.0434 ± 0.0006	99.10	0.87	0.555	7.19
		“	“	0.332	6.86
		98.06	1.76	22.8	11.1
		“	“	22.8	11.1
Ethylbenzene	0.050 ± 0.004	“	“	23.2	11.1
		98.78	1.04	1.64	8.01
		98.57	1.25	12.6	10.2
Butene-1	0.057 ± 0.004	“	“	7.44	9.52
		98.91	0.91	3.78	8.78
		98.82	1.00	2.39	8.34
		98.80	1.03	5.21	9.12
Butanone	0.075 ± 0.004	98.78	1.05	9.95	9.88
		99.11	0.71	2.67	8.44
		98.96	0.86	7.41	9.52
		“	“	12.9	10.2

<sup>a</sup> The balance of the feed, usually less than 0.2%, was benzene used as the initiator solvent.

<sup>b</sup>  $\bar{M}_n \times 10^{-3}$  determined by osmometry. The melt index was unmeasurably low.

TABLE II  
Activation Energy of the Chain-Transfer Constant

Transfer agent	Chain-transfer constant		$\Delta E^*$ with approximate 95% confidence limits	$\Delta E^*$ esti- mated from ethyl radical data	$C_s$ at 130°C calculated from $\Delta E^*$ and $C_s$ values in ref. 2
	130°C	200°C			
Ethyl acetate	0.0045 ± 0.0003	0.0121 ± 0.0004	5.3 ± 0.7		0.022
Hydrogen	0.0159 ± 0.0008	0.040 ± 0.002	5.0 ± 0.8		0.0032
Propane	0.00302 ± 0.00008	0.00652 ± 0.00002	4.2 ± 0.3		0.0094
Cyclohexane	0.0095 ± 0.0003	0.019 ± 0.001	3.8 ± 0.7	3.7	0.0052
Isobutane	0.0072 ± 0.0003	0.0136 ± 0.0005	3.5 ± 0.6		
Cyclopentane	0.0126 ± 0.0005	0.0228 ± 0.0009	3.2 ± 0.6		
Ethanol	0.0075 ± 0.0003	0.0135 ± 0.0002	3.2 ± 0.4		0.013
Acetone	0.0168 ± 0.0005	0.0282 ± 0.0006	2.8 ± 0.4		
Propylene	0.0122 ± 0.0008	0.0200 ± 0.0006	2.7 ± 0.8		
Isopropanol	0.0144 ± 0.0005	0.0234 ± 0.0005	2.6 ± 0.5		0.014
Toluene	0.0154 ± 0.0005	0.022 ± 0.001	2.0 ± 0.8		
Tetrahydrofuran	0.0288 ± 0.0006	0.0401 ± 0.0009	1.8 ± 0.3		
<i>p</i> -Xylene	0.0317 ± 0.0009	0.0434 ± 0.0006	1.7 ± 0.3		
Butanone	0.060 ± 0.005	0.075 ± 0.004	1.2 ± 1.1	1.1	
Butene-1	0.047 ± 0.002	0.057 ± 0.004	1.1 ± 1.0	1.4	
Ethylbenzene	0.052 ± 0.002	0.050 ± 0.004	-0.2 ± 1.0		

Extrapolation of the data on various transfer agents indicated that the limiting  $\bar{M}_n$  for these conditions was between 70 000 and 90 000. Since there was a strong possibility that polymer of this  $\bar{M}_n$  would stay in solution at 1360 atm at 200°C, an attempt to make polymer without added transfer agent was made. Indeed, polymer was successfully made reproducibly in the absence of transfer agent. However, any variations in temperature or abnormalities in the agitation either had a snowballing effect or were a signal that something else was amiss, for unless the reactor ran perfectly the runs were not reproducible. Since, according to the data of Ehrlich,<sup>5</sup> the ragged edge of solubility is being approached here, this sensitivity of the reaction is understandable.

The limiting molecular weight was thus established by direct experimentation to be about 86 000. The nonreproducible runs where temperature and/or agitation did not behave normally gave higher  $\bar{M}_n$  values than the reproducible runs.

The 86 000 limiting  $\bar{M}_n$  is lower than the 140 000 value found at 130°C.<sup>3</sup> Since the radical concentration was kept about the same by using equal concentration of initiators which had comparable half-lives at the two temperatures, the energetics of propagation versus termination would suggest that  $\bar{M}_n$  could rise as temperature is increased.<sup>6</sup> The lower observed  $\bar{M}_n$  at 200°C indicates that chain-breaking reactions have increased in rate more than propagation. These reactions could include transfer to initiator, transfer to the trace of benzene solvent, transfer to monomer, and  $\beta$ -elimination.<sup>7</sup> No attempt was made to estimate the relative importance of these separate possibilities.

The first conclusion to be drawn from the  $\Delta E^*$  values in Table II is that the experimental error in the activation energy for the chain-transfer constant can be surprisingly small: 95% confidence limits of  $\pm 0.3$  kcal/mole were obtained from present equipment and techniques by making sufficient runs. This degree of precision is better than is needed to indicate differences between transfer agents and is sufficient to allow some valid comparisons between this and other related work to be made.

The objective of this work was to determine the activation energy of the chain-transfer constant. This activation energy  $\Delta E^*$  was defined above as the activation energy for hydrogen abstraction (the chain-transfer step)  $E_s^*$  minus the activation energy for the radical addition (or propagation) step  $E_p^*$ . Since  $E_p^*$  is constant, the variations in  $\Delta E^*$  must depend entirely on  $E_s^*$  for each transfer agent.

As a rough rule of thumb, compounds having low chain-transfer constants (on a per-hydrogen basis) will have high activation energies, and vice versa. Thus, esters, alcohols, and alkanes have high activation energies. Compounds which have activated hydrogen atoms and thus have high  $C_s$  values and low  $\Delta E^*$  values include aralkanes, olefins, and ketones. These patterns of radical reactivity are the same as seen in nonpolymerizing free-radical systems.<sup>8</sup>

Hydrogen is an apparent exception to this rule, in that it has a high activation energy and a moderately high  $C_s$  value on a per-transferrable-hy-

drogen basis. The obvious difference between it and the other transfer agents in Table II is that it is the only one in which a C—H bond is not the bond broken in the transfer step. Its rate of transfer is probably different from hydrocarbon-type compounds because of a larger pre-exponential factor in its Arrhenius expression.<sup>9</sup> Thus, it falls in a different series than hydrocarbons, and within this series the rule probably holds. Other transfer agents which break bonds other than C—H in the transfer step (such as  $\text{CCl}_3$ ,  $\text{CH}_2\text{Cl}_2$ ,<sup>10</sup> mercaptans, secondary amines,<sup>11,12</sup> etc.) may also have unusual pre-exponential factors.

It is instructive to compare the present  $\Delta E^*$  values in Table II with values which are estimated from the reactions of alkyl radicals at subatmospheric pressures. These values have been estimated from the ethyl radical data compiled by Kerr and Trotman-Dickenson.<sup>8</sup> The value  $E_p^*$  was assumed to be equal to the value of the activation energy for the addition of ethyl radicals to ethylene for which a mean value of 6.9 kcal/mole was obtained from the published values.<sup>8</sup> This is also the mean value obtained by averaging  $E^*$  values for the addition of *n*-propyl<sup>13</sup> and *n*-butyl<sup>14</sup> radicals to ethylene.  $E_s^*$  for alkanes which transfer at secondary carbon atoms was assumed to be the same as that for abstraction of hydrogen from normal heptane by ethyl radical, which value is 10.6 kcal/mole.<sup>15</sup> The ( $E_s^* - E_p^*$ ) value, 3.7 kcal/mole, is very close to that calculated for chain transfer of cyclohexane and the other alkanes studied. The somewhat higher and apparently quite precise  $\Delta E^*$  value for propane is reasonable because transfer of the six primary hydrogens is relatively more important for propane which has a primary: secondary hydrogen ratio of 3:1 than for heptane which has a primary: secondary ratio of 3:5. It is known that primary hydrogens show a higher activation energy than secondary in transfer reactions.<sup>8</sup>

The estimated  $E_s^*$  for butene-1, which transfers preferably the secondary allylic hydrogens,<sup>16</sup> was taken as the arithmetic average of the values of  $E_s^*$  for ethyl radical reacting with four different olefins containing secondary allylic hydrogens.<sup>15</sup> Thus, ( $E_s^* - E_p^*$ ) for butene-1 was estimated to be  $8.3 - 6.9 = 1.4$  kcal/mole, an answer in good agreement with the value obtained in this work of 1.1 kcal/mole for transfer during ethylene polymerization.

Butanone has been directly studied with ethyl radicals in the gas phase.<sup>17</sup> From the reported value  $E_s^* = 8.0$  kcal/mole, the value  $\Delta E^*$  is calculated to be 1.1, in excellent agreement with our value of 1.2 kcal/mole.

Because of the lack of ethyl radical data on the other compounds in Table II, the comparisons cannot be carried further. The excellent correspondence between  $\Delta E^*$  values calculated from gas-phase ethyl radical data at subatmospheric pressures and the data in this report is striking to say the least, and indicates that ethyl radical is a good model for polyethyl radical. Hydrogen atoms and methyl radicals are not good models for polyethyl radicals and do not give such close correspondence of chain-transfer data, although they do give a rough correlation with polyethylene data.<sup>1</sup>

An additional aspect of the data in Table II deserves consideration. The similarity in  $C_s$  values at 130°C between phenyl derivatives and their vinyl analogs has been pointed out.<sup>16</sup> It is, therefore, noteworthy that, upon further study, it is seen that the transfer constants at 1360 atm for toluene and ethylbenzene are essentially equal to those for propylene and butene-1 respectively at about 170°C. At 130°C they are higher and at 200°C lower, as a result of the fact that the activation energies for the phenyl compounds are roughly 1.0 kcal/mole lower than for the vinyl analogs. Presumably, the greater delocalization possible for the free electron in an aromatic system is responsible for the lower activation energies. Ethylbenzene is noteworthy in that its chain-transfer constant is practically temperature insensitive.

Since this work was begun in order to permit recalculation of chain-transfer data to a common basis, it is instructive now to do just this. The chain-transfer constants given in Hill and Doak's<sup>2</sup> Table IV, for compounds for which  $\Delta E^*$  values were obtained in the present work, were recalculated to the common basis of 130°C. The published value for cyclohexane was assumed to be for 200°C as for all other compounds of the same series reported by Hill and Doak. No correction for pressure differences was made. Since all their Table IV data are for high-pressure bulk polymerizations, it is probably not serious to ignore pressure effects. The agreement between the recalculated values (shown in Table II), and our measured 130°C values is good. A factor of about 2.4 difference was found in making the same correction for data in Hill and Doak's Table III which were obtained at low pressure in benzene solution. This factor is probably due to the necessity of making additional corrections.

It is concluded that the effect of temperature on chain-transfer constants is adequately accounted for by an Arrhenius expression, the activation energy of which may be either directly measured or adequately estimated from data on reactions of ethyl radical in the gas phase at subatmospheric pressures.

## References

1. G. A. Mortimer, *J. Polym. Sci. A-1*, **4**, 881 (1966).
2. A. Hill and K. W. Doak in *Crystalline Olefin Polymers*, Part I, R. Raff and K. W. Doak, Eds., Interscience, New York, 1964, pp. 285-291.
3. P. W. Tidwell, and G. A. Mortimer, *J. Polym. Sci. A-1*, in press.
4. G. A. Mortimer, *J. Polym. Sci. A-1*, this issue.
5. P. Ehrlich, *J. Polym. Sci. A*, **3**, 131 (1965).
6. H. Sobue and H. Kubota, *Makromol. Chem.*, **90**, 276 (1966).
7. J. C. Woodbrey and P. Ehrlich, *J. Amer. Chem. Soc.*, **85**, 1580 (1963).
8. J. A. Kerr and A. F. Trotman-Dickenson in *Progress in Reaction Kinetics*, G. Porter, Ed., Pergamon Press, New York, 1961.
9. M. H. J. Wijnen and E. W. R. Steacie, *J. Chem. Phys.*, **20**, 205 (1952).
10. J. Harmon, T. A. Ford, W. E. Hanford, and R. M. Joyce, *J. Amer. Chem. Soc.*, **72**, 2213 (1950).
11. P. Gray and A. Jones, *Trans. Faraday Soc.*, **61**, 2161 (1965).

12. P. Gray, A. Jones, and J. C. J. Thynne, *Trans. Faraday Soc.*, **61**, 474 (1965).
13. J. A. Kerr and A. F. Trotman-Dickenson, *Trans. Faraday Soc.*, **55**, 572 (1959).
14. J. A. Kerr and A. F. Trotman-Dickenson, *J. Chem. Soc.*, **1960**, 1602.
15. D. G. L. James and E. W. R. Steacie, *Proc. Roy. Soc. (London)*, **A244**, 289 (1958).
16. L. Boghetich, G. A. Mortimer, and G. W. Daues, *J. Polym. Sci.*, **61**, 3 (1962).
17. P. Ausloos and E. W. R. Steacie, *Can. J. Chem.*, **33**, 1062 (1955).

Received October 20, 1969

Revised December 17, 1969

## Chain Transfer in Ethylene Polymerization. VI. The Effect of Pressure

GEORGE A. MORTIMER, *Hydrocarbons and Polymers Division,  
Monsanto Company, Texas City, Texas 77591*

### Synopsis

The chain-transfer reaction, which controls the molecular weight level of the polymer, apparently has not been studied as a function of pressure for ethylene. Therefore, the chain-transfer constants for eleven transfer agents were determined at 1360 and 2380 atm at 130°C. The results were interpreted according to transition-state theory as the difference between the volumes of activation for the transfer and propagation steps. It was found that the effect of pressure on the transfer constant is small for most transfer agents, indicating that the volumes of activation for hydrogen abstraction and addition to the ethylene double bond are similar. Alkanes, however, gave anomalous results.

### INTRODUCTION

It has been pointed out that chain-transfer constants in ethylene polymerization measured at different reaction conditions cannot be directly compared unless there is some way of converting them to a common basis.<sup>1,2</sup> A method of accounting for the temperature effect has been presented.<sup>2</sup> The task left for this paper is to study and account for the effect of pressure.

The study of the pressure effect for ethylene polymerization has particular significance. Although the effect of pressure on the chain-transfer reaction for a few other polymer systems has been briefly investigated, it is not commercial practice to polymerize these other monomers at high pressure. However, ethylene is routinely polymerized commercially at high and widely varying pressures, and generally in the presence of a chain-transfer agent. Therefore, this study has a very practical application.

### EXPERIMENTAL

All polymerizations were carried out in the second polymerization system described previously<sup>1</sup> by use of the same procedures. The only difference was that, in the present work, the reaction pressure was 2380 atm. The pertinent data are given in Table I.

### CALCULATIONS

Chain-transfer constants  $C_s$  were calculated as their logarithms by the nonlinear least-squares method<sup>3</sup> and are listed in Table I.



TABLE I. Chain Transfer Data at 2380 atm, 130°C

Transfer agent	$C_s^a$	Feed composition, mole-% <sup>b</sup>		Transfer agent	Melt index	$1/\bar{P} \times 10^4$
		Ethylene	Propane			
Acetone	$0.016 \pm 0.001$	83.70	14.61	1.56	12.6	10.2
		85.59	12.44	1.84	11.4	10.1
		82.99	14.61	2.26	33.5	11.7
		"	"	"	37.6	11.9
Butane	$0.0045 \pm 0.0002$	87.14	12.72	0	0.071	6.03
		"	"	"	0.149	6.40
		85.35	14.51	"	0.570	7.21
		83.37	16.49	"	2.67	8.45
		"	"	"	1.04	7.65
		80.55	19.32	"	8.30	9.66
		"	"	"	5.14	9.10
		76.31	23.56	"	24.2	11.2
		69.76	30.11	"	101.	14.1
		69.62	30.25	"	110.	14.3
		90.93	0	8.94	0.066	5.99
		"	"	"	0.542	7.18
		"	"	"	0.498	7.12
		89.14	"	10.72	0.480	7.10
		88.03	"	11.83	2.68	8.45
		86.07	"	13.80	8.90	9.74
		83.81	"	16.05	26.3	11.3
		87.39	2.83	9.65	2.73	8.47
		87.04	4.24	8.58	3.10	8.59
		85.97	"	9.65	4.77	9.02
87.51	7.07	5.29	2.23	8.28		
87.43	"	5.36	1.19	7.75		
83.37	9.38	7.11	6.53	9.37		
83.34	"	7.15	8.67	9.71		
Butanone	$0.055 \pm 0.005$	84.75	14.61	0.51	16.8	10.6
		"	"	"	16.4	10.6

According to transition-state theory,<sup>4</sup> which appears to hold for ethylene polymerization,<sup>5</sup> the effect of pressure for any reaction having a rate constant  $k$  can be described by eq. (1).

$$d(\ln k)/dP = -\Delta V_{\ddagger}^{\ddagger}/RT \quad (1)$$

where  $P$ ,  $R$ , and  $T$  have the usual gas-equation meanings and  $\Delta V_{\ddagger}^{\ddagger}$  is the difference in volume between the transition state and the reactants in a standard state. In the context of chain-transfer measurements, this equation may be rewritten as eq. (2), where the differential has been rendered as the finite difference between states 1 and 2 and subscripts s and p refer to transfer and propagation steps respectively.

$$(\ln C_{s1} - \ln C_{s2})/(P_1 - P_2) = -(\Delta V_{s\ddagger} - \Delta V_{p\ddagger})/RT \quad (2)$$

In actually performing the calculation of  $(\Delta V_{s\ddagger} - \Delta V_{p\ddagger})$ ,  $C_s$  values were not used as such, but the values of  $(\ln C_s)$  were computed directly along with the standard deviation of the logarithm value<sup>3</sup> by using the 2380 atm data of Table I and the corresponding 1360 atm data.<sup>3,6</sup> By using this transformation, the method of Welch<sup>7</sup> could be used to approximate the 95% confidence limits of the  $(\Delta V_{s\ddagger} - \Delta V_{p\ddagger})$  values. Had  $C_s$  values them-

TABLE I (continued)

Transfer agent	$C_s^a$	Feed composition, mole-% <sup>b</sup>		Transfer agent	Melt index	$1/\bar{P} \times 10^4$
		Ethylene	Propane			
Cyclohexane	0.0090 ± 0.0009	85.22	12.72	1.92	10.7	9.98
		83.33	14.61	"	9.54	9.83
		82.57	"	2.69	13.1	10.2
		82.18	"	3.08	20.0	10.9
Cyclopentane	0.0109 ± 0.0009	"	"	"	12.4	10.2
		82.77	14.56	2.54	11.8	10.1
		82.39	14.61	2.87	27.3	11.4
		"	"	"	30.2	11.5
Ethanol	0.0068 ± 0.0006	80.81	"	4.45	29.0	11.5
		"	"	"	22.7	11.1
Ethylbenzene	0.043 ± 0.003	84.71	14.56	0.59	7.49	9.53
		84.41	14.61	0.85	28.8	11.5
		"	"	"	28.7	11.5
		"	"	"	44.9	12.3
Isopropanol	0.012 ± 0.001	83.10	14.32	2.44	20.8	10.9
		82.91	14.51	"	16.8	10.6
		82.81	14.61	"	22.4	11.0
Propane <sup>a</sup>	0.00276 ± 0.00011					
Toluene	0.018 ± 0.001	83.01	14.61	2.25	26.6	11.3
		"	"	"	29.6	11.5
		"	"	"	87.1	13.7
<i>p</i> -Xylene	0.040 ± 0.003	84.67	"	0.59	14.6	10.4
		86.56	12.63	0.67	7.34	9.51
		84.25	14.61	1.01	32.5	11.7
		"	"	"	52.6	12.6

<sup>a</sup> Chain-transfer constants were calculated as described in ref. 3 by use of all of the data listed under butane in all calculations.

<sup>b</sup> The balance of the feed, usually less than 0.2%, was benzene used as initiator solvent.

selves been used in the calculation, no estimate of the error in ( $\Delta V_{s\ddagger} - \Delta V_{p\ddagger}$ ) values would be available. The results of these calculations are given in Table II.

TABLE II  
Pressure Effect on the Chain-Transfer Constant at 130°C

Transfer agent	$C_s$		$(\Delta V_{s\ddagger} - \Delta V_{p\ddagger})$ and approximate 95% confidence limits, cc/mole
	130°C	200°C	
Isopropanol	0.0144 ± 0.0005	0.012 ± 0.001	6.1 ± 5.5
Cyclopentane	0.0126 ± 0.0005	0.0109 ± 0.0009	4.7 ± 5.7
Butane	0.00494 ± 0.00009	0.0045 ± 0.0002	3.2 ± 3.8
Propane	0.00302 ± 0.00008	0.00276 ± 0.00011	3.1 ± 2.9
Ethanol	0.0075 ± 0.0003	0.0068 ± 0.0006	3.1 ± 6.1
Butanone	0.060 ± 0.005	0.055 ± 0.005	2.9 ± 8.3
Cyclohexane	0.0095 ± 0.0003	0.0090 ± 0.0009	1.5 ± 6.4
Acetone	0.0168 ± 0.0005	0.016 ± 0.001	1.1 ± 4.4
Ethylbenzene	0.052 ± 0.002	0.043 ± 0.003	6.7 ± 4.7
Toluene	0.0154 ± 0.0005	0.018 ± 0.001	-4.7 ± 5.5
<i>p</i> -Xylene	0.0317 ± 0.0009	0.040 ± 0.003	-7.8 ± 4.4

## DISCUSSION

Examination of the data in Table II leads to several conclusions. The effect of pressure on chain transfer constants is small and is negligible for many purposes. For most of the transfer agents, the effect is of marginal statistical significance. The average of the  $(\Delta V_{s\ddagger} - \Delta V_{p\ddagger})$  values for the first eight transfer agents listed in Table II is +3 cc/mole. Since  $\Delta V_{p\ddagger}$  has been shown to be about -23 cc/mole,<sup>5</sup>  $\Delta V_{s\ddagger}$  for these eight compounds would be roughly -20 cc/mole.

These rather terse statements require some amplification. Regardless of whether  $\Delta V_{p\ddagger}$  is accurately known or not, it is constant for ethylene. Therefore, the variations seen in Table II may be due to differences in  $\Delta V_{s\ddagger}$  between transfer agents, to random experimental error, or to both. The approximate 95% confidence limits give an estimate of the extent of random error, which is seen to be large in comparison with the magnitude of the quantity  $(\Delta V_{s\ddagger} - \Delta V_{p\ddagger})$ . There seems to be no *a priori* reason to suspect that the volumes of the transition states for chain transfer to the eight aliphatic compounds should be greatly different from one another, so a simple lumping of all the values into an overall average of about +3 cc/mole seems to be as justified as any other treatment.

It may be emphasized, in passing, that the whole argument for the validity of such a lumping or averaging is based on the availability of an appropriate statistical estimate of the magnitude of random experimental error in the  $(\Delta V_{s\ddagger} - \Delta V_{p\ddagger})$  values. Such an estimate can be obtained, based on our present knowledge in mathematical statistics, only if the standard error of  $(\ln C_s)$ , rather than the error in  $C_s$ , is known. The ability to draw realistic conclusions about volumes of activation is ample justification for using a procedure for computing  $C_s$  values which may be more cumbersome than Mayo's method.<sup>3</sup>

The aromatic transfer agents, the last three compounds listed in Table II, show a peculiar behavior in that the methyl-substituted derivatives have a negative net value and the ethyl-substituted one a high positive net value of  $(\Delta V_{s\ddagger} - \Delta V_{p\ddagger})$ . This result is puzzling but has been verified by careful repetition of experiments. It might be argued that there is no *a priori* reason to suspect that aromatics should be different from the just-discussed aliphatics, or, for that matter, from each other. Assuming however, that the approximate 95% confidence limits in Table II are indeed good approximations of the true level of uncertainty in the data, there is no question but that xylene is different from the eight aliphatics and from ethylbenzene, *a priori* assumptions notwithstanding. Furthermore, the difference between toluene and the aliphatics is significant and between toluene and ethylbenzene highly significant in the statistical sense. Without further experimentation on other aromatic compounds, no rationale for these surprising results can be offered.

The effects of pressure on chain transfer with a few other monomers have been reported. Walling has estimated  $\Delta V_{s\ddagger}$  to be in the range of -6 to

-15 cc/mole for the systems he has studied.<sup>8</sup> No exact comparisons can be made between this work and his, but it appears that possible values for  $\Delta V_s^\ddagger$  extend over greater than a 9 cc/mole span. Table II shows a span of 14.5 cc/mole and, assuming  $\Delta V_p^\ddagger$  is -23 cc/mole, covers a range of  $\Delta V_s^\ddagger$  values of roughly -16 to -31 cc/mole. Imoto et al. reported for vinyl acetate a difference of 32.6 cc/mole between the activation volume of transfer to polymer and that of transfer to monomer,<sup>9</sup> again indicating that a wide span of values is possible. An equally wide span is found for polyethylene if short-chain branching can be considered a transfer reaction, as discussed in the next paragraph. In view of the limited number of monomers and chain-transfer agents for which data are available in the literature, no further conclusions are drawn.

The initial step in the short-chain branching reaction has been described as an intramolecular chain-transfer reaction.<sup>10</sup> Thus, a discussion of the effect of pressure upon this reaction is appropriate at this time. By using the portion of the 130°C data of Woodbrey and Ehrlich<sup>11</sup> which gives an essentially linear plot of (ln methyl ratio) versus pressure, a value of  $(V_b^\ddagger - V_p^\ddagger)$ , where b refers to short-chain branching, can be calculated to be about +24 cc/mole. A value of comparable magnitude was also found for the effect of pressure on branching in poly(vinyl acetate).<sup>9</sup> For a  $(V_b^\ddagger - V_p^\ddagger)$  value of 24 cc/mole, the value  $V_b^\ddagger$  is seen to be +1 cc/mole, indicating that pressure has little effect on the abstraction of hydrogen atoms in short-chain branching. This result is consistent with the concept that short-chain branching occurs following hydrogen abstraction via a six-membered ring which is already about as compact as it can be.

The extrapolated value of  $1/\bar{P}_0$  at 2380 atm, which is a result of the chain-transfer calculation, is  $2.5 \pm 0.3 \times 10^{-4}$ , giving the limiting  $\bar{M}_n$  as 110 000  $\pm$  10 000. This result is puzzling. The polymerization rate nearly doubles in going from 1360 atm to 2380 atm.<sup>5</sup> Since the termination rate should be nearly pressure-independent,<sup>8</sup> especially since the viscosity is quite low, the rate increase should be due to an increased rate of propagation.<sup>13</sup> Thus, the molecules should grow twice as long before being terminated, and the limiting  $\bar{M}_n$  should be about double that found at 1360 atm.<sup>6</sup>

Since it is not, other chain-breaking reactions must be considered to see if their rate might be increased sufficiently to account for the low limiting molecular weight. One possibility is  $\beta$ -elimination; however, this gives rise to unsaturation, particularly of the vinylidene type. Since both total and vinylidene double bonds are decreased at higher pressures,  $\beta$ -elimination is seen not to be increased by pressure.<sup>11</sup> Another possibility is that transfer to monomer is accelerated relative to propagation: that is,  $(V_s^\ddagger - V_p^\ddagger)$  for ethylene is large and negative. In vinyl acetate polymerization, strong acceleration of transfer to monomer was found as pressure was raised.<sup>9</sup> However, transfer to monomer should produce vinyl end-groups in the polymer, whereas no increase in vinyl content (which is very low anyway) has been observed as pressure is raised.<sup>11</sup> This possibility is therefore also excluded.

Changes in the rate of termination or initiation might be considered. These appear to be negligible.<sup>13</sup> Even if they were not, the effect of their variation on  $1/\bar{P}_0$  is negligible because their contribution to the limiting molecular weight is so small.<sup>6,11</sup>

A possible explanation that cannot be eliminated with data presently available is that increased transfer to the traces of initiator and/or benzene may be responsible for the lowered  $\bar{M}_n$ . There is no reason to suspect that transfer of a hydrogen atom from di-*tert*-butyl peroxide will be any different from transfer of a hydrogen atom from the aliphatic compounds in Table II. However, with peroxides, transfer at the peroxy linkage is also possible, and the effects of pressure on such a reaction are hard to predict. It is doubtful, however, that the effect would be large enough to account for the magnitude of  $\bar{M}_n$  lowering observed. Also, no direct data were obtained on the effect of pressure on relative rates of transfer of hydrogen atoms on aromatic rings. Much of the increase in  $C_s$  for toluene and xylene might come from the ring hydrogens. However, even if all of the effect were from ring hydrogens, the magnitude of the effect is too small to account for the raising of  $1/\bar{P}_0$  considering the small amount of benzene present as the initiator solvent. Thus, the exact reason that the limiting  $\bar{M}_n$  is low is not yet established.

Although the pressure effect on the chain-transfer agents studied seems to be easily enough accounted for by the transition state theory, the present data still leave unanswered questions. In terms of correcting chain-transfer data to a standard condition, one may as a first approximation assume that the pressure effect is negligible. However, more data on other transfer agents will be required before any safe predictions can be made about compounds which have not been studied inasmuch as no clear patterns of reactivity change due to pressure have emerged from this study.

### References

1. G. A. Mortimer, *J. Polym. Sci. A-1*, **4**, 881 (1966).
2. G. A. Mortimer, *J. Polym. Sci. A-1*, this issue.
3. P. W. Tidwell and G. A. Mortimer, *J. Polym. Sci. A-1*, in press.
4. M. G. Evans and M. Polanyi, *Trans. Faraday Soc.*, **31**, 875 (1935).
5. R. O. Symcox and P. Ehrlich, *J. Amer. Chem. Soc.*, **84**, 531 (1962).
6. G. A. Mortimer, *J. Polym. Sci. A-1*, this issue.
7. B. L. Welch, *Biometrika*, **34**, 28 (1947).
8. C. Walling, *J. Polym. Sci.*, **48**, 335 (1960).
9. H. Nakamoto, Y. Ogo, and T. Imoto, *Makromol. Chem.*, **111**, 93 (1968).
10. M. J. Roedel, *J. Amer. Chem. Soc.*, **75**, 6110 (1953).
11. J. C. Woodbrey and P. Ehrlich, *J. Amer. Chem. Soc.*, **85**, 1580 (1963).
12. P. Ehrlich and J. C. Woodbrey, *J. Appl. Polym. Sci.*, **13**, 117 (1969).
13. R. O. Symcox and P. Ehrlich, *J. Amer. Chem. Soc.*, **84**, 531 (1962).

Received October 20, 1969

Revised December 17, 1969

## Chain Transfer in Ethylene Polymerization. III. An Improved Method of Calculating Polymerization Chain-Transfer Constants

PAUL W. TIDWELL and GEORGE A. MORTIMER, *Hydrocarbons and  
Polymers Division, Monsanto Company, Texas City, Texas 77591*

### Synopsis

The method of determining chain-transfer constants in polymer systems, originally developed by Mayo, has been extended to the simultaneous determination of constants for several transfer agents. The validity of various calculation methods was examined. Particular attention was devoted to the question of how precisely chain-transfer constants are known. This extended method was applied to the determination of chain-transfer constants in ethylene polymerization under conditions where the limiting molecular weight in the absence of transfer agents cannot be directly measured, and it was shown that precision is improved (uncertainty reduced) by simultaneously determining more than one transfer constant.

### INTRODUCTION

Since Mayo<sup>1</sup> first showed the derivation and illustrated the concept of the chain-transfer constant, the procedures described by him have been used extensively to determine the numerical values of chain-transfer constants. This paper will show that the simple procedure described by Mayo may be employed in least-squares estimation procedures for determining chain-transfer constants and that these concepts can readily be extended to the simultaneous determination of several chain-transfer constants when mixed solvents are employed in a free-radical polymerization system.

### THEORY

#### Chain Transfer

Mayo<sup>1</sup> has shown that the degree of polymerization  $\bar{P}$  at low conversion of monomer to polymer in a properly conducted free-radical polymerization, can be adequately represented by eq. (1)

$$1/\bar{P} = 1/\bar{P}_0 + C_s([S]/[M]) \quad (1)$$

where  $\bar{P}$  is the number-average degree of polymerization ( $\bar{M}_n$  divided by monomer molecular weight),  $[S]$  is the initial solvent (or chain-transfer agent) molar concentration,  $[M]$  is the initial monomer molar concentra-

tion;  $C_s$  is the chain-transfer constant, and  $\bar{P}_0$  is the degree of polymerization in the absence of a chain-transfer agent. Chain-transfer constants have been computed for a variety of systems by preparation of graphs of  $1/\bar{P}$  versus  $[S]/[M]$ .

In some polymerization systems, it is necessary to use more than one solvent to avoid phase separation during the course of the polymerization runs. The polymerization of ethylene is one such system where propane and butane may be used separately or together as solvents.<sup>2</sup> Since chain transfer to solvent occurs for both of these solvents, eq. (1) must be extended to the general form for  $n$  transfer agents shown in eq. (2).

$$1/\bar{P} = 1/\bar{P}_0 + \sum_{i=1}^n C_{si}([S_i]/[M]) \quad (2)$$

### Estimation of Chain-Transfer Constants

While graphical methods for determining the chain-transfer constant have been used extensively where the determination of a single chain-transfer constant was required, the use of graphical methods is difficult when more than one chain-transfer constant is to be computed. An alternate method for determining one or more chain-transfer constants is to utilize the method of least squares.

The method of least squares to compute chain-transfer constants is attractive for several reasons. These include the possibility of automation of the calculation procedure by using a digital computer and the securing of a valid measure of the precision with which the computed values of  $1/\bar{P}_0$  and the chain-transfer constants are known.

The computations required in the use of the method of least squares are described in most numerical analysis and elementary statistics textbooks, however, the assumptions implicit in the use of this procedure are not often stated. These are shown below in the order of their importance.

It is assumed that: (1) the mathematical model used describes the physical system; (2) the errors in the dependent variables are independent of each other; (3) the variances of the errors in the dependent variables are constant for all observations; (4) the distribution of the errors in the dependent variables is described by the normal (Gaussian) distribution function. The user of the method of least squares is obligated to establish the validity of these assumptions for the system with which he is working.

Sufficient work has established that the model derived by Mayo is correct, hence assumption (1) is not in jeopardy. The validity of assumption (2) about the independence of the errors is frequently compromised by commonly used experimental practices. The consequences of assumption (2) being invalid can be serious, and may result in the computed values of the chain-transfer constants being biased.

The techniques introduced by Fisher<sup>3</sup> of making the experimental runs in a random order and other good experimental practices discussed by Wilson<sup>4</sup> assure that any nonindependence in the errors in successive experi-

mental runs will not affect the validity of inferential statements concerned with the calculated chain-transfer constants.

Questions about the validity of assumptions (3) and (4) are important in the chain-transfer computational (or graphical) procedures, because the assumptions made determine how the data are to be weighted in the computational procedures used to calculate the chain-transfer constants. For example, if it can be shown that the variances of the observed values of  $1/\bar{P}$  are proportional to the numerical values of  $1/\bar{P}$ , then the data should be weighted differently in the calculation procedure than for the situation where the variances of the observed values of  $1/\bar{P}$  are constant regardless of the numerical value of  $1/\bar{P}$ . In using graphical methods the user often utilizes this information without realizing that it is being done.

There are two principle sources of error in the observed values of  $1/\bar{P}$ . One source of error stems from the procedures employed in the determination of the molecular weight of the polymer made in the experimental run. The other source of error arises from the experimental run itself. Both of these sources of error must be considered in attempting to determine how to treat the data so that the variance of each of the observations of the dependent variables to be fitted is approximately constant.

If it can be shown from a sequence of repetitive experimental polymerization runs and from a sequence of repetitive measurements of the molecular weight of a polymer that the principal cause of variation in the results arises from the run to run variation, then there is reason to expect that  $1/\bar{P}$  is more likely to be normally distributed and to have constant variance than is  $\bar{P}$ . This expectation arises from the fact that variations in pressure, temperature, and concentrations of reactants have a linear or nearly linear theoretical relationship with  $1/\bar{P}$ .

If the principal cause of variation in the results arises from the analytical procedures used to determine the molecular weight of the polymer, then the question about which form of  $\bar{P}$  is more likely to be normally distributed and have constant variance can be answered (usually) by knowledge about the analytical procedures used. Thus, if a colligative property measurement is used to determine the polymer molecular weight, then  $1/\bar{P}$  is more likely to be normally distributed with constant variance than is  $\bar{P}$ . If, however, viscosity methods are used to determine the molecular weight, the converse is true.

Clearly, if a least-squares method of computation is to be used validly, it is important to determine whether it is  $\bar{P}$  or  $1/\bar{P}$  which more nearly fits the least squares assumptions. Thus, if  $1/\bar{P}$  has constant variance, then the model to which the data should be fitted is eq. (2). However, if  $\bar{P}$  has constant variance, then the data should be fitted by using eq. (3).

$$\bar{P} = 1/\left\{1/\bar{P}_0 + \sum_{i=1}^n C_{si}([S_i]/[M])\right\} \quad (3)$$

Equation (3) weights the data during the calculation differently than does eq. (2) and also requires the use of a nonlinear rather than a linear least-squares procedure.



### Transformation of Variables

It is permissible, as long as assumptions (1)–(4) of the least-squares treatment are preserved, to transform the parameters which are being calculated. Thus, in eq. (4), a transformation has been made such that the value  $t$  is computed rather than  $C_{s_i}$ , where  $t$  is the natural logarithm of the chain-transfer constant.

$$1/\bar{P} = 1/\bar{P}_0 + \sum_{i=1}^n e^t([S_i]/[M]) \quad (4)$$

where

$$t_i = \ln C_{s_i}$$

The reason for making this transformation is that in subsequent papers we shall wish to compute activation energies and volumes of activation for chain transfer. In both of these calculations the logarithm of the chain-transfer constant is involved. When a calculation in the form shown in eq. (4) has been performed, the standard deviation of the logarithm of the chain-transfer constant is directly calculable. A method is available<sup>5</sup> for approximating from the standard deviation of the logarithms the confidence that can be attached to these activation energies and volumes of activation. If the chain-transfer constant were determined by eq. (2), there would be no known method of estimating the amount of uncertainty in activation energies and volumes of activation.

Equation (4), like eq. (3), requires the use of a nonlinear least-squares procedure. Where this is necessary, we prefer the method of Marquardt.<sup>6</sup>

## EXPERIMENTAL

All experimental work was carried out in reaction system 2\* as previously described.<sup>7</sup> The pertinent data are given in Table I. The column in the table labeled  $1/\bar{P}$  represents the reciprocal degree of polymerization as calculated from the polymer melt index as previously described.<sup>7,8</sup> The reaction is carried out in a single, supercritical phase.<sup>9</sup>

### FITTING OF DATA

Repetition of experimental runs and molecular weight measurements led us to conclude that the principal cause of variation in our results is in the

\* A referee raised the question why there was a change in the base  $1/\bar{P}$  in changing from system 1 to 2,<sup>7</sup> inasmuch as the sureness with which  $1/\bar{P}_0$  is known is a substantial point in this and succeeding papers. There was strong evidence that, for some unknown reason, gaseous transfer agents were not being completely and reproducibly added to the reactor in system 1. Several changes were made to overcome this problem. Following these changes, all evidence suggested that reproducible, quantitative addition of gaseous additives was achieved. Thus, the base  $1/\bar{P}$  in system 2 is reliable, and the base  $1/\bar{P}$  in system 1 was slightly in error due to incomplete additive addition.

TABLE I. Chain-Transfer Data at 1360 Atm, 130°C, 0.2 mmole/l. Di-*tert*-butyl Peroxide Initiator

Feed composition <sup>a</sup>			Melt index <sup>b</sup>	$1/\bar{P} \times 10^5$	Residual $\times 10^5$	Data source
Ethylene, mole-%	Propane, mole-%	Butane, mole-%				
87.93	11.92	—	0.0525	58.9	-2.2	c
87.82	12.02	—	0.0818	61.0	-0.5	c
"	"	—	0.0824	61.0	-0.5	e
87.02	12.82	—	0.111	62.4	-2.2	d
85.47	14.37	—	0.463	70.7	-0.2	e
"	"	—	0.428	70.2	-0.7	e
"	"	—	0.548	71.9	0.9	e
85.42	14.43	—	0.296	67.9	-3.3	e
"	"	—	0.580	72.3	1.1	e
"	"	—	0.435	70.3	-0.8	e
"	"	—	0.394	69.7	-1.5	e
"	"	—	0.410	70.0	-1.2	c,d
"	"	—	0.553	71.9	0.7	c,d
"	"	—	0.502	71.3	0.1	c,d
82.74	17.10	—	3.75	87.7	5.1	d
"	"	—	3.87	88.1	5.5	d
"	"	—	1.70	80.4	-2.2	d
"	"	—	2.37	83.4	0.7	d
79.81	20.04	—	7.60	95.5	-0.6	e
"	"	—	9.52	98.3	2.2	e
"	"	—	6.54	93.7	-2.3	e
79.65	20.20	—	6.08	92.9	-3.9	d
79.16	20.68	—	11.3	100.	1.4	d
77.03	22.82	—	22.6	111.	0.8	d
88.57	6.41	4.86	0.361	69.1	0.1	e
85.75	8.02	6.08	3.73	87.7	4.3	e
81.05	10.69	8.11	21.9	110.	0.7	e
85.36	4.76	9.73	8.00	92.2	-1.0	e
82.49	6.41	10.94	19.9	109.	-0.6	e
84.14	4.76	"	11.0	100.	-1.2	e
85.69	3.21	"	6.07	92.9	-1.6	e
90.12	—	9.73	0.904	75.4	2.1	e
"	—	"	0.855	75.0	1.6	e
88.98	—	10.86	1.40	78.8	-1.6	e
88.90	—	10.94	1.88	81.3	0.4	e
"	—	"	1.82	81.0	0.2	e
"	—	"	1.54	79.6	-1.3	e
87.76	—	12.08	6.35	93.4	5.4	e
86.47	—	13.38	7.38	95.2	-1.3	e
84.85	—	15.00	16.6	106.	-1.5	e
82.49	—	17.35	48.9	124.	0.5	e
"	—	"	43.8	122.	-1.7	e
82.33	—	17.51	48.9	124.	-0.7	e
82.21	—	17.63	54.8	127.	0.8	e

<sup>a</sup> The balance of the feed, usually less than 0.2%, was benzene used as initiator solvent.

<sup>b</sup> See Mortimer<sup>7,8</sup> for the use of melt index data to estimate  $\bar{M}_n$ .

<sup>c</sup> Data of Mortimer.<sup>7</sup>

<sup>d</sup> Data of Mortimer.<sup>9</sup>

<sup>e</sup> This work.

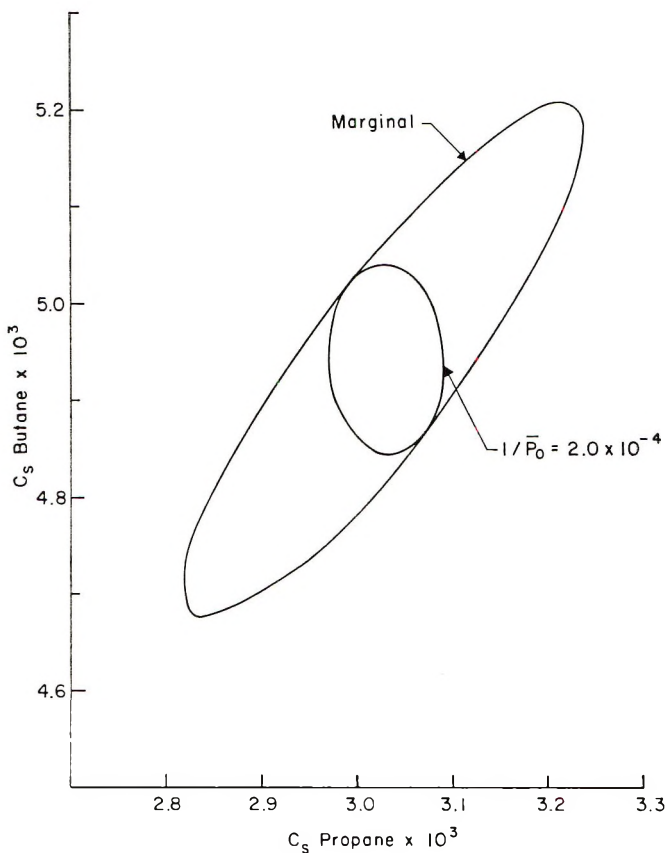


Fig. 1. Approximate 95% confidence limits with  $1/\bar{P}_0$  fixed and not fixed.

conducting of the experimental runs rather than in the molecular weight measurements. Therefore, the data in Table I were fitted to eq. (2) where  $n = 2$ . The best values obtained and their simple standard deviations were:  $C_{s1}$  (propane) =  $0.00302 \pm 0.00008$ ;  $C_{s2}$  (butane) =  $0.00494 \pm 0.00009$ ;  $1/\bar{P}_0 = 0.000200 \pm 0.000015$ . The column in Table I labeled "Residual" is the difference between the observed value of  $1/\bar{P}$  and the computed value of this variable using the constants shown above.

Since the three parameter values  $C_{s1}$ ,  $C_{s2}$ , and  $1/\bar{P}_0$  were jointly determined, the error limits for the parameter estimates are properly defined by joint confidence limits rather than the simple confidence limits given above. This point is illustrated in Figures 1 and 2. Figure 1 shows a confidence interval for the chain-transfer constants of propane and butane, that is, the joint confidence limits for these two parameters without regard for the value of  $1/\bar{P}_0$ . This is calculated from an approximation of the marginal distribution function. The small confidence interval labeled  $1/\bar{P}_0 = 2.0 \times 10^{-4}$  is the confidence limit for these two parameters at the point where

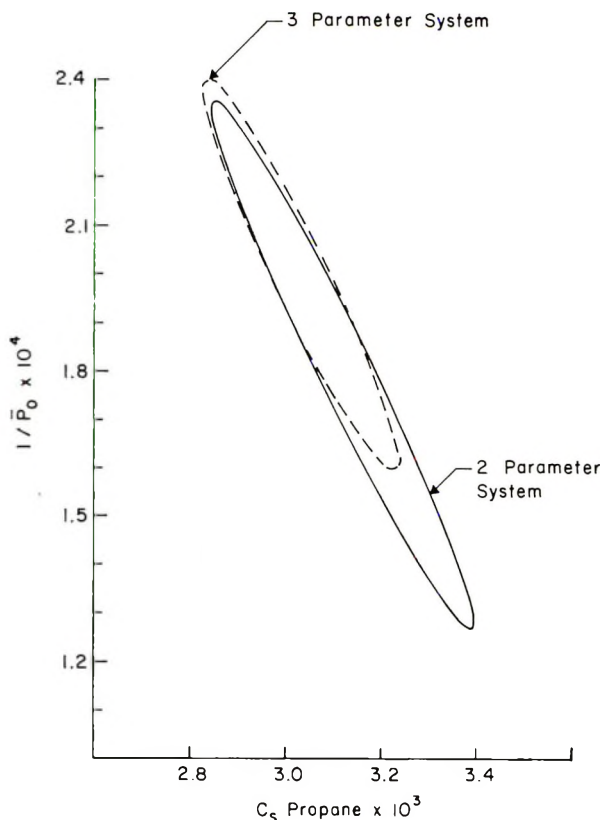


Fig. 2. Approximate confidence limits for three-parameter system and joint confidence contour for two-parameter system in which butane data were not used.

$1/\bar{P}_0$  is fixed at its most probable value. This is calculated from the conditional distribution given  $1/\bar{P}_0$ . From this figure it can be seen that the value given to  $1/\bar{P}_0$  has a considerable effect on the confidence limits for the chain-transfer constants for propane and butane.

Some knowledge of the magnitude of  $1/\bar{P}_0$  lessens considerably the uncertainty associated with the chain-transfer constants. This is illustrated even more clearly in Figure 2, in which the same information is shown in a different manner. In this figure, confidence limits for  $1/\bar{P}_0$  and  $C_s$  for propane are shown. One curve was obtained from data containing information only about  $1/\bar{P}_0$  and  $C_s$  for propane by excluding data on runs containing butane. The other curve was obtained from all of the data and thus contains information on  $1/\bar{P}_0$  and both of the chain-transfer constants without regard to the value of  $C_s$  for butane. It was calculated from an approximation of the marginal distribution function over all values of  $C_s$  for butane. These latter data clearly provide a more precise estimate for  $1/\bar{P}_0$ , and hence also reduce the uncertainty associated with  $C_s$  for propane.

## DISCUSSION

It will be noted that the data in Table I are arranged in order of changing feed concentration. It will be further noted that, with one minor exception, the residuals are randomly distributed as to their algebraic sign and are of comparable magnitude over the entire range of feed compositions studied. The one area of exception is at low propane concentrations in the absence of butane where phase separation has previously been postulated.<sup>9</sup> The excellence of fit of the model to the data, as indicated by this pattern in the residuals, is evidence of the correctness of eq. (2) and the attendant assumptions.

The relatively large joint uncertainty in  $1/\bar{P}_0$  and  $C_s$  is ample reason why  $1/\bar{P}_0$  should be determined as accurately as possible. Were it not for phase separation, a direct determination of  $1/\bar{P}_0$  would be made. Figure 2 shows that the simultaneous use of two transfer agents reduces the uncertainty in  $1/\bar{P}_0$  when a direct measurement in the absence of any transfer agent is not possible.

From Figure 1 it can be seen that minor variations in the concentration of one transfer agent and uncertainty in its transfer content will have a relatively small effect on the calculated transfer constant of a second transfer agent, at least in our system. Thus, although there is some uncertainty in the absolute values of  $C_s$  because of the joint uncertainty between  $C_s$  and  $1/\bar{P}_0$ , there is less uncertainty between the relative values of different transfer agents. To our knowledge, this paper represents the first application of the use of joint confidence contours to represent the degree of uncertainty in the measurement of chain transfer constants. It is clear that simple  $\pm$  values did not convey a true picture of the uncertainty in the parameters estimated from the data in Table I. The use of techniques such as illustrated in the paper would seem to be essential whenever  $1/\bar{P}_0$  cannot be directly measured or when more than one transfer agent is used simultaneously.

## References

1. F. R. Mayo, *J. Amer. Chem. Soc.*, **65**, 2324 (1943).
2. P. Ehrlich and J. J. Kurpen, *J. Polym. Sci. A*, **1**, 3217 (1963).
3. R. A. Fisher, *Statistical Methods for Research Workers*, 10th ed., Oliver and Boyd, London, 1948.
4. E. B. Wilson, Jr., *An Introduction to Scientific Research*, McGraw-Hill, New York, 1952.
5. B. L. Welch, *Biometrika*, **34**, 28 (1947).
6. D. W. Marquardt, *J. Soc. Ind. Appl. Math.*, **1963**, 431.
7. G. A. Mortimer, *J. Polym. Sci. A-1*, **4**, 881 (1966).
8. G. A. Mortimer, G. W. Daues, and W. F. Hamner, *J. Appl. Polym. Sci.*, **8**, 839 (1964).
9. G. A. Mortimer, *J. Polym. Sci. A-1*, **4**, 1895 (1966).

Received October 20, 1969

Revised December 17, 1969

## Preparation, Reaction, and Polymerization of the Nuclear Chlorinated $\alpha,\alpha'$ -Xylylene Diallyl Ethers\*

J. P. STALLINGS, *T. R. Evans Research Center, Diamond Shamrock Corporation, Painesville, Ohio 44077*

### Synopsis

A process has been developed in which the diallyl ethers of the tetrachloroxylenes are produced in 90-95% yield. The starting materials are the appropriate chlorinated xylene, sodium hydroxide, and allyl alcohol. Epoxidation of the diallyl ethers with perbenzoic acid gave the corresponding diepoxides. The above diallyl ethers are capable of entering into both homo- and copolymerization reactions in the presence of free-radical initiators. With 2% *tert*-butyl perbenzoate, the diallyl ethers are polymerized to soluble prepolymers at 130-138°C in about 1 hr. These prepolymers can be formulated with appropriate reinforcing materials and peroxide initiator to give hard, tough thermosetting resins. The optimization of various molding and formulation conditions is also described.

### INTRODUCTION

The polymerization of diallylic monomers to form soluble, fusable prepolymers has been shown with diallyl phthalate and diallyl isophthalate.<sup>1-5</sup> These prepolymers find utility commercially when formulated and cured to a thermosetting resin.<sup>6-11</sup> Such resins are used for specialty applications where good dimensional stability, optical clarity and heat resistance are required.

It is the purpose of this work to describe polymerization of some new diallylic xylene ethers to thermosetting resins. Our interest in allyl resins was motivated by activity in xylene chemistry<sup>12</sup> and the production of diallylic ethers from various chlorinated xylenes. The scope of the work includes the preparation and reaction of the starting monomers, prepolymerization of these monomers, compounding of the prepolymers, and final cure of the formulated prepolymer. The properties of the finished resins are also discussed.

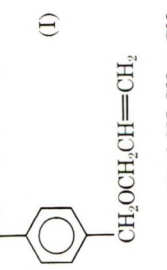
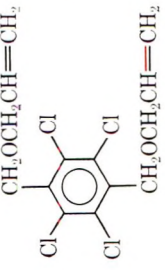
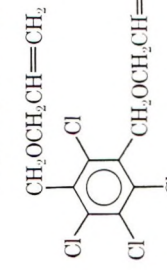
### EXPERIMENTAL

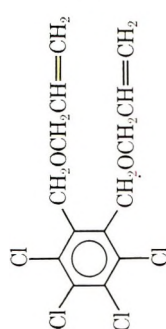
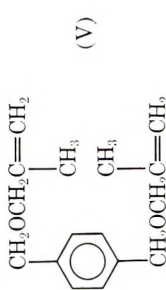
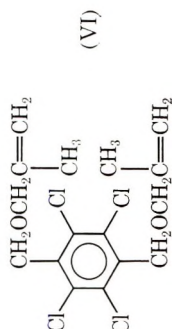
#### Reagents

All chemicals were of reagent grade. The starting chlorinated xylenes had melting or boiling ranges of less than 2°C.

\* Presented at the 158th Meeting of the American Chemical Society, Division of Organic Coatings and Plastics Chemistry, New York, 1969.

TABLE I  
 Preparation of the Diallyl Ethers

Reactants		Conditions		Product					
Dihalide (1 mole)	Alcohol (1 liter)	Base (2 mole)	Temp, °C	Reaction time, hr	Product	Mp, °C, or bp, °C/mm Hg	Yield, % (isol.)	Analysis, (%) Calcd	Found
<i>p</i> -Xylylene dichloride	allyl	NaOH	96	6	 (I)	107-109/0.5 mm	77	77.1 C	77.6 C
$\alpha,\alpha',2,3,5,6$ - Hexachloro- <i>p</i> - xylene	allyl	NaOH	96	8	 (II)	92.3-93.3 (lit. <sup>14</sup> 88-90)	87		
$\alpha,\alpha',2,4,5,6$ - Hexachloro- <i>m</i> - xylene	allyl	NaOH	96	8	 (III)	56.2-58.2	80	47.2 C 4.0 H 40.0 Cl	47.1 C 4.1 H 39.8 Cl

$\alpha,\alpha'$ -Dibromo-3,4,5,6-tetra-chloro- <i>o</i> -xylylene	allyl	NaOH	96	8	 <p>(IV)</p>	165/0.5 mm 34-37°C (lit. <sup>13</sup> 154/0.2 mm)	70
<i>p</i> -Xylylene dichloride	methallyl	NaOH	114	5	 <p>(V)</p>	123-128/0.5-0.7 mm	83 78.0 C 9.0 H 9.2 H
$\alpha,\alpha'$ -2,3,5,6-Hexachloro- <i>p</i> -xylylene	methallyl	NaOH	114	7.5	 <p>(VI)</p>	54.5-55.5	48 50.0 C 49.1 C 4.7 H 4.7 H 37.0 Cl 37.6 Cl



### Physical Measurements

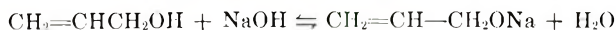
Melting points were determined with an open capillary in an electrically heated oil bath and are uncorrected.

### Preparation of the Diallyl Ethers

All of the allylic monomers were prepared in a similar manner. Sodium hydroxide (2 mole) was dissolved in one liter of the allyl alcohol (containing 0.010 g hydroquinone) by heating in a three-necked, round-bottomed flask fitted with thermometer, mechanical stirrer and reflux condenser. After the sodium hydroxide had dissolved, the solution was cooled to about 40°C. A 2-*eq.* portion of the chlorinated xylene was added to the flask. The stirred slurry was heated to reflux and the temperature was controlled carefully, since at 50–70°C (depending on the dihalide), an exothermic reaction occurred. At this point, it was necessary to turn off the heating mantle or remove it until the temperature reached a maximum. The heating was then continued to reflux the mixture with stirring. A reflux time of 5–8 hr was required for 90–95% conversion to the desired diallyl ether.

Liquid products could be easily separated from the excess allyl alcohol by fractional distillation. With solid products, purification was accomplished by: (1) vacuum distillation of one-half of the allyl alcohol followed by precipitation of the residue with water, filtration, and recrystallization from methanol, or (2) treatment of the reaction mixture with water to precipitate the product as above, followed by distillation of the alcohol.

All of the above techniques necessarily involve the removal of an alcohol–water azeotrope since water is formed in the reaction:



In order to distill the anhydrous alcohol, it is necessary to introduce an additional low-boiling component which will azeotrope with water at a boiling temperature lower than the boiling temperature of any of the pure components. Chloroform performed well in this application, since it fits the above requirements, is inert, and is completely soluble in the reaction mixture. In practice, a Dean-Stark trap and reflux condenser are attached to the reaction flask, and reflux is maintained until no further water is collected. The chloroform and alcohol (which do not azeotrope) are then fractionated with a packed insulated column and variable take-off head. The column is 50 × 2 cm packed with 8 mm glass helices. By using the above method, an alcohol recovery of about 80% is realized in most preparations. Table I summarizes the data.

Several of the diallyl monomers were epoxidized with perbenzoic acid in chloroform or benzene. Higher yields were observed in benzene. Table II shows the yields and purities of the diepoxides. Oxirane oxygen was titrated via HBr dissolved in acetic acid with monochlorobenzene as the solvent for the diepoxide. Crystal violet was used as the indicator. Figure 1 shows that the epoxidation reaction obeys second-order kinetics and that unchlorinated monomer (I) reacts faster than chlorinated monomer (II).

TABLE II  
Epoxidation of the Diallyl Ethers

Starting diallyl ether	Yield of crystallized diepoxide, %	Purity via oxirane oxygen, %	Mp, °C, or bp, °C/mm Hg
$\alpha,\alpha'$ -Diallyloxy-3,4,5,6-tetrachloro- <i>o</i> -xylene (IV)	59	95	77.8-77.9
$\alpha,\alpha'$ -Diallyloxy-2,4,5,6-tetrachloro- <i>m</i> -xylene (III)	90	92	88.8-90.8
$\alpha,\alpha'$ -Diallyloxy-2,3,5,6-tetrachloro- <i>p</i> -xylene (II)	67	99	123-125
$\alpha,\alpha'$ -Diallyloxy- <i>p</i> -xylene (I)	78	91	188-204/- 1.8-2.9 mm

### Copolymerization of the Diallyl Ethers

Although the diallyl ethers exhibited low rates of polymerization, they copolymerized readily with several olefinic monomers. The data are seen in Table III.

It can be seen that both maleic anhydride and ethylene glycol maleate were copolymerized with the diallyl ethers. Extraction studies showed that both monomers had entered into the polymerization. It is believed that a true copolymer is formed since maleic anhydride does not homopolymerize under the conditions employed. The unreacted maleic anhydride is present in 10% to 49%, depending on conditions and monomers used.

### Homopolymerization of the Diallyl Ethers

Samples of the monomer (III) were tested for thermal stability as a preliminary examination of polymerization behavior. The monomer shows

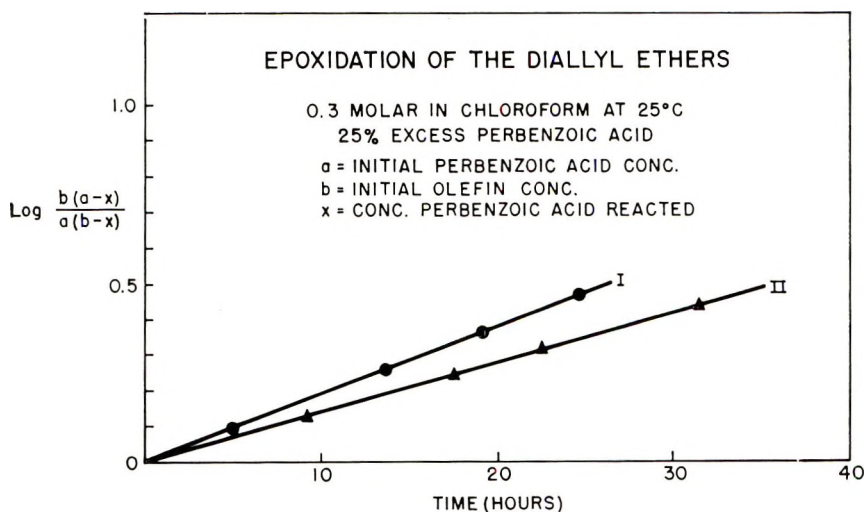


Fig. 1. Epoxidation of the diallyl ethers.

TABLE III  
Copolymerization of Diallyl Ethers

Diallyl ether Moles	Diallyl ether Type	Comonomer Moles	Comonomer Type	Initiator (%)	Temp, °C	Time, hr	Polymer appearance	Diallyl ether lost in CHCl <sub>3</sub> extraction, wt-%	Comonomer lost in water extraction, wt-%
0.10	I	0.10	Maleic anhydride	Di- <i>tert</i> - butyl peroxide	105	1.5	Clear, hard	—	49
0.10	II	0.10	Maleic anhydride	Di- <i>tert</i> - butyl peroxide	95	0.75	Clear, hard unburnable	2	40
0.10	V	0.10	Maleic anhydride	Di- <i>tert</i> - butyl peroxide	120	2.0	Clear, hard	9	10
0.10	VI	0.10	Maleic anhydride	Di- <i>tert</i> - butyl peroxide	120	2.0	Clear, hard unburnable	5	10
0.003	I	0.0083	Ethylene glycol maleate	Di- <i>tert</i> - butyl peroxide	150	8	Clear, hard	0	—
0.0040	II	0.0083	Ethylene glycol maleate	Di- <i>tert</i> - butyl peroxide	150	8	Clear, hard burned	0	—
0.0030	I		Selectron 5003L <sup>a</sup>						

<sup>a</sup> Ethylene glycol maleate polyester (PPG Industries), 1.7 g.

some sensitivity to air oxidation and polymerization at 150–200°C but shows excellent stability under nitrogen at 200°C for 8 hr. It was thus indicated that prepolymers might be prepared in a controlled manner without the interference of premature polymerization or gelation.

A brief study was undertaken to determine the relative reactivity toward polymerization of the isomers of the  $\alpha,\alpha'$ -diallyloxy tetrachloroxylenes. Thus, the *ortho*, *meta*, and *para* isomers were homopolymerized at 150°C with 5% di-tertiary butyl peroxide. The time was recorded in which each monomer polymerized to give a hard infusible polymer. The following data were recorded: *ortho*, 56 hr; *meta*, 7.0 hr; *para*, 8.5 hr. The order of reactivity towards homopolymerization was then *meta* > *para*  $\gg$  *ortho*.

Consequently,  $\alpha,\alpha'$ -diallyloxy-2,4,5,6-tetrachloro-*m*-xylene (III) and  $\alpha,\alpha'$ -diallyloxy-2,3,5,6-tetrachloro-*p*-xylene (II) were selected for further polymerization studies.

### Prepolymers of the Diallyl Ethers

Figure 2 shows the prepolymer reactor. The polymerization temperature could be controlled  $\pm 0.5^\circ\text{C}$  and polymerization could be quenched from 138°C to 120°C in 2 min—representing considerable decrease in initiator activity.

All prepolymers of II and III were prepared in three-necked, round-bottomed flasks or glass resin kettles. Since the monomers melt at 93 and 58°C, all prepolymers were prepared in bulk above 93°C. The polymerization could be followed by the use of a capillary viscometer immersed in the prepolymer melt. By using a 1.00 mm capillary at 130°C, the melt viscosity (poises) was  $8.2 \times$  efflux time (sec) from a height of 33 mm. Table IV shows the experimental data. The scale was 0.5–5.0 moles and all polymerizations were carried out under a nitrogen blanket. The pre-

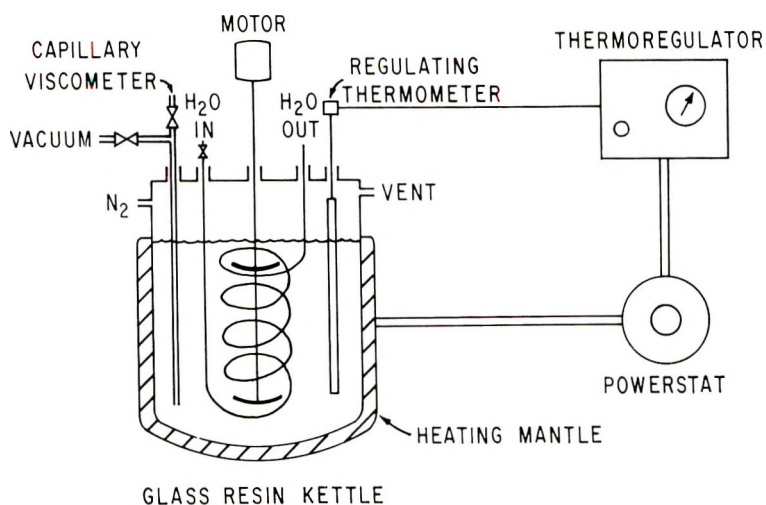


Fig. 2. Prepolymer Reactor.

TABLE IV  
Preparation of Diallyl Ether Prepolymer

Mono- mer	Initiator <sup>a</sup> Type	Wt-%	Temp, °C	Poly- merization time, min	Final efflux time, sec <sup>b</sup>	Conversion, %	$\bar{M}_n^c$	Bromine no.
II	TBPB	3.0	130	84	20	13.5	—	—
II	DTBP	3.0	130	51	123	25.7	—	—
III	Bz <sub>2</sub> O <sub>2</sub>	4.0	95	135	2.4	21.5	3436	339
III	DTBP	2.0	130	121	10.5	43.0	5645	429
III	DTBP	2.0	136	75	10.6	42.0	4979	416
III	DTBP	2.0	138	52	13.0	44.0	7974	391
III	DTBP	2.0	138	58	3.6	41.0	5547	392
III	DTBP	2.0	138	70	3.6	37.6	8436	189
III	DTBP	2.0	138	52	1.6	32.0	6185	565
III	DTBP	2.0	138	61	1.2	25.0	6900	415
III	DTBP	2.0	138	67	2.0	30.0	5500	348

<sup>a</sup> TBPB = *tert*-butyl perbenzoate; DTBP = di-*tert*-butyl peroxide; Bz<sub>2</sub>O<sub>2</sub> = benzoyl peroxide.

<sup>b</sup> By use of a 1.00-mm capillary at polymerization temperature at 33 mm height.

<sup>c</sup> By osmometry.

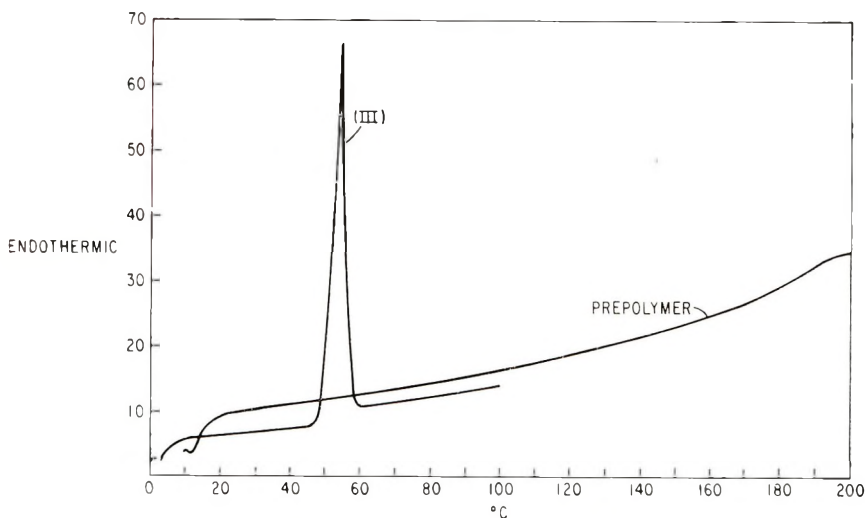


Fig. 3. Differential scanning calorimeter curve.

polymer was isolated from monomer either by precipitation from methanol (in which monomer is soluble), or by distillation of monomer via a molecular still at  $190^{\circ}\text{C}$  at  $5\ \mu$  pressure. The prepolymer residue was allowed to cool and was then pulverized.

A differential scanning calorimeter was used to characterize the monomer and prepolymer shown in Figure 3. The thermogram shows no evidence of residual monomer in the amorphous prepolymer.

#### Formulation and Cure of $\alpha,\alpha'$ -Diallyloxy-2,4,5,6-tetrachloro-*m*-xylene (III) Prepolymer

A brief study was undertaken to assess the optimum initiator type, concentration and cure temperature required for final polymerization of prepolymers (III). The prepolymers were formulated with 5 phr each of initiator and lauric acid mold release agent. The samples were compression molded with a Buehler press at 4000 psi for 5 min. Sample size was  $1 \times \frac{1}{8}$  in. Table V shows the results of this study.

In order to compound fillers with the prepolymer, optimum mixing was achieved by: (1) physical mixing in a Hobart Mixer followed by (2) hot-roll milling to effect good filler-prepolymer interaction, and (3) chopping to give final prepolymer compound. The results of this work are seen in Table VI.

### DISCUSSION

The high yields of the diallyl ethers are not unexpected since benzylic halides are quite reactive in  $\text{S}_{\text{N}}2$  reactions. In addition, the allylate anion is resonance stabilized and available for the desired Williamson reaction:



TABLE V  
Formulation and Cure of  $\alpha, \alpha'$ -Diallyloxy-2,4,5,6-Tetrachloro-*m*-xylene Prepolymers

Initiator	Mold temperature, °F	Mold leakage	Sample appearance		
			Continuous button	Strength	Appearance
Benzoyl peroxide	200	Yes	No	Weak	Clear
MEK peroxide	250	No	Yes	Weak	Clear
<i>Tert</i> -butyl perbenzoate	300	No	Yes	Strong	Clear
Di- <i>tert</i> -butyl peroxide	350	No	Yes	Strong	Discolored
Dicumyl peroxide	400	No	Yes	Strong	Discolored

The precipitation of sodium chloride also adds to the driving force of the reaction. Previous workers<sup>13,14</sup> have found it necessary to use sodium and allyl alcohol as the base for the reaction. The present method using NaOH and allyl alcohol offers a favorable cost advantage.

As the bulk prepolymerization proceeds, there is considerable melt viscosity increase, as shown in Figure 4. Similar results are seen (Fig. 5) when efflux time is plotted versus conversion.

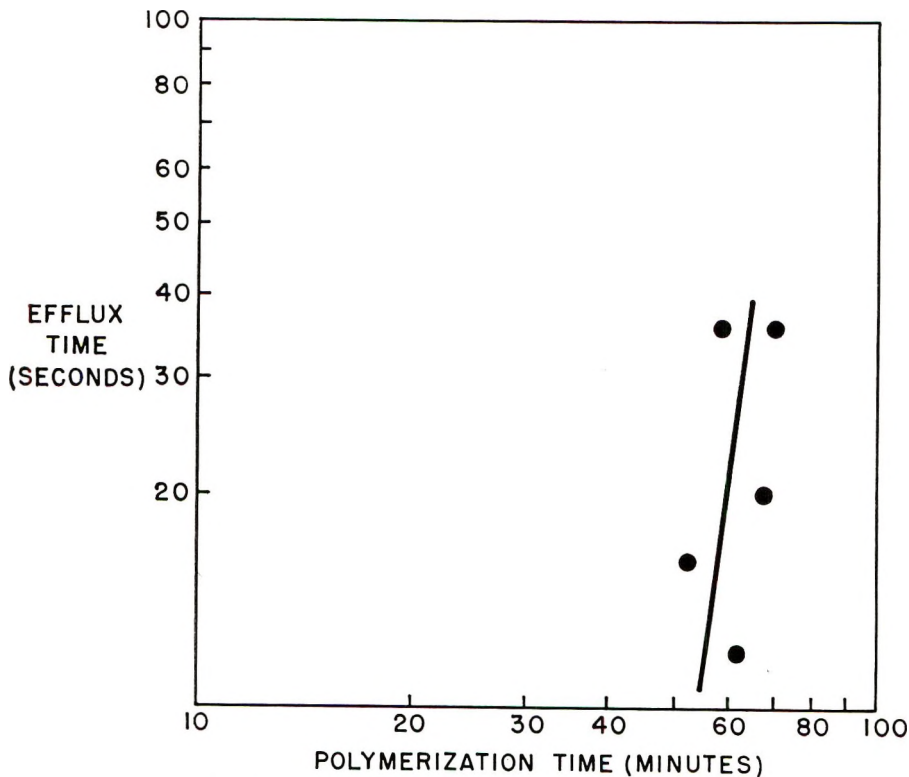


Fig. 4. Efflux time vs. polymerization time for monomer III.

TABLE VI  
 Compounding and Final Cure of  $\alpha,\alpha'$ -Diallyloxy-2,4,5,6-Tetrachloro-*m*-xylylene Prepolymers

Ingredient	Composition, parts by weight											
	16	16	16	16	16	16	16	16	116	116	116	116
III prepolymer	100	100	100	100	100	100	100	100	116	116	116	116
1/8" in. Fiberglass	107	107	107	107	107	107	107	107	107	107	107	107
Wollastonite F-1	27	27	27	27	27	27	27	27	27	27	27	27
Lauric acid	4	4	4	4	4	4	4	4	4	4	4	4
Sb <sub>2</sub> O <sub>3</sub>	8	8	8	8	8	8	8	8	8	8	8	8
TBP <sup>a</sup>	8	8	8	8	8	8	8	8	8	8	8	8
DTBP <sup>b</sup>	—	—	—	—	—	—	—	—	—	—	—	—
Two-roll milling at 220°F	Banded	Banded	Banded	Banded	Banded	Banded	Banded	Banded	No band	No band	No band	No band
Compression in molding of chopped band at 4000 psi	Hard	Hard	Hard	Hard	Hard	Hard	Hard	Hard	—	—	—	—
315°F.	disk	disk	disk	disk	disk	disk	disk	disk	—	—	—	—
350°F	Hard	Hard	Hard	Hard	Hard	Hard	Hard	Hard	—	—	—	—
	disk	disk	disk	disk	disk	disk	disk	disk	—	—	—	—

<sup>a</sup> *Tert*-butyl perbenzoate.

<sup>b</sup> Di-*tert*-butyl peroxide.



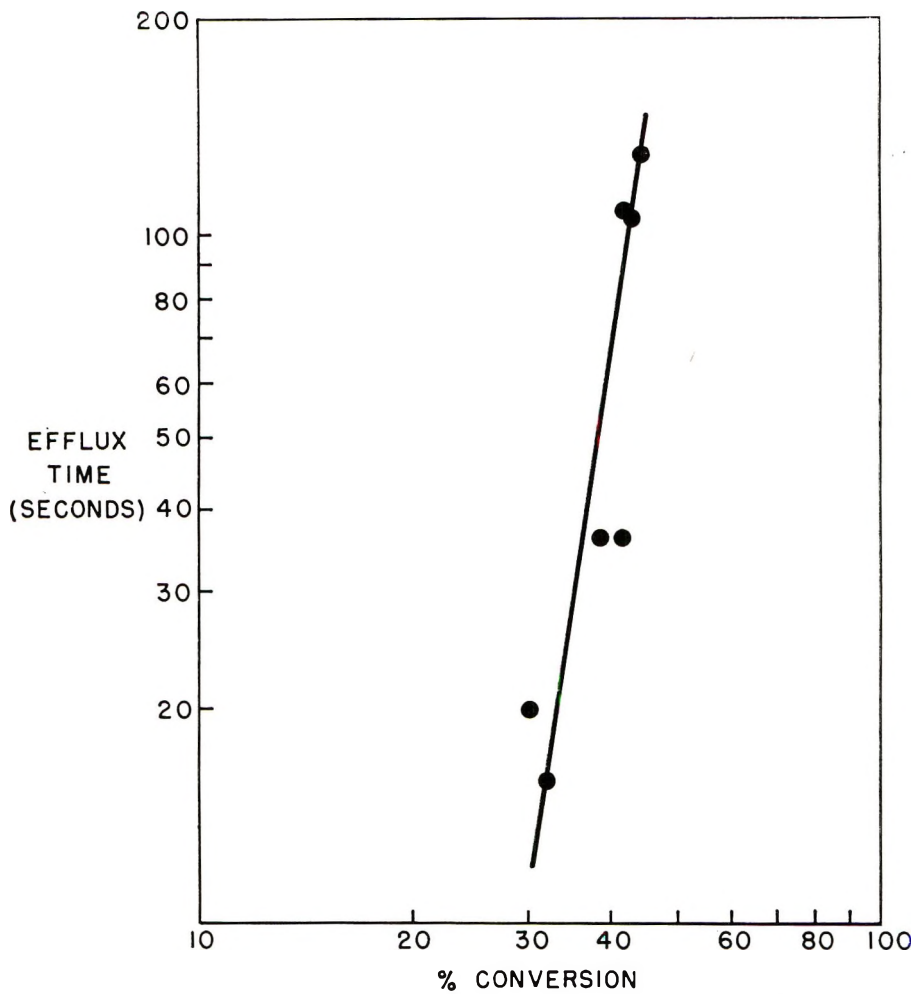


Fig. 5. Efflux time vs. % conversion to prepolymer for monomer III.

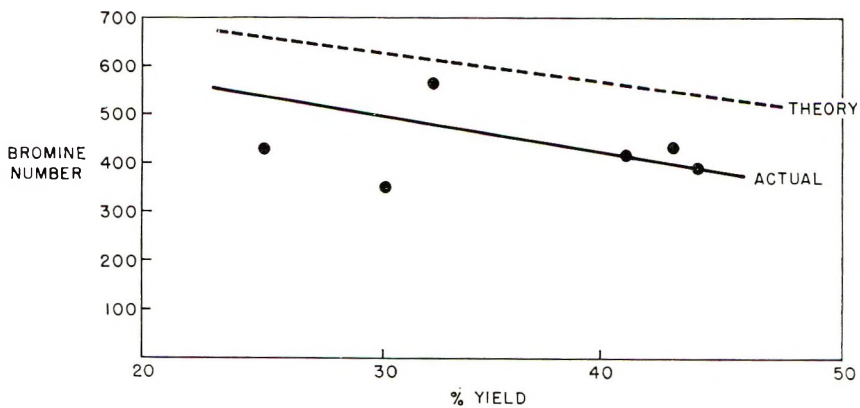


Fig. 6. Bromine number vs. conversion for monomer III.

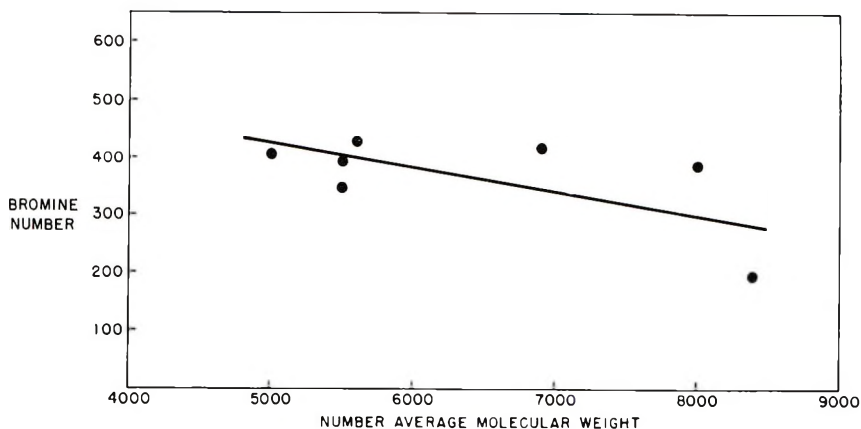
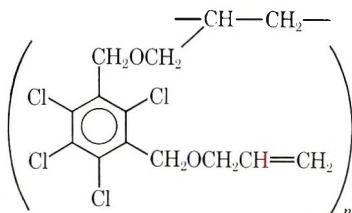


Fig. 7. Bromine number vs. number-average molecular weight for monomer III.

The optimum conditions for the prepolymerization reaction are 95–138°C depending upon the initiator used. Although all of the prepolymer were soluble in chloroform, the lower than calculated bromine numbers shown in Figure 6 indicate a small amount of branching, crosslinking, or cyclization<sup>15</sup> had occurred in some cases. Increased scatter at high molecular weights, shown in Figure 7, is believed caused by this phenomenon. By analogy with diallyl phthalate, the predominant prepolymer structure is



with  $n = 10\text{--}24$ .

The final polymerization of  $\alpha,\alpha'$ -diallyloxy-2,4,5,6-tetrachloro-*m*-xylene prepolymer involved an initiator screening study. At 200–250°F with benzoyl peroxide or methyl ethyl ketone peroxide, the prepolymer could not be polymerized in a compression mold with a sufficient rate or conversion to prevent mold leakage or formation of weak specimens. At 350–400°F, with di-*tert*-butyl peroxide or dicumyl peroxide, discoloration occurred. The best balance of conditions for molding employed tertiary butyl perbenzoate at 300°F. Under these conditions, a strong, clear thermoset was obtained with no evidence of thermal degradation.

## CONCLUSIONS

A process has been developed in which the diallyl ethers of the tetrachloroxylenes are produced in 90–95% yield. The starting materials are the appropriate chlorinated xylene, sodium hydroxide and allyl alcohol.

The above diallyl ethers are capable of entering into both homo- and copolymerization reactions in the presence of free-radical initiators. In the presence of 2% *tert*-butyl perbenzoate, the diallyl ethers are polymerized to soluble prepolymers at 130–138°C in about 1 hr. These prepolymers can be formulated with appropriate reinforcing materials and peroxide initiator to give hard, tough thermosetting resins.

The author wishes to thank Dr. R. L. Harris and Mr. J. N. Jenkins for assistance in the preparation and evaluation of the resins.

### References

1. G. Nowlin and L. S. Burnett, *SPE J.*, **17**, 1093 (1961).
2. Anon., *Brit. Plastics*, **40**, No. 5, 86 (1967).
3. H. H. Beacham, *Plastics Design Process*, **7**, No. 4, 20 (1967).
4. H. Raech, Jr., *Allylic Resins and Monomers*, Reinhold, New York, 1956.
5. D. Porret, U. S. Pat. 3,390,116 (June 25, 1968).
6. I. Sakurada and G. Takahashi, *Kobunshi Kagaku*, **11**, 266 (1954).
7. L. Lynn, *Mod. Plastics*, **31**, No. 2, 139, 219 (1953).
8. C. A. Heibeiger and J. L. Thomas, Brit. Pat. 861,817, (Mar. 1, 1961).
9. H. R. Simonds, M. H. Bigelow, and J. V. Sherman, *The New Plastics*, Van Nostrand, New York, 1945, p. 63.
10. H. Beacham, J. Litwin, and C. W. Johnston, *Plastics Technol.*, **9**, No. 5, 44 (1963).
11. D. W. Sundstrom and L. A. Walters, *SPE ANTEC, Tech. Papers*, **15**, 163 (1969).
12. F. B. Slezak, J. P. Stallings, and J. A. Bungs, *Ind. Eng. Chem., Prod. Res. Develop.*, **4**, 259 (1965).
13. S. D. Ross and M. Markarian, U. S. Pat. 2,564,214 (Aug. 14, 1951).
14. S. D. Ross and M. Markarian, U. S. Pat. 2,799,694 (July 16, 1957).
15. G. Nowlin, J. A. Gannon, and L. Jungster, *J. Appl. Polym. Sci.*, **13**, 463 (1969).

Received November 13, 1969

## Polymerization of Vinyl Monomers with Salts of Brønsted Acids

KOICHI YAMAGUCHI and YUJI MINOURA,  
*Department of Chemistry, Faculty of Engineering,  
Osaka City University, Sumiyoshi-ku, Osaka, Japan*

### Synopsis

The polymerization of vinyl monomers (*N*-phenylmaleimide, acrylamide, acrylonitrile, methyl vinyl ketone, methyl methacrylate, vinyl chloride, and styrene) with sodium salts of Brønsted acids (sodium cyanide, sodium nitrite, sodium hydroxide, etc.) were investigated at 0°C in dimethylformamide. *N*-Phenylmaleimide, acrylonitrile, and methyl vinyl ketone were found to undergo polymerization with sodium cyanide, however the other monomers were not polymerized with this salt. In the polymerizations of acrylonitrile and *N*-phenylmaleimide with sodium cyanide, the rates of the polymerizations were found to be proportional to the initiator concentration and to the square of the monomer concentration. The activation energy of acrylonitrile polymerization was 3.7 kcal/mole, and that of *N*-phenylmaleimide was 3.0 kcal/mole. The results of the copolymerization of acrylonitrile with methyl methacrylate at 0°C in dimethylformamide with sodium cyanide confirm that these polymerizations proceeded by an anionic mechanism initiated by the Michael addition reaction of the monomers with the salts. In these polymerizations, the monomer reactivity increased with increase in the  $e$  values. The initiation ability of sodium salts increased with increasing  $pK_a$  of the conjugate acids and with decreasing electronegativity of metal ion in the series of lithium, sodium, and potassium cyanide. The polymerizations took place only in aprotic polar solvents, and did not occur in weak polar solvents and in protonic solvents.

### INTRODUCTION

Inorganic salts are known to initiate the radical or ionic polymerization of vinyl monomers. For example,  $K_2S_2O_8$  is an initiator radical and Lewis acids such as  $AlCl_3$ ,  $BF_3$ , and  $SnCl_4$  are cationic catalyst. It is known that monomers such as vinylidene cyanide and nitropropene were polymerized with weak bases such as water and amine<sup>1-3</sup> and acrylonitrile (AN) and cyanoacetylene were polymerized with sodium cyanide.<sup>4</sup> In anionic polymerization, Tsuruta<sup>5</sup> showed that polymerization of vinyl monomers having a large Alfrey-Price  $+e$  value is favored. The relationship between initiators and  $e$  values of the vinyl monomers is shown in Table I.

In this paper, vinyl monomers were polymerized in dimethylformamide (DMF) at 0°C with the use of various sodium salts of Brønsted acids. It was found that *N*-phenylmaleimide (NPMI), which has a large  $e$  value, underwent polymerization as well as AN and methyl vinyl ketone (MVK) with sodium cyanide, sodium hydride, sodium nitrile, disodium hydrogen

phosphate, sodium dihydrogen phosphate, and sodium hydroxide. It was found that the initiation abilities of sodium salts increased with increasing  $pK_a$  of the conjugate acids.

In the polymerization of AN and NPMI with sodium cyanide, the rates of polymerization were proportional to the concentration of the initiator and the square of the concentration of the monomer; the activation energy for AN was 3.7 kcal/mole.

Copolymerization of AN and methyl methacrylate (MMA) and the reaction of AN with sodium cyanide were carried out to confirm the mechanism of these polymerizations. It was found that these polymerizations were an anionic reaction by the Micheal addition reaction of the monomer with sodium salts.

The polymerizations were carried out in order to investigate the effect of metal ions (sodium, lithium, and potassium) of the salts. The effect of solvents (DMF, dimethyl sulfoxide, tetrahydrofuran, benzene, acetone) on the polymerization was also studied.

## EXPERIMENTAL

### Monomer

Vinyl monomers used were styrene (St), MMA, AN, MVK, vinyl chloride (VC), acrylamide (AA), and NPMI.

St, MMA, MVK, and AN were purified by the usual method, dried over calcium hydride, and then distilled under nitrogen atmosphere. The monomers were redistilled over calcium hydride before use. The boiling points of monomers were: St, 53–53.5°C/30 mm Hg; MMA, 45–45.5°C/100 mm Hg; AN, 78.5–79.0°C. VC was distilled through a calcium chloride column. AA supplied by Nitto Chemical Industrial Co. was purified by recrystallization from the mixed solvent of benzene and methanol (mp 85.0–85.5°C). NPMI was prepared by the reaction of aniline with maleic anhydride<sup>6</sup> and recrystallized from benzene (mp 89–89.9°C).

### Solvent

DMF, dimethyl sulfoxide (DMSO), hexamethylphosphoramide (HMPA), toluene, acetone, benzene, tetrahydrofuran (THF), and water were purified by distillation.

### Salts

Inorganic salts were analytical reagents, reduced to powder in a mill and dried by heating before use.

### Polymerization

Monomer, catalyst, and solvent were placed in a glass tube connected to a vacuum line, and the tube was thoroughly degassed, sealed, and placed in an ice-water bath. The reaction mixture was poured into a large excess of

TABLE I

Monomer	Hammett constant $\sigma$	$e$	KR, NaR, LiR	SrR <sub>2</sub>	RMgX	ROK, RONa, ROLi NaOH, KOH	NR <sub>2</sub> , NaHCO <sub>3</sub> ROR, H <sub>2</sub> O
CH <sub>2</sub> =C(CH <sub>3</sub> )C <sub>6</sub> H <sub>5</sub>	-0.161	-1.27	→	→	→	→	→
CH <sub>2</sub> =CHCH=CH <sub>2</sub>	—	-0.8	→	→	→	→	→
CH <sub>2</sub> =CHC <sub>6</sub> H <sub>5</sub>	0.009	-0.8	→	→	→	→	→
CH <sub>2</sub> =C(CH <sub>3</sub> )CO <sub>2</sub> C <sub>2</sub> H <sub>5</sub>	0.352	0.17	→	→	→	→	→
CH <sub>2</sub> =CHCOCH <sub>3</sub>	0.516	0.68	→	→	→	→	→
CH <sub>2</sub> =CHCO <sub>2</sub> C <sub>2</sub> H	0.522	0.22	→	→	→	→	→
CH <sub>2</sub> =CHCN	0.628	1.20	→	→	→	→	→
CH <sub>2</sub> =CHNO <sub>2</sub>	0.778	1.78	→	→	→	→	→
CH <sub>2</sub> =C(CO <sub>2</sub> C <sub>2</sub> H <sub>5</sub> ) <sub>2</sub>	1.044		→	→	→	→	→
CH <sub>2</sub> =C(CN)CO <sub>2</sub> C <sub>2</sub> H <sub>5</sub>	1.150		→	→	→	→	→
CH <sub>2</sub> CH=CHCH=C(CN)- CO <sub>2</sub> C <sub>2</sub> H <sub>5</sub>	1.150		→	→	→	→	→
CH <sub>2</sub> =C(CN) <sub>2</sub>	1.256	2.58	→	→	→	→	→

methanol containing dilute hydrochloric acid after a suitable time interval. The polymer precipitated was filtered, washed with methanol and dried in a vacuum to constant weight.

### Reaction of Acrylonitrile with Sodium Cyanide

In a 200-ml flask, a solution of 1.5 g (0.03 mole) of sodium cyanide and 1.88 ml (0.03 mole) of AN in 50 ml of DMF was allowed to react at room temperature for 1 hr with stirring, and then few drops of water were added. The mixture was filtered and the solution was distilled in order to remove AN, DMF, and water. The residue was extracted with acetone, and the product (bp 100–105°C /1 mm Hg) was isolated by distillation under reduced pressure. The melting point, the elemental analysis, and the infrared spectrum of the product were measured.

### Reaction of Acrylamide with Sodium Cyanide

In a 200-ml flask, a solution of 2.5 g (0.05 mole) of sodium cyanide and 3.6 g (0.05 mole) of AA in 100 ml of DMF was allowed to react at room temperature for 2 hr, and then few drops of water were added.

The mixture was filtered and the solution was distilled to remove DMF and water. The distillation residue was extracted with acetone. The infrared spectrum of the insoluble part was determined in order to confirm the endgroup.

### Measurements

The intrinsic viscosities of polymers were measured by means of a Ubbelohde viscometer in DMF.

The infrared spectra of polymers as KBr pellets were measured on an infrared spectrometer (Jasco IR-I, Japan Spectroscopic Co., Ltd).

## RESULTS AND DISCUSSION

### Polymerization of Acrylonitrile with Sodium Cyanide

**Kinetics.** The polymerization of AN with sodium cyanide was carried out at 0°C in DMF at various monomer and initiator concentrations. The relationship between the rate of the polymerization obtained from time-conversion curves and the initiator or the monomer concentrations are shown in Figure 1.

From the results, it was found that the rate of polymerization  $R_p$  was proportional to the initiator concentration and to the square of the monomer concentration:

$$R_p = K[\text{AN}]^2[\text{NaCN}]$$

The activation energy of the reaction was found to be 3.7 kcal/mole. The intrinsic viscosity of the poly-AN was measured at 25°C in DMF.

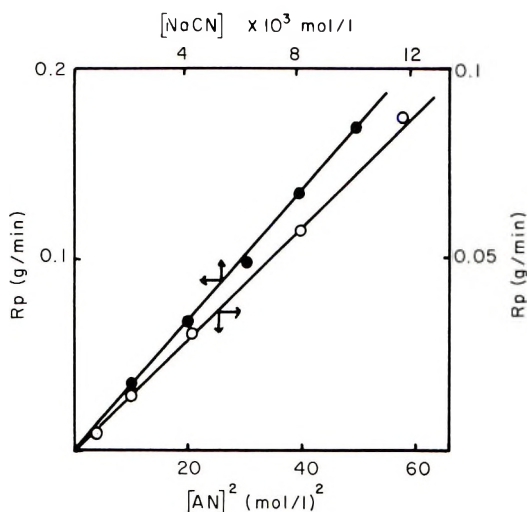


Fig. 1. Relationship between the rate of polymerization and concentration of initiator or monomer at 0°C in DMF. (●)  $[AN] = 7.55$  mole/l.; (○)  $[NaCN] = 1 \times 10^{-2}$  mole/l.

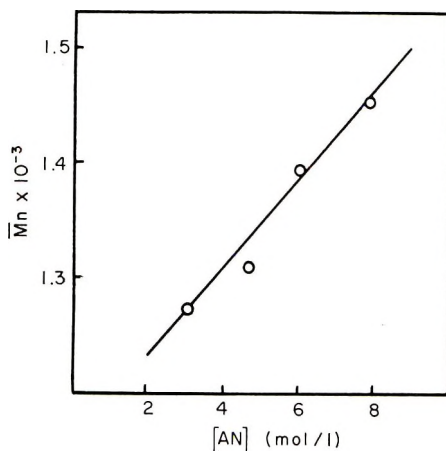


Fig. 2. Relationship between the molecular weight ( $\bar{M}_n$ ) and the concentration of the monomer ( $[AN]$ ).  $[NaCN], 1 \times 10^{-2}$  mole/l.; at 0°C, in DMF.

From the intrinsic viscosity, the molecular weight of poly-AN was calculated by using the following equation obtained by Bisschops:<sup>7</sup>

$$[\eta] = 1.66 \times 10^{-4} M^{0.81}$$

The relationship between the molecular weight and the initiator and monomer concentration is shown in Figures 2 and 3.

As can be seen in Figures 2 and 3, the molecular weight increased with increasing AN concentration and decreasing initiator concentration. From the results, the polymerization of AN with sodium cyanide was considering to be an anionic polymerization.



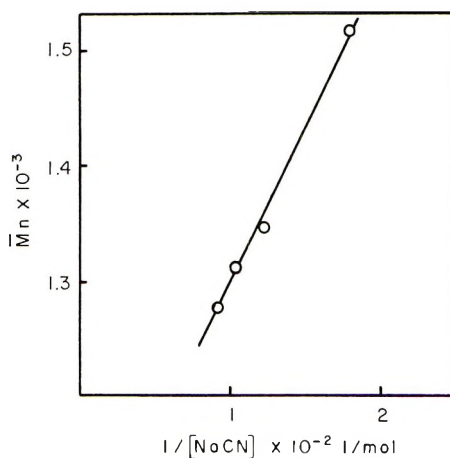


Fig. 3. Relationship between the molecular weight ( $\bar{M}_n$ ) and the concentration of the initiator  $[AN] = 7.55$  mole/l at  $0^\circ\text{C}$  in DMF.

**Copolymerization.** The copolymerization of AN with MMA was carried out with the use of sodium cyanide at  $0^\circ\text{C}$  in DMF in order to investigate the mode of the polymerization. The polymer yield and the compositions calculated from the elementary analysis are shown in Table II, and the copolymer composition curve is shown in Figure 4.

TABLE II  
Copolymerization of Acrylonitrile and Methyl  
Methacrylate at  $0^\circ\text{C}$  in DMF<sup>a</sup>

AN, mole/l.	MMA, mole/l.	Yield of copolymer at 1 hr, g	Nitrogen content in copolymer, %	Acrylonitrile content in copolymer, mole-%
1	4	0.0336	—	—
2	3	0.2438	23.91	94.73
2.5	2.5	0.4060	25.32	96.83
3	2	0.6542	25.63	98.39
4	1	1.0940	26.06	99.28

<sup>a</sup>  $[NaCN] = 8 \times 10^{-3}$  mole/l.

In Figure 4, curve 1 shows the results of the copolymerization of AN with MMA with the use of sodium cyanide; curves 2, 3, and 4 show the results of anionic copolymerization with  $\text{C}_6\text{H}_5\text{MgBr}$ ,<sup>8</sup> the radical copolymerization with benzyl peroxide,<sup>9</sup> and the redox copolymerization with  $(\text{NH}_4)_2\text{S}_2\text{O}_8$ – $\text{Na}_2\text{S}_2\text{O}_8$ ,<sup>10</sup> respectively. Curve 1 showed a similar trend as curve 2, and the polymerization reaction of AN with sodium cyanide was considered to be an anionic polymerization.

**Mechanism.** In order to confirm the initiation reaction of AN with sodium cyanide, the reaction of AN and sodium cyanide was studied at

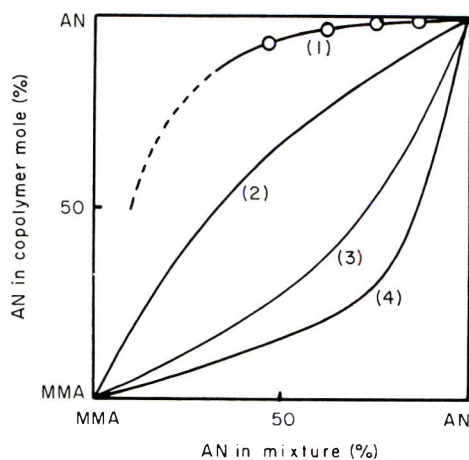


Fig. 4. Relationship of the monomer composition and the polymer composition in copolymerization of AN and MMA with NaCN ( $2 \times 10^{-3}$  mole/l.) in DMF at  $0^\circ\text{C}$ : (1) NaCN; (2)  $\text{C}_6\text{H}_5\text{MgBr}$ ; (3) BPO; (4)  $(\text{NH}_4)_2\text{S}_2\text{O}_8\text{-Na}_2\text{S}_2\text{O}_8$ .

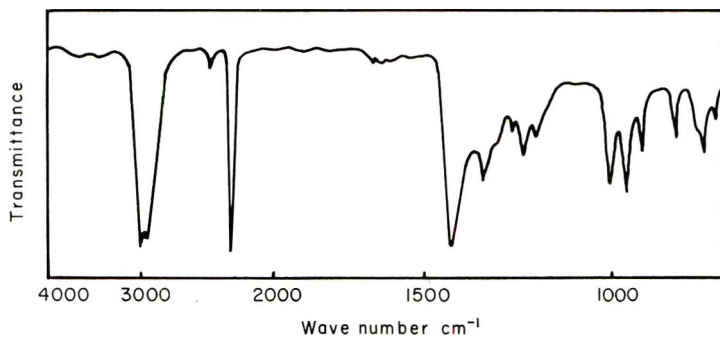


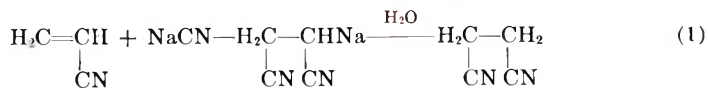
Fig. 5. Infrared spectrum of the product obtained from acrylonitrile and NaCN.

room temperature in DMF. The product obtained had a melting point of  $50\text{--}51^\circ\text{C}$ .

ANAL. Calcd. for  $\text{C}_3\text{H}_4\text{N}_2$ : C, 59.99%; H, 5.03%; N, 34.98%. Found: C 60.12%; H, 5.19%; N, 34.98%.

The infrared spectrum is shown in Figure 5. The product showed infrared absorption at  $2250\text{ cm}^{-1}$  due to  $\text{—CN}$  and bands at  $2950$  and  $1470\text{ cm}^{-1}$  due to  $\text{—CH}_2\text{—}$ . The infrared spectrum was identical to the spectrum of ethylene dicyanide obtained by the reaction of hydrogen cyanide with AN.

From the results, it was found that the product was ethylene dicyanide ( $\text{NCCH}_2\text{CH}_2\text{CN}$ ). The reaction scheme is shown in eq. (1):



Therefore, it is thought that the initiation reaction was the Micheal addition reaction, and the polymerization reaction considered to follow eqs. (2)–(4).

#### Initiation



#### Propagation



#### Termination



If the stationary state is assumed, the rate equation of the polymerization is:

$$R_p = (k_i k_p / k_t) [\text{M}]^2 [\text{NaCN}]$$

The termination reaction was assumed to be a unimolecular termination, and the termination occurred by the formation of a six membered ring in the chain end<sup>11</sup> [eq. (5)].

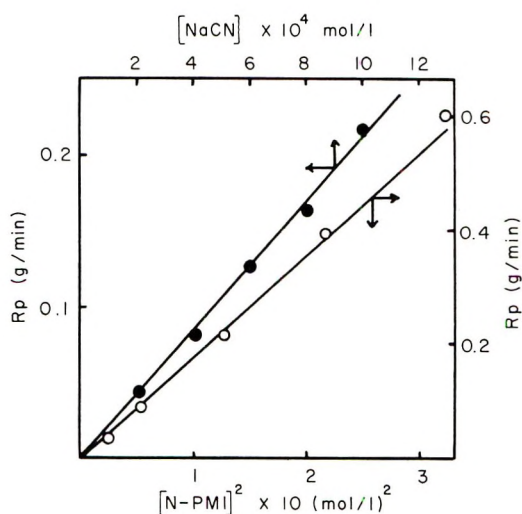
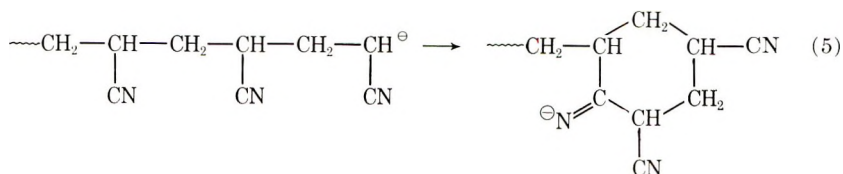


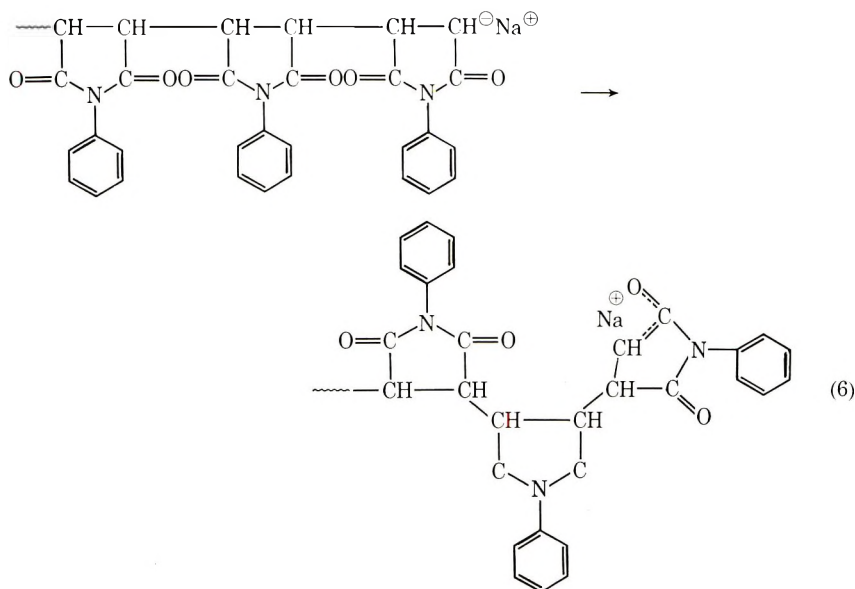
Fig. 6. Relationship between the rate of the polymerization and the concentration of initiator or monomer at 0°C in DMF: (O) [NaCN] =  $6.0 \times 10^{-4}$  mole/l.; (●) [NPMI] =  $5.78 \times 10^{-1}$  mole/l.

### Polymerization of *N*-Phenylmaleimide with Sodium Cyanide

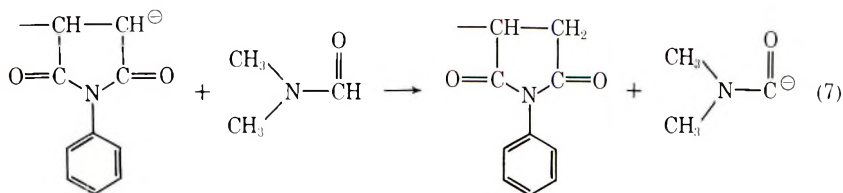
The polymerization of NPMI with sodium cyanide was studied at 0°C in DMF at various monomer and initiator concentrations. The relationship between the rate of polymerization and the initiator or the monomer concentration is shown in Figure 6. The rate equation was the same as in the polymerization of AN:

$$R_p = K[\text{NPMI}]^2[\text{NaCN}]$$

and the activation energy was 2.7 kcal/mole. The polymer obtained was a red powder, and the intrinsic viscosity was 0.080–0.085 in DMF at 35°F. In the mechanism of the polymerization, the initiation, propagation, and termination reactions were identical to those in the polymerization of AN. However, the termination reaction may follow two paths: one involves ring formation of the chain end as in case of AN or MMA [eq. (6)],



the other mode is the termination by the proton of the solvents [eq. (7)].



Due to steric hindrance, the second termination mechanism was considered more likely.

### Polymerization of Vinyl Monomers with Sodium Salts of Brønsted Acids

The polymerization of vinyl monomers (NPMI, AA, AN, MVK, MMA, VC, St) with sodium salts of Brønsted acids (sodium hydroxide, sodium cyanide, sodium hydrogen phosphate, sodium tetraborate, sodium cyanide, sodium carbonate, sodium hydride, sodium nitrile, sodium dihydrogen phosphate, sodium sulfide) was carried out at 0°C in DMF for 2r hr. The concentration of vinyl monomers and initiator were 3.0 mole/l. and  $2 \times 10^{-2}$  mole/l., respectively. The results are shown in Table III.

TABLE III  
Polymerization of Vinyl Monomer with Sodium Salts of Brønsted Acids<sup>a</sup>

Catalyst	$pK_a^b$	Polymer yield, %		
		NPMI ( $e = 1.57$ )	AN ( $e = 1.20$ )	MVK ( $e = 0.68$ )
NaOH <sup>c</sup>	15.7	18.3	10.0	Trace
Na <sub>2</sub> HPO <sub>4</sub> <sup>e</sup>	12.1	11.4	0	0
Na <sub>2</sub> B <sub>4</sub> O <sub>7</sub> <sup>e</sup>	9.2	22.1	0	0
NaCN <sup>d</sup>	9.0	99.0	66.7	32.4
Na <sub>2</sub> S <sup>d</sup>	7.1	44.6	0	0
NaH <sub>2</sub> PO <sub>4</sub> <sup>e</sup>	7.0	Trace	0	0
NaOCN <sup>e</sup>	4.5	49.9	0	0
NaNO <sub>2</sub> <sup>d</sup>	3.4	38.3	15.1	Trace
NaCO <sub>3</sub> <sup>e</sup>	3.3	19.1	0	0
NaH <sup>e</sup>		51.7	20.0	Trace

<sup>a</sup> [M] = 3 mole/l., [C] =  $2 \times 10^{-2}$  mole/l., in DMF, 0°C, 24 hr.

<sup>b</sup>  $pK_a$  of conjugate acid of catalyst.

<sup>c</sup> Insoluble in DMF.

<sup>d</sup> Soluble in DMF.

Sodium cyanide, sodium hydride, sodium nitrile, and sodium thiocyanide were soluble in DMF and the other sodium salts of Brønsted acids were insoluble. The other sodium salts, i.e., sodium hydrogen sulfate ( $pK_a = 1.8$ ),<sup>12</sup> sodium sulfate ( $pK_a = 1.8$ ),<sup>12</sup> sodium nitrate ( $pK_a = -1.64$ ),<sup>12</sup> sodium hydrogen sulfite ( $pK_a = -1.1$ ),<sup>12</sup> sodium sulfite ( $pK_a = -3.0$ ),<sup>12</sup> sodium chloride ( $pK_a = -7.0$ ),<sup>12</sup> sodium bromide ( $pK_a = -9.0$ ),<sup>12</sup> sodium iodide ( $pK_a = -11.0$ ),<sup>12</sup> sodium hydrogen carbonate, and sodium thiocyanide, were ineffective for the polymerization of these vinyl monomers at 0°C in DMF for 48 hr. The polymerizations of AA and VC at room temperature and MMA and St at 0°C did not take place with these sodium salts at 24 hr.

It was found that the initiation ability of sodium salts increased with increasing  $pK_a$  of the conjugate acids. The vinyl monomers [NPMI ( $Q = 0.57$ ,  $e = 1.57$ ),<sup>13</sup> AN ( $Q = 0.60$ ,  $e = 1.20$ ),<sup>14</sup> and MVK ( $Q = 0.15$ ,  $e = 0.68$ )<sup>14</sup>] which have large  $+e$  values were polymerized with the salts of small  $pK_a$  values. However, AA ( $Q = 0.18$ ,  $r = 1.30$ )<sup>14</sup> did not polymerize with sodium salts. The other monomers [MMA ( $Q = 0.74$ ,  $e = 0.40$ ),<sup>14</sup> VC

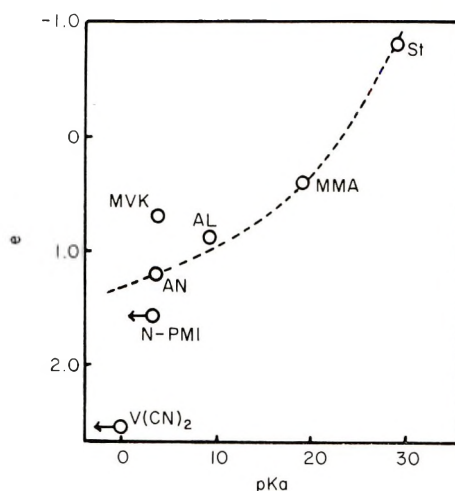


Fig. 7. Relationship between  $e$  of monomer and  $pK_a$  of conjugate acid.

( $Q = 0.044$ ,  $e = 0.20$ ),<sup>14</sup> and St ( $Q = 1.0$ ,  $e = 0.8$ )<sup>14</sup> which have small  $e$  values underwent polymerization with  $n$ -BuLi ( $pK_a = 40$ )<sup>15</sup> but not with sodium salts.

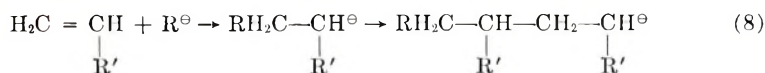
It is known that St polymerizes in the presence of catalysts of having  $pK_a$  values higher than that of sodium salts of xanthene ( $pK_a = 29$ )<sup>15</sup> and that MMA polymerizes with catalysts having  $pK_a$  values higher than that of *tert*-BuONa ( $pK_a = 19$ ).<sup>15</sup> For some monomers [St, MMA, MVK, AN, AA, NPMI, aerolein (AL) and vinylidene cyanide, V(CN<sub>2</sub>)<sup>2</sup>] with organometallic compounds or inorganic salts, the relationships between  $e$  values of monomers and  $pK_a$  values of the conjugate acid are shown in Figure 7; however, the reactivities of monomers changed with solvent used.

From the curve, we can estimate the lowest  $pK_a$  which can initiate polymerization when the  $e$  value of the monomer is known. The point for MVK was shifted off the left side of the curve. In the study of Tsuruta and Yasuda,<sup>16</sup> it was found that the rate of the Micheal addition reaction of MVK was faster than that for AN and methacrylonitrile. We considered that the reaction was accelerated by the strong  $\delta^{\oplus}$  charge of the double bond which was induced by the carbonyl group of MVK. The relationship of Figure 7 was replotted on a log-log scale, and the following equation was introduced:

$$e = A(pK_a)^{-1/2} + B$$

where  $A$ ,  $B$  are constants ( $A = -3.0$ ,  $B = 1.3$ ).

The initiation reaction of the monomer with salts of Brønsted acids was found to be the Micheal addition reaction. In case of the reaction of AN with sodium cyanide, the Micheal addition reaction is as follows:

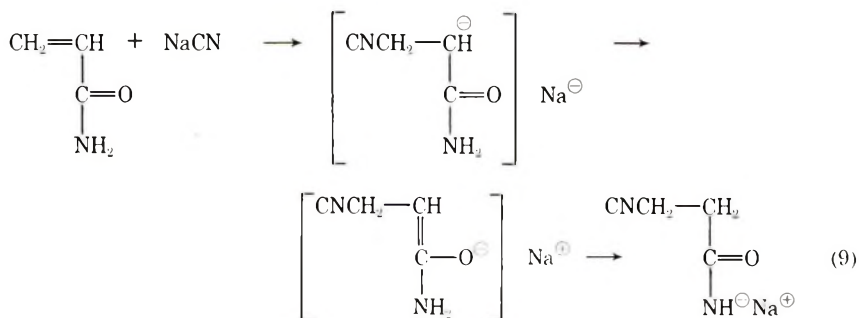


As the initiation reaction is Michael addition, the nucleophilic rapidly added to the electrophilic double bond. Especially in an aprotic polar solvent, the nucleophilicity of the initiator increases with increasing  $pK_a$  of the negative ion and the electrophilicity of the double bond increases with increasing  $e$  value of the vinyl monomer. In the case of catalysts of which the conjugate acids have a large  $pK_a$  value, the initiation is addition of the vinyl monomer of large  $e$  values and initiation produces an anion. It was considered that the polymerization was not dependent on low basicity of the initiator.

### Polymerization of Acrylamide with Sodium Cyanide

As described above, AA was not polymerized with sodium salts in spite of its large  $e$  values. In order to clarify this, AA was polymerized with sodium cyanide at  $100^\circ\text{C}$  in DMF for 24 hr. The infrared spectrum of the polymer obtained ( $[\eta] = 0.08$  in formic acid) is shown in Figure 8. The infrared spectrum was same as that obtained with hydrogen transfer polymerization. From the results, it was found that the polymerization at elevated temperature resulted a hydrogen-transfer reaction, even with a weak base such as sodium cyanide.

The reaction of equimolar amounts AA and sodium cyanide was studied at room temperature in DMF for 2 hr. The infrared spectrum of the product is shown in Figure 8b. The melting point of the product was  $70\text{--}71^\circ\text{C}$ , and the infrared spectrum showed the absorption due to  $\text{—C}\equiv\text{N}$  ( $2300\text{ cm}^{-1}$ ) and due to hydrogen transfer polymerization ( $3040\text{ cm}^{-1}$ ,  $1538\text{ cm}^{-1}$ ). The reaction mechanism is considered to be as shown in eq. (9).



Although the addition of initiator to AA was thought to take place, polymerization did not occur at  $0^\circ\text{C}$ .

### Effect of Other Inorganic Salts on Polymerization of Vinyl Monomers

The polymerization of vinyl monomers (NPMI, AN, MVK, and MMA) with lithium cyanide, sodium cyanide, and potassium cyanide was studied at  $0^\circ\text{C}$  in DMF. The results are shown in Figure 9 and Table IV.

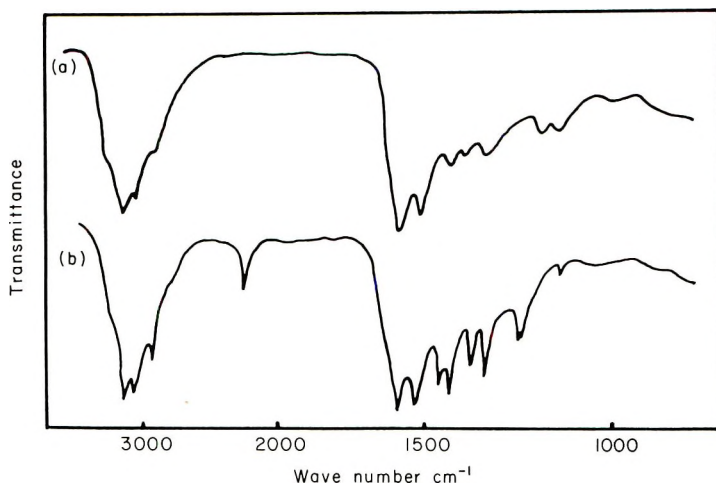


Fig. 8. Infrared spectra: (a) polymer obtained with NaCN; (b) product obtained with acrylamide and NaCN.

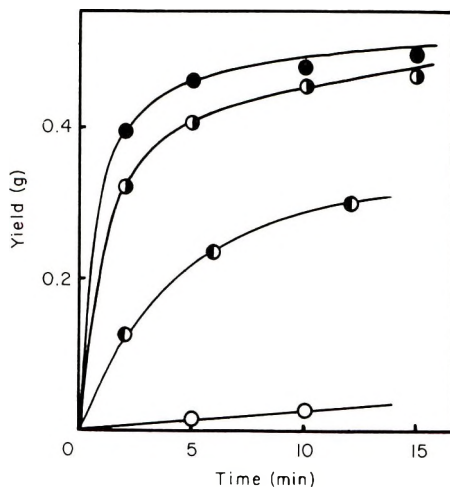


Fig. 9. Time-conversion plots for polymerization of NPMI with LiCN, NaCN, and KCN in DMF at 0°C,  $[M] = 5.78 \times 10^{-1}$  mole/l.: (●)  $[\text{NaCN}] = 2 \times 10^{-3}$  mole/l.; (○)  $[\text{NaCN}] = 1 \times 10^{-4}$  mole/l.; (◐)  $[\text{LiCN}] = 2 \times 10^{-3}$  mole/l.; (◑)  $[\text{KCN}] = 1 \times 10^{-4}$  mole/l.

The order of the solubility of cyano salts in DMF is as follows;  $\text{LiCN} > \text{NaCN} > \text{KCN}$ . From the results of Table IV and Figure 9, it was found that NPMI, AN, and MVK are polymerized with these salts, but MMA is not, and the rate of the polymerization increased in the order of following:  $\text{KCN} > \text{NaCN} > \text{LiCN}$ . The relationship between the electronegativity<sup>17</sup> of the metal ion and the rate of the polymerization ( $R_p$ ) of NPMI is



TABLE IV  
Polymerization of Vinyl Monomers with Metal Cyano Salts<sup>a</sup>

Salts	Electro- negativity <sup>b</sup>	Conversion, g/min				
		NPMI <sup>c</sup>	NPMI <sup>d</sup>	AN <sup>e</sup>	MVK <sup>e</sup>	MMA <sup>e</sup>
LiCN	1.0	—	0.17	0.11	0.01	0
NaCN	0.9	0.01	0.27	0.19	0.10	0
KCN	0.8	0.06	0.16	0.13 <sup>f</sup>	0.05 <sup>f</sup>	0

<sup>a</sup> [M](NPMI)  $5.78 \times 10^{-1}$  mole/l.; [AN], [MVK], [MMA], 3 mole/l. at 0°C in DMF.

<sup>b</sup> Data of Pritchard and Skinner.<sup>17</sup>

<sup>c</sup> [Cat] =  $1 \times 10^{-4}$  mole/l.

<sup>d</sup> [Cat] =  $2 \times 10^{-3}$  mole/l.

<sup>e</sup> [Cat] =  $2 \times 10^{-2}$  mole/l.

<sup>f</sup> Catalyst did not dissolve completely in DMF.

shown in Figure 10. From the log-log plot of electronegativity and  $R_p$ , the relationship is represented as

$$R_p = A [\text{electronegativity}]^{-a}$$

where  $a$  is a constant and  $A$  is a constant dependent on the concentration of the monomer and initiator. For concentrations of monomer and initiator of  $5.78 \times 10^{-1}$  mole/l. and  $1 \times 10^{-4}$  mole/l., respectively,  $A$  is  $4.1 \times 10^{-3}$  and  $a$  is 12.

The polymerizations of vinyl monomers (NPMI, AN, MVK, and MMA) with metal hydroxides (sodium hydroxide, lithium hydroxide, potassium hydroxide, calcium hydroxide, and magnesium hydroxide), metal oxides (calcium oxide, magnesium oxide, and barium oxide) and metal acetates (sodium acetate, lithium acetate, calcium acetate, barium acetate, mercury acetate, cadmium acetate, zinc acetate, and lead acetate)

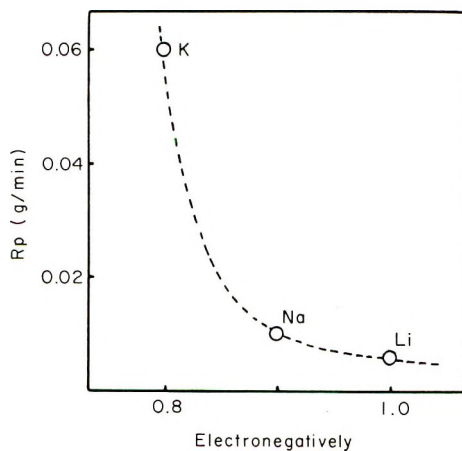


Fig. 10. Relationship between  $R_p$  and electronegativity of metal ion in polymerization of NPMI with cyano salts. [M] =  $5.78 \times 10^{-1}$  mole/l.; [Ca+] =  $1 \times 10^{-4}$  mole/l.; in DME, at 0°C.

were studied at 0°C or 30°C in DMF for 24 hr. The results are shown in Table V. As shown in Table V, it was found that NPMI and AN were polymerized with lithium hydroxide, sodium hydroxide, and potassium hydroxide, that MVK showed some polymerization and that MMA did not. With the other metal hydroxides as initiator, none of the monomers underwent polymerization. In the polymerization of monomer with metal oxide, only NPMI underwent polymerization.

TABLE V  
Polymerization of Vinyl Monomers with Oxide, Hydroxide,  
and Acetate Salts in DMF at 0°C, 24 hr<sup>a</sup>

Catalyst	EN <sup>b</sup>	pK <sub>a</sub> <sup>c</sup>	Polymer yield, %			
			NPMI	AN	MVK	MMA
KOH	0.8		34.4	14.3	Trace	0
NaOH	0.9		37.0	10.0	Trace	0
LiOH	1.0	14.1	21.9	8.1	Trace	0
Mg(OH) <sub>2</sub>	1.2	11.4	0	0	0	0
Ca(OH) <sub>2</sub>	1.0	12.7	0	0	0	0
MgO <sup>d</sup>	1.2	11.4	2.12	0	0	0
CaO <sup>d</sup>	1.0	12.7	5.08	0	0	0
BaO <sup>d</sup>	0.9	13.4	7.26	0	0	0
Na(CH <sub>3</sub> COO)	0.9		26.6	0	0	0
Li(CH <sub>3</sub> COO)	1.0	14.1	18.2	0	0	0
Ca(CH <sub>3</sub> COO) <sub>2</sub>	1.0	12.7	8.9	0	0	0
Ba(CH <sub>3</sub> COO) <sub>2</sub>	0.9	13.4	0	0	0	0
Zn(CH <sub>3</sub> COO) <sub>2</sub>	1.5	9.7	0	0	0	0
Cd(CH <sub>3</sub> COO) <sub>2</sub>	1.4	9.0	0	0	0	0
Pb(CH <sub>3</sub> COO) <sub>2</sub>	2.0	7.8	0	0	0	0
Hg(CH <sub>3</sub> COO) <sub>2</sub>	1.9	3.7	0	0	0	0

<sup>a</sup> [M] = 3 mole/l., [Caf] = 2 × 10<sup>-2</sup> mole/l.

<sup>b</sup> Electronegativity of metal ion.<sup>15</sup>

<sup>c</sup> pK<sub>a</sub> of metal ion.

<sup>d</sup> At 30°C.

With metal acetate as the initiator, NPMI was polymerized with sodium acetate, lithium acetate, and potassium acetate, but the other monomers did not.

These results confirmed that the initiation ability increased with decreasing electronegativity and with increasing pK<sub>a</sub><sup>12</sup> of the metal ion.

### Effect of Solvents

The polymerization of NPMI with sodium cyanide was carried out at 0°C or 30°C in various solvents (DMF, DMSO, THF, HMPA, acetonitrile, acetone, toluene, benzene, water). The results are shown in Table VI. The sodium cyanide initiator dissolved in all solvents except THF, acetonitrile, acetone, toluene, and benzene. The polymer of NPMI was not obtained by the polymerization without sodium cyanide at 0°C in these solvents; polymerization of NPMI occurred with sodium cyanide in DMF, DMSO, HMPA and acetonitrile but not in the other solvents.

TABLE VI  
 Effect of Solvent<sup>a</sup>

Solvent	Dielectric constant <sup>b</sup>	Temp, °C	Time, min	Yield, %
DMF	37	0	20	93.2
DMSO	45	30	50	39.8
HMPA	34	0	20	13.4
Acetonitrile	37.5	0	240	10.0
Acetone	21	0	240	0
THF	7	0	120	0
Toluene	2.4	0	240	0
Benzene	2.3	0	2880	0
Water	80	0	2880	0

<sup>a</sup> [NPMI] =  $5.78 \times 10^{-1}$  mole/l.; [NaCN] =  $2 \times 10^{-2}$  mole/l.

<sup>b</sup> Data of Kornblum et al.<sup>18</sup> and Okawara.<sup>19</sup>

The solvents in which polymerization took place had larger dielectric constants, i.e., DMF (37),<sup>18</sup> DMSO (47),<sup>18</sup> acetonitrile (37.5),<sup>18</sup> and HMPA (34).<sup>19</sup> In general, a polar solvent having a large dielectric constant shows increased solvation of the anion. Therefore, the polymerization takes place in a solvent having a relatively large dielectric constant.

It was confirmed that these anionic polymerizations took place only in aprotic polar solvents such as DMF, DMSO, polymerization did not occur in weakly polar solvents such as THF or in protonic solvents.

### References

1. F. B. Joyner and G. F. Hawkins, U. S. Pat. 2,721,858 (1955).
2. H. Gilbert and F. F. Miller, *J. Amer. Chem. Soc.*, **76**, 1074 (1954).
3. A. T. Blomoust, *J. Amer. Chem. Soc.*, **67**, 1519 (1945).
4. C. S. Marvel and D. J. Casey, *J. Org. Chem.*, **24**, 957 (1959).
5. T. Tsuruta, *Kobunshi no Gosei*, Kagakudojin, Japan, 1961, p. 53.
6. M. P. Cava, in *Organic Syntheses*, Vol. 41, J. D. Roberts, Ed., Wiley, New York, 1961, p. 93.
7. J. Bisschops, *J. Polym. Sci.*, **17**, 81 (1955).
8. F. Dawans and G. Smets, *Makromol. Chem.*, **59**, 163 (1963).
9. F. M. Lewis and F. R. Mayo and W. F. Hulse; *J. Amer. Chem. Soc.*, **67**, 1701 (1945).
10. M. Watanabe and S. Yaguchi, *Kobunshi Kagaku*, **15**, 129 (1958).
11. A. Ottolenghi and A. Zilkha, *J. Polym. Sci. A*, **1**, 687 (1963).
12. A. Albert and E. P. Serjeant, *Ion Constants*, Maruzen, 1963, p. 145.
13. Y. Suzuki and Y. Minoura, unpublished data, 1966.
14. L. J. Young, *J. Polym. Sci.*, **54**, 411 (1961).
15. M. Schlosser, *Angew. Chem.*, **76**, 124 (1964).
16. T. Tsuruta and Y. Yasuda, *J. Macromol. Sci.*, **A-2**, 943 (1968).
17. H. O. Pritchard, and H. A. Skinner, *Chem. Revs.*, **55**, 745 (1955).
18. N. Kornblum, R. Seltzer, and P. Haberfield, *J. Amer. Chem. Soc.*, **85**, 1148 (1963).
19. M. Okawara, *Yuki Gosei Kiyokashi*, **25**, 1223 (1967).

Received November 3, 1969

Revised December 2, 1969

## NOTES

***Polymerization-Induced Electrical Effects in Sulfur.  
The Electrical Resistance of Sulfur as a  
Function of Temperature***

Sulfur was heated at atmospheric pressure in a pyrophyllite container with tantalum electrodes silver-soldered to platinum leads. A chromel-alumel thermocouple was imbedded within the center of the sulfur sample and temperature was measured by a null point method with a potentiometer. Resistance was monitored as a function of temperature by the use of a calibrated vacuum tube voltmeter.

Results plotted in Figure 1 indicate that resistance measurements are capable of clearly showing the effect of polymerization and depolymerization (polymer breakdown) in liquid sulfur. In studying Figure 1 more closely, the effects of the orthorhombic  $\rightarrow$  monoclinic phase transformation and the individual melting of both the orthorhombic and monoclinic phases can also be noticed.

With the exception of polymerization, each of the above phenomena is accompanied by a decrease in resistance and hence a decrease in resistivity. The results show that shortly after the inception of polymerization, known to occur at 159°C, the resistance of sulfur rises. This is presumably due to the bonding of short chains and the resulting decrease in the number of conducting diradically-terminated chains present in the liquid. The observation that the electrical resistance does not appear to begin increasing until achieving a temperature of about 166°C may be ascribed to kinetic phenomena. It is very doubtful that this six degree discrepancy is due to systematic error in measuring temperature in view of the observation that the melting of both orthorhombic and monoclinic sulfur took place within 0.2 and 0.1°C, respectively, of the known values. Furthermore, the error in measuring temperature is judged to be at the most  $\pm 2$  to 3 °C. The resistance of liquid sulfur continues to increase until the long chains begin to break up at about 190 °C, at which point some electrons become available for conduction and the diradical concentration rises thus causing the electrical resistance to decrease as the temperature is further increased. In addition to these effects, a sharp decrease in resistance is observed at 212 °C that is probably associated with accelerated chain scission. Experimental data is summed up in Table I.

The experiment proves unequivocally that electrical resistance is very noticeably influenced by the reactions that take place in liquid sulfur. Thus, we would expect that a high-pressure apparatus in which electrical resistance is monitored could be successfully utilized to study pressure effects on the polymerization or depolymerization temperatures

TABLE I  
Comparison of Experimental Results with Known Data for Polymorphism,  
Melting, and Polymerization Effects in Sulfur at Atmospheric Pressure

Phenomenon	Accepted temperature, °C	Experimental temperature (from graphical plot), °C
Orthorhombic $\rightleftharpoons$ monoclinic phase transformation	95.6	100
Orthorhombic $\rightleftharpoons$ pure liquid S	112.8	113
Monoclinic $\rightleftharpoons$ pure liquid S	118.9	119
Polymerization	159	166
Depolymerization (maximum viscosity and chain length)	188	192

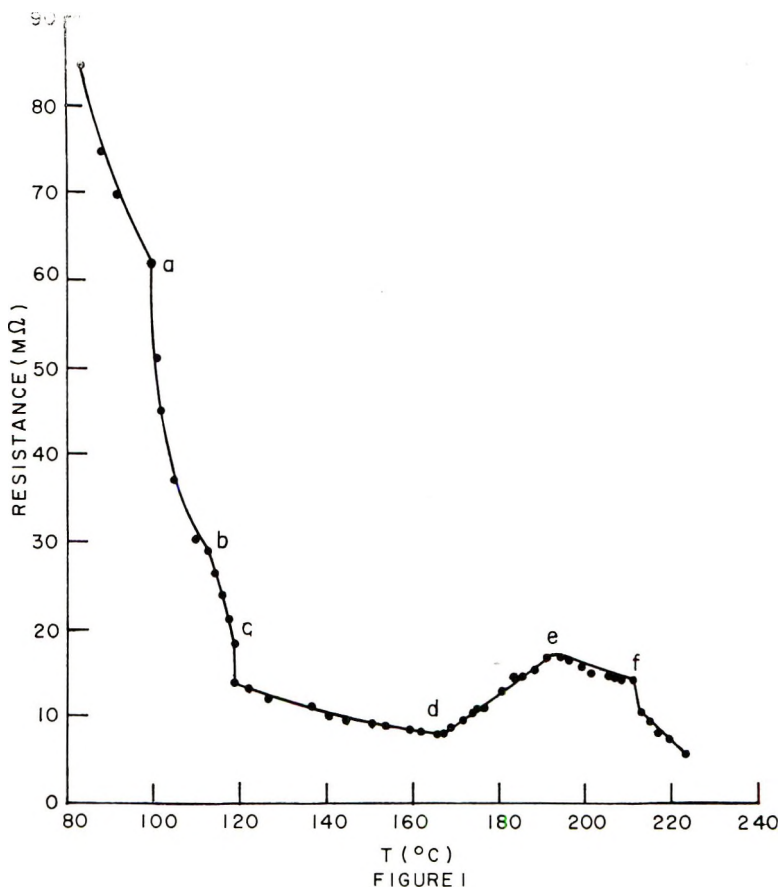


Fig. 1. Electrical resistance as a function of temperature for sulfur showing the effects of: (a) orthorhombic  $\rightleftharpoons$  monoclinic phase transformation; (b) melting of orthorhombic sulfur; (c) melting of monoclinic sulfur; (d) polymerization of liquid sulfur; (e) depolymerization or chain breakup; (f) suspected to be associated with accelerated chain scission.

and on other liquid reactions in sulfur. These effects have so far only been studied to 1 kb by differential thermal analysis and to about 20 kb by the opposed anvil-quenching technique.<sup>1, 2</sup> Thus electrical measurements should contribute significantly to an understanding of the processes involved in these reactions. We expect, in the future, to conduct this type of experiment in our cubic or hexahedral high-pressure high temperature apparatus.

#### References

1. G. C. Vezzoli, F. Dacheille, and R. Roy, *J. Polym. Sci. A-1*, **7**, 1557 (1969).
2. G. C. Vezzoli, Ph.D. thesis, "The Polymorphism and Polymerization of Sulfur under Pressure," The Pennsylvania State University, 1969.

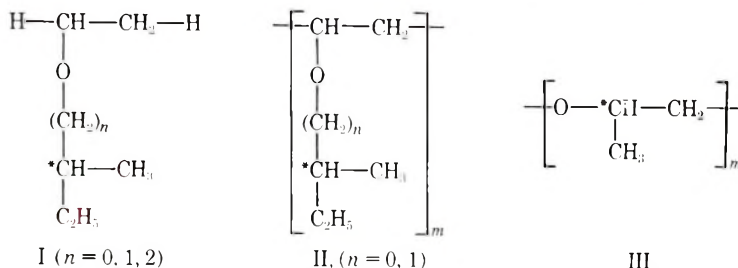
GARY C. VEZZOLI

Institute for Exploratory Research  
U. S. Army Electronics Command  
Fort Monmouth, New Jersey 07703

Received October 14, 1969

**Optical Activity of Poly[(*R*)-Propylene Oxide] Samples of Different Stereoregularity**

In the course of our research on the rotatory properties of optically active ethers (I) and poly(vinyl ethers) (II),<sup>1</sup> we have investigated the optical activity and the optical



rotatory dispersion (ORD)<sup>2</sup> of samples of poly[(*R*)-propylene oxide] (PPO) (III) having different stereoregularity.

It seemed of interest to establish whether the chromophoric system, connected with the oxygen atom on every monomeric unit, was modified when included in the polymer chain backbone (as in PPO) with respect to that found in poly(vinyl ethers),<sup>1,3</sup> in which the oxygen atom is included in the side chains.

The ORD curves of PPO have not been studied in detail up to now; Tsuruta and co-workers<sup>4</sup> reported that the ORD in benzene and chloroform are normal<sup>2</sup> between 700 and 300 nm, and Livshits<sup>5,6</sup> found that the ORD in methanol and chloroform between 600 and 300 nm is described by the one-term Drude equation.<sup>2</sup>

On the other hand, no satisfactory explanation has yet been given for the observed strong dependence of the optical rotatory power of PPO on the nature of the solvent.<sup>4-7</sup> The optical rotation at 589 nm of three samples having different solubility in acetone and different stereoregularity<sup>8</sup> has been measured in various solvents; the ORD curves of these same samples in trifluoroethanol, chloroform, and diethyl ether have also been examined.

The molar rotation at 589 nm, corrected for the refractive index of the solvent,<sup>9</sup> of samples A, B, and C in different solvents (Table I) shows that none of the regularities found by Rule<sup>10</sup> in the study of the influence of solvent on optical activity seem to be followed.

The ORD curve of sample B in trifluoroethanol and that in chloroform are normal between 600 and 210 and between 600 and 250 nm, respectively, the former being negative and the latter positive (Fig. 1).

These curves, however, are not simple;<sup>2</sup> in both cases the  $\lambda_0$  value calculated by the one-term Drude equation\* is lower than 150 nm and hence does not correspond to the wavelengths where the first optically active absorption band has been found for ethers<sup>11</sup> or has been predicted for paraffins.<sup>12</sup> The ORD of sample B in diethyl ether (Fig. 1), shows a maximum at about 235 nm, which is not connected to a Cotton effect,<sup>2</sup> while the circular dichroism (CD)<sup>2</sup> spectrum in the same solvent does not show any dichroic band in the region 300-210 nm.

The negative ORD curve of a film of III (sample B) shows, at about 210 nm, the first extremum of a Cotton effect corresponding to the negative CD maximum observed at about 188 nm (Fig. 2). From this point of view the situation can be considered very similar to that observed in the case of low molecular weight alkyl ethers (I).<sup>1</sup>

\* On suggestion of a referee we report the definition of  $\lambda_0$  according to the one-term Drude equation,  $[\Phi] = K/(\lambda^2 - \lambda_0^2)$ , where  $[\Phi]$  is the molar rotation (referred to one monomeric unit),  $K$  is a constant,  $\lambda$  is the wavelength of the incident light and  $\lambda_0$  is the wavelength of the closest optically active absorption band.<sup>2</sup>

TABLE I  
Molar Rotatory Power in Different Solvents of Some Samples of Poly[(R)-propylene Oxide] of Different Stereoregularity

Solvent	Fraction A <sup>a</sup>			Fraction B <sup>b</sup>			Fraction C <sup>b</sup>		
	$\alpha_{580}^{25}$ ( $l = 1$ ) <sup>c</sup>	$[\Phi]_{589}^{25}$	$[\Phi]_{589}^{25}$ (corr.) <sup>d</sup>	$\alpha_{580}^{25}$ ( $l = 1$ ) <sup>c</sup>	$[\Phi]_{589}^{25}$	$[\Phi]_{589}^{25}$ (corr.) <sup>d</sup>	$\alpha_{580}^{25}$ ( $l = 1$ ) <sup>c</sup>	$[\Phi]_{589}^{25}$	$[\Phi]_{589}^{25}$ (corr.) <sup>d</sup>
Chloroform	+0.092°	+2.28	+1.42	+0.110°	+7.80	+5.71	+0.150°	+9.89	+7.27
Diethyl ether	+0.104°	+2.01	+1.57	+0.084°	+6.97	+5.45	+0.126°	+9.04	+7.06
Dibutyl ether	+0.100°	+2.02	+1.54	+0.120°	+6.56	+5.00	+0.080°	+9.71	+7.36
<i>p</i> -Xylene	-0.120°	-2.45	-1.74	-0.104°	-6.02	-4.26	-0.105°	-7.03	-4.98
Trifluoro- ethanol	-0.072°	-3.02	-2.47	-0.079°	-9.68	-7.76	-0.082°	-11.23	-9.19
Pyridine	-0.105°	-3.62	-2.55	-0.090°	-10.45	-7.39	-0.194°	-12.86	-9.10
Benzene	-0.090°	-3.67	-2.60	-0.161°	-11.19	-7.90	-0.202°	-13.44	-9.50

<sup>a</sup> Soluble in acetone at 0°C.

<sup>b</sup> Derived from the fraction insoluble in acetone at 0°C (see experimental section).

<sup>c</sup> Using a Perkin-Elmer polarimeter, Model 141.

<sup>d</sup>  $[\Phi]_{589}^{25}$  (corr.) =  $3/12 + (n_D^{25})^2[\Phi]_{589}^{25}$  obs.<sup>9</sup>

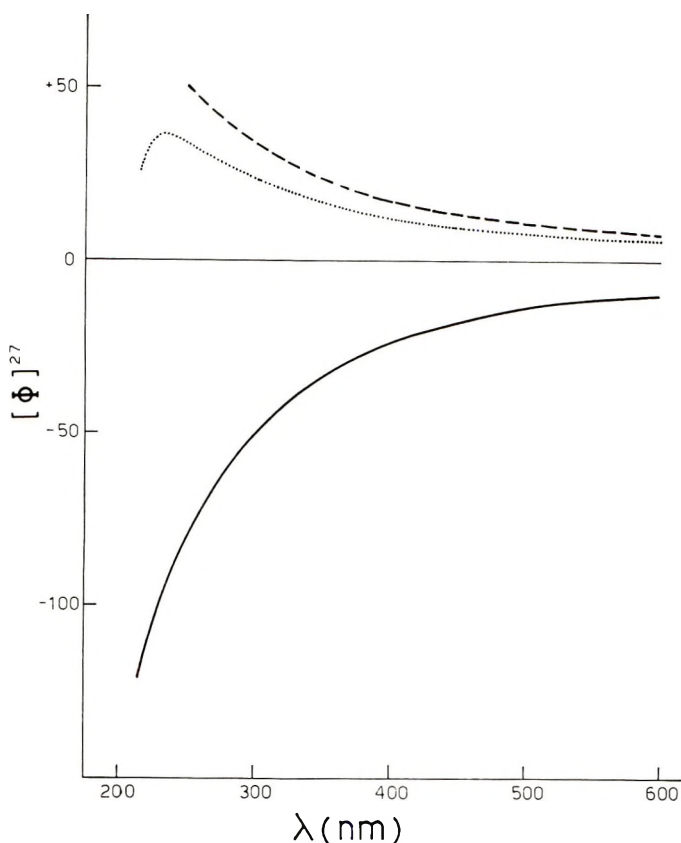


Fig. 1. ORD curves of PPO sample B: (---) chloroform; (···) diethyl ether; (—) trifluoroethanol.

The ORD curves in diethyl ether of all the three samples of PPO examined (Fig. 3) are similar, being in all cases complex and characterized by a maximum centered nearly the same wavelength (about 235 nm), which, as indicated earlier, is not attributable to a Cotton effect.  $[\Phi]_{235}$  increases as the solubility of the fraction in acetone decreases, that is, with increasing stereoregularity of the polymer fraction.

The complex ORD curves of samples of II ( $n = 1$ ) having different stereoregularity are also characterized by a maximum which has the highest intensity in the most stereoregular sample, but in this case  $\lambda_{\text{max}}$  decreases with increasing stereoregularity.<sup>3</sup>

Finally, taking in account the previous data on optically active ethers and poly(vinyl ethers),<sup>1</sup> the variation of optical activity of PPO with changing solvent and degree of stereoregularity can be interpreted on the basis of the following considerations.

The variations of stereoregularity in poly(vinyl ethers) cause a change in the position of the conformational equilibria of the macromolecules, which is responsible for differences in average contribution to the optical activity by monomeric units inserted in chain segments having different stereoregularity.<sup>1</sup> By contrast, the structural variations\* in the PPO samples, related to differences in stereoregularity and solubility in

\* According to the observation of Price and co-workers<sup>8</sup> these structural variations can correspond not only to the change of the configuration of the main-chain asymmetric tertiary carbon atoms, that is, a change of stereoregularity, but to the presence of head-to-head and tail-to-tail monomeric units that contain asymmetric carbon atoms having opposite absolute configurations.



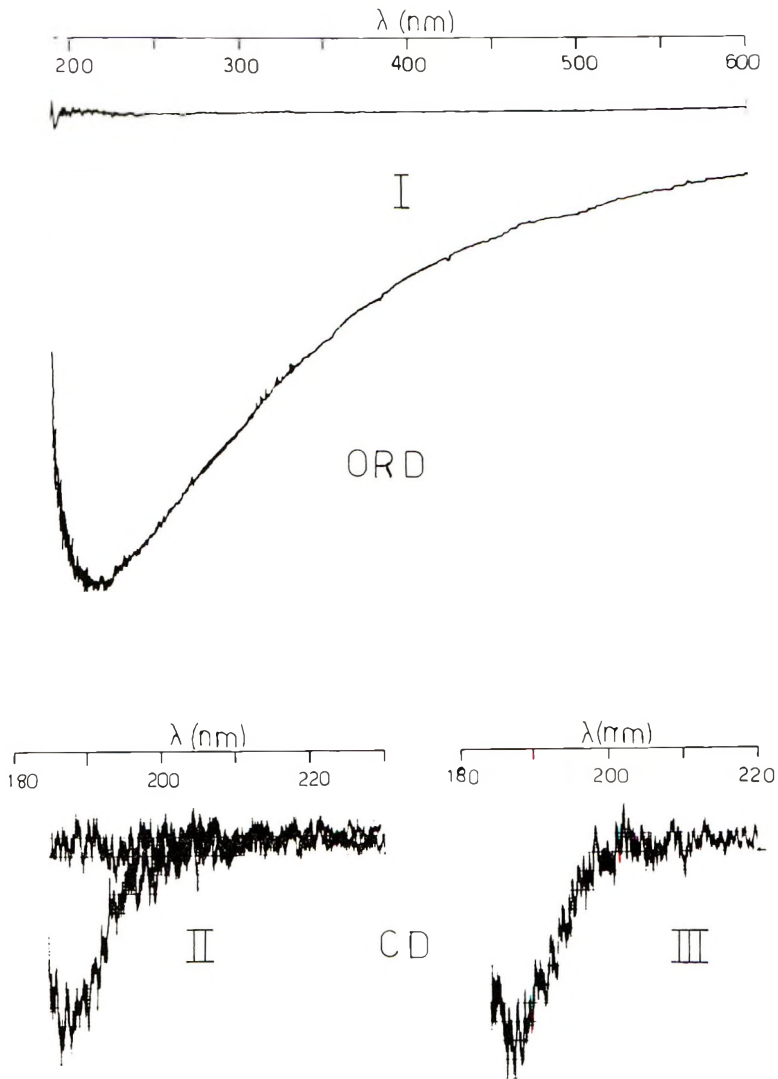


Fig. 2. ORD and CD curves of PPO sample B in the solid state: (I) ORD; (II) CD, initial position of the film; (III) CD, after a rotation of  $90^\circ$ . Photographic reproductions of the experimental curves.

acetone, do not seem to change appreciably the ratio between the absolute value of the contributions with opposite sign given to the optical rotation by the chromophores present in each monomeric unit. This experimental fact can be taken as an indication that stereoregularity does not affect markedly the conformational equilibria of III.

These data are not inconsistent with the relationship, found by Price and co-workers,<sup>8</sup> between molar rotatory power and number of configurational inversions in PPO, but do not permit a distinction to be made between the configurational inversions which could be present in PPO having a regular head-to-tail enchainment of monomeric units and those which are strictly related to a head-to-head, tail-to-tail enchainment of the monomeric units.<sup>8</sup>

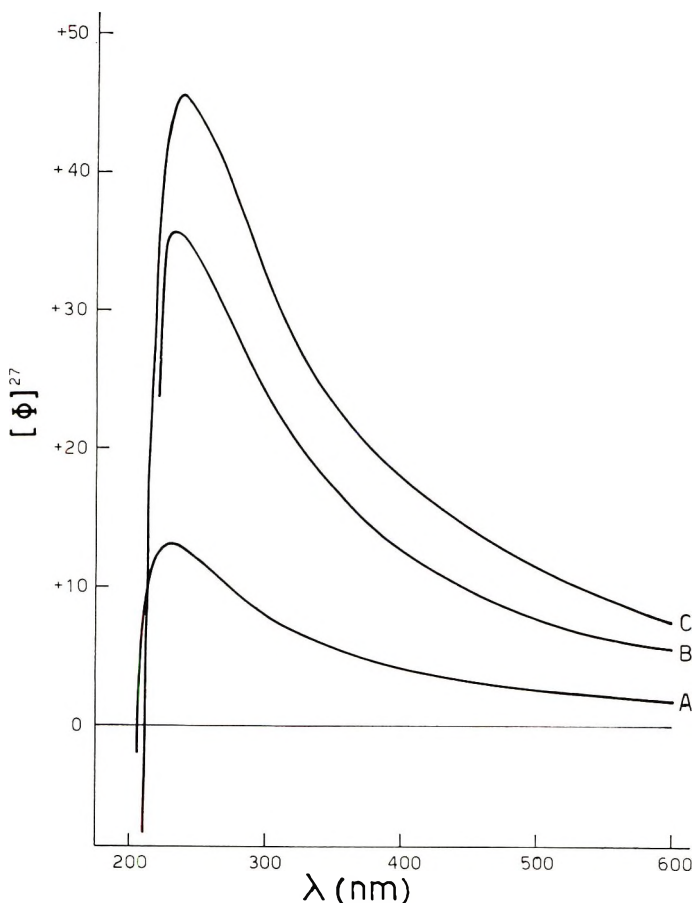


Fig. 3. ORD curves in diethyl ether of the three PPO samples A, B, and C.

According to the above conclusions, the average length of the isotactic blocks does not influence, at least for the set of solvents examined, the optical rotation per monomeric unit in PPO, contrary to what has been found for optically active isotactic vinyl polymers.<sup>13</sup>

The ultraviolet absorption spectra in solution and the ORD and CD spectra in the solid state of III have shown that the first optically active absorption band is at the same wavelength as in low molecular weight optically active ethers.<sup>11</sup> Therefore, large differences in electronic interactions among the ethereal groups in III can be excluded.

The variation of optical activity with solvent in PPO as well as in low molecular weight ethers<sup>14</sup> should be attributed mainly to the influence of the solvation on the position of the conformational equilibria of III and I.

## EXPERIMENTAL

### Preparation of the Poly[(R)-propylene Oxide] Samples

The samples were obtained, as previously reported,<sup>7,15</sup> by fractionating the crude polymer derived from the polymerization of (+)(R)-propylene oxide (PO) having  $[\alpha]_D^{27} + 15.0$  (diethyl ether) with a ferric acetate hydroxide [approximate composition

$2\text{Fe}_2\text{O}_3 \cdot \text{Fe}(\text{OH}) \cdot \text{FeO} \cdot \text{OCOC}_2\text{H}_5$ ]<sup>15</sup> as catalyst. The monomer was prepared<sup>7</sup> from (-)(R)-propylene glycol having  $[\alpha]_D^{27} = 16$  (neat).

In a typical polymerization experiment, 5.40 g of PO, after stirring on freshly ground calcium hydride, was distilled by use of an all-glass vacuum line into an ampoule containing 2.0 ml of catalyst slurry (0.2 g of catalyst in dry heptane).

The ampoule was sealed, heated for 60 hr at 70°C, cooled to -70°C, and then broken. The crude polymer, after purification,<sup>15</sup> weighed 4.92 g (91.0% yield).

Crude polymer (2.91 g), after dissolution in acetone ( $c = 0.65$  g/dl) was fractionated<sup>7, 15</sup> by cooling to 0°C into two fractions: (1) soluble in acetone at 0°C (52.9 wt-%), fraction A; (2) insoluble in acetone at 0°C (47.1 wt-%). The second fraction, on repeated dissolutions in acetone ( $c = 0.1$ - $0.2$  g/dl) and successive coolings to 10-15°C, till incipient precipitation of the polymer, gave two fractions: fraction B (37.2 wt-%), which was soluble in acetone, and fraction C (9.9 wt-%), which was insoluble in acetone under the reported conditions.

### ORD, CD, and UV Measurements

The ORD, CD, and UV measurements were performed by using a Cary 60 spectropolarimeter, a Roussel-Jouan Dichrograph II, and a Cary 14 spectrophotometer, respectively.

The ORD and CD spectra of the polymer in the solid state were studied on a practically unoriented film of PPO (fraction B), prepared by slow evaporation of the solvent from 0.3 ml of diethyl ether solution ( $c = 0.5$  g/dl) over a quartz plate of 8 cm<sup>2</sup> area, presenting the film in three different positions. These were obtained by rotation of the film around its normal axis, by an angle of 90° and 270°, with respect to its initial position.

The authors thank Mr. Carlo Bertucci for assistance in performing ORD, CD, and UV measurements.

### References

1. P. Pino, P. Salvadori, E. Chiellini, and P. L. Luisi, *Pure Appl. Chem.* **16**, 469 (1968), and references there reported.
2. C. Djerassi, *Optical Rotatory Dispersion: Applications to Organic Chemistry*, McGraw-Hill, New York, 1960.
3. P. Pino, P. Salvadori, and E. Chiellini, in preparation.
4. K. Matsuura, S. Inoue, and T. Tsuruta, *Makromol. Chem.*, **86**, 316 (1965).
5. V. S. Livshits, Candidate's Thesis, Institute of Chemical Physics, USSR Academy of Sciences, Moscow, 1965.
6. I. N. Topchieva, *Russ. Chem. Rev.*, **35**, 741 (1966).
7. C. C. Price and M. Osgan, *J. Amer. Chem. Soc.*, **78**, 4787 (1956).
8. C. C. Price, R. Spector, and A. L. Tumolo, *J. Polym. Sci. A-1*, **5**, 407 (1967).
9. W. Kauzmann, F. B. Clough, and I. Tobias, *Tetrahedron*, **13**, 57 (1961).
10. J. R. Partington, *An Advanced Treatise on Physical Chemistry*, Green, London, Vol. IV, 1953, p. 368.
11. P. Salvadori, L. Lardicci, G. B. Consiglio, and P. Pino, *Tetrahedron Letters*, **1966**, 5343.
12. P. Pino, F. Ciardelli, G. P. Lorenzi, and G. Montagnoli, *Makromol. Chem.*, **61**, 207 (1963).
13. P. Pino, *Adv. Polym. Sci.*, **4**, 393 (1965).

14. G. B. Consiglio, Thesis, University of Pisa, 1965
15. M. Osgan, *J. Polym. Sci. A-1*, **6**, 1249 (1968).

EMO CHIELLINI  
PIERO SALVADORI

Istituto di Chimica Organica Industriale  
Università di Pisa,  
Istituto di Chimica delle Macromolecole  
del C.N.R., Nucleo di Pisa, Italy

MASEH OSGAN\*

Mellon Institute  
Pittsburgh, Pennsylvania, U. S. A.

PIERO PINO

Swiss Federal Institute of Technology  
Zurich, Switzerland

\* Present address: Laboratoire de Chimie Macromoléculaire, Institut Français du Pétrole, Hauts de Sein, France.

Received August 12, 1969  
Revised November 3, 1969

### *Thermal Degradation of Poly(vinyl chloride) in Presence of a Second Polymer*

In a preceding study<sup>1</sup> it was observed in our laboratory that in a sample of poly(vinyl chloride) (PVC) grafted by mechanochemical polymerization of methyl methacrylate (MMA), which was in fact a mixture of practically pure PVC and pure poly(methyl methacrylate) (PMMA) with a small amount of true grafted copolymer,<sup>2</sup> the thermal degradation of the PMMA part was more rapid at 210°C than that of a pure PMMA sample. This was indicative that the thermal degradation of PVC follows a radical mechanism and that then radicals escaped from the PVC portion then initiate the thermal depolymerization of the PMMA part. Independently, using mixtures of PVC and PMMA and the technique of thermovolatilization analysis (TVA), McNeill<sup>3</sup> has made the same observation. His experiments have been extended to other systems,<sup>4</sup> and more precise results for the PVC-PMMA system show clearly that chlorine radicals and HCl cause change in the degradation process of the PMMA.<sup>5</sup> Chlorine radicals initiate the degradation and HCl decreases the depolymerization rate because it allows the formation of anhydride structures blocking the "zip" process. McNeill states also that in presence of PMMA, the dehydrochlorination process of the PVC is slower, and he explains that the PMMA is competing with PVC for chlorine radicals and acts as rather inefficient radical scavenger.

On the other hand, Ouchi<sup>6</sup> has shown that during the pyrolysis of PVC rather stable carbonaceous radicals may accumulate in the degraded residue. Then it may be expected that with a mixture of PVC with a second polymer, because part of the radicals escape from the PVC, the process of accumulation of stable radicals would be slower.

Experiments have been done in isothermal conditions at 270°C under a nitrogen atmosphere, which corresponds nearly to the maximum of spins observed by Ouchi,<sup>6</sup> in a Bruker ESR apparatus, model BER 400 S (X band), equipped with a variable temperature probe (100-700°K).

Four samples have been used: sample I was a commercial PVC (Pechiney Saint-Gobain, bulk process); sample II was a grafted 80:20 PVC-PMMA copolymer prepared by mastication of PVC (sample I) in the presence of MMA in a Brabender plastograph;<sup>7</sup> sample III was a grafted 80:20 PVC-polystyrene (PST) copolymer prepared by mastication of PVC (sample I) in the presence of styrene and 0.5 part of benzoyl peroxide in a Brabender plastograph;<sup>7</sup> sample IV was a mixture of PVC (sample I, 60 parts) and poly- $\alpha$ -methylstyrene (PMST) (40 parts) polymerized anionically at low temperatures.

About 5 mg of each sample was introduced in a closed quartz tube in the probe of the apparatus. The required temperature level was attained after 2 min, and the spectra were obtained from time to time over a period of about 2 hr. In all cases the ESR signals are similar to those described by Ouchi, except that, due to the higher temperature of measurements, the half-width of the singlet is broader (9 gauss instead of 6 gauss). The relative intensities observed are plotted in Figure 1. The values are not very rigorous because of partial saturation of the signals. However it may be seen that the accumulation of free radicals is slower in the mixtures than in pure PVC. The efficiency of the second polymer with decreasing accumulation rate is in the order PMMA > PST > PMST. In the better case, the rate is slower but the amount of the second polymer is double, so that the amount of PVC is lower.

A second series of experiments was carried out with the use of the same samples and the same conditions (270°C, nitrogen atmosphere); these studies consisted of simultaneous thermogravimetric analysis and argentopotentiometric titration of the hydrochloric acid evolved.<sup>8</sup> The temperature rise from room to 270°C was controlled manually so that the time scale could be slightly shifted from an experiment to another.

The loss of hydrochloric acid (Fig. 2) represents the degradation of the PVC portion. Except for the case of sample III, where the degradation is slower, and due to the un-

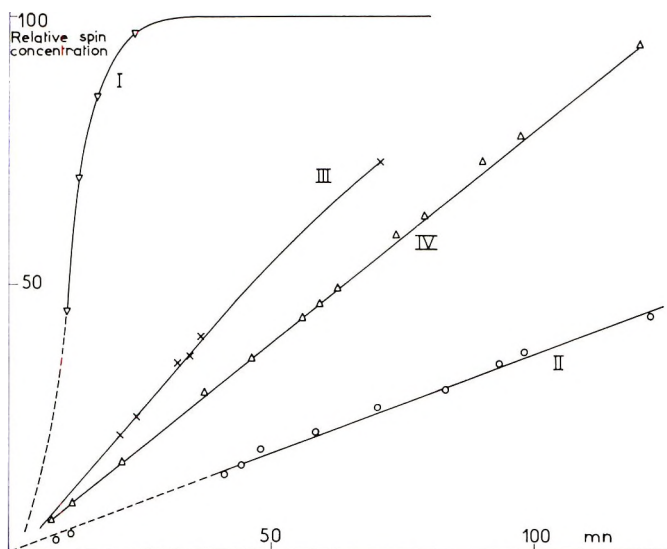


Fig. 1. Relative spin concentration vs. time of the four samples: (I) pure PVC; (II) PVC-PMMA, (III) PVC-PST (IV) PVC-PMST. All heated at 270°C in the cavity of the ESR apparatus.

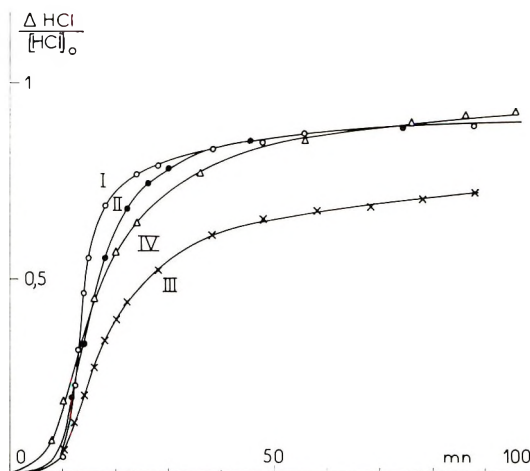


Fig. 2. Dehydrochlorination yield (ratio of HCl evolved relative to theoretical total dehydrochlorination) of the PVC portions of the four samples vs. time.

certainty of the origin of the time scale, it may be stated that there is practically no difference in the dehydrochlorination rates. Then it is possible to suppose that the dehydrochlorination of the PVC portion is associated with the same degradation process as in the pure PVC; this degradation process is represented by the small difference between the loss of weight and the loss of HCl in the case of the pure PVC. For samples II, III, and IV a part of the difference was then assigned to the PVC portion and was calculated from the dehydrochlorination results. The remaining part of the difference was attributed to the degradation of the second polymer. The results are shown in Figure 3. It may be observed at first that the degradation rate of the second polymer is very much

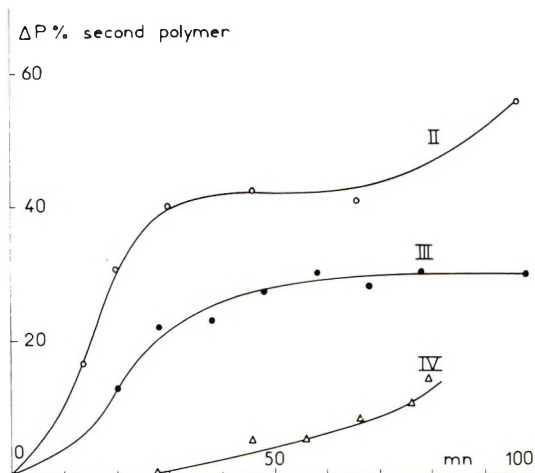


Fig. 3. Loss of weight (per cent) of the second polymer of samples II, III, and IV vs. time.

higher than expected for the pure polymer at the same temperatures, in agreement with the results of McNeill.<sup>4,5</sup> They indicate further that the degradation rates of the second polymer decrease in the order PMMA > PST > PMST, the same as for the decreasing of the accumulation rate of the conjugated polydienyl or aromatic radicals.

Comparison of the two curves relative to pure PVC in Figures 1 and 2 shows that the accumulation of radicals is related to the dehydrochlorination. The dehydrochlorination is at first very rapid and then slows as the spin number levels off. This levelling off is probably the result of an equilibrium between the formation of new radicals and their destruction by combination reactions with labile chlorine radicals; such an explanation is in agreement with the results of Ouchi which show a maximum of the spin number at 275°C, as at higher temperatures the combination reactions take place with more ease. Although the duration of the experiments at 270°C in the ESR apparatus was limited for practical reasons, it is probable that the maximum number of spins in the case of samples III and IV (and possibly II) would be greater than in the case of pure PVC; obviously the reason for such a situation is that after their migration, the labile chlorine radicals, upon reaction with the second polymer, give HCl and a macromolecular radical which cannot react with the radicals in the PVC part. The differences in the behavior of samples III and IV are easily explained on the base of the transfer of the hydrogen atom from the  $\alpha$  carbon of the polystyrene, giving a radical which easily causes chain scission and depolymerization. The transfer of a hydrogen atom from poly- $\alpha$ -methylstyrene is more difficult, and although the depolymerization rate is higher, the net result is a lower degradation rate of the second polymer. In the other hand, the higher efficiency of the polystyrene in capturing the chlorine radicals explains also its higher stabilizing power with respect to the dehydrochlorination reaction.

The behavior of PMMA is quite different: the dehydrochlorination rate is rather high, although the accumulation of radicals is the slowest. These facts might be explained by the action of the methyl methacrylate monomer upon the PVC part of the sample. The formation of monomer is caused by depropagation of the PMMA initiated either thermally at the chain ends or by the chlorine radicals. It may swell the PVC and increase the mobility of its molecules, either allowing an increased combination rate of the radicals or facilitating the escape of chlorine radicals. The latter event would cause a lower dehydrochlorination rate. But on the other hand, it has been shown<sup>2</sup> that the thermal stability of the PVC is decreased after it has been dissolved in boiling methyl methacrylate; then this monomer may also increase the dehydrochlorination rate

of the PVC part. The net balance of these two differences effects might be very small, as actually observed in Figure 2.

#### References

1. A. Michel, M. Bert, and A. Guyot, *J. Appl. Polym. Sci.*, **13**, 945 (1969).
2. A. Michel, M. Galin, and A. Guyot, *J. Appl. Polym. Sci.*, **13**, 929 (1969).
3. I. C. McNeill and D. Neil, *Makromol. Chem.*, **117**, 265 (1968).
4. I. C. McNeill and D. Neil, *Europ. Polym. J.*, in press.
5. I. C. McNeill and D. Neil, *Europ. Polym. J.*, in press.
6. I. Ouchi, *J. Polym. Sci. A*, **3**, 2685 (1965).
7. A. Guyot and A. Michel, *J. Appl. Polym. Sci.*, **13**, 911 (1969).
8. A. Guyot and J. P. Benevise, *J. Appl. Polym. Sci.*, **6**, 98 (1962).

A. GUYOT  
M. BERT  
A. MICHEL  
R. SPITZ

C. N. R. S., Institut de Recherches sur la Catalyse  
Villeurbanne 69, France

Received December 12, 1969



*Contents (continued)*

## NOTES

- GARY C. VEZZOLI: Polymerization-Induced Electrical Effects in Sulfur: The Electrical Resistance of Sulfur as a Function of Temperature..... 1587
- EMO CHIellini, PIERO SALVADORI, MASEH OSGAN, and PIERO PINO: Optical Activity of Poly [(R)-Propylene Oxide] Samples of Different Stereoregularity.. 1589
- A. GUYOT, M. BERT, A. MICHEL, and R. SPITZ: Thermal Degradation of Poly-(vinyl chloride) in Presence of a Second Polymer..... 1596

The *Journal of Polymer Science* publishes results of fundamental research in all areas of high polymer chemistry and physics. The *Journal* is selective in accepting contributions on the basis of merit and originality. It is not intended as a repository for unevaluated data. Preference is given to contributions that offer new or more comprehensive concepts, interpretations, experimental approaches, and results. Part A-1 *Polymer Chemistry* is devoted to studies in general polymer chemistry and physical organic chemistry. Contributions in physics and physical chemistry appear in Part A-2 *Polymer Physics*. Contributions may be submitted as full-length papers or as "Notes." Notes are ordinarily to be considered as complete publications of limited scope.

Three copies of every manuscript are required. They may be submitted directly to the editor: For Part A-1, to C. G. Overberger, Department of Chemistry, University of Michigan, Ann Arbor, Michigan 48104; and for Part A-2, to T. G. Fox, Mellon Institute, Pittsburgh, Pennsylvania 15213. Three copies of a short but comprehensive synopsis are required with every paper; no synopsis is needed for notes. Books for review may also be sent to the appropriate editor. Alternatively, manuscripts may be submitted through the Editorial Office, c/o H. Mark, Polytechnic Institute of Brooklyn, 333 Jay Street, Brooklyn, New York 11201. All other correspondence is to be addressed to Periodicals Division, Interscience Publishers, a Division of John Wiley & Sons, Inc., 605 Third Avenue, New York, New York 10016.

Detailed instructions in preparation of manuscripts are given frequently in Parts A-1 and A-2 and may also be obtained from the publisher.

# Wiley-Interscience Books for Chemists

## The Science and Technology of Polymer Films

Volume I.

Edited by ORVILLE J. SWEETING, *Yale University.*

Bringing together the scientific basis for plastic film products and current technology, this book presents useful and reliable data, with attention given to anticipated development of new polymers as well as new achievements with modifications of old polymers. Each chapter is written by an authority using modern terminology and accuracy with strong practical knowledge. Among other features are a special emphasis on packaging films, a new construct concerning the structure of films, and careful selection in the chapters on testing, coating, extrusion and others (but especially testing) to give fullest treatment to those tests or methods known to be of practical value.

**CONTENTS:** Introduction (O. J. Sweeting). Molecular Constitution of Film-Forming Polymers (O. J. Sweeting and R. N. Lewis). Synthetic Organic Polymers as Film Formers (O. J. Sweeting and R. N. Lewis). Natural Polymers as Film Formers: Cellulose for Film Manufacture (D. R. Walton). Cellophane Viscose and Its Conversion into Film (V. C. Haskell). Properties of Regenerated Cellulose (E. Wellisch). Other Organic Natural Polymers (O. J. Sweeting). Inorganic Polymers as Film Formers (O. J. Sweeting and R. N. Lewis). Melt Rheology of Film-Forming Polymers (H. J. Karam). Characterization of Deformation in Polycrystalline Polymer Films (R. J. Samuels). The Technology of Melt Casting (J. L. Hecht). The Friction and Lubrication of Polymer Films (D. K. Owens). Film Orientation (J. B. Mauro and J. J. Levitzky). Web-Coating Equipment and Applications (G. L. Booth). Properties and Methods of Identification of Commercial Films (P. M. Hay). Measurement of Physical Properties of Flexible Films (K. W. Ninnemann). The Analytical Chemistry of Cellulosic Films (F. J. Reindinger). The Analytical Chemistry of Vinyl Film-Forming Polymers (J. G. Cobler, M. W. Long, and E. G. Owens II). Polymer Safety for Uses in Contact with Food (R. Henderson). Author Index. Subject Index.

1968 887 pages \$37.50

## Plastic Foams

Volume I: Chemistry and Physics of Foam Formation.

Volume II: Structure, Properties, and Application.

By CALVIN J. BENNING, *International Paper Company.*

A unique, up-to-date compilation and coordination of Plastic (Polymeric) Foam Technology, creating a single body of knowledge with common laws of physics and chemistry. Included in its scope are the only complete treatments of polyethylene and polypropylene foam technology, lab procedure for evaluating performance, one-step polystyrene foam processes, foam applications, polyvinyl chloride foams, phenol, urea, and polyvinyl alcohol formaldehyde foams.

**Contents of Volume I:** Polystyrene Foam. Polyurethane Foam. Polyolefin Foams. Polyvinyl-chloride Foam. Phenolic Foam. Urea-formaldehyde Foams. Polyvinyl Alcohol-formaldehyde Foam. Epoxy Foams. Acrylonitrile and Acrylate Copolymer Foams. Pyranil Foam. Synthetic Rubber and Silicone Foams. Miscellaneous Cellular Plastics. Expandable Beads and Spheres. Inorganic Foams. Index. **Contents of Volume II:** Physics and Chemistry of Foam Formation and Stability. Relationship between Foam Morphology and the Physical Properties of Cellular Plastics. Relationship between Polymer Structure and Properties in Plastic Foams. Modification of Foam Structures. Laboratory Procedures for Predicting Foam Process and Performance. Engineering Properties of Cellular Plastics. Applications for Cellular Materials. Appendices: Raw Materials. How to Pick the Proper Foam for a Specific Application. Economics and Markets.

Volume I: 665 pages.

Volume II: 363 pages.

1969 \$75.00 for the set

## Encyclopedia of Polymer Science and Technology

Plastics, Resins, Rubbers, Fibers

Executive Editor: NORBERT M.

BIKALES, *Consultant.*

Editorial Board: HERMAN F. MARK (Chairman), *Polytechnic Institute of Brooklyn*; NORMAN G. GAYLORD, *Gaylord Associates, Inc.*

"... The definitive reference tool in the polymer field. ..."

—*Library Journal*

Contains comprehensive treatments of all monomers and polymers, their properties, methods, and processes for their preparation and manufacture, as well as broad treatments of theoretical fundamentals.

The articles are written and reviewed by specialists from around the world, and provide a unique source of original and authoritative references. All subjects are dealt with strictly from the polymer point of view.

Eleven volumes now available.

\$50 each; \$40 by subscription.

**wiley!**

**WILEY-INTERSCIENCE**

A division of

JOHN WILEY & SONS, Inc.

605 Third Ave., N.Y., N.Y. 10016

In Canada: 22 Worcester Road, Rexdale, Ontario